

The impact of fine sediments in small rivers: Method development and effects on brown trout redds

Inauguraldissertation

zur Erlangung der Würde eines Doktors der Philosophie
vorgelegt der
Philosophisch-Naturwissenschaftlichen Fakultät der Universität Basel

Yael Schindler Wildhaber
aus Rüti (GL), Schweiz

Basel, 2013

Originaldokument gespeichert auf dem Dokumentenserver der Universität Basel
edoc.unibas.ch



Dieses Werk ist unter dem Vertrag „Creative Commons Namensnennung-Keine kommerzielle Nutzung-Keine Bearbeitung 3.0 Schweiz“ (CC BY-NC-ND 3.0 CH) lizenziert. Die vollständige Lizenz kann unter creativecommons.org/licenses/by-nc-nd/3.0/ch/ eingesehen werden.

Genehmigt von der Philosophisch-Naturwissenschaftlichen Fakultät
auf Antrag von

Prof. Dr. Christine Alewell
Fakultätsverantwortliche / Dissertationsleiterin

PD. Dr. Christopher Robinson
Korreferent

Basel, den 11.12.2012

Prof. Dr. Jörg Schibler
Dekan



Namensnennung-Keine kommerzielle Nutzung-Keine Bearbeitung 3.0 Schweiz
(CC BY-NC-ND 3.0 CH)

Sie dürfen: Teilen — den Inhalt kopieren, verbreiten und zugänglich machen

Unter den folgenden Bedingungen:



Namensnennung — Sie müssen den Namen des Autors/Rechteinhabers in der von ihm festgelegten Weise nennen.



Keine kommerzielle Nutzung — Sie dürfen diesen Inhalt nicht für kommerzielle Zwecke nutzen.



Keine Bearbeitung erlaubt — Sie dürfen diesen Inhalt nicht bearbeiten, abwandeln oder in anderer Weise verändern.

Wobei gilt:

- **Verzichtserklärung** — Jede der vorgenannten Bedingungen kann aufgehoben werden, sofern Sie die ausdrückliche Einwilligung des Rechteinhabers dazu erhalten.
- **Public Domain (gemeinfreie oder nicht-schützbar Inhalte)** — Soweit das Werk, der Inhalt oder irgendein Teil davon zur Public Domain der jeweiligen Rechtsordnung gehört, wird dieser Status von der Lizenz in keiner Weise berührt.
- **Sonstige Rechte** — Die Lizenz hat keinerlei Einfluss auf die folgenden Rechte:
 - Die Rechte, die jedermann wegen der Schranken des Urheberrechts oder aufgrund gesetzlicher Erlaubnisse zustehen (in einigen Ländern als grundsätzliche Doktrin des fair use bekannt);
 - Die **Persönlichkeitsrechte** des Urhebers;
 - Rechte anderer Personen, entweder am Lizenzgegenstand selber oder bezüglich seiner Verwendung, zum Beispiel für **Werbung** oder Privatsphärenschutz.
- **Hinweis** — Bei jeder Nutzung oder Verbreitung müssen Sie anderen alle Lizenzbedingungen mitteilen, die für diesen Inhalt gelten. Am einfachsten ist es, an entsprechender Stelle einen Link auf diese Seite einzubinden.

Abstract

Native brown trout populations are declining in Swiss rivers. This could be due, among other reasons, to a clogged riverbed caused by fine sediment deposition, leading to a decrease in interstitial flow and therefore in a reduced oxygen supply to the salmonid embryos. Furthermore, suspended sediment (SS) could directly harm health and fitness of free swimming fish. The aim of this dissertation was to develop and apply methods to measure SS and the effects of weekly fine sediment infiltration and net fine sediment accumulation over the entire egg incubation season on oxygen concentrations in artificial redds and the survival of the implemented brown trout eggs. Furthermore, the effects of riverbed structure, redd morphology and hydrological and hydrogeological conditions on interstitial oxygen and egg survival was assessed. In addition, source areas of SS and organic matter were assessed by C/N atomic ratio, $^{13}\text{C}_{\text{tot}}$, $^{13}\text{C}_{\text{org}}$ and ^{15}N isotopes. The study was conducted at three sites named A, B and C, from up- to downstream along the canalized and partly stabilized river Enziwigger in the Swiss Plateau. Data were collected weekly or measured continuously during two spawning seasons (2009/10 and 2010/11) from November to March in a total of 36 redds.

Weekly fine sediment infiltration rates in redds were relatively high and generally increased with higher SS concentrations. Both, infiltrated sediments and SS showed strong temporal variations between low flow and peak discharge conditions. Fine sediment infiltration was at maximum during high flow events with sediments mainly in the size of sand (0.063 - 2 mm). These sediments originated for the most part in the upper watershed. Small amounts of fine sediments infiltrated during base flow periods with particles mainly in the size of silt and clay ($< 63 \mu\text{m}$) and with increasing organic matter concentrations. Organic matter was generally of allochthonous origin and major sediment source areas were pasture and arable land during those low flow periods.

Less fine sediment accumulated over the entire egg incubation period in upwelling zones on the local scale and within areas of higher mean water levels due to corresponding flushing of fine sediments. Even though SS and bedloads increased from up- to downstream, less fine sediment accumulated downstream. Higher flushing of fine sediments and generally increased sediment dynamics downstream due to higher water levels are probably the reasons for this observation. Increased sediment dynamics also caused remarkably scouring of redds: 50% of the redds in the two downstream sites were excavated or buried during high flow events in early winter due to sediment movements. Redd loss at the upstream site A was substantially lower (8%).

The high permeability of the redd substratum and the typical pit-tail structure of redds led to high dissolved oxygen (DO) concentrations in redds shortly after redd construc-

tion. Specific infiltration rates q decreased substantially within one month due to riverbed sediment displacements and fine sediment infiltration. This resulted in lower DO concentrations in redds. In individual redds, DO concentration decreased temporally to almost 0%, leading to a depleted redd environment unfavorable for embryo survival. Interstitial DO concentration and q generally increased during high flows. In contrast they decreased during the falling limb of the water level, likely indicating exfiltration of depleted ground- or interstitial water. Similarly, DO concentrations decreased under prolonged base flow conditions. This paralleled the higher percentage of silt and clay particles in the infiltrated sediment, probably triggering riverbed clogging and therefore reducing q .

Even though organic matter in SS increased from up- to downstream due to an increase of pasture and arable land downstream of the river, egg survival was better at the downstream sites. Organic matter concentrations were with means between 5.1% at site A and 6.5% at site C relatively low. The low egg survival at site A was likely due to the high fine sediment accumulation at the site, triggering low specific infiltration rates and consequently decreased DO concentrations. This was especially true at spots with low mean water levels, where flushing of fines is inhibited.

Enhanced soil erosion processes on pasture and arable land are expected with increasing heavy rain events and less snow during winter seasons due to climate change. Consequently, SS and organic matter in the river will increase, which will possibly affect brown trout negatively. Furthermore, a higher frequency of high flows in the future could potentially enhance scouring of redds especially in the downstream sites, which could further reduce egg survival rates.

Contents

1	Introduction	1
1.1	The impact of fine sediments in rivers	1
1.2	Fine sediments in Swiss rivers	2
1.3	Causes for brown trout decline in Switzerland	3
1.4	Aims and outline of the thesis	4
1.5	Further scientific contributions within the thesis	4
2	Measurement of spatial and temporal fine sediment dynamics	7
2.1	Abstract	7
2.2	Introduction	8
2.3	Materials and methods	9
2.3.1	Study site and general setup	9
2.3.2	OBS sensors and time integrated samplers to measure suspended sediment	10
2.3.3	Sediment baskets to measure fine sediment infiltration and accumulation	11
2.3.4	Bedload traps to measure sediment transported along the bed	12
2.3.5	Hydraulic conditions	13
2.3.6	Freeze core samples	13
2.3.7	Sample analyses	13
2.4	Results and discussion	14
2.4.1	Suspended sediment	14
	Turbidity measured by optical backscatter sensors	14
	Suspended sediment samplers	16
2.4.2	Sediment infiltration	17
2.4.3	Sediment accumulation	20
2.4.4	Fine sediment transported along the bed	22

2.4.5	Comparison of the different methods	23
	SS samplers and OBS turbidity sensors	23
	Sediment infiltration baskets and bedload traps	24
	Sediment accumulation baskets	26
2.5	Conclusion	27
3	Organic matter dynamics and stable isotopes to trace SS source areas	29
3.1	Abstract	29
3.2	Introduction	30
3.3	Materials and methods	31
3.3.1	Study site and general setup	31
	Sample collection	32
	Sample analyses	33
	Data interpretation	33
3.4	Results and discussion	34
3.4.1	Spatial and temporal dynamics of C_{org} in sediments and of DOC .	34
3.4.2	Spatial and temporal dynamics of TN in sediments and of nitrate .	37
3.4.3	Spatial and temporal dynamic of C/Na	38
3.4.4	Spatial and temporal dynamics of C_{inorg} in sediments	39
3.4.5	Carbon and nitrogen isotopes for tracing suspended sediment sources	39
3.5	Conclusions	45
4	Evaluation of a new method to measure riverbed colmation	47
4.1	Abstract	47
4.2	Introduction	48
4.3	Materials and methods	49
4.4	Results and discussion	49
4.4.1	Comparing penetration depth with the sediment size of the riverbed	49
4.4.2	Spatial distribution of penetration depths and redd locations . . .	50
4.4.3	Reproducibility and comparability of the method	51
4.5	Conclusion and outlook	52
5	Multidimensionale Untersuchung der Fluss-Grundwasser-Interaktion	55
5.1	Zusammenfassung	56
5.2	Einleitung	56

CONTENTS

5.3	Untersuchungsgebiet	57
5.4	Methoden und Datengrundlagen	60
5.4.1	Hydrologische Grundlagen	60
5.4.2	Messsysteme zur Aufzeichnung hydraulischer und physikalischer Parameter	61
5.4.3	Flussbetttopographie	61
5.4.4	Grundwasserströmungsmodell und Szenarienberechnungen	62
5.5	Resultate	63
5.5.1	Hydrologie	63
5.5.2	Hydraulische und physikalische Parameter	63
5.5.3	Lokales und regionales Grundwasserströmungsmodell	66
5.5.4	Szenarienberechnungen mit dem lokalen Grundwasserströmungsmodell	68
5.6	Diskussion	71
5.7	Schlussfolgerungen	73
6	Effects of river morphology, hydraulic gradients, and sediment deposition on water exchange and oxygen dynamics in salmonid redds	75
6.1	Abstract	75
6.2	Introduction	76
6.3	Materials and methods	78
6.3.1	Study site and general setup	78
6.3.2	Sediment collections and analyses	80
6.3.3	Oxygen	81
6.3.4	Riverbed and redd morphology	81
6.3.5	Hydraulic investigations	81
6.3.6	Groundwater flow modeling	83
6.4	Results and discussion	83
6.4.1	Spatiotemporal changes in riverbed and redd morphology	83
6.4.2	Hydraulic dynamics in redds	86
	Spatial patterns of the hydraulic dynamics	86
	Temporal pattern of the hydraulic dynamics	90
6.4.3	Oxygen	93
	Manual vs. continuous oxygen measurements	93
	Spatial oxygen dynamics	93
	Temporal oxygen dynamics	94

6.5	Conclusion	96
6.6	Supplementary information	97
7	Artificial steps mitigate fine sediment effects on brown trout embryo survival in a heavily modified river	99
7.1	Summary	99
7.2	Introduction	100
7.3	Methods	104
7.3.1	Study River and experimental setup	104
7.3.2	Quantification of embryo survival	105
7.3.3	Statistical analysis	106
7.4	Results	106
7.4.1	Redd loss during bed scouring	106
7.4.2	Embryo survival among years and sites	107
7.4.3	Oxygen dynamics and embryo survival	107
7.4.4	Fine sediment, river structure and embryo survival	109
7.5	Discussion	109
7.5.1	Embryo survival among years and sites	110
7.5.2	Oxygen dynamics in redds and embryo survival	111
7.5.3	Factors affecting brown trout embryo survival	112
7.6	Supplementary information	114
8	Final remarks and outlook	115
	Acknowledgements	116
	Bibliography	118
A	Sediment oxygen demand	133
A.1	Objective	133
A.2	Materials and methods	133
A.3	Results, discussion and outlook	135
	Curriculum vitae	137

List of Figures

1.1	Used methods/measurements to assess fine sediment input, the abiotic redd environment and egg survival.	5
2.1	Watershed of the river Enziwigger with the three field sites A, B and C and the towns Willisau and Hergiswil (Canton of Lucerne, Switzerland). . . .	10
2.2	Devices used to measure fine sediment dynamics in the redds. (A) : suspended sediment sampler, (B) : sediment infiltration/accumulation basket, (C) : bedload trap.	12
2.3	Correlation between turbidity in NTU and suspended sediment concentration (SSC). Dashed lines are the 95 % confidence intervals; RSE = residual standard error (degree of freedom = 154)	14
2.4	Example of the temporal variation of the suspended sediment concentration (SSC) and water level (Site A, Season 1).	15
2.5	Weekly D_{50} of the suspended sediment (SS) caught by the SS samplers ($n=6$ /site) during three weeks at the three sites A, B and C. Mean total amount of SS load \pm standard deviation is given below/above the boxes. The 6 samples of 3 rd of December 2009 had to be merged for grain size analysis because of the small quantity of SS.	16
2.6	Sediment infiltration rate in relation to the highest mean daily water level above the redds during the measurement week. The relationship at site B and C is described by a Weibull growth function.	18
2.7	Weekly silt and clay infiltration at site C in absolute values (A) and relative values (i.e., fraction of silt and clay of the total fine sediment deposition; (B)) in relation to the daily infiltration rate of sediment <2 mm. Dashed lines are the 95 % confidence intervals.	19
2.8	Weekly sediment infiltration in relation to the total weekly SS load assessed with SS samplers at the three sites. R^2 and p of the nonlinear regressions were calculated after Gail et al. (2009).	25
2.9	Relationship between infiltration rate of fine sediment measured with sediment baskets and bedload measured with bedload traps at site A. (A) : all data with a nonlinear regression line, R^2 and p were calculated after Gail et al. (2009); (B) : linear regression for data with infiltration rates smaller $2 \text{ kg m}^{-2} \text{ d}^{-1}$, dashed lines are the 95 % confidence intervals.	26

3.1	Watershed of the river Enziwigger with the three field sites A, B and C including their altitude, soil sample spots and the towns Willisau and Hergiswil (Canton of Lucerne, Switzerland).	32
3.2	Sediment, nutrient and isotope composition dynamics during the field period. Plotted are mean values of all samples from all three sites. (A) Water level at site B, the weekly infiltration of sediment <2 mm (IS) and the weekly suspended sediment (SS); (B) C_{org} and TN of IS and SS; (C) C/Na and $\delta^{15}N$ of SS; (D) $\delta^{13}C$ of C_{org} and C_{tot} of the SS.	36
3.3	Relationship between C_{org} and (A) total IS <2 mm; (B) total SS; (C) clay and silt fraction of sediment <2 mm and (D) TN. Solid circles and solid lines: Infiltrated sediment, stars and dotted lines: SS. Dashed lines in (A) and (B) are the 95 % confidence intervals.	38
3.4	Relationship between maximal mean daily water level of a week and $\delta^{13}C_{tot}$ and $\delta^{15}N$ values of the weekly captured SS at the three sites. Dashed lines are the 95 % confidence intervals.	40
3.5	$\delta^{13}C_{tot}$ and $\delta^{15}N$ values of SS and soil samples collected above each sites (average \pm sd). Dashed line: SS regression line.	42
3.6	Total suspended sediment (SS) per week at the three sites and soil source contribution from the three/four possible sources to SS at the three sites, determined with the dual isotope mixing model <i>IsoSource</i> . Air temperature was measured close to site B in Hergiswil.	43
3.7	Schematic view of the groundwater table and bedrock at site B with the installed piezometers (P).	45
4.1	Correlation between penetration depth and (A) clay fraction of the upper 10 cm of the riverbed sediment (u10), (B) clay and silt fraction of u10, (C) sediment < 2 mm fraction of u10, and (D) D_{50} of the riverbed sediment. Linear regression line is only for data with penetration depth > 3 cm. Dashed lines are the 95 % confidence intervals.	50
4.2	Mean penetration depth of two measurements per measuring point at the site B, terrace 4.	51
4.3	Relationship between penetration depths conducted twice at the same spot by (A) the same person and (B) two persons. Dashed lines are the 95 % confidence intervals.	52

LIST OF FIGURES

- 5.1 Untersuchungen auf verschiedenen Skalen. **a)** Lage des Untersuchungsgebiets in der Schweiz. **b)** Digitales Höhenmodell (5 m-Auflösung) des Untersuchungsgebiets und Modellperimeter für das regionale Grundwasserströmungsmodell. Dargestellt ist die Verteilung von berechneten Grundwassergleichen (1 m-Äquidistanz) während einer Mittelwassersituation (siehe Abb 5.2). **c)** Digitales Höhenmodell (5 m-Auflösung) und Modellperimeter des lokalen Grundwasserströmungsmodells. Dargestellt sind die Verteilung von berechneten Grundwassergleichen (0.2 m-Äquidistanz) während einer Mittelwassersituation (siehe Fig. 5.2) sowie die Lage der Grundwassermessstellen, Sohlswellen und künstlich angelegten Forellenlaichgruben. **d)** 5-fach überhöhtes laterales Höhenprofil durch den Talgrundwasserleiter der Enziwigger, dargestellt mit einem, aus den Bohrtiefen abgeleiteten Schotter-Grundwasserkörper; die Enziwigger wurde über weite Bereiche an den östlichen Talrand verlegt. **e)** Darstellung des untersuchten Flussbettabschnittes und Resultate der Flussbettvermessungen zusammen mit der Lage der ufernahen Grundwassermessstellen, Sohlswellen und künstlich angelegten Forellenlaichgruben. 59
- 5.2 Zeitreihen von: **a)** meteorologischen Daten im Einzugsgebiet der Enziwigger; **b)** Pegelraten im Fluss; **c)** Pegelraten im ufernahen Grundwasser (BP3 und 5); **d)** Pegelraten im Talgrundwasserleiter (BP1); **e)** Temperaturdaten im Fluss und im Grundwasser (BP1, 3 und 5); und **f)** Daten der elektrischen Leitfähigkeiten im Fluss und im Grundwasserpegel BP5 (BP5). Für die Lage der Grundwassermessstellen siehe Fig. 5.1. 64
- 5.3 **a)** Berechnete Austauschraten für drei Szenarien während Mittel- und Hochwasser (Fig. 5.2). Auch dargestellt sind der Flusspegel und der Verlauf des Flussbettes in der Mitte der Enziwigger. Der 20. April 2010 sowie der 29. Juli 2010 entsprechen einem niedrigen Wasserstand, während der 30. Juli 2010 fand ein Hochwasserereignis statt (Fig. 5.2). Positive Werte entsprechen einer Infiltration vom Flusswasser in das hyporheische Interstitial; negative Werte entsprechen einer Exfiltration vom Grundwasser in den Fluss. **b)** Räumliche Verteilung der Austauschraten im Flussbett des untersuchten Gewässerabschnittes der Enziwigger für das lokale Grundwasserströmungsmodell (Szenario 1). 68
- 5.4 Flusspegel in der Enziwigger und zeitliche Verläufe der berechneten Austauschraten durch die künstlich angelegten Forellenlaichgruben (B42, 51 und 52, siehe Fig. 5.1) für den gesamten instationär modellierten Zeitraum. Positive Werte entsprechen einer Infiltration vom Flusswasser in das hyporheische Interstitial; negative Werte entsprechen einer Exfiltration vom Grundwasser in den Fluss. Die Unterschiedliche Skalierung bei Szenario 3 ist zu beachten. 69
- 5.5 **a)** Strömungsvektoren und Zuströmbereiche zu den Grundwassermessstellen dargestellt für die drei Szenarien. **b)** Räumliche Verteilung der Austauschprozesse für die drei berechneten Szenarien über die gesamte Simulationszeit. Kalibrierte Durchlässigkeit der Flusssohle: C1 = 19 ($\text{m}^2 \text{d}^{-1}$) m^{-2} , C2 = 50 ($\text{m}^2 \text{d}^{-1}$) m^{-2} , C3 = 42 ($\text{m}^2 \text{d}^{-1}$) m^{-2} , C4 = 62 ($\text{m}^2 \text{d}^{-1}$) m^{-2} , C5 = 19 ($\text{m}^2 \text{d}^{-1}$) m^{-2} 70

6.1	Schematic view of (A) longitudinal section of an artificial redd (modified after Greig et al., 2007b) including the location of the mini piezometers, the egg pockets (square) and temperature probes (bullet points) with the local scale flow pattern, (B) the hyporheic flow on an intermediate scale induced by riverbed steps according to the model calculations of Huber et al. (2013) (Chap. 5), and (C) the intermediate and regional scale water exchange processes (top view). Modeled data from Huber et al. (2013) (Chap. 5). Black: only exfiltration, gray: ex- and infiltration, light gray: only infiltration. Arrows indicate the main direction of the interstitial- / groundwater flow, ovals represent the position of the redds (for naming see Fig. 6.2).	77
6.2	Location of the Enziwiggerwatershed in Switzerland. The photograph shows the step and terrace structure at study site B. The watershedmap of the river Enziwigger and the towns Willisau and Hergiswil (Canton of Lucerne, Switzerland) shows the locations of the three field sites A, B and C, while the schematic on the right illustrates the location of the redds within each field site. Here, superscripts indicate redds with continuous temperature (T) and oxygen (O) measurements.	79
6.3	Differences between the riverbed topography measured in October and December 2009 at the two downstream sites B and C. Negative values indicate gravel bed erosion, and positive values indicate sediment deposition. Black ovals are the positions of the artificial redds. Redds lost during season 1 are marked by a star on the left side, while redds lost during season 2 are marked by a star on the right side.	86
6.4	In each panel, the black graph represents the flowstage at site B. Symbols within panels denote (A) the mean \pm standard deviation (SD) of the riverbed level differences between tail and pit (B) mean \pm SD of the vertical hydraulic gradients (VHGs) in the tail of the redds, and (C) mean \pm SD of the horizontal hydraulic gradients (HHGs) between pit and tail of the redds. Values were calculated from all 18 redds during season 2. A positive hydraulic gradient indicates upwelling, and a negative gradient indicates downwelling.	87
6.5	Specific infiltration rate in the upper (q_u) and the bottom part (q_b) of the redds during the two seasons. Negative values indicate upwelling, positive values indicate downwelling. For each redd the horizontal line indicates the median, the box interquartile range (i.e., center 50% of the data), whiskers mark maximum and minimum values, and points denote values exceeding 1.5 times the interquartile range. Among seasons, redds were built in the same location (Fig. 6.2) with the exception of redds A31 and A32 (see beginning of Section 6.4.2).	89
6.6	Relationship between water level and vertical hydraulic gradient (VHG) for individual redds from season 2. Within each panel Spearman correlation coefficient ρ and the p -value are given. Positive VHG indicates upwelling, and negative VHG indicates downwelling. The location of each redd is given in Fig. 6.2.	90

LIST OF FIGURES

6.7 Example of the temporal dynamics of the specific infiltration q in the upper part of the redd gravel (q_u), the oxygen concentration and the water level. Shown are data from redd C21.S2 (cf. Fig. 6.2). A period when oxygen and temperature probes were dug out is marked with vertical dashed lines. 91

6.8 Temporal changes of the specific infiltration rate q in the upper and the bottom part of the redd C22.S2 (cf. Fig. 6.2 for location of the redd). Negative values indicate upwelling, positive values indicate downwelling. The arrows point to periods with increased upwelling during the falling limb of high flow events. 92

6.9 Example for temporal oxygen concentration and water level dynamics (redd A31.S2, see Fig. 6.2 for location of the redd). Arrows mark the decrease of oxygen concentrations during the falling limb of high flow events. 94

6.10 Relationships between the mean daily oxygen concentrations in redds and the specific infiltration rates q_t with non-linear regression lines. Within each panel Spearman correlation coefficient ρ (ρ) and the p -value are given. See Fig. 6.2 for location of the redds. 95

6.11 Correlation between dissolved oxygen and accumulated fine sediment in the redds. Dashed lines are the 95% confidence intervals. 97

7.1 Conceptual process-based summary of the interaction of investigated parameters and how they relate to brown trout embryo survival in our heavily modified study river. In each box a general descriptive term (in italics) is given on top, with parameters investigated in our project listed below. Superscripts indicate References: 1- Huber et al. (2013) (Chap. 5), 2 - Schindler Wildhaber et al. (2012b) (Chap. 2), 3 - Schindler Wildhaber et al. (2012a) (Chap. 3), 4 - Schindler Wildhaber et al. (2014) (Chap. 7), and 5 - this study (bold parameters are identified most important variables). Arrows indicate that parameter affects the response parameter directly, and the open circle indicates that parameters jointly affect the response parameter. Dashed arrow indicates that water exchange might also affect embryo STH directly, e.g., by removing metabolic waste, but this was not tested in the current study. 102

7.2 Study river and experimental setup. **(a)** Location of the Enziwigger watershed in Switzerland. The photograph shows the step and terrace structure at study site B. The watershed map of the river Enziwigger shows the towns Willisau and Hergiswil (Canton of Lucerne, Switzerland) and the location of the three field sites, **(b)** Schematic of the experimental setup, showing a top view on one of the artificial redds with the pit (white) and tail (light grey) areas. Symbols mark the position of the piezometer pipes (grey stars), egg capsules (white circles), and the Aandera oxygen probe (white rectangle) introduced in some redds for continuous oxygen monitoring. The fine sediment infiltration (IB) and accumulation (AB) baskets were located just behind the egg-capsules. For a schematic lateral view on one of the artificial redds see Fig. 6.1 in Schindler Wildhaber et al. (2014) (Chap. 7) and **(c)** egg-capsule used to incubate brown trout embryos. . . . 104

7.3	(a) mean embryo survival to hatch for all study sites during seasons 1 (S1) and 2 (S2) and (b) Mean embryo survival to hatch in the individual field sites (A, B and C) for seasons 1 and 2. Bars represent mean \pm SEM.	107
7.4	Interstitial oxygen concentration in the four redds where continuous measurements and embryo survival to hatch data were available. Horizontal gray bars mark periods of missing data.	108
7.5	Relationship between brown trout survival to hatch and significant predictor variables identified in the multivariate logistic regression (Table 7.2). Lines are mean regression line \pm 95% point-wise confidence intervals as predicted from the fitted generalized linear model. Symbol filling denotes seasons (2009/10 = open, 2010/11 = filled) and shape denotes field sites (\circ = Site A, \triangle = Site B, and \square = Site C). Arrows in graph c mark influential data-points mentioned in the results section.	110
7.6	Relationship between influential predictor variables identified in partial least squares regression (VIP > 1, 7.4). Pearson product-moment correlation coefficients (r) and the p-values (p) are given. The black line is the best fit line. Abbreviations: FS = fine sediment, Distance step up = Distance to next upstream step.	114
A.1	Recirculation system used for measuring sediment oxygen demand (SOD). The red arrows indicate the flow direction.	134
A.2	Decline of oxygen concentration within the circulation system with sediment samples from the three sites A,B and C. Accumulation baskets from the same redd are indicated with $_a$ and $_b$. $_1$ and $_2$ refers to the accumulation basket which was run twice. The samples are sorted after the date of procedure. The date behind the site label stands for the day when samples have been collected in the field.	135

List of Tables

2.1	Site characteristics: D_{50} of the riverbed sediment was defined by freeze core samples and with line-number-analyses (Fehr, 1987). Data are given as mean \pm standard deviation.	11
2.2	Mean and standard deviation of suspended sediment concentration (SSC_{NTU}) measured with the OBS sensors and suspended sediment (SS) load caught by suspended sediment samplers at the three sites during the two field seasons.	15
2.3	Range or mean \pm standard deviation of infiltration rate (IR) of sediment < 2 mm in permeable sediment baskets.	17
2.4	Mean and range of daily sediment < 2 mm infiltration rate (IR) during the two seasons at the three sites and of the coefficient of variation (CV) of the weekly values within the six samplers per site.	18
2.5	Mean values \pm standard deviation of the fraction of fine sediment (< 2 mm) in the accumulation baskets and the fraction of sediment $< 63 \mu m$ of the accumulated fine sediment during the two spawning seasons S1 (2009/2010) and S2 (2010/2011) and in freeze cores (FC) taken in winter 2008/2009 at the three sites.	20
2.6	Fine sediment (< 2 mm) and silt and clay ($< 63 \mu m$) accumulation in the accumulation baskets as % of the whole baskets and the silt and clay fraction of the sediment < 2 mm. Range (mean) or mean \pm standard deviation.	21
2.7	Mean and range of daily bedload (BL) < 2 mm, of the percentage of BL < 2 mm of the total BL and of the coefficient of variation (CV) of the weekly values within the six samplers at the three sites.	22
2.8	Spearman rank correlation coefficients (ρ) between the measured parameters of both seasons for the three sites with mean weekly SSC_{NTU} measured with OBS sensors, total weekly suspended sediment (SS) load measured by SS samplers, daily fine sediment infiltration rate, fine sediment accumulation, daily bedload of fine sediment, the percentage of fine sediment of the total bedload, highest mean daily water level of a week and vertical hydraulic gradient (VHG). The accumulation baskets were correlated with the mean values of the parameters during the whole field seasons. The sample size (n) is given in parentheses.	24

3.1	Mean values and standard deviation at the three sites sampled of organic and inorganic carbon (C_{org} and C_{inorg}) in infiltrated sediment (IS) and suspended sediment (SS), dissolved organic carbon (DOC) in the river and the interstitial (int.), total nitrogen (TN) in IS and SS, nitrate in the river and interstitial, C/Na , $\delta^{13}C_{org}$, $\delta^{13}C_{tot}$ and $\delta^{15}N$ of SS. The sample numbers are given in parentheses.	35
3.2	Range (mean) of C/Na , $\delta^{13}C_{org}$, $\delta^{13}C_{tot}$ and $\delta^{15}N$ values of algae ($n = 4$), manure ($n = 6$), and riverbed sediment (riverbed S, $n = 5$) as well as of forest ($n = 14$), pasture ($n = 12$) and arable land ($n = 8$) soils of the watershed. 39	39
3.3	Mean (range and standard deviation) source contribution (%) to the suspended sediment at the three sites. Riverbed S = riverbed sediment.	44
4.1	Mean \pm standard deviation of the penetration depths and number of integrated values at the three sites A, B and C. Each value consists of two replicates. Data of fine sediment (< 2 mm) accumulation, fraction of sediment $< 63 \mu m$ of the fine sediment and D_{50} of the riverbed sediment (defined by freeze core samples and with line-number-analyses; Fehr, 1987) are taken from Schindler Wildhaber et al. (2012b)(Chap. 2).	52
5.1	Fragen und Ziele für die verschiedenen Untersuchungsskalen sowie Untersuchungsmethoden und Ergebnisse.	58
5.2	Definition Modellrandbedingungen (Fig. 5.1).	62
5.3	Zusammenfassung der Resultate der Fluss- und Grundwassermessungen (BP1, 3 und 5, siehe Fig. 5.1 und 5.2), der Temperaturanalysen in den Forellenlaichgruben (B42, 51 und 52, siehe Fig. 5.1) und der Grundwasserströmungsmodellierung. Mittelwerte \pm Standardabweichung. T = Temperatur, P = Pegel, GW=Grundwasser	65
5.4	Berechnete Aufenthaltszeiten (t) und Fließpfade (d) zu den Grundwassermessstellen (BP1, 3 und 5, siehe Fig. 5.1) für die regionale und lokale Grundwasserströmungsmodellierung und die verschiedenen Szenarienberechnungen.	67
6.1	Physical parameters used for calculating specific infiltration rates q in alphabetic order (1. Roman letters, 2. Greek letters).	84
6.2	Spearman rank correlation coefficients between median specific infiltration rate q in the upper part (ca. 0 - 12 cm; q_u) and the total part (ca. 0 - 20 cm, q_t) with total accumulated fine sediment (< 2 mm), accumulated silt and clay fraction, sum of the weekly infiltrated fine sediment, <i>fredle index</i> of the accumulation baskets, maximal water level above the redd and distance of the redd to the upstream and downstream step. The sample size (n) is given in parentheses.	88

LIST OF TABLES

6.3 Mean oxygen concentrations calculated from continuous measurement with permanent oxygen probes in one redd per site during season 1 (S1) and two redds per site during season 2 (S2). Given are mean \pm standard deviations, minimum (Min) and number of days wherein oxygen concentration was below 7 mg l^{-1} 94

7.1 Explanatory variables included in multivariate analyses. For each variable a short description and references (Ref.) describing the methodology how the parameter was measured are given. The hypothesized effect on embryo STH (\uparrow = increase; \downarrow = decrease) based on the process understanding developed in our project (Fig. 7.1) are also given. Finally, the variable influence on prediction score (VIP) inferred in the partial least squares regression analysis is given. The most important predictor variables identified in the multivariate logistic regression analysis are marked in bold. 103

7.2 Results of the multivariate logistic regression analyses. Given are the explained deviance (D_{exp}), parameter estimates (Estimate) and their standard error (SE), as well as their significance levels (p) from the optimal logistic regression model. Dist. step up = distance to upstream step, HHG = Horizontal hydraulic gradient, see also Table 7.1. 109

LIST OF TABLES

Chapter 1

Introduction

1.1 The impact of fine sediments in rivers

In rivers throughout the world increasing fine sediment loads (sediments < 2mm) were assessed in catchments that are impacted both directly and indirectly by human activities (Owens et al., 2005). Sediment supply in the alpine Rhine basin e.g., is estimated to increase between 220% and 284% by the year 2100 due to the combined effect of expected climate and land use change (Asselman et al., 2003). Several authors have noticed higher suspended sediment concentrations in alpine rivers during winter and spring due to the combination of more intensive rainfall together with changes in land use over the last decades (for a review see Scheurer et al., 2009). The United States Environmental Protection Agency (EPA) has identified both sediments and turbidity among the top 10 causes of river and stream impairment (EPA, 2009). A chemical, physical and biological survey in 1392 wadeable rivers indicated that an increase in nutrients (e.g., nitrogen and phosphorus) and streambed sediments have the highest negative impact on biological condition (EPA, 2007). 25% of the investigated stream length had streambed sediment characteristics in poor conditions compared to a regional reference. Soil erosion from road construction, poor agricultural practices, and other disturbances likely caused this increase in fine sediment on the stream bottom (EPA, 2007).

Increased fine sediment loads in rivers generally trigger higher fine sediment infiltration rates in the riverbed gravel (Greig et al., 2005; Zimmermann and Lapointe, 2005b). The local retention and transport of fine sediment are, however, determined by many factors as flow conditions (e.g., shear stress, water depth and hydraulic gradient), by the properties of the suspended load (e.g., grain size distribution and cohesivity) and by the channel sediment structure (Brunke, 1999). If fine sediment settles on the top of the streambed in areas of low water velocity (= external colmation) or passes through the coarse top layer (= armor layer) and accumulates in the underlying layer (= internal colmation), pore spaces of the riverbed get reduced, resulting in a smaller hydraulic conductivity (Schälchli, 1995; Brunke, 1999). Schälchli (1995) divided the colmation process of a riverbed into three phases. In phase 1, the coarse particles (> 30 μm) play the dominant role by closing the big pores. The consequence is only a minor reduction of the hydraulic conductivity. The pores are filled up by medium-sized particles (3 - 30 μm) in phase 2, reducing the hydraulic conductivity substantially, while in phase 3 the very fine particles (< 3 μm) play the dominant role by building an almost impermeable matrix. With increas-

ing discharge and bed shear stress, decolmation, an expression referring to all processes that contribute to an increase of hydraulic conductivity, starts (Schälchli, 1995; Brunke, 1999). During the decolmation process, the positions of single grains of the armor layer can be altered, affecting the underlying clogged layer and consequently locally increasing hydraulic conductivity. High floods can totally break up the armor layer and hydraulic conductivity increases to a maximum value (Schälchli, 1995; Schälchli et al., 2002). A new colmation cycle begins during the following falling limbs. However, the development of new colmation is also possible when discharge remains constant and the suspended load is high (Brunke, 1999). Thus, increasing colmation can occur due to I) higher fine sediment loads and II) due to less decolmation processes attributable to anthropogenic modifications as riverbed stabilizations, dams or water abstractions.

The observed and predicted changes of fine sediment dynamics in rivers can provide a serious threat to aquatic ecosystems, including phytoplankton, aquatic invertebrates and fish (for reviews see Bilotta and Brazier, 2008; Newcombe and MacDonald, 1991). High levels of nutrients and excess streambed sedimentation more than double the risk of poor biological condition (EPA, 2007). Possible effects of fine sediment particles on salmonid fish differ between development stages (Bilotta and Brazier, 2008). While suspended particles can directly impact free swimming fish (Newcombe and Jensen, 1996; Newcombe and MacDonald, 1991), colmated riverbed can lower the oxygen supply to the developing salmonid embryos and the flushing of harmful metabolic waste products of embryos, and hence potentially reduce their survival (Greig et al., 2005).

1.2 Fine sediments in Swiss rivers

Suspended sediment (SS) concentration data of Swiss rivers of the last years do not show a clear trend (Bucher, 2002). Measured SS concentrations in 12 rivers by the NADUF program (National river monitoring and survey program) did not increase during the last 20 years. But no data exist from small rivers, which are likely to react stronger on changes in the river catchment (Bucher, 2002). Soil erosion in Switzerland has likely increased since the second world war due to land use change (Bucher, 2002). Arable farm land has increased from 1965 to 1990, but in the recent years it decreased again. The percentage of corn, which is known to trigger high erosion rates, grew since 1965 (approx. 4%) continuously to 23% in the year 2011 (BSF, 2012).

Quantifying soil erosion is, however, difficult. Prasuhn (2011) assessed soil erosion on arable lands during ten years in the Swiss midlands and concluded that fields affected by erosion differed from year to year. Each year, about 30% of the 203 analyzed fields were affected. The total annual soil loss in the investigated area did not decrease during the monitoring period, even though soil tillage practices have significantly changed toward soil conserving tillage methods. This could be due to weather fluctuations, obliterating the effect of tillage methods (Prasuhn, 2012). About 22% of the total eroded soil was transported directly or indirectly via road gullies to surface water (Prasuhn, 2011). Mosimann (2003) compared soil erosion in the Canton of Baseland of the years 1992 and 2002. He concluded that soil erosion tends to decrease thanks to the improved crop management and soil cultivation. But heavier agricultural machinery triggered soil compaction and thus the danger of runoff increased. Meusburger and Alewell (2008) found in the Urseren Valley, a valley in the Alps, an increase of landslide area of 92% within 45

1.3. CAUSES FOR BROWN TROUT DECLINE IN SWITZERLAND

years, likely due to land use change e.g., increased stocking number, and the increased intensity of torrential rain events.

In Switzerland, many rivers were straightened and canalized. This highly increased the sediment transport capacity, causing erosion of riverbed and riverbanks. As a consequence, steps were inserted to break down the riverbed slope and decrease the sediment load. The decreased sediment transport can, however, colmate the riverbed due to fine particles settling down during low flow velocity and less decolmation processes (Schälchli et al., 2005). Additionally, increased water infiltration above steps can cause higher fine sediment infiltration in the river gravel (Bucher, 2002). Residual flow reach below dams are also vulnerable for colmation due to the reduced discharge (Bucher, 2002). Finally, hydro-peaking below hydro-power plants can trigger river colmation since the production of hydro-power is connected with flushes with often very high SS concentrations (Baumann et al., 2012).

1.3 Causes for brown trout decline in Switzerland

Brown trout *salmo trutta* is one of the most common as well as an ecologically and economically highly important riverine fish species in Switzerland. They spawn in loose gravel riverbeds and require clean and well oxygenated river water. This makes brown trout a reliable indicator for the river condition in Switzerland (Fischnetz, 2004). Brown trout catches by anglers declined in Switzerland considerably since the 1980s by around 50%. Furthermore, an increase in fish diseases and organ damages has been observed in the catch. In the year 1998, the Swiss Federal Office for the Environment and the Swiss Federal Institute of Aquatic Science and Technology lanced a project called "Fischnetz" (network for declining fish yields in Switzerland) to assess this decrease of brown trout catches and population abundance, identify the most important causes, and develop possible solutions. All Swiss cantons joined the project. The project was concluded in the year 2003 (Fischnetz, 2004; Burkhardt-Holm, 2007). The decline in brown trout catches has been attributed to reduced fishing activities, to a change in stocking and to a decrease of brown trout populations (Fischnetz, 2004). More than one factor are likely contributing to this population decline and many factors are interrelated. Driving factors are insufficient spawning habitats and protection areas for adults and a lack of connections between habitats due to e.g., dams or high steps. Further, the proliferative kidney disease (PKD) can strongly effect brown trout populations locally. Its clinical outbreak is aggravated by confounding factors, such as increased river water temperature. Chemical pollutions in the river due to waste water treatment plants or diffuse inputs from agriculture or urban areas also effected brown trout negatively. But more data are needed for a clear conclusion (Fischnetz, 2004; Burkhardt-Holm and Scheurer, 2007).

Suspended fine sediments in rivers are probably not a main cause for the brown trout population decline. Measured suspended sediment concentrations in 12 rivers by the NADUF program were mostly below the critical threshold of 100 mg l^{-1} (Bucher, 2002). The abundance of young-of-the-year (YOY) brown trout assessed by electro fishing in 35 Swiss rivers and a total of 64 sites did, however, significantly correlate with the degree of colmation of the riverbed (Schager et al., 2007). The degree of colmation was assessed by estimating the force needed to "kick" in the riverbed and break up the sediment structure by feet (Schager and Peter, 2001). But high densities of YOY of over 2000 individual per

hectare were also assessed in some parts with medium or high colmation rates. This could potentially be a measuring bias since colmation was only assessed punctually and only during summer time and thus not during the spawning and egg incubation season (Bucher, 2002).

1.4 Aims and outline of the thesis

This PhD thesis was part of the interdisciplinary SNF project "Methodologies to measure and characterize fine sediment input to rivers and their effect on health and reproduction of gravel spawning brown trout". The project aimed to understand the complex interactions of sediment input and their effects on brown trout (Burkhardt-Holm et al., 2008). The project was built on the "biotic" and "abiotic part". The main objective of the "abiotic part" was to develop and optimize methods to assess fine sediment input in rivers and their impact on the abiotic environment. The used and developed methods and measurements can be roughly divided in methods to I) measure fine sediment input and II) assess the abiotic redd environment (Fig. 1.1). Investigations of brown trout survival were part of the "biological part" of the project and conducted by Christian Michel (Program MGU, University of Basel).

A comparisons of different methods to measure fine sediment loads and their application at three sites along the river Enziwigger can be found in chapter 2. The source areas of the captured suspended sediments were assessed by $^{13}\text{C}_{\text{tot}}$ and ^{15}N isotopes. The method and results are described in chapter 3. Chapter 4 assesses a new method to determine internal colmation of the riverbed, which is a consequence of the infiltrated sediment (Fig. 1.1).

Regional and local hydraulic settings can have a high influence on the redd environment. This is described in chapter 5. Chapter 6 focuses on the effects of fine sediments, redd morphology and the hyporheic flow regime on the oxygen concentration in the redds. A laboratory experiment to asses sediment oxygen demand of the redd substratum is shortly described in the Appendix. Finally, chapter 7 reports the effect of the measured abiotic factors on brown trout egg survival (Fig. 1.1).

1.5 Further scientific contributions within the thesis

Within the abiotic part of the project, three bachelor theses were conducted and successfully completed. Rudolf (2010) assessed the influence of precipitation and water level on sediment dynamics in the river Enziwigger. She could show an increase of suspended sediments with increasing water level and precipitation. Suspended sediment concentrations increased quickly if the total precipitation in the watershed raised above 11.4 mm per day or 21.5 mm per three days. Brun (2011) investigated the temporal and spatial dynamic of nitrate, ammonium and DOC and their impact on the oxygen concentration in redds. He could not show a correlation between nutrient and oxygen concentrations. Measured values are incorporated in Chap. 3. Liechti (2011) measured carbon and nitrogen isotopes of suspended sediments to determine their source areas. Her results are part of Chap. 3.

1.5. FURTHER SCIENTIFIC CONTRIBUTIONS WITHIN THE THESIS

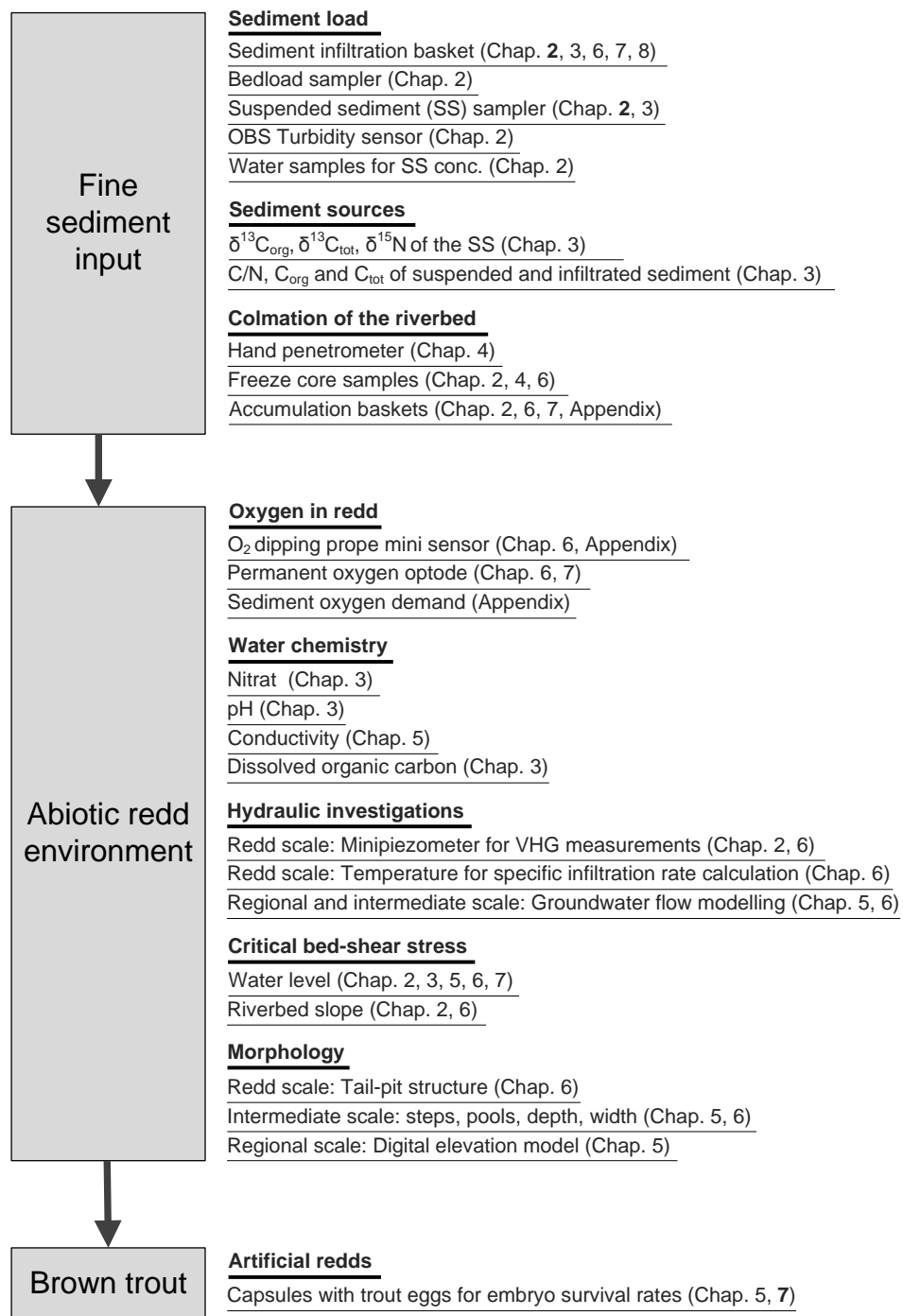


Figure 1.1: Used methods/measurements to assess fine sediment input, the abiotic redd environment and egg survival.

Chapter 2

Measurement of spatial and temporal fine sediment dynamics

This chapter is published as:

Schindler Wildhaber Y, Michel C, Burkhardt-Holm P, Bänninger D, Alewell C. Measurement of spatial and temporal fine sediment dynamics in a small river. Hydrol. Earth Syst. Sci. 16: 1501-1515, 2012.

2.1 Abstract

Empirical measurements on fine sediment dynamics and fine sediment infiltration and accumulation have been conducted worldwide, but it is difficult to compare the results because the applied methods differ widely. We compared common methods to capture temporal and spatial dynamics of suspended sediment (SS), fine sediment infiltration and accumulation and tested them for their suitability in a small, canalized river of the Swiss Plateau. Measurement suitability was assessed by data comparison, relation to hydrological data and in the context of previously published data. SS concentration and load were assessed by optical backscatter (OBS) sensors and SS samplers. The former exhibit a better temporal resolution, but were associated with calibration problems. Due to the relatively low cost and easy mounting of SS samplers, they can provide a higher spatial distribution in the river's cross section. The latter resulted in a better correlation between sediment infiltration and SS load assessed by SS samplers than SS concentrations measured with OBS sensors. Sediment infiltration baskets and bedload traps capture the temporal and spatial distribution of fine sediment infiltration. Data obtained by both methods were positively correlated with water level and SS. In contrast, accumulation baskets do not assess the temporal behaviour of fine sediment, but the net accumulation over a certain time period. Less fine sediment accumulated in upwelling zones and within areas of higher mean water level due to scouring of fine sediments. Even though SS and sediment infiltration assessed with the bedload traps increased from up- to downstream, less fine sediment accumulated downstream. This is probably also attributable to more scouring downstream.

2.2 Introduction

Fine sediment (<2 mm) load in rivers are generally increasing throughout the world in catchments that are impacted both directly and indirectly by human activities (Owens et al., 2005). Sediment supply in the alpine Rhine basin is estimated to increase between 220 % and 284 % by the year 2100 due to climate and land use change (Asselman et al., 2003). These observed and anticipated changes in fine sediment dynamics in rivers can provide a serious threat to aquatic ecosystems, including phytoplankton, aquatic invertebrates and fish (for a review see Bilotta and Brazier, 2008). Salmonid fish can be affected by suspended sediments (SS) in several ways. While SS can directly impact health and fitness of free swimming fish (Newcombe and Jensen, 1996), fine sediment deposition in the gravel bed can induce siltation of the riverbed resulting in a decrease in hydraulic conductivity (Schälchli, 1995). This affects the oxygen supply to the developing salmonid embryos in the redd negatively, which inhibits the incubation success (Greig et al., 2005). The consequences of climate and land use change on the transport of sediment into rivers, on sediment transport in the river and on clogging processes are poorly known. Studies for the Alps, pre-Alps and the hilly regions of the Swiss Plateau are rare. This includes small rivers, which are habitats for gravel spawning fish (Scheurer et al., 2009).

Several studies have shown a strong correlation between sediment deposition and the occurrence of fine sediment in the water column. Higher fine sediment load in rivers generally lead to increased fine sediment infiltration into the riverbed (Acornley and Sear, 1999; Zimmermann and Lapointe, 2005b), while periods of low flow and smaller SS concentration and load trigger low sediment infiltration rates with finer grain sizes (Sear, 1993; Soulsby et al., 2001b). Consequently, direct measurements of SS concentration and load may be a straight forward method to assess sediment deposition. The estimation of SS concentrations from turbidity measurements with optical backscatter (OBS) sensors depends on the content of fine particulate organic matter as well as grain size distribution of the SS and colour and shape of the grains (Packman et al., 1999). Accordingly, OBS turbidity measurements require calibration at individual test sites.

Deposition of fine sediments is not only controlled by SS concentration, but also by flow hydraulics and inter-gravel flow. These specific hydraulic conditions, influenced by the topography and the permeability of the riverbed, can have a large influence on sediment deposition (Brunke, 1999; Seydell et al., 2009). Seydell et al. (2009) found significantly higher fine sediment infiltration rates in downwelling zones than upwelling zones. Furthermore, sediment infiltration is dependent on flow velocity (Brunke, 1999). Rivers of the hilly regions of the Swiss Plateau and other regions in Europe are generally canalized and laterally stabilized by terraces for land drainage and flood control. These terraces lower the flow velocity and trigger downwelling processes upstream of the terraces, resulting in an increase of fine sediment infiltration (Bucher, 2002). Additionally, terraces may impede desiltation, i.e., processes that increase hydraulic conductivity attributable to higher bed-shear stress (Schälchli, 1995).

Numerous studies have been conducted on fine sediment dynamics and fine sediment infiltration and accumulation in Canada (e.g., Julien and Bergeron, 2006; Levasseur et al., 2006; Zimmermann and Lapointe, 2005b), the USA (e.g., Lisle and Lewis, 1992), and the United Kingdom (e.g., Greig et al., 2005; Heywood and Walling, 2007; Sear, 1993; Soulsby et al., 2001b). The results of those empirical studies of fine sediment infiltration rates are

2.3. MATERIALS AND METHODS

difficult to generalize mostly due to different measurement methodologies (Sear et al., 2008). Hence, there is a need to compare methodologies as well as data on sediment input and riverbed clogging to achieve a better comparability of results from different studies and to increase knowledge on the interaction between fine sediment dynamics and fine sediment infiltration and accumulation (Scheurer et al., 2009). The aim of this study was to I) compare results obtained by different methods used to capture temporal and spatial dynamics of suspended sediment and fine sediment infiltration and accumulation, II) test their suitability for a river in the Swiss Plateau, III) compare the results with hydrological data, and IV) compare the results with literature data. Because these questions are crucial for gravel spawning salmonid embryos, the study was conducted in artificial redds.

2.3 Materials and methods

2.3.1 Study site and general setup

The river Enziwigger is a small canalized river located near Willisau (Canton of Lucerne, Switzerland) with a total watershed area of about 31 km² (Fig. 2.1). The flow regime of the Enziwigger is not affected by hydro-power and no waste water treatment plant is located above Willisau. Like most rivers in the Swiss Plateau, its morphology is strongly modified: only 5% of the ecomorphology is close to natural or natural, 21% is little affected and 74% is strongly affected or even artificial, including terraces that have been inserted to prevent deep channel erosion and scouring of the bed during flood events (classified with the Swiss modular stepwise procedure for ecomorphology after Huette and Niederhauser, 1998; EBP-WSB-Agrofutura, 2005). In spite of these strong modifications its biological condition (classified with the macrozoobenthos module of the Swiss modular stepwise procedure; Stucki, 2010) is considered good (EBP-WSB-Agrofutura, 2005). The only fish species in the Enziwigger is the brown trout, *Salmo trutta* (EBP-WSB-Agrofutura, 2005).

The bedrock of the watershed consists of Upper Freshwater Molasse. The soil types are mainly (stagnic) Cambisol and Leptosol (classified according to WRB; IUSS, 2006). The mean annual temperature in Willisau is 8.5°C, with a mean annual rainfall of 1050 mm. Mean annual rainfall on the peak of the mountain Napf, where the river Enziwigger originates, is 1700 mm per year (1961–2007; data from MeteoSwiss). Discharge was measured in Willisau from November 2007 until November 2008 by the Canton of Lucerne. Mean discharge was 2.1 m³ s⁻¹, minimum discharge was 1.1 m³ s⁻¹, and maximum 10.1 m³ s⁻¹.

Measurements were set up in artificial salmonid redds located at three experimental sites along the river named A, B and C (from up- to downstream; Fig. 2.1) at altitudes of 757, 625 and 583 m above sea level (for site characteristics see Table 2.1). Each site was equipped with six artificial redds in places where natural brown trout redds had been mapped in November 2008. The locations of the redds are mostly consistent over years (Philip Amrein, fish warden of the Canton of Lucerne, personal communication, 2009). Data were assessed during two spawning seasons (Season 1: November 2009 to end of March 2010; Season 2: November 2010 to end of March 2011) in 18 artificial redds per year ($n_{\text{tot}} = 36$).

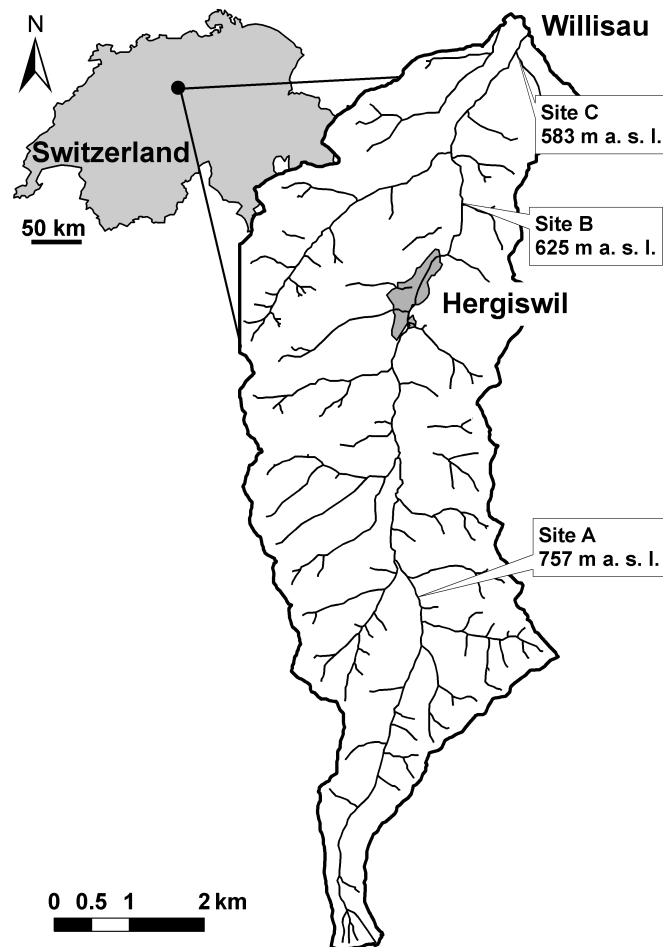


Figure 2.1: Watershed of the river Enziwigger with the three field sites A, B and C and the towns Willisau and Hergiswil (Canton of Lucerne, Switzerland).

2.3.2 OBS sensors and time integrated samplers to measure suspended sediment

Turbidity was measured continuously every 15 s during both field periods at each site with one optical back scatter (OBS) probe (Campbell Scientific, OBS-3+). The median from 40 measurements was logged every 10 min. The probes were mounted about 5 cm above the riverbed (about 20 cm depth during baseflow conditions). To calibrate the nephelometric turbidity unit (NTU) to suspended sediment concentration (SSC_{NTU}) in $mg\ l^{-1}$, water samples were taken every seven hours with an automatic water sampler (ISCO 6700, Isco Inc., USA). Because of freezing of the suction hose during the first field season, manual water samples were taken weekly during the second field season. The latter were complemented with samples collected by local habitants during storm events. Water samples were taken to the laboratory to assess the total SSC (see Sect. 2.3.7).

Time-integrated suspended sediment (SS) samplers following Phillips et al. (2000) were installed behind each redd and emptied at weekly intervals to determine the spatial variation of the SS load (Fig. 2.2A). The SS samplers were one meter long and consisted of

2.3. MATERIALS AND METHODS

Table 2.1: Site characteristics: D_{50} of the riverbed sediment was defined by freeze core samples and with line-number-analyses (Fehr, 1987). Data are given as mean \pm standard deviation.

Site	A	B	C
Altitude (m a.s.l.)	757	625	583
Watershed area (km ²)	5.5	22.6	28.9
Mean watershed slope (°) ^a	26.0	20.3	19.5
River slope at the site (°) ^b	5.0	1.5	1.4
River slope of riffle between 2 terraces (°)	0.27	0.24	0.23
D_{50} (freeze core) (mm)	20 \pm 4	19 \pm 6	16 \pm 1
D_{50} (line-nr-analysis) (mm)	25 \pm 8	25 \pm 4	16 \pm 4
Channel width (m)	3–3.5	4–4.5	4.5–5
Water depth above redds (cm)	10.9 \pm 3.9	23.2 \pm 6.0	20.9 \pm 7.9
Step length (m)	11–15	9–12	7–10
Mean bed shear stress above redds (Pa) ^c	5.0	9.5	8.2

^a Calculation based on the slope value for each pixel from a digital elevation model of the watershed.

^b Based on the slope value from a digital elevation model.

^c Calculated by the reach-average bed shear stress formula: $\tau_0 = \rho g R S$, where τ_0 is bed shear stress, ρ is water density, g is acceleration due to gravity, R is hydraulic radius at mean water level and S is the slope.

commercially available PE pipes with an outer diameter of 110 mm and a wall thickness of 4.2 mm. They were sealed with a plugged polyethylene funnel at the inlet and a cap at the outlet. An aluminum tube with an inner diameter of 4 mm was passed through the funnel and the cap as inlet and outlet. The SS samplers were mounted parallel to the riverbed at two upright steel bars driven into the channel bed, with the inlet tube pointing directly into the direction of the flow. The greater cross-sectional area of the main cylinder compared to that of the inlet tube reduces the flow velocity within the samplers by a factor of 600 relative to that of the ambient flow. This reduction in flow velocity induces sedimentation of the SS particles as the water moves through the cylinder towards the outlet tube (Phillips et al., 2000). The SS samplers collect a statistically representative sample under field conditions (Phillips et al., 2000).

2.3.3 Sediment baskets to measure fine sediment infiltration and accumulation

Fine sediment infiltration and accumulation was determined with sediment baskets (Fig. 2.2B; cf. Acornley and Sear, 1999; Heywood and Walling, 2007; Greig et al., 2005). They consisted of two baskets made of 20 \times 20 mm wire mesh with 2.5 mm wire and a solid bottom. The inner baskets had a diameter of 125 mm and were 160 mm deep. They were filled with riverbed sediment >4 mm to start with initial conditions without fine sediments. A second basket with a diameter of 150 mm was dug in the riverbed as a placeholder. A polyethylene bag with two long handles was placed around the inner baskets and stuffed between the two baskets. The bag was pulled over the inner basket during sampling to prevent loss of fine sediment during removal of the inner basket.

Each redd was equipped with two sediment baskets. One of them was emptied at weekly intervals to investigate the weekly fine sediment infiltration rates (= sediment infiltration

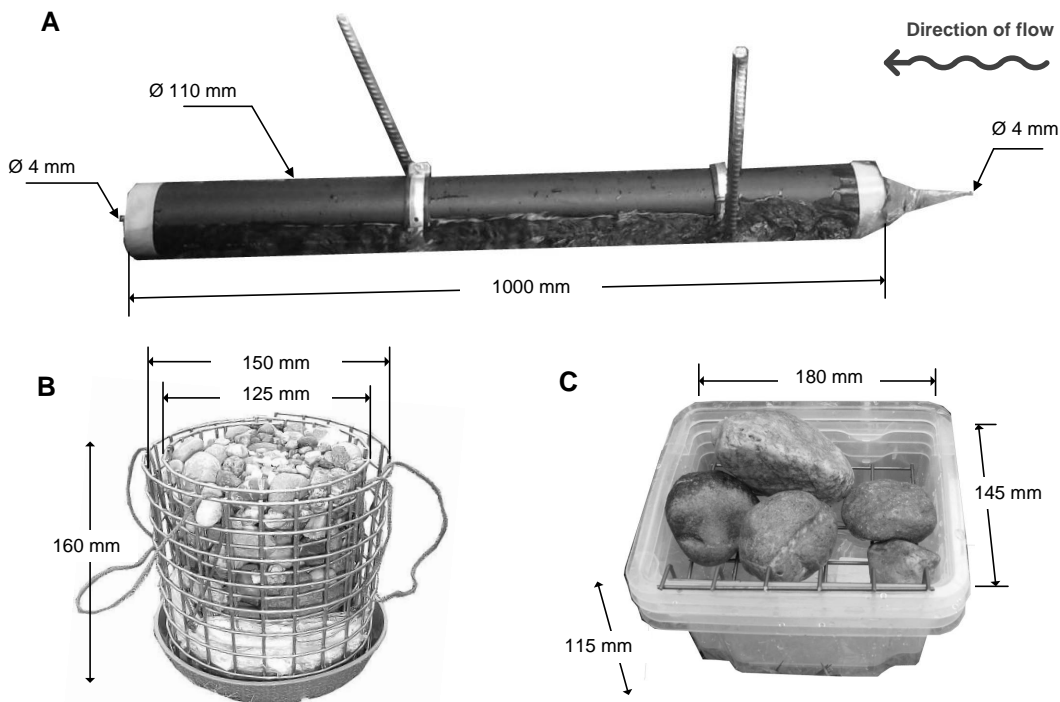


Figure 2.2: Devices used to measure fine sediment dynamics in the redds. (A): suspended sediment sampler, (B): sediment infiltration/accumulation basket, (C): bedload trap.

basket). The baskets' sediment was sieved with a 4 mm sieve and refilled with the same sediment during each sampling event. Sediment <4 mm was taken to the laboratory for grain size analyses. The second set of sediment baskets was emptied only at the end of the spawning season to assess the total net accumulation of fine sediment during the incubation period (= accumulation basket; Sear et al., 2008). During Season 1 (2009/2010) 10 of the initial 18 accumulation baskets were washed away at high flow. Two accumulation baskets in each redd were, therefore, installed during Season 2 (2010/2011).

2.3.4 Bedload traps to measure sediment transported along the bed

The volume of the described sediment infiltration baskets is small and most of the space within the trap is taken up by coarse bed material. Thus, these baskets can fill very quickly in situations where sediment loads are high, resulting in an underestimation of the sediment infiltration rate (Bond, 2002). Bedload traps similar to Bond (2002) were designed to overcome this problem. They consisted of two nestable $180 \times 145 \times 115$ mm dug boxes with a 25×25 mm wire lid, above which coarse bed material was placed to avoid resuspension of the settled material in the trap (Fig. 2.2C). To empty the box, it was covered by a lid and the inner box was removed. The coarse bed material above the trap caused turbulence; consequently, part of the settled fine sediment might not be material transported as bedload, but also as suspension. We still call the described traps "bedload samplers" to clearly distinct them from the sediment infiltration baskets and to

2.3. MATERIALS AND METHODS

use the same nomenclature as Bond (2002). During the first field season, each redd was equipped with one bedload trap, which was emptied weekly. No bedload traps were installed during the second field season.

2.3.5 Hydraulic conditions

The temporal dynamic of the water level at the three sites was measured every 15 s during both seasons with pressure transmitter probes (STS, Sensor Technik Sirmach, Switzerland). Average values were logged at 10 min intervals. The water level above each redd was measured weekly to assess its spatial and temporal variability within a site.

The vertical hydraulic gradient in the redds was measured weekly within mini piezometers designed after Baxter et al. (2003) and installed in the pit and tail of each redd. The piezometers had a length of 300 mm and consisted of a 25 mm diameter polypropylene (PP) pipe with an inner diameter of 21.4 mm. They were perforated with approximately 30 evenly spaced holes in the lower 160 mm and plugged at the bottom. The vertical hydraulic gradient is a unitless measure that is positive under upwelling conditions and negative under downwelling condition. It is calculated by the formula

$$\text{VHG} = \Delta h / \Delta l \quad (2.1)$$

where VHG is the vertical hydraulic gradient, Δh is the difference in head between the water level in the piezometer and the level of the stream surface and Δl is the depth from the streambed surface to the first opening in the piezometer sidewall (Baxter et al., 2003).

2.3.6 Freeze core samples

Freeze core samples were taken with a copped and plugged 400 mm diameter steel pipe. The pipe was pounded in the river sediment to a depth of approximately 350 mm and filled with liquid nitrogen. Freeze cores with a length of roughly 350 mm and a diameter of about 150 mm were removed and divided vertically in 100 mm wide layers. Sediment from the cores was taken to the laboratory, dried and sieved.

2.3.7 Sample analyses

The grain size distributions of the sediments were determined with the standardized sieve technique using sieves of different mesh sizes. Grains with a diameter $<32 \mu\text{m}$ were measured with a sedigraph (Micrometrics 100, Coulter Electronics, Germany). Grain size fractions were named according to the German soil taxonomy: Sand: $63 \mu\text{m}$ – 2mm , silt: $2 \mu\text{m}$ – $63 \mu\text{m}$ and clay: $<2 \mu\text{m}$ (Sponagel et al., 2005). Water samples for determination of suspended sediment concentrations were filtered through pre-weighed Whatman-filters with $11 \mu\text{m}$ pore diameter, dried at 40°C and weighed. Organic carbon concentration was measured with a CHN-Analyzer (Leco, USA).

2.4 Results and discussion

2.4.1 Suspended sediment

Turbidity measured by optical backscatter sensors

The calibration of NTU values to suspended sediment concentration (SSC_{NTU}) was difficult and associated with a high variance (Fig. 2.3). The calibration curve has an offset to the zero-point, indicating a systematic measurement error. Some general statements, however, were possible: SSC_{NTU} varied at all sites between 2 and 10 mg l^{-1} during low flow conditions and increased at high flow ranging from around 150 mg l^{-1} (site A) to around 300 mg l^{-1} (site C). Only small floods occurred during the second field season, resulting in significant smaller mean SSC_{NTU} at all sites with an overall mean of 17.0 mg l^{-1} compared to an overall mean of 42.7 mg l^{-1} during the first season (*t*-test, $p < 0.01$; Table 2.2). SSC_{NTU} increased significantly from upstream (site A) to the two downstream sites (B and C) during both seasons (ANOVA, $p < 0.01$; Table 2.2). The high mean SSC_{NTU} at site B for the second season might partly be related to measurement artifacts since the OBS sensor at this site was often shielded by leaves. Even though obvious outliers were excluded from the dataset, many high value data points remained in the dataset. These values could not be excluded with certainty, but might still be influenced by measurement artifacts.

The high temporal resolution in SSC_{NTU} data is an advantage of the OBS sensors. SSC_{NTU} increased rapidly with increasing water level at all sites and there is evidence of sediment exhaustion during the falling limb of flood events (Fig. 2.4). The observed simultaneous peaks in discharge and SSC_{NTU} correspond to the remobilization and transport of in-

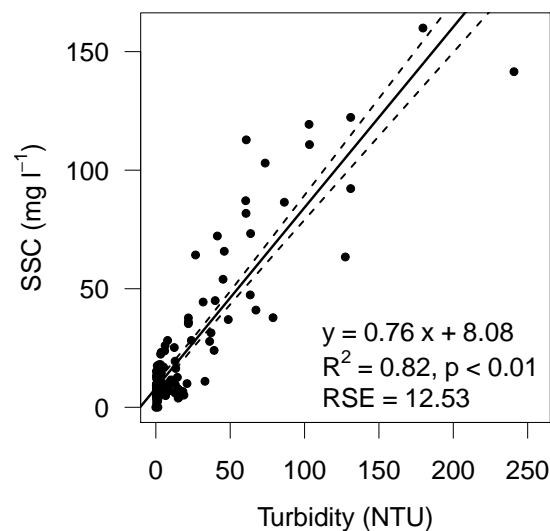


Figure 2.3: Correlation between turbidity in NTU and suspended sediment concentration (SSC). Dashed lines are the 95% confidence intervals; RSE = residual standard error (degree of freedom = 154)

2.4. RESULTS AND DISCUSSION

Table 2.2: Mean and standard deviation of suspended sediment concentration (SSC_{NTU}) measured with the OBS sensors and suspended sediment (SS) load caught by suspended sediment samplers at the three sites during the two field seasons.

Site	Field season 1 (2009/2010)		Field season 2 (2010/2011)	
	SSC_{NTU} ($mg\ l^{-1}$)	SS ($g\ week^{-1}$)	SSC_{NTU} ($mg\ l^{-1}$)	SS ($g\ week^{-1}$)
A	$28.0 \pm 37.8^{**}$	$14.4 \pm 3.5^*$	$12.9 \pm 7.6^{**}$	$7.0 \pm 1.7^{**}$
B	49.1 ± 56.5	16.8 ± 3.3	$21.4 \pm 12.8^*$	$11.5 \pm 0.4^*$
C	$54.9 \pm 62.8^*$	$20.3 \pm 2.5^{**}$	16.2 ± 23.3	11.2 ± 0.5
mean	42.7 ± 53.3	17.2 ± 3.9	17.0 ± 16.5	9.9 ± 2.3

Differences between seasons are highly significant for all sites and both measurement devices (*t*-test, $p < 0.01$).

* Differs significantly from the two other sites (ANOVA, $p < 0.05$).

** Differs highly significantly from the two other sites (ANOVA, $p < 0.01$).

channel sediments (e.g., Duvert et al., 2010). Although OBS sensors are widely used for turbidity measurements, their handling is an often underestimated problem (for a review see Downing, 2006). The most frequent problems with OBS sensors are their signal dependence on grain size distribution and on sediment composition (shape of particles) as well as algal growth on the sensor windows (Downing, 2006; Minella et al., 2008; Packman et al., 1999). An infinite number of combinations of sediment characteristics, including size, shape, mineral compositions and surface texture, is possible. Each combination produces a unique signal and each metre has a unique emitter-detector geometry that samples the signal in a particular way (Downing, 2006). NTU is consequently an arbitrary unit, incomparable to NTU measured at other times and places or with different turbidity metres (Downing, 2006). A calibration of NTU to SSC_{NTU} in $mg\ l^{-1}$ is necessary for the comparison to other studies. Measurement uncertainty is, however, introduced into the SSC_{NTU} data when converting NTU to SSC_{NTU} (Downing, 2006; Navratil et al., 2011).

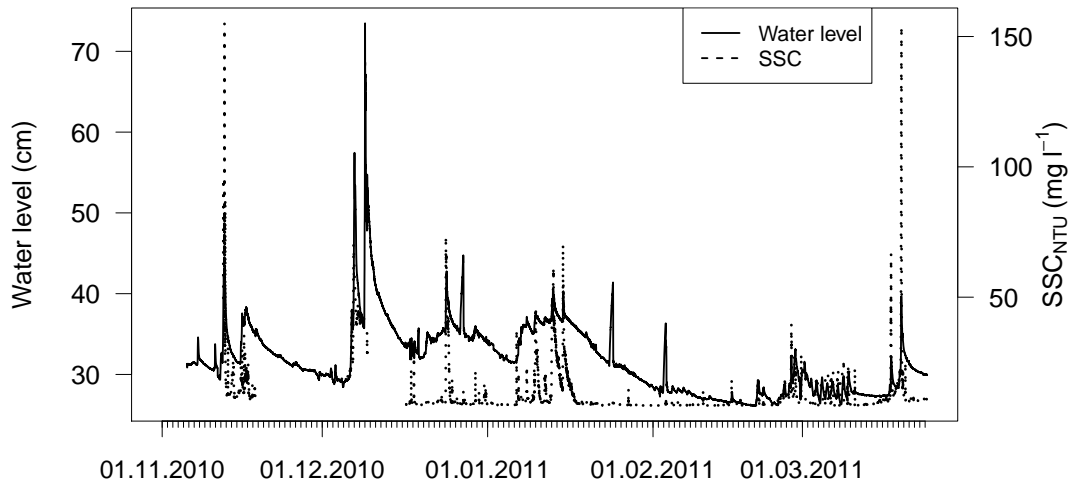


Figure 2.4: Example of the temporal variation of the suspended sediment concentration (SSC) and water level (Site A, Season 1).

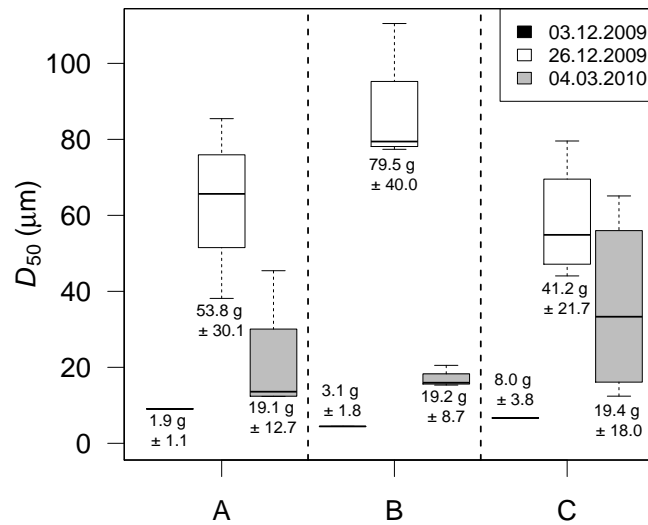


Figure 2.5: Weekly D_{50} of the suspended sediment (SS) caught by the SS samplers ($n = 6/\text{site}$) during three weeks at the three sites A, B and C. Mean total amount of SS load \pm standard deviation is given below/above the boxes. The 6 samples of 3rd of December 2009 had to be merged for grain size analysis because of the small quantity of SS.

Several problems with the OBS sensors were observed during the two field seasons. Drifting leaves were caught by the sensors in the fall months, resulting in abnormally high NTU values. This was particularly the case at site B during Season 2. More frequent checks at the field site, similar to the SS samplers (see below), could partly counterbalance this shortcoming. Moreover, freezing of the suction hose of the ISCO samplers during the winter interrupted sediment concentration sampling. Regular sediment concentration samples are, however, necessary for a good calibration. Finally, the D_{50} of the SS (50th percentile grain size diameter; data assessed by SS samplers, see below) fluctuated strongly during the field season with a minimum of $6.7 \mu\text{m}$ at low flow with low SSC_{NTU} and a maximum of $110.5 \mu\text{m}$ at high flow associated with high SSC_{NTU} (Fig. 2.5). The large effect of the change in grain size distribution on the OBS signal has been documented in numerous studies (for a review see Downing, 2006). Organic carbon concentrations of the suspended sediment were also highly variable with minimum values around 1.5% at high flow and maximum values around 10.5% at low flow. This change in organic carbon concentrations has again an influence on the conversion of NTU to SSC_{NTU} values (Downing, 2006).

Suspended sediment samplers

Results from the SS samplers paralleled the observations with the OBS sensors, showing significant higher SS loads during the first season than the second season (t -test, $p < 0.01$) and a SS increase from upstream to downstream (ANOVA, $p < 0.01$; Table 2.2). The SS loads captured during one week by the six SS samplers per site varied highly with coefficients of variation between 12 and 100%. This might represent the well known variation in suspended sediment concentration through the cross-section of rivers (Horowitz et al.,

2.4. RESULTS AND DISCUSSION

Table 2.3: Range or mean \pm standard deviation of infiltration rate (IR) of sediment < 2 mm in permeable sediment baskets.

Reference	Study site	IR ($\text{kg m}^{-2} \text{d}^{-1}$)	Sampling interval
This study	Enziwigger, LU, Switzerland	0.01–10.36	weekly
This study	Enziwigger, LU, Switzerland	0.21–0.70	4 month
Acornley and Sear (1999)	River Test, Hampshire, UK	0.02–1.00	monthly
Acornley and Sear (1999)	Wallop Brook, UK	0.04–0.40	monthly
Sear (1993)	North Tyne, Northumberland, UK	0.005–1.60	monthly
Seydell et al. (2009)	River Lahn, near Marburg, Germany	0.16 ± 0.07	two weeks interval
Zimmermann and Lapointe (2005b)	Cascapédia River, Québec, Canada	0.006–6.80	after suspension event

1990; Spreafico et al., 2005). The D_{50} of the SS varied highly across the channel and with time, again representing the variation of SS within a river both with low and high mean SS concentrations in the water column (Fig. 2.5). The described differences could also partly be attributable to instrumental biases.

The deposited sediments can be retained for further analyses of their composition, which is a major advantage of the SS samplers. In addition, the SS samplers can be installed in a relatively dense sampling network because they are inexpensive and easily fabricated. An installation at specific test sites, for example behind individual artificial redds, is possible. Thus, they can provide information about cross-sectional differences of SS loads and about the SS load at a specific test locations. Problems of this method include clogging of the inlet with leaves and the difficulty of placing the samplers horizontally with the inlet tube directly pointing into the flow direction. Consequently, distinguishing instrumental and sampling errors from spatial and temporal heterogeneity can be difficult. It is, therefore, suggested to closely monitor the samplers to ensure their proper performance, especially during fall when a large number of leaves drift in the river.

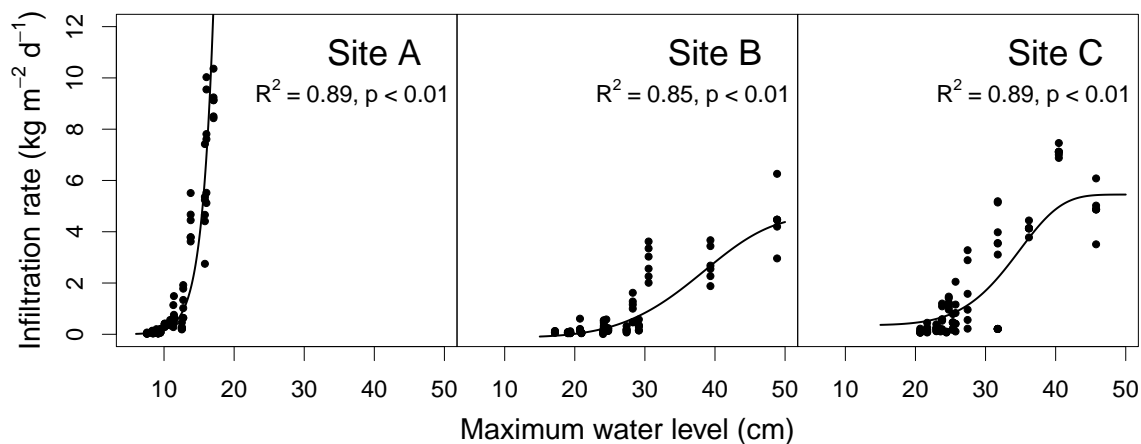
2.4.2 Sediment infiltration

A strong temporal variation of fine sediment infiltration with values ranging between $0.01 \text{ kg m}^{-2} \text{d}^{-1}$ during low flow conditions and $10.36 \text{ kg m}^{-2} \text{d}^{-1}$ during peak discharge was found (Table 2.3). Our results confirm the conclusions of previous field studies showing maximum fine sediment infiltration during peak discharge when sediment transport is high (Soulsby et al., 2001b; Zimmermann and Lapointe, 2005b; Acornley and Sear, 1999; Greig et al., 2005). At all sites, an exponential increase in sediment infiltration with increasing water level was found. Sediment infiltration rates below a certain water level threshold (site A: about 15 cm, site B and C: about 25 cm) were very small (Fig. 2.6). At

Table 2.4: Mean and range of daily sediment <2 mm infiltration rate (IR) during the two seasons at the three sites and of the coefficient of variation (CV) of the weekly values within the six samplers per site.

Site	Field season 1 (2009/2010)		Field season 2 (2010/2011)	
	IR (kg m ² day ⁻¹)	CV (%)	IR (kg m ² day ⁻¹)	CV (%)
A	1.67 (0.02–10.36)	32.9 (7.6–58.4)	0.68 (0.02–7.57)	31.1 (10.5–67.3)
B	1.29 (0.01–8.22)	40.6 (17.2–75.1)	0.62 (0.03–5.31)	27.5 (14.7–50.0)
C	1.55 (0.06–7.46)	38.3 (0–86.4)	0.66 (0.05–7.38)	48.7 (15.5–106.1)

Differences between seasons are significant for all sites (*t*-test, $p < 0.01$).
There are no significant differences between the sites (ANOVA).

**Figure 2.6:** Sediment infiltration rate in relation to the highest mean daily water level above the redds during the measurement week. The relationship at site B and C is described by a Weibull growth function.

site B and C, sediment infiltration reached a maximum at a water level around 45 cm. This indicates a saturation or equilibrium of input and scouring at higher water level. This equilibrium was never reached at site A, most likely due to an overall lower water level and, therefore, less scouring (Table 2.1, Fig. 2.6).

The sediment infiltration baskets were not filled with homogeneous gravel, but with riverbed gravel collected during redd construction; consequently, the D_{50} (27.1 ± 2.1 mm; note here and in the following all values are given as mean \pm sd) as well as the sorting coefficient ($SO = (D_{75}/D_{25})^{0.5}$; 1.6 ± 0.1) among the cleaned sediment baskets differed. Spearman rank correlation tests showed, however, that these differences had no influence on the amount of fine sediment infiltration ($p = 0.5$ and 0.2 respectively).

Sediment infiltration rates during the first season were significantly higher at all sites with a mean of 1.54 ± 0.24 kg m² day⁻¹ compared to the second season with a mean of 0.74 ± 0.21 kg m² day⁻¹ (*t*-test, $p < 0.01$). This is attributable to numerous high flows during the first field season. No significant differences of infiltration rates between the three sites were found (ANOVA, $p < 0.3$ – 0.8). The variation of sediment infiltration rates among infiltration baskets at each site was very high with coefficients of variation up to 100% (Table 2.4). The most likely explanation for these differences is the cross-channel

2.4. RESULTS AND DISCUSSION

variation due to the differences in flow velocity caused by bank roughness effects (Acornley and Sear, 1999).

Overall, the observed sediment infiltration rates are relatively high compared to other sediment infiltration studies conducted with sediment baskets (Table 2.3). These high sediment infiltration rates can partly be explained by the high input of fine sediment from the molasse bedrock in the catchment. Furthermore, the sampling was conducted at a higher frequency than in the other studies (Table 2.3). The efficiency of newly cleaned gravel in trapping fine sediments is at its maximum with initial conditions and decreases with time (Heywood and Walling, 2007). Hence, weekly sampled sediment baskets will yield higher daily means compared to monthly sampled baskets. Additionally, part of the deposited sediments might be washed out again. The difference between unequal sampling intervals can also be seen in the large discrepancy between the sediment infiltration rates calculated from the weekly obtained sediment infiltration data and those calculated from the accumulation baskets, which were only sampled at the end of the seasons after four months (Table 2.3). As such, quantitative comparisons of sediment infiltration rates from studies with different sampling intervals have to be done with caution.

Grain size analyses showed an increase of silt and clay with increasing fine sediment infiltration in absolute values (Fig. 2.7, left), but a decrease in relative values (i.e., fraction of silt and clay of the total fine sediment deposition; Fig. 2.7, right). During periods with low sediment infiltration rates, up to 94 % of the sediment consisted of sediment <0.25 mm; thus, sediments of a size most likely to be transported in suspension. This agrees with Acornley and Sear (1999) and Sear (1993). They found mainly sediment infiltration composed of sediments transported in suspension (<0.25 mm) during low flow and a greater proportion of sediments with a diameter between 0.25 and 4 mm during high flow. This fraction is large enough to be in intermittent contact with the bed, yet small enough to pass through small interstices of the weekly cleaned sediment infiltration baskets (Lisle, 1989).

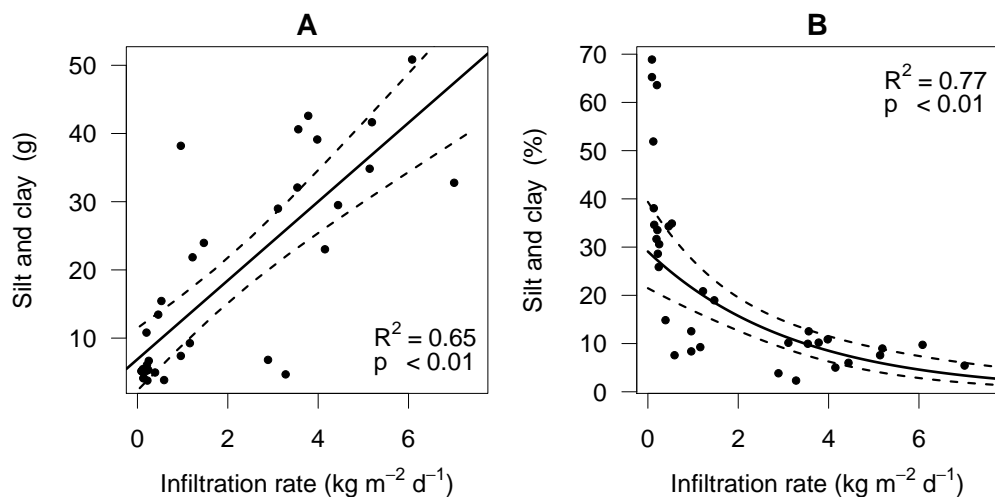


Figure 2.7: Weekly silt and clay infiltration at site C in absolute values (**A**) and relative values (i.e., fraction of silt and clay of the total fine sediment deposition; **B**) in relation to the daily infiltration rate of sediment <2 mm. Dashed lines are the 95 % confidence intervals.

Table 2.5: Mean values \pm standard deviation of the fraction of fine sediment (<2 mm) in the accumulation baskets and the fraction of sediment $<63 \mu\text{m}$ of the accumulated fine sediment during the two spawning seasons S1 (2009/2010) and S2 (2010/2011) and in freeze cores (FC) taken in winter 2008/2009 at the three sites.

Site	% <2 mm S1	% <2 mm S2	% <2 mm mean	% <2 mm in FC	% $<63 \mu\text{m}$ S1	% $<63 \mu\text{m}$ S2	% $<63 \mu\text{m}$ mean	% $<63 \mu\text{m}$ in FC
A	25.5 \pm 1.4** (<i>n</i> = 4)	18.0 \pm 3.3 (<i>n</i> = 10)	20.1 \pm 4.5* (<i>n</i> = 14)	13.6 \pm 4.1 ⁺⁺ (<i>n</i> = 6)	8.2 \pm 1.3 (<i>n</i> = 4)	11.3 \pm 2.1** (<i>n</i> = 10)	10.4 \pm 2.4 (<i>n</i> = 14)	5.1 \pm 1.7 ⁺⁺ (<i>n</i> = 6)
B	16.0 \pm 4.3 (<i>n</i> = 2)	20.1 \pm 4.4 (<i>n</i> = 4)	18.7 \pm 4.5 (<i>n</i> = 6)	13.3 \pm 4.5 (<i>n</i> = 6)	9.3 \pm 2.4 (<i>n</i> = 2)	7.0 \pm 1.0** (<i>n</i> = 4)	7.8 \pm 1.8 (<i>n</i> = 6)	4.8 \pm 1.1 ⁺ (<i>n</i> = 6)
C	15.4 \pm 3.3 (<i>n</i> = 2)	13.1 \pm 2.6 (<i>n</i> = 4)	13.9 \pm 2.8* (<i>n</i> = 6)	12.5 \pm 4.1 (<i>n</i> = 6)	13.8 \pm 4.1* (<i>n</i> = 2)	8.9 \pm 0.6 (<i>n</i> = 4)	10.5 \pm 3.1 (<i>n</i> = 6)	5.0 \pm 2.5 ⁺ (<i>n</i> = 6)

* Differs significantly from the two other sites (ANOVA, $p < 0.05$).

** Differs highly significantly from the two other sites (ANOVA, $p < 0.01$).

+ Differs significantly from the mean fraction of the accumulation baskets (t -test, $p < 0.05$).

++ Differs highly significantly from the mean fraction of the accumulation baskets (t -test, $p < 0.01$).

Sediment infiltration baskets do not represent natural conditions. Sediments <4 mm is removed in a regular interval, causing an overestimation of the real capacity of sediment infiltration occurring in the undisturbed riverbed. The suitability of the infiltration baskets strongly depends on the purpose of the research question. They are a quasi standardized method to obtain spatial and temporal differences of fine sediment infiltration or to assess the time needed for siltation of a freshly cut redd. To assess sediment infiltration rates close to natural conditions, Greig et al. (2005) assessed the temporal sediment accumulation by installing multiple small, porous infiltration pots. At each time step (2 weeks), two small pots were randomly removed. This allowed them to conduct seven measurements during the spawning period. Problems with this method are the possible spatial variability among the pots and the loss of pots at high flow (see Sect. 2.4.3). Another measurement strategy could consist of measuring sediment infiltration from week to week without removing the fine sediment trapped in the baskets, but this also does not represent true natural conditions, since the sediment structure would get disturbed while measuring the infiltrated sediment.

2.4.3 Sediment accumulation

The highest values for fine sediment accumulation over the two seasons were observed at site A, the most upstream site (ANOVA, $p < 0.05$). On average, 20.1 % of the sediment basket consisted of particles <2 mm at site A, 18.7% at site B and 13.9 % at site C (Table 2.5). The decrease in fine sediment accumulation downstream could be related to higher scouring of fine sediment down the stream due to the higher water level. Sediment accumulation at site B and C did not differ significantly between the two seasons (t -test, $p = 0.3$ and 0.5 respectively), despite the significant higher fine sediment infiltration during the first field season at all sites. Only at site A, significantly higher fine sediment accumulation rates were obtained during the first season (t -test, $p < 0.01$, Table 2.5). Consequently, downstream scouring of fine sediment seems to have a greater effect on sediment accumulation than SS load and sediment infiltration on sediment accumulation.

The sediment accumulation baskets were not filled with standardized gravel but with riverbed gravel to represent natural conditions. These differences in D_{50} as well as in

2.4. RESULTS AND DISCUSSION

Table 2.6: Fine sediment (<2 mm) and silt and clay (<63 μ m) accumulation in the accumulation baskets as % of the whole baskets and the silt and clay fraction of the sediment <2 mm. Range (mean) or mean \pm standard deviation.

Reference	Study site	<2 mm (%)	<63 μ m (%)	<63 μ m of <2 mm (%)
This study	Enziwigger, Lucerne	9.6–26.7 (18.3)	0.9–2.4 (1.7)	6.1–16.7 (9.8)
Greig et al. (2005)	River Test and Blackwater, Hampshire	10.0, 12.2		
Greig et al. (2005)	River Ithon and Aran, Wales	28.9, 15.7		
Heywood and Walling (2007)	Avon catchment, Hampshire	1.3–17.2		31 \pm 14
Levasseur et al. (2006)	Sainte Margerite River, Quebec	0.4–27 (13.2)	0.04–0.72 (0.16)	
Lisle (1989)	Coast Range of northern California			4.8–5.9
Julien and Bergeron (2006)	Sainte Margerite River, Quebec	3.3–29.2*	0.03 \pm 0.02–0.41 \pm 0.2	
Zimmermann and Lapointe (2005b)	Cascapédia River watershed, upper reaches; Québec	3.5–10		4–9

* Sediment <1 mm.

sorting coefficient of the accumulation baskets had no influence on the amount of sediment accumulation (Spearman rank correlation, $p = 0.5$).

Comparisons with other studies revealed similar rates of sediment accumulation to those reported in this study (Table 2.6). $90 \pm 2.6\%$ of the accumulated fine sediment was sand and $67 \pm 5.6\%$ had a diameter >0.25 mm. Thus, the size most likely carried in suspension (<0.25 mm) accounted for only 33 % of the sediment accumulated in the sediment basket. This is in the same range as found by Lisle (1989). During high flow the main component of the infiltrated sediment is in the bedload fraction (see Sect. 2.4.2). This fraction is deposited and accumulated at all depths down to the bottom of the basket as long as size distributions of transported sediment and the riverbed particles do not overlap (Lisle, 1989).

The fine sediment fraction (<2 mm) in the accumulation baskets was greater than in the riverbed sediment obtained by freeze core samples (Table 2.5). Because of the high variation among the accumulation baskets and among the freeze core samples, the differences were only significant at site A (t -test, $p < 0.01$). According to Zimmermann et al. (2005), these differences could reflect the influence of the effective size of the pore spaces available in the substrate on sediment infiltration. The overestimation of fine sediment in the baskets in this study could also be due to the small gap of about 4 mm between the inner and the outer sediment basket, in which the fine sediment (mainly in the bedload fraction) was able to infiltrate. This gap accounts for about 13 % of the volume of the

Table 2.7: Mean and range of daily bedload (BL) <2 mm, of the percentage of BL < 2 mm of the total BL and of the coefficient of variation (CV) of the weekly values within the six samplers at the three sites.

Site	BL < 2 mm (kg m ² d ⁻¹)	CV (%)	% < 2 mm of BL	CV % < 2 mm of BL (%)
A	1.93 (0.02–14.26)	72.0 (10.7–193.4)	73.8 (32.2–98.3)**	45.0 (0–86.6)
B	2.01 (0.01–10.80)	79.8 (0–183.2)	30.3 (4.0–60.6)*	64.2 (24.3–96.3)
C	2.24 (0.02–8.5)	61.9 (0–178.2)	58.7 (23.7–92.5)	27.5 (0–62.8)

* Differs significantly from the two other sites (ANOVA, $p < 0.05$).

** Differs highly significantly from the two other sites (ANOVA, $p < 0.01$).

inner baskets and was entirely filled with fine sediment at the end of the spawning season. The differences could also reflect an overestimation of the coarse fraction by freeze cores since individual pieces of coarse gravel and cobbles protruding out of the freeze cores can result in a smaller percentage of fine sediment of the sample (Young et al., 1991; Zimmermann et al., 2005).

Comparisons with the freeze core samples showed significantly higher silt and clay fractions of the total fine sediment in the accumulation baskets with 7.8 to 10.5 % compared to 4.8 to 5.1 % in the freeze core samples (t -test, $p < 0.05$; Table 2.5). This high fraction in the accumulation baskets is probably attributable to silt and clay particles which would have infiltrated to deeper layers in a natural environment. At the beginning of the measurement campaign, the sediment in the sediment baskets is comparable to a freshly cut redd. This cleaned gravel is vulnerable to deep infiltration by fines before a seal is formed during entrainment of the armor layer (Lisle, 1989). Sediments can only infiltrate to the bottom of the baskets. Freeze core data support this assumption indicating a significant higher silt and clay fraction at a depth of 10–20 cm and 20–30 cm with silt and clay content of $6.0 \pm 2.0\%$ and $6.3 \pm 2.5\%$, respectively, compared to the upper layer (0–10 cm) with a silt and clay content of $3.6 \pm 2.4\%$ (ANOVA, $p < 0.01$). The fraction of particles $< 63 \mu\text{m}$ of the accumulated sediment within a site and between the two seasons varied greatly (Table 2.5). Therefore, no general conclusions concerning the differences between the three sites and the two seasons can be drawn. The hydraulic differences within a site and the forming of a surface seal of sand (Lisle, 1989) influences the deposition and accumulation of silt and clay particles probably to a larger extent than their abundance in the water column. Silt and clay fractions assessed in other studies were also highly variable, making a comparison difficult (Table 2.6).

2.4.4 Fine sediment transported along the bed

Mean sediment caught by the bedload samplers increased along the river from $1.93 \text{ kg m}^2 \text{ d}^{-1}$ at site A to $2.24 \text{ kg m}^2 \text{ d}^{-1}$ at site C (Table 2.7). This pattern parallels the data from the SS samplers and OBS sensors and could be related to an increasing shear stress attributable to higher water levels down the stream or/and to a higher input of fine sediments from the arable corn fields in the lower part of the catchment.

At all sites, bedload rates were very small until a certain water level (data not shown).

2.4. RESULTS AND DISCUSSION

Above this level, bedload increased exponentially with increasing water level. This matches the pattern we found with the sediment infiltration baskets (Fig. 2.6).

The percentage of fines in the total captured bedload was highest at site A (ANOVA, $p < 0.01$). This is probably also attributable to the low water level compared to the other two sites and the relatively small slope due to the frequent artificial terraces, resulting in lower shear stress (Table 2.1). The fraction of the bedload smaller than 2 mm decreased with higher water level and total bedload (Spearman rank correlation, $p < 0.01$; Table 2.8).

Bedload rates and the percentage of fine sediment of the total bedload caught by the six bedload samplers varied highly per site (Table 2.7). This variations can be partly accounted for by cross-channel differences also observed in the SS load, sediment infiltration and accumulation data. The higher coefficients of variation of the bedload data compared to the other methods is likely explained by (i) the variation in precision in placing the traps flush with the sediment surface. If the border of the trap is not flush with the bed, fine sediment transported along the bed was not trapped and (ii) the turbulence caused by the coarse bed material above the trap, which differs between traps and triggers different trapping efficiencies.

In total 26 bedload traps were lost at the 18 research plots during the first field season. Thus, on average, at every sampling spot the traps were lost 1.5 times. Hence, we found that a major disadvantage of the bedload samplers is their big contact surface, making them more susceptible to scouring at high discharge. For those reasons, no bedload traps were installed during the second field season.

2.4.5 Comparison of the different methods

SS samplers and OBS turbidity sensors

Results clearly suggest that both the SS samplers and the OBS turbidity sensors are suitable to capture large scale spatial and temporal variations in suspended sediment concentrations or loads (Table 2.2). The two methods revealed a significant increase in suspended sediment (both SS load and SS concentration) along the river and significantly higher suspended sediment in the 2009/1010 season than the 2010/2011 season. Similarly, both methods showed a significantly positive Spearman correlation between SS and water level (Table 2.8). The weak correlation between SSC_{NTU} and water level at site B was probably related to measurement problems with the OBS sensor due to leaves caught by the sensor (see Sect. 2.4.1). Even though the methods differ in their quantitative results, correlation analysis showed a significant correlation between SS load caught by the sampler during one week and the average SSC_{NTU} that week (Table 2.8).

The advantage of the SS samplers is their relatively low cost and their easy mounting, making a high spatial distribution across the channel possible. Therefore, the correlation between SS loads obtained with the SS samplers and the sediment infiltration rate was better than the correlation between SSC_{NTU} assessed by OBS sensors and the sediment infiltration rates (Table 2.8). SS sampler data are positively correlated to fine sediment infiltration (Table 2.8, Fig. 2.8). At a deposition of about 40 kg m^{-2} , saturation or equilibrium of input and scouring was reached at site B and C. At site A, deposition increased until about 60 kg m^{-2} . This can be explained by less scouring at site A attributable to lower

Table 2.8: Spearman rank correlation coefficients (ρ) between the measured parameters of both seasons for the three sites with mean weekly SS_{NTU} measured with OBS sensors, total weekly suspended sediment (SS) load measured by SS samplers, daily fine sediment infiltration rate, fine sediment accumulation, daily bedload of fine sediment, the percentage of fine sediment of the total bedload, highest mean daily water level of a week and vertical hydraulic gradient (VHG). The accumulation baskets were correlated with the mean values of the parameters during the whole field seasons. The sample size (n) is given in parentheses.

	SS	Infiltration	Accu.	Bedload	Bedload (%)	Water level	VHG
SS_{NTU} ($mg\ l^{-1}$)	0.8 (212)**	0.8 (218)**	0.8 (14)**	0.7 (104)**	-0.4 (104)**	0.7 (196)**	0.2 (131)*
	0.2 (204)*	0.2 (204)**	0.2 (6)	-0.4 (96)*	0.1 (96)	0.2 (204)**	0.1 (121)
	0.7 (204)**	0.5 (204)**	0.6 (6)	0.8 (90)**	-0.5 (90)**	0.9 (180)**	0.2 (90)
SS ($g\ week^{-1}$)		0.9 (212)**	0.8 (14)**	0.8 (104)**	-0.4 (104)**	0.6 (212)**	0.3 (131)**
		0.9 (204)**	-0.4 (6)	0.8 (96)**	-0.4 (96)**	0.8 (204)**	0.4 (121)**
		0.8 (204)**	0.8 (6)	0.8 (90)**	-0.5 (90)**	0.8 (204)**	0.2 (90)
Infiltration ($kg\ m^2\ d^{-1}$)			0.6 (14)*	0.9 (104)**	-0.4 (104)**	0.7 (218)**	0.3 (131)**
			0.0 (6)	0.8 (96)**	-0.5 (96)**	0.8 (204)**	0.4 (121)**
			0.3 (6)	0.9 (90)**	-0.6 (90)**	0.6 (204)**	0.0 (90)
Accu.(% <2 mm)				- (4)	- (4)	-0.6 (14)*	-0.3 (14)
				- (2)	- (2)	0.1 (6)	-0.6 (6)
				- (2)	- (2)	-0.2 (6)	-0.1 (6)
Bedload ($kg\ m^2\ d^{-1}$)					-0.4 (104)**	0.9 (104)**	0.2 (57)
					-0.4 (96)**	0.7 (96)**	0.2 (39)
					-0.6 (90)**	0.8 (90)**	0.0 (35)
Bedload (% < 2mm)						-0.5 (104)**	0.1 (57)
						-0.2 (96)*	0.1 (39)
						-0.6 (90)**	-0.2 (35)
Water level(cm)							0.1 (131)
							0.4 (121)**
							0.2 (90)

* $p < 0.05$.

** $p < 0.01$.

water levels. OBS data are only weakly correlated with sediment infiltration (Table 2.8) probably due to the cross channel differences in SS or measurement biases discussed earlier. Cross channel differences cannot be assessed with only one point measurement of SS_{NTU} per site. Certainly, a higher cross channel resolution could also be obtained by mounting multiple OBS sensors across the channel. But the installation of the sensors across the channel could be quite difficult and would also be connected with high costs.

Sediment infiltration baskets and bedload traps

Fine sediment infiltration rates measured with the sediment baskets correlated significantly with sediment transported as bedload measured with the bedload traps (Table 2.8). A nonlinear regression (saturation curve) describes the observed relationship best (Fig. 2.9, left). Values above a sediment infiltration rate of $2\ kg\ m^{-2}\ d^{-1}$ are highly variable, probably attributable to higher scouring. While sediment infiltration baskets reach a saturation around $10\ kg\ m^{-2}\ d^{-1}$, bedload traps can capture sediments until about $15\ kg\ m^{-2}\ d^{-1}$ because of their large volume (Fig. 2.9, left). Consequently, sediment

2.4. RESULTS AND DISCUSSION

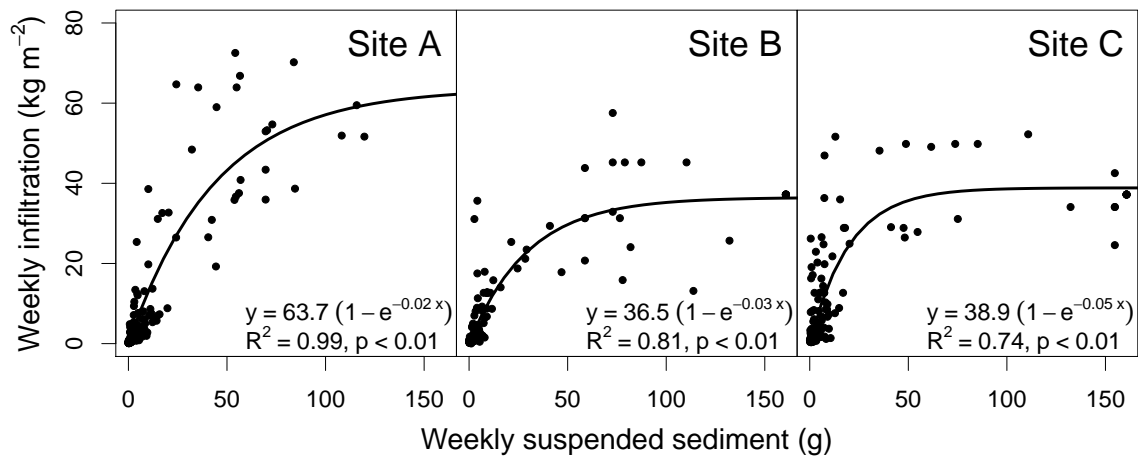


Figure 2.8: Weekly sediment infiltration in relation to the total weekly SS load assessed with SS samplers at the three sites. R^2 and p of the nonlinear regressions were calculated after Gail et al. (2009).

infiltration baskets are filled very quickly at high water level if not emptied in short enough intervals.

Results suggest a linear relationship of the data with smaller sediment infiltration rates (0 to $2 \text{ kg m}^{-2} \text{ d}^{-1}$; Fig. 2.9, right). According to Bond (2002), sediment infiltration is governed primarily by sediment supply or transport rates until the point when interstitial spaces become clogged with fine sediments. The data from this study support this statement qualitatively (see Sect. 2.4.2 and the highly significant correlation between both water level and SS load with sediment infiltration rates as well as with bedload rates, Table 2.8). The sediment infiltration rates are, however, almost twice the bedload until the mentioned level at a sediment infiltration rate of $2 \text{ kg m}^{-2} \text{ d}^{-1}$ (Fig. 2.9, right). This is probably attributable to an instrumental bias of the bedload samplers. According to Bond (2002), trapping efficiency of the bedload traps is lower for the silt and fine sand ($<0.25 \text{ mm}$) fractions (only 20–40 % at some sites). During low sediment infiltration rates, this fraction accounted for most of the infiltrated sediments (Fig. 2.7). In contrast to the sediment infiltration baskets, where infiltrated sediments are caught in a matrix of coarse sediment, fines can be easier washed out of bedload traps. A closer assessment of the differences in trapping efficiency of the sediment infiltration baskets and the bedload traps can only be accomplished under well defined conditions in a stream channel.

Sediment caught by bedload traps is mainly dependent on the water level and SS load. Because of the solid wall of the traps, the vertical hydraulic gradient has no influence on this process (Table 2.8). In contrast, less fine sediment infiltration was expected with a positive vertical hydraulic gradient (= upwelling) in the sediment infiltration baskets. This has been shown in previous studies (Brunke, 1999; Seydell et al., 2009). This relationship, however, was not observed in this study: at sites A and B, fine sediment infiltration was slightly higher in upwelling zones compared to downwelling zones (Table 2.8). This is likely attributable to the high variability of hydrological exchange processes (e.g., Brunke and Gonser, 1997). The vertical hydraulic gradient measurements represent only

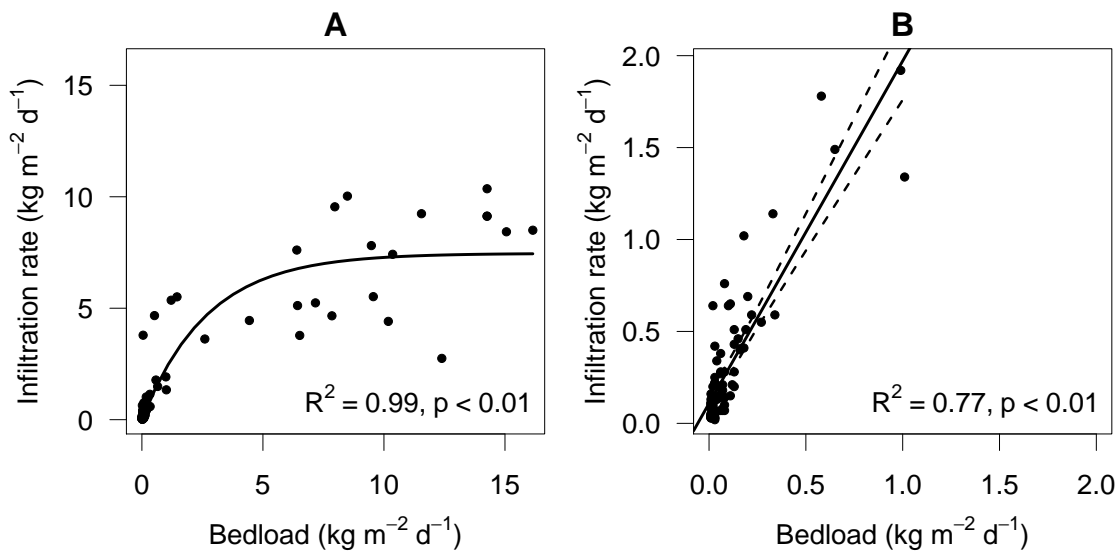


Figure 2.9: Relationship between infiltration rate of fine sediment measured with sediment baskets and bedload measured with bedload traps at site A. **(A):** all data with a nonlinear regression line, R^2 and p were calculated after Gail et al. (2009); **(B):** linear regression for data with infiltration rates smaller $2 \text{ kg m}^{-2} \text{ d}^{-1}$, dashed lines are the 95 % confidence intervals.

the specific hydraulic conditions at a certain time while sediment infiltration was measured over a week with possible changing vertical hydraulic gradients.

Multiple regression analyses for sediment infiltration as response variable with SS load (measured by SS sampler), SSC_{NTU} , bedload, water level and vertical hydraulic gradient as explanatory variables were conducted. SS load as single explanatory variable was the best predictor for sediment infiltration at all sites. Due to the equilibration or saturation of sediment infiltration, the sediment infiltration rate is best described by a nonlinear regression model (Fig. 2.8). As such, the strong correlation between sediment infiltration and the occurrence of fine sediment in the water column found in other studies (Acornley and Sear, 1999; Zimmermann and Lapointe, 2005b) could be confirmed.

Sediment accumulation baskets

Only a small number of accumulation baskets resisted the flood; consequently, only a small data set across the two field seasons was available (site A: $n = 14$, site B: $n = 6$, site C: $n = 6$). This makes statistical analyses difficult and only general conclusions concerning the net fine sediment accumulation are possible (see Sect. 2.4.3). Fine sediment accumulation decreased from upstream to downstream, i.e., from site A to site C. In contrast, SS concentration and load and bedload increased from upstream to downstream, while fine sediment infiltration did not differ significantly between the sites. This is probably attributable to the higher resuspension and scouring of fines downstream due to higher water level, resulting in higher SS concentration and bedload, but smaller net sediment infiltration and accumulation.

Spearman rank analyses between sediment accumulation and other methods are only feasible at site A, which has the largest dataset. These analyses indicate a positive corre-

2.5. CONCLUSION

lation between accumulated fine sediment and mean SS load ($\rho = 0.8, p < 0.01$) as well as mean infiltration of fines ($\rho = 0.6, p < 0.05$; Table 2.8).

Higher mean water levels above the accumulation baskets lead to resuspension of fine sediment, resulting in a negative Spearman rank correlation between water level and sediment accumulation ($\rho = -0.6, p < 0.05$; Table 2.8). A smaller amount of fine sediment accumulation in plots with higher water level and flow velocity compared to plots with lower water level was reported previously (e.g., Acornley and Sear, 1999; Levasseur et al., 2006). Finally, multiple linear regression analyses with SS load and vertical hydraulic gradient (VHG) as explanatory variables indicate less sediment accumulation in upwelling zones than in downwelling zones:

$$\text{Accumulation} = 14.2 + 0.6 \times \text{SS} - 21.5 \times \text{VHG}, \quad R^2 = 0.7, p < 0.05 \quad (2.2)$$

The results of Seydell et al. (2009) support these findings. They even noted that subsurface flow patterns have a larger influence on sediment deposition than the suspended sediment concentration in the river. Due to cross correlations between the mentioned dependent variables (Table 2.8), other multiple regressions are not possible.

2.5 Conclusion

We compared different methods to capture temporal and spatial dynamics of suspended sediment (SS), fine sediment infiltration and accumulation. These methods were correlated and tested for their suitability for a river in the Swiss Plateau. A comparison to other studies as well as a cross-comparison between methods indicated a general agreement between the methods. All methods are, however, connected with some instrumental and sampling errors, which can not always be distinguished from spatial heterogeneity in the river. This calls for laboratory tests to assess the instrumental biases under controlled hydraulic and sediment conditions.

Methods to capture SS (OBS sensors and SS samplers) indicate big spatial and temporal differences in SS. OBS data have a higher temporal resolution. SS samplers can provide important information on the composition of SS and a better spatial distribution can be achieved because of their relatively low construction cost. Due to the dense sampling network the correlation between SS load collected with SS samplers and sediment infiltration rate was better than between sediment infiltration rate and SSC_{NTU} assessed by a single OBS sensor per site.

Sediment infiltration baskets are a quasi standardized method to obtain spatial and temporal differences of fine sediment infiltration but do not represent natural conditions. Sediment $<4\text{mm}$ are removed at regular intervals, causing an overestimation of the real capacity of sediment infiltration in an undisturbed riverbed. Sediment infiltration is mainly governed by water level and SS concentration. A major hydrological event can result in a total siltation of the sediment infiltration baskets. With higher water levels, scouring increases, resulting in an equilibrium between SS input and scouring. Bedload traps have a larger volume than sediment infiltration baskets, but they are associated with other problems as the difficulty to dig them flush into the riverbed. Furthermore, they are susceptible to scouring at high flows due to their large contact surface. We con-

clude that sediment infiltration baskets are better suited for a highly dynamic canalized river of the Swiss Plateau.

Sediment accumulation baskets do not assess the temporal behaviour of fine sediment infiltration but the accumulation over a certain time period. The loss of baskets at high flow generated the biggest problem associated with the accumulation baskets. They can not be renewed as their purpose is the assessment of accumulation during the entire field period. Additionally, they overestimate the fine sediment proportion. Differences in the effective size of the pore spaces, the gap between the inner and the outer sediment baskets or the solid bottom of the baskets are possible reasons for this overestimation. Less fine sediment accumulates in upwelling zones and with a higher mean water level due to scouring. Even though SS concentration and load and sediment assessed with the bedload traps increased from up- to downstream, less fine sediment accumulated downstream. This was probably due to more scouring downstream.

Acknowledgments This study was funded by the Swiss national foundation (SNF K-32K1-32K1-120486). We would like to thank Nicolas Gratiot and the RIVER team, Dirk de Boer, an anonymous reviewer and the editor Ilja van Meerveld for the constructive comments. They were a great help to improve the manuscript. We thank Annina Gysel, Sandra Rudolf and Bastian Brun for their help in the field, Philipp Amrein and Sepp Lustenberger for support during the field work, Marianne Caroni and Ruth Strunk for laboratory assistance and Claude Schneider for technical support.

Chapter 3

Organic matter dynamics and stable isotopes to trace SS source areas

This chapter is published as:

Schindler Wildhaber Y, Liechti R, Alewell C. Organic matter dynamics and stable isotope signature as tracers of the sources of suspended sediment. *Biogeosciences*, 9: 1985-1996, 2012.

3.1 Abstract

Suspended sediment (SS) and organic matter in rivers can harm brown trout *Salmo trutta* by affecting the health and fitness of free swimming fish and by causing siltation of the riverbed. The temporal and spatial dynamics of sediment, carbon (C), and nitrogen (N) during the brown trout spawning season in a small river of the Swiss Plateau were assessed and C isotopes as well as the C/N atomic ratio were used to distinguish autochthonous and allochthonous sources of organic matter in SS loads. The visual basic program *IsoSource* with $^{13}\text{C}_{\text{tot}}$ and ^{15}N as input isotopes was used to quantify the temporal and spatial sources of SS. Organic matter concentrations in the infiltrated and suspended sediment were highest during low flow periods with small sediment loads and lowest during high flow periods with high sediment loads. Peak values in nitrate and dissolved organic C were measured during high flow and high rainfall, probably due to leaching from pasture and arable land. The organic matter was of allochthonous sources as indicated by the C/N atomic ratio and $\delta^{13}\text{C}_{\text{org}}$. Organic matter in SS increased from up- to downstream due to an increase of pasture and arable land downstream of the river. The mean fraction of SS originating from upper watershed riverbed sediment decreased from up to downstream and increased during high flow at all measuring sites along the course of the river. During base flow conditions, the major sources of SS are pasture, forest and arable land. The latter increased during rainy and warmer winter periods, most likely because both triggered snow melt and thus erosion. The measured increase in DOC and nitrate concentrations during high flow support these modeling results. Enhanced soil erosion processes on pasture and arable land are expected with increasing heavy rain events and less snow during winter seasons due to climate change. Consequently, SS and organic matter in the river will increase, which will possibly affect brown trout negatively.

3.2 Introduction

All streams carry some suspended sediment (SS) under natural conditions (Ryan, 1991). An increase of SS due to anthropogenic perturbation, however, has been observed in the last decades (e.g., Owens et al., 2005). Perturbation includes forestry, pasture and agricultural activities, which enhance soil erosion processes and hence the sediment delivery into rivers (e.g., Pimentel and Kounang, 1998). In addition, it is expected that the frequency and intensity of heavy rain events in middle Europe will increase due to climate change (IPPC, 2007), enhancing soil erosion triggered by water. According to model calculations, the sediment supply from the Alpine region into the Rhine basin, for example, is expected to increase by about 250 % (Asselman et al., 2003). Increasing SS loads in rivers generally lead to a higher fine sediment infiltration rate in the riverbed gravel (Greig et al., 2005; Zimmermann and Lapointe, 2005b; Schindler Wildhaber et al., 2012b). SS and fine sediment infiltration (SI) can provide a serious threat to aquatic ecosystems including phytoplankton, aquatic invertebrates, and salmonid fish (for a review see Bilotta and Brazier, 2008). Salmonid fish can be affected by SS in several ways. Their eggs develop in so-called redds, a shallow depression created by the female brown trout, where eggs and sperms are deposited. The female covers the fertilized eggs with gravel. While SS can directly impact health and fitness of free swimming fish (Newcombe and Jensen, 1996), fine sediment infiltration in redds can induce siltation of the gravel resulting in a decrease in hydraulic conductivity (Schälchli, 1995). This affects the oxygen supply to the developing salmonid embryos in redds negatively, and hence their survival (Greig et al., 2005, 2007a; Heywood and Walling, 2007). The presence of high organic matter in the IS and interstitial water can have additionally disproportionately impact on spawning habits (Greig et al., 2005). As respiration is strongly dependent on the availability of organic matter, oxygen demand within riverbeds will increase as the pool of organic matter increases (for a review see Greig et al., 2007b). Organic material is derived either from in-stream sources (autochthonous), for example macrophyte vegetation or from external sources (allochthonous), for example leaf litter or runoff from agricultural fields (Sear et al., 2008).

Schindler Wildhaber et al. (2012b) reported in a study on sediment dynamics in a small Swiss headwater river of the Swiss Plateau with a native brown trout *Salmo trutta* population increasing SS loads and concentrations from up- to downstream (Chap. 2). This finding could be related to an increased shear stress attributable to a higher water level down the stream and/or to a higher fine sediment input from the arable land in the lower part of the catchment. Furthermore, organic carbon concentrations of the SS were found to be highly variable with minimum values around 1.5 % at high flow and maximum values around 10.5 % at low flow (Schindler Wildhaber et al., 2012b, Chap. 2).

An identification of SS source areas is required to improve site management and possibly restrain the described negative consequences for brown trouts. Sediment tracer-based methods have been used to distinguish possible sources in watersheds. Stable carbon (C) and nitrogen (N) isotopes as well as the carbon to nitrogen atomic ratio (C/N_a) have been found to be reliable tracers in recent studies (Onstad et al., 2000; McConnachie and Peticrew, 2006; Fox and Papanicolaou, 2007; Gao et al., 2007; Fox et al., 2010). Stable isotope compositions as well as C/N_a are affected by many factors including soil depth, vegetation, climate and cultural history (Kendall, 1998). By assessing the ratio of ¹³C to

3.3. MATERIALS AND METHODS

^{12}C , ^{15}N to ^{14}N and Ca to Na in the SS as well as in surface soils of the catchment, conclusions concerning possible SS origin can be drawn. The isotopic compositions of SS samples may represent a mixture of potential sources. The proportional contributions of different sources can be assessed by linear mixing models. The disadvantage of these models is generally the limitation in detecting potential sources by the number of isotope tracers. With n isotope tracers, $n + 1$ potential sources can be detected. The model is mathematically under-determined if the number of potential sources exceeds $n + 1$, resulting in an equation system with less equations than unknown variables and therefore no single solution is possible (Phillips and Gregg, 2001). Phillips and Gregg (2003) developed a visual basic program called *IsoSource* to assess potential source contributions if more than $n + 1$ sources are present. The program examines in small increment steps all possible combinations of each source contribution, resulting in several feasible solutions. This program was used in this study to quantify source contributions to SS during the brown trout spawning season.

The objective of this study was I) to assess the temporal and spatial C and N dynamics during the brown trout spawning season in suspended and infiltrated sediments and river as well as interstitial water, II) the use of C_{org} isotopes as well as C/Na to distinguish autochthonous and allochthonous sources of the organic matter in the SS, and III) the use of C_{tot} and N isotopes as tracers to quantify the sources of SS with respect to time and space.

3.3 Materials and methods

3.3.1 Study site and general setup

The river Enziwigger is a small canalized river located near Willisau, Canton of Lucerne, Switzerland with a total watershed area of about 31 km² (Fig. 3.1). The flow regime of the Enziwigger is not affected by hydro-power facilities and there is no waste water treatment plant located above Willisau. Like most rivers in the Swiss Plateau, its morphology is strongly modified: Only 5% is close to natural or natural, 21% is little affected and 74% is strongly affected or even artificial, including terraces that have been inserted to prevent deep channel erosion and scouring of the bed during flood events (classified with the Swiss modular stepwise procedure for ecomorphology after Huette and Niederhauser, 1998; EBP-WSB-Agrofutura, 2005).

The bedrock of the watershed consists of Upper Freshwater Molasse. The soil types are mainly (stagnic) Cambisols and Leptosols (classified according to WRB; IUSS, 2006). The mean annual temperature in Willisau is 8.5 °C with a mean annual rainfall of 1050 mm. Mean annual rainfall on the peak of the mountain Napf, where the river Enziwigger originates, is 1700 mm per year (1961–2007; data from MeteoSwiss).

SS, IS and water samples were collected at three sites named A, B and C; from up- to downstream (Fig. 3.1) during the brown trout spawning season from November 2009 to end of March 2010. The sites had an altitude of 757, 625 and 583 m above sea level. For more information regarding the characteristics of the river and the three sites, see (Schindler Wildhaber et al., 2012b, Chap. 2).

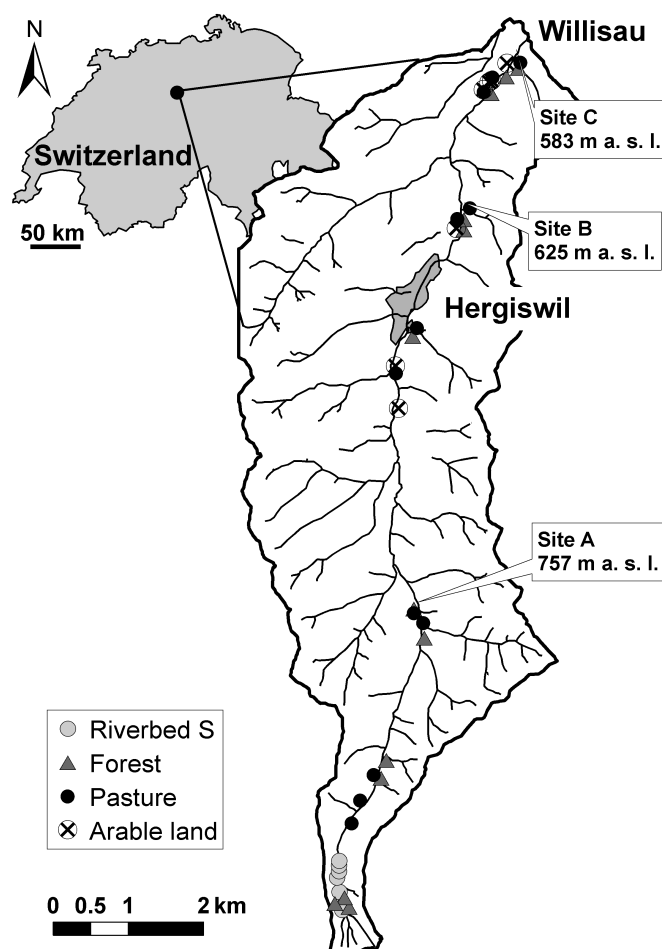


Figure 3.1: Watershed of the river Enziwigger with the three field sites A, B and C including their altitude, soil sample spots and the towns Willisau and Hergiswil (Canton of Lucerne, Switzerland).

Sample collection

SS were sampled with 6 time-integrated SS samplers at each site following Phillips et al. (2000). The aperture of the SS samplers were about 60–70 mm above the riverbed. IS samples were collected in 6 sediment baskets per site. SS samplers and sediment baskets were both emptied in a weekly interval. The basket's sediment was sieved with a 4 mm sieve and the basket refilled with the remaining coarse sediment during each sampling event. Sediments <4 mm were taken to the laboratory for further analyses. The term infiltrated sediment (IS) refers to the total sediment <2 mm infiltrated during one week in the sediment basket and suspended sediment (SS) refers to the total amount of sediment caught during one week in the SS samplers. For a detailed description and discussion of the used methods for SS and IS see Schindler Wildhaber et al. (2012b) (Chap. 2).

Interstitial water samples for dissolved organic carbon (DOC) and nitrate analyses were obtained in approximately two week intervals in 12 mini piezometers per site. The mini piezometers were 300 mm deep and perforated in the lower 160 mm. They were de-

3.3. MATERIALS AND METHODS

signed after Baxter et al. (2003) and are described in detail in Schindler Wildhaber et al. (2012b)(Chap. 2). The interstitial water samples represent the water at the depth of the buried eggs in natural redds. Water samples were filtered in the field with $0.45 \mu\text{m}$ filters and laboratory analyses were conducted the following day. Soil samples for isotope and organic matter analyses were collected in forest, pasture and arable land with erosion evidences (Fig. 3.1). Soil profiles were determined at each sampling spot to ensure sampling of representative areas. In total, 40 topsoil samples of the watershed were analyzed. Additionally, an algae sample of each site, six manure samples close to site B and C, and 5 riverbed sediment samples from the upper most accessible reach of the river were collected. No surface water ran at the upper most accessible reach of the river during dry periods, which allowed sediment sampling with a simple corer. It is assumed that these sediments represent mainly the original bedrock molasse. Downstream riverbed sediments were not sampled, as those samples would possibly represent a mixture of the other four sources. Source samples that are not independent would complicate the modeling results.

Water level at the three sites was measured every 15 s with pressure transmitter probes (STS Sensore Technik, Sirmach) and logged at 10 min intervals. Air temperature und precipitation was measured near site B at the town Hergiswil (Fig. 3.1) by a private company (KELAG Künzli Elektonik AG) in 5 min intervals on behalf of the Canton of Lucerne. Air temperature for site A and C was calculated from these data by assuming an increase of mean air temperature by 0.6°C per 100 m in altitude (Leser et al., 2005).

Sample analyses

Soil and sediment samples were dried at 40°C . Grain size distributions of the IS and SS were assessed with the standardized sieve techniques, grains with a diameter $<32 \mu\text{m}$ with a sedigraph (Micrometrics 100, Coulter Electronics, Germany). Grain size fractions were classified according to the German soil taxonomy: Clay: $<2 \mu\text{m}$, silt: $2\text{--}63 \mu\text{m}$ and sand: $63 \mu\text{m}\text{--}2 \text{mm}$ (Sponagel et al., 2005). Organic and total carbon (C_{org} and C_{tot}) of the IS was measured by a Leco RC612 multiphase analyzer. C_{org} , C_{tot} , total nitrogen (TN) and C and N isotopes of SS and soil samples were measured with a continuous flow isotope ratio mass spectrometer (Thermo Finnigan, Germany) in line with a FLASH Elemental Analyzer 1112 (Thermo Finnigan, Italy) following standard processing techniques. For C_{org} analyses, inorganic carbon was eliminated with HCl vapor. Stable isotope ratios are reported as δ values per mil (‰) as: $\delta X = [(R_{\text{sample}}/R_{\text{standard}}) - 1] \times 1000$ where X is ^{13}C or ^{15}N and $R = ^{13}\text{C}/^{12}\text{C}$ or $^{15}\text{N}/^{14}\text{N}$. Standard reference materials are PDB limestone for C and air for N. The samples were corrected to internal standards EDTA ($\delta^{13}\text{C} = -30.3\text{‰}$, $\delta^{15}\text{N} = -1.1\text{‰}$) and AO-1, ammonium oxalate ($\delta^{13}\text{C} = -17.0\text{‰}$ and $\delta^{15}\text{N} = 32.7\text{‰}$). The precision reported for $\delta^{13}\text{C}$ and $\delta^{15}\text{N}$ analyzes was 0.1‰ . DOC was measured with a TOC-Analyzer 5000A (Shimadzu Corporation), nitrate with an ion chromatograph with a Metrosep A Supp 5 column (Metrohm AG).

Data interpretation

Differences between two groups of data were tested with the Student's *t*-test. ANOVA was performed to determine significant differences between three or more groups. The

relationship between a response variable and a possible predictor variable was assessed by linear regression models, backward stepwise linear regression models were used with several possible predictor variables. Relationships of data which were not normally distributed were tested with the Spearman rank correlation test. Significance level for all statistical analyses was set at 0.05.

The visual basic program *IsoSource* was used to quantify soil and sediment source contribution to SS (Phillips and Gregg, 2003). This program is available free at <http://www.epa.gov/wed/pages/models/stableIsotopes/isosource/isosource.htm> and has been successfully applied in different studies (e.g., Phillips et al., 2005; Gibbs, 2008; Phillips and Gregg, 2003). The program examines all possible combinations of each source contribution (0–100 %) in user-defined increment steps. Combinations that sum up to the measured isotopic compositions within a specified tolerance are considered to be feasible solutions from which the range of potential source contributions can be determined. Reporting the mean of the feasible solutions would only lead to misinterpretation of the results since every feasible solution may be the correct one (Phillips and Gregg, 2003). Thus, the means of the possible solutions with standard deviations are reported in this study. Source increments of 1 % and mass balance tolerance levels of $\pm 0.1\text{‰}$ were defined. In few cases, where no solution was found with these defaults, mass balance tolerance level was set to 1 ‰.

3.4 Results and discussion

3.4.1 Spatial and temporal dynamics of C_{org} in sediments and of DOC

C_{org} concentrations of the IS samples were significantly smallest at the upstream site A (mean = $1.7 \pm 1.3\%$). The highest mean C_{org} concentration in IS was found at site B ($3.0 \pm 2.5\%$). IS at the most downstream site C had a mean C_{org} concentration of $2.3 \pm 1.8\%$ (Table 3.1). Overall, the assessed C_{org} concentrations of the IS are relatively low. Sear et al. (2008) reported in a review organic matter concentrations of infiltrated fine sediment from 13 rivers in Europe. Concentrations ranged from 3.4 % to 24.5 % with a mean of 13 %. Heywood and Walling (2007) measured 15 % C_{org} in infiltrated fine sediment.

C_{org} concentration of the SS showed a similar spatial pattern as C_{org} concentration of the IS: the smallest concentrations were assessed at site A with a mean of 5.1 %, site B and C had significant higher concentrations with means of 6.6 and 6.5 %, respectively (Table 3.1). Again, these concentrations are relatively low. Acornley and Sear (1999) assessed 25 to 40 % C_{org} in the SS during low flows in summer and 15 to 20 % during high flows in autumn in two rivers in Hampshire, England, which were also brown trout spawning habitats. The relatively low C_{org} concentrations could partly be due to an instrumental bias of the SS samplers. Phillips et al. (2000) reported that SS samplers underestimate smallest SS particles to some extent. This would also include the light weighted organic material. They concluded, however, that the mean grain size does not statistically differ from point samples and that SS samplers collect statistically representative samples. The weekly assessed C_{org} concentrations of the SS are about four times higher than the concentrations in IS. This is probably due to the low specific gravity of organic material, holding it longer in suspension than inorganic material (Sear et al., 2008). The degrada-

3.4. RESULTS AND DISCUSSION

Table 3.1: Mean values and standard deviation at the three sites sampled of organic and inorganic carbon (C_{org} and C_{inorg}) in infiltrated sediment (IS) and suspended sediment (SS), dissolved organic carbon (DOC) in the river and the interstitial (int.), total nitrogen (TN) in IS and SS, nitrate in the river and interstitial, C/Na, $\delta^{13}C_{org}$, $\delta^{13}C_{tot}$ and $\delta^{15}N$ of SS. The sample numbers are given in parentheses.

	Site A	Site B	Site C
C_{org} IS (%)	1.7 ± 1.3 (29)*	3.0 ± 2.5 (30)*	2.3 ± 1.8 (27)
C_{inorg} IS (%)	2.1 ± 0.4 (29)	2.4 ± 0.8 (30)	2.1 ± 0.9 (27)
C_{org} SS (%)	5.1 ± 1.9 (29)	6.6 ± 2.7 (16)	6.5 ± 1.7 (27)
C_{inorg} SS (%)	2.1 ± 0.3 (29)	2.3 ± 0.7 (16)	2.0 ± 0.4 (27)
DOC river (mg l ⁻¹)	2.1 ± 0.6 (6)	1.8 ± 0.8 (7)	3.2 ± 1.7 (7)*
DOC int. (mg l ⁻¹)	2.0 ± 0.6 (36)*	2.5 ± 1.1 (27)	2.5 ± 1.0 (29)
TN IS (%)	0.2 ± 0.1 (17)	0.2 ± 0.2 (15)	0.2 ± 0.1 (14)
TN SS (%)	0.4 ± 0.1 (18)*	0.5 ± 0.3 (16)	0.5 ± 0.2 (12)
Nitrate river (mg l ⁻¹)	5.2 ± 0.7 (7)*	8.9 ± 0.6 (7)*	9.0 ± 1.2 (7)*
Nitrate int. (mg l ⁻¹)	4.9 ± 0.6 (34)*	8.9 ± 0.5 (27)*	9.0 ± 0.6 (29)*
C/N atomic IS	14.2 ± 2.0 (17)	16.8 ± 3.7 (15)	14.8 ± 2.9 (14)
C/N atomic SS	16.7 ± 2.1 (18)	15.3 ± 3.1 (16)	15.8 ± 2.1 (12)
$\delta^{13}C_{org}$ SS (‰)	-28.0 ± 0.5 (18)	-28.1 ± 0.9 (16)	-27.8 ± 0.9 (15)
$\delta^{13}C_{tot}$ SS (‰)	-20.1 ± 2.8 (18)*	-21.8 ± 2.6 (16)	-22.9 ± 3.0 (12)*
$\delta^{15}N$ SS (‰)	-0.4 ± 0.9 (18)*	2.0 ± 1.1 (16)*	1.8 ± 0.6 (12)

* Differs significantly from the two other sites (ANOVA, $p < 0.05$).

tion of C_{org} is considered to be negligible (see Sect. 3.4.3). The increase of C_{org} in IS and SS from up to downstream can be explained by the higher percentage of agriculturally exploited land downstream of the watershed. Site A is surrounded by forest and pasture, while dominant land use at site B and C are arable farm land and pasture, which were both regularly manured.

C_{org} concentrations and the total amount of IS and SS showed remarkable inverse dynamics (Fig. 3.2A, B). IS and SS generally increased with increasing water levels. C_{org} concentrations in IS and SS showed a significant inverse relationship with water level and total IS and SS (Fig. 3.3A, B). Lowest C_{org} concentrations in IS (about 0.1 %) were measured during high flows in January and peak concentrations during base flows in February (about 6 to 8 %; Fig. 3.2A). Minimum C_{org} concentrations of the SS were also measured in January and were around 1.5 % and maximum at the end of February with concentrations around 10 % (Figs. 3.2B and 3.3B). A decrease of particulate organic carbon with increasing SS is reported in studies worldwide (Onstad et al., 2000; Meybeck, 1982; Gao et al., 2007; Zhang et al., 2009). The pattern can be explained by a dilution of C_{org} during high sediment loads with mineral matter derived from terrigenous soil erosion or remobilizing of mineral matter of the riverbed (Zhang et al., 2009). C_{org} has a very low specific gravity holding it longer in suspension than inorganic material, thus during base flow, the C_{org} proportion increases compared to heavier inorganic material. The significant relationship between the concentration of C_{org} in IS and SS and the silt and clay fraction (sediment $< 63 \mu m$) of IS and SS support this assumption (Fig. 3.3C). Silt and clay are also held in suspension more easily than sediment in the sand fraction.

It is assumed that the concentrations of C_{org} in the IS and SS are low enough that they do not have negative effects on the developing brown trout embryos in the river Enziwigger.

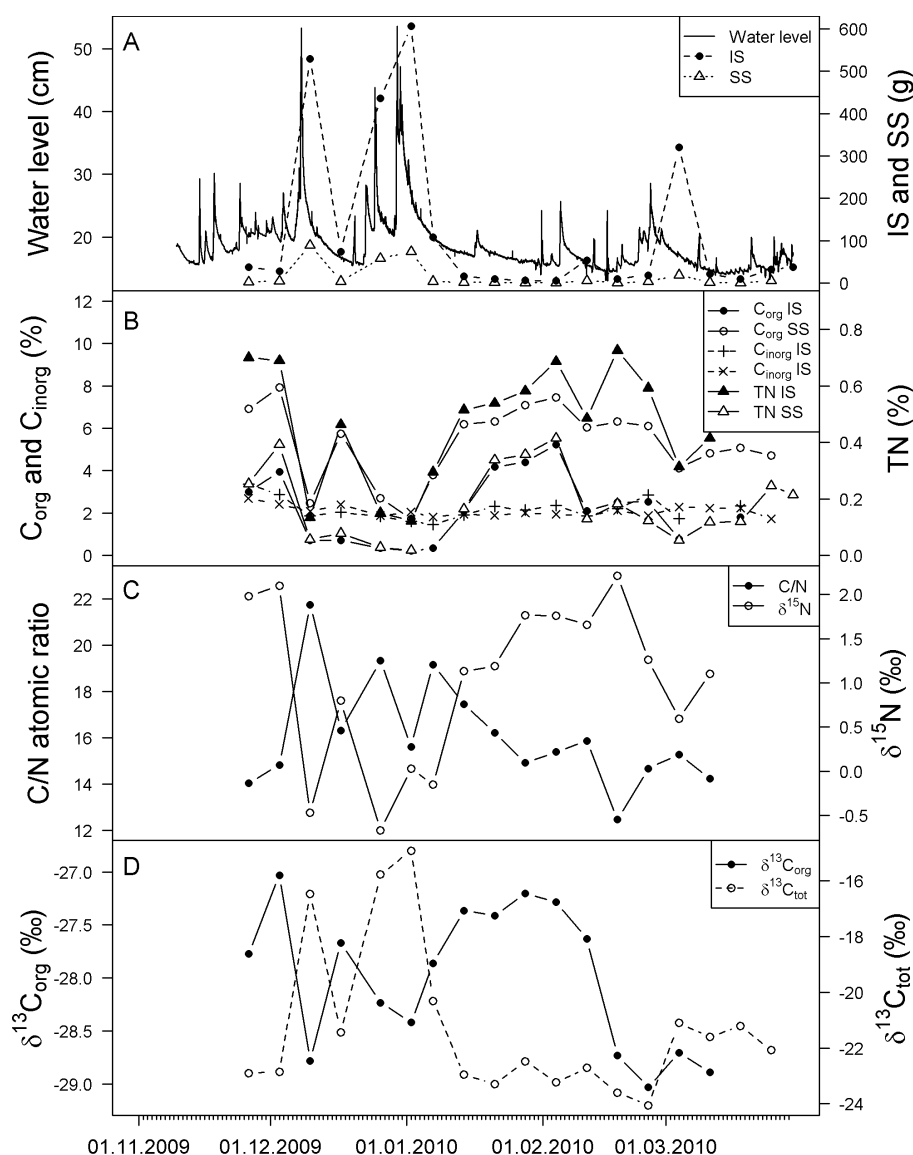


Figure 3.2: Sediment, nutrient and isotope composition dynamics during the field period. Plotted are mean values of all samples from all three sites. **(A)** Water level at site B, the weekly infiltration of sediment <2 mm (IS) and the weekly suspended sediment (SS); **(B)** C_{org} and TN of IS and SS; **(C)** C/N_{a} and $\delta^{15}N$ of SS; **(D)** $\delta^{13}C$ of C_{org} and C_{tot} of the SS.

Only during long periods of low flow with enhanced C_{org} concentrations in the SS and IS, C_{org} might induce a negative environments for the brown trout embryos. A high concentration of C_{org} can additionally block interstitial pore spaces, reduce gravel permeability and promote the growth of biofilms, leading to a decrease of oxygen availability (Greig et al., 2005).

The mean values of the measured DOC concentrations of the river and interstitial water samples were around 2 mg l^{-1} at all sites (Table 3.1). No significant differences in DOC concentrations in the river water and the interstitial water close to the brown trout eggs

3.4. RESULTS AND DISCUSSION

were assessed. DOC values around 2 mg l^{-1} represent a good mean water quality during the measured winter period in terms of DOC classified with the Swiss modular stepwise procedure for chemistry (Liechti, 2010). DOC values of the measured samples at site A never exceeded 4 mg l^{-1} ; thus, they were always in the category “good water quality” (Liechti, 2010). DOC values in river and interstitial water at site B and C exceeded 4 mg l^{-1} at three out of seven sampling dates. This indicates a “moderate” water quality in terms of DOC (Liechti, 2010). One of these relatively high values was assessed at the beginning of December during a high flow following strong precipitation. During heavy precipitation, previously unsaturated layers of the soil and river channel get connected to the drainage network. This delivers further carbon to the stream as new sources of DOC in upper organic soil horizons are assessed with rising water tables (Dawson et al., 2010). Otherwise, DOC can also be exported with near-surface soil runoff and/or overland flow generated during the storm event (Inamdar et al., 2004). DOC values $>4 \text{ mg l}^{-1}$ were also measured in February during low flow conditions but with relatively high temperature (mean daily temperature around 5°C), which followed a cold period with mean temperature below freezing point. Biological activity might have been increased due to the higher temperature, resulting in an increase of DOC (Dawson et al., 2008) or DOC is flushed out from arable land to the river through infiltrating melt water (Hornberger et al., 1994).

3.4.2 Spatial and temporal dynamics of TN in sediments and of nitrate

TN increased similar to C_{org} from the upstream site A to the two downstream sites B and C (Table 3.1), most probably due to the increased sediment input from manured arable land and pasture. The increase of TN in the SS from site A with a mean of 0.4 % to site B and C with means around 0.5 % was significant (Table 3.1). The percentage of TN in SS was about 4 times higher than in the IS, thus showing the same pattern as C_{org} . The temporal dynamic of TN concentrations of IS and SS showed the same characteristics as the C_{org} dynamic (Fig. 3.2B): low levels at high discharge and high sediment yield and high levels at low discharge and low sediment yields (see previous section for explanation of this pattern). Overall, a highly significant relationship between TN and C_{org} concentration of captured sediments was found (Fig. 3.3D). The linear regressions between C_{org} and TN gives a y -intercept for IS of $0.09 (\pm 0.08)$ and for SS of 1.0 ± 0.2 (Fig. 3.3D). These small intercepts indicate mainly organic TN in these samples (Onstad et al., 2000).

Nitrate concentrations in the river and the interstitial water increased significantly from site A with a mean of 5.2 and 4.9 mg l^{-1} , respectively, to site B and C with means for river and interstitial water of 8.9 and 9.0 mg l^{-1} (Table 3.1). Nitrate concentrations for the two arable sites B and C did not differ significantly. A nitrate concentration below 5.6 mg l^{-1} represents a “good” water quality with respect to nitrate according to the Swiss modular stepwise procedure for chemistry (Liechti, 2010). All but one measurement at site A was below this threshold concentration. The only sample exceeding this concentration was taken at high flow. This indicates nitrate leaching during high flow from the nearby pasture. Nitrogen leaching during storm events was described by other authors (e.g., Inamdar et al., 2004; Wagner et al., 2008). All samples at site B and C exceeded the concentration of 5.6 mg l^{-1} and two and three out of seven samples, respectively, even exceeded 8.4 mg l^{-1} . 8.4 mg l^{-1} is set as threshold concentration between the category

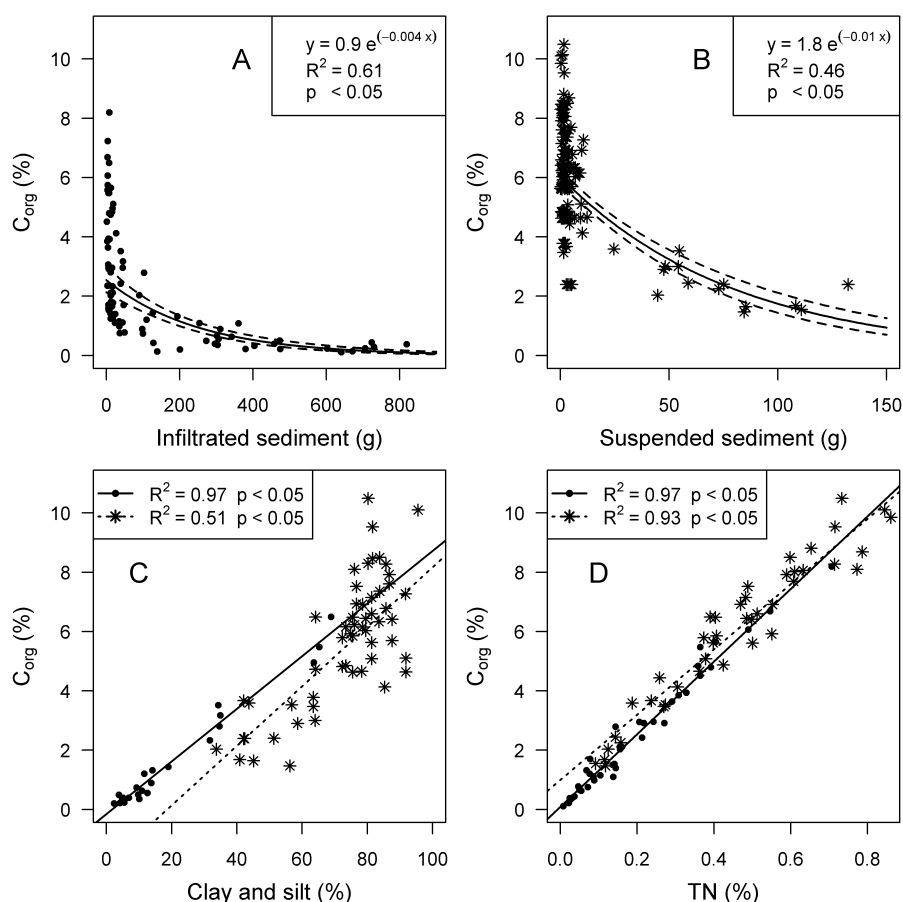


Figure 3.3: Relationship between C_{org} and (A) total IS <2 mm; (B) total SS; (C) clay and silt fraction of sediment <2 mm and (D) TN. Solid circles and solid lines: Infiltrated sediment, stars and dotted lines: SS. Dashed lines in (A) and (B) are the 95% confidence intervals.

“moderate” and “unsatisfying” water quality in terms of nitrate (Liechti, 2010). Thus, the nitrate concentrations of the river and interstitial water are too high, which is most probably due to manuring of the arable land and pasture at the two downstream sites. Nitrate concentrations in the interstitial water at the depth of brown trout eggs were not significantly different from nitrate concentrations in the river water. The lack of chemical gradients might indicate strong river water flux to the brown trout eggs (Malcolm et al., 2003a).

3.4.3 Spatial and temporal dynamic of C/Na

Mean C/Na of SS are between 12.5 and 21.8 (Fig. 3.2C). C/Na generally decrease with increasing decomposition while $\delta^{15}N$ values increase (Conen et al., 2008). The correlation between mean C/Na and mean $\delta^{15}N$ of SS is significantly negative ($\rho = -0.8$). This inverse relationship can also be seen in Fig. 3.2C.

C/Na of the IS do not differ significantly from C/Na of the SS. Mean C/Na were between 14.2 and 16.8 for IS and SS at all three sites (Table 3.1). Values are similar to data reported

3.4. RESULTS AND DISCUSSION

Table 3.2: Range (mean) of C/Na, $\delta^{13}\text{C}_{\text{org}}$, $\delta^{13}\text{C}_{\text{tot}}$ and $\delta^{15}\text{N}$ values of algae ($n = 4$), manure ($n = 6$), and riverbed sediment (riverbed S, $n = 5$) as well as of forest ($n = 14$), pasture ($n = 12$) and arable land ($n = 8$) soils of the watershed.

	C/Na	$\delta^{13}\text{C}_{\text{org}}$ (‰)	$\delta^{13}\text{C}_{\text{tot}}$ (‰)	$\delta^{15}\text{N}$ (‰)
Algae	7.9–9.6 (9.1)*	–41.4––31.1 (–35.0)*	–40.1––16.7 (–24.3)	–0.7––3.5 (2.1)*
Manure	14.6–34.9 (20.8)*	–28.7––25.3 (–27.9)	–29.0––25.7 (–27.9)	7.4–11.9 (8.9)*
Riverbed S	12.1–25.5 (17.8)	–28.1––26.7 (–27.3)	–3.2––0.7 (–1.9)*	–5.9––3.44 (–4.7)*
Forest	13.4–31.8 (16.8)	–28.4––26.8 (–27.5)*	–28.7––11.0 (–23.0)	–4.0––4.7 (–0.8)*
Pasture	11.4–26.1 (13.9)	–29.2––27.8 (–28.6)	–29.5––20.7 (–27.6)*	–1.0––6.4 (3.0)
Arable land	9.5–11.3 (10.7)*	–28.5––27.1 (–27.8)	–28.3––19.9 (–25.9)	4.3–7.7 (6.0)*

* Differs significantly from the five other potential sources (ANOVA, $p < 0.05$)

for worldwide rivers (Meybeck, 1982), continental US rivers (Onstad et al., 2000), and in the Zhujiang River, China (Zhang et al., 2009). Mean C/Na of arable land, pasture and forest soil samples were between 10.7 and 16.8 (Table 3.2). C/Na of the analyzed algae as autochthonous sources of organic matter were significantly smaller with a mean of 9.1 ± 0.8 . The highest concentration of autochthonous organic matter would most likely occur during low flow conditions. No significant correlations between C/Na and SS or IS and between C/Na and water level at the sites were found. Consequently, the measured C/Na of IS and SS pointed to an allochthonous origin (e.g., soil or litter) of the organic matter in sediment. C/Na were excluded from further sediment tracer modeling because of the missing significant relationships between C/Na of the SS and water levels at the sites.

3.4.4 Spatial and temporal dynamics of C_{inorg} in sediments

IS and SS had a C_{inorg} concentration around 2% at all sites (Table 3.1, Fig. 3.2b) due to carbonaceous bedrocks in the area. No significant differences between C_{inorg} concentrations of the IS and SS as well as between the three sites were found, which is consistent with a steady pH value of the river water around 8.2 at all site. The C_{inorg} concentrations varied only marginally during the season and no correlation between C_{inorg} concentrations and the total IS, SS and the maximal water level during the week was assessed (Fig. 3.2B). Consequently, the concentration of C_{inorg} of IS and SS can not be used to draw any conclusions about the origin of the sediments.

3.4.5 Carbon and nitrogen isotopes for tracing suspended sediment sources

$\delta^{13}\text{C}_{\text{org}}$ values of SS were around -28.0 ± 0.9 ‰ and did not differ significantly between the three sites (Table 3.1). $\delta^{13}\text{C}_{\text{org}}$ values of soil and sediment samples from the catchment were in the same range (Table 3.2). Algae were highly depleted in $^{13}\text{C}_{\text{org}}$ resulting in $\delta^{13}\text{C}_{\text{org}}$ values between –41 and –31‰. Thus, $^{13}\text{C}_{\text{org}}$ isotopes indicate an allochthonous origin of the organic matter in SS, supporting the conclusion drawn from C/Na. $\delta^{13}\text{C}_{\text{tot}}$ values of the SS decreased significantly from upstream (mean site A: –20.0‰) to downstream (mean site C: –22.9‰), indicating different source contributions to the sediments (Table 3.1). The significantly higher $\delta^{15}\text{N}$ values at sites B and C

with means of 2.0 ± 1.1 and 1.8 ± 0.6 ‰, respectively, support this assumption ($\delta^{15}\text{N}$ mean of site A = -0.4 ± 0.9 ‰, Table 3.1).

SS isotope compositions varied highly during the brown trout spawning season. $\delta^{13}\text{C}_{\text{tot}}$ values increased with higher water level and higher amount of SS while $\delta^{13}\text{C}_{\text{org}}$ and $\delta^{15}\text{N}$ values decreased (Fig. 3.2c, d). This indicates different SS sources related to the discharge pattern. Linear regression models showed significant relationships for all three sites between water level and $\delta^{13}\text{C}_{\text{tot}}$ values ($R^2 = 0.51$ to 0.95) and between water level and $\delta^{15}\text{N}$ values ($R^2 = 0.51$ to 0.66 , Fig. 3.4). No significant relationship was found between water level and $\delta^{13}\text{C}_{\text{org}}$. The relatively small range of $\delta^{13}\text{C}_{\text{org}}$ values (-29.9 to -26.5 ‰) compared to $\delta^{13}\text{C}_{\text{tot}}$ (-25.6 to -13.8 ‰) and $\delta^{15}\text{N}$ (-2.2 to 3.6 ‰) might be a reason for this missing significance. For this reason only, C_{tot} and N isotope compositions were used for further tracer modeling and $\delta^{13}\text{C}_{\text{org}}$ values were excluded.

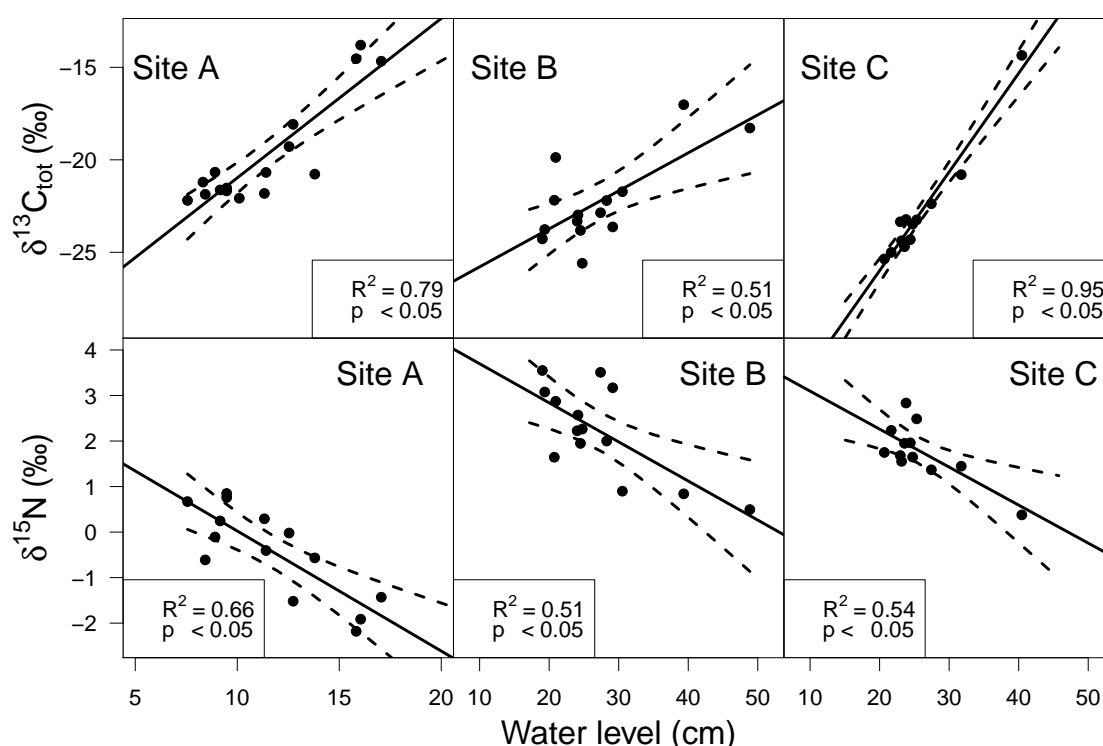


Figure 3.4: Relationship between maximal mean daily water level of a week and $\delta^{13}\text{C}_{\text{tot}}$ and $\delta^{15}\text{N}$ values of the weekly captured SS at the three sites. Dashed lines are the 95 % confidence intervals.

Riverbed sediment in the upper watershed had $\delta^{13}\text{C}_{\text{tot}}$ values as high as -0.7 ‰ due to enrichment with carbonate. The carbonate contents of the sediment were between 2.2 and 3.4 %. In parallel, ^{15}N was depleted resulting in $\delta^{15}\text{N}$ values around -5 ‰ (Table 3.2, Fig. 3.5). These low values indicate young, poorly-decomposed material (Conen et al., 2008). The riverbed sediment probably originates mainly from the bedrock molasse. Very low C_{org} concentrations with a mean of 0.2 % support this assumption. $\delta^{13}\text{C}_{\text{tot}}$ of the forest soils varied highly (Table 3.2). Two of the six forest samples above site A had carbonate contents around 1.5 %. Those two soils were enriched in $^{13}\text{C}_{\text{tot}}$ resulting in $\delta^{13}\text{C}_{\text{tot}}$ values around -14 ‰. The remaining forest soil samples contained no carbonate resulting in $\delta^{13}\text{C}_{\text{tot}}$ similar to $\delta^{13}\text{C}_{\text{org}}$ around -28 ‰ (Fig. 3.5). $^{13}\text{C}_{\text{tot}}$ values of the forest soils

3.4. RESULTS AND DISCUSSION

upstream of site B and C were around -26‰ . Again, carbonated soils (C_{inorg} around 0.3‰) were enriched in $^{13}C_{tot}$ compared to decarbonated soils. Mean $\delta^{15}N$ of the forest soil samples above site A was -2.5‰ . The downstream forest soil samples around site B and C were enriched with ^{15}N (mean $\delta^{15}N = 1.5\text{‰}$). A decrease of $\delta^{15}N$ with increasing elevation and declining temperature has been assessed in several studies (for a review see Amundson et al., 2003) and can be explained by poorly-decomposed material. The steep slopes of the forests above site A can have an additional influence on the low $\delta^{15}N$ values. The soil residence time decreases with increasing slope and therefore $\delta^{15}N$ values decrease (Amundson et al., 2003).

$\delta^{13}C_{tot}$ values of pasture and arable land soil samples were between -19.9 and -29.5‰ at all sites (Table 3.2, Fig. 3.5). Differences between sites and between pasture and arable land in $\delta^{13}C_{tot}$ were not significant. Again, higher $\delta^{13}C_{tot}$ values were assessed in carbonaceous soils. $\delta^{15}N$ of pasture and arable land was significantly higher than in the forest. The significantly highest $\delta^{15}N$ values were assessed in arable land with a mean of 6.0‰ (Table 3.2). These high values are attributable to an acceleration of soil N loss through enhanced decomposition rates because of cultivation (Amundson et al., 2003). Additionally, manure is commonly enriched in ^{15}N (Amundson et al., 2003; Alewell et al., 2008). The manure samples, which were collected on arable land at site B and C, had a mean $\delta^{15}N$ of 8.9‰ (Table 3.2).

These findings lead to the assumption that during high flow and high SS loads with high $\delta^{13}C_{tot}$ and low $\delta^{15}N$ values (Fig. 3.4), SS source is mainly the riverbed sediment in the upper watershed. During low flow and low SS loads with lower $\delta^{13}C_{tot}$ and higher $\delta^{15}N$ values (Fig. 3.4), SS sources are soils of forests, pasture and arable land (Fig. 3.5). The *IsoSource* program was used to quantify the proportion of the different sources (Phillips and Gregg, 2003). While interpreting the results, it is recommended to concentrate on the distribution of the feasible solutions rather than focus on a single value such as the mean to avoid misrepresenting the uniqueness of the results (Phillips and Gregg, 2003).

Algae samples were excluded from the modeling because C/Na and $\delta^{13}C_{org}$ values indicated none or minimal autochthonous C contributions. As described in Sect. 3.3.1, riverbed sediment samples were only taken in the upper most accessible reach of the river. Fox et al. (2010) noted that transformation of nitrogen could occur during temporary storage of sediments in the streambed, thus potentially masking their provenance. The sediment study in the Enziwigger was only conducted during winter time when biological activity is low. Consequently, it is assumed that N and C_{tot} isotopic compositions would not significantly change during the temporary storage in the river. With biotic fractionation, higher isotope values and lower C/Na values with less organic concentrations are expected. The opposite was measured: With less organic material in the sediments, $\delta^{15}N$ values decreased and C/Na increased (Fig. 3.2). Additionally, decomposition processes triggered higher isotope values with smaller grain sizes since larger soil particles break into smaller particle sizes during these decomposition processes (e.g., Fox and Papanicolaou, 2007). This was not the case for $\delta^{13}C_{tot}$, but it did apply to $\delta^{15}N$. This is, however, probably not attributable to physical fractionation but due to the fact that the mean sediment size as well as the source contributions varied in dependence of the water level.

SS at site A can possibly originate from forest and pasture soils or from riverbed sediment of the upper watershed. $\delta^{13}C_{tot}$ and $\delta^{15}N$ values of the three possible sources are clearly

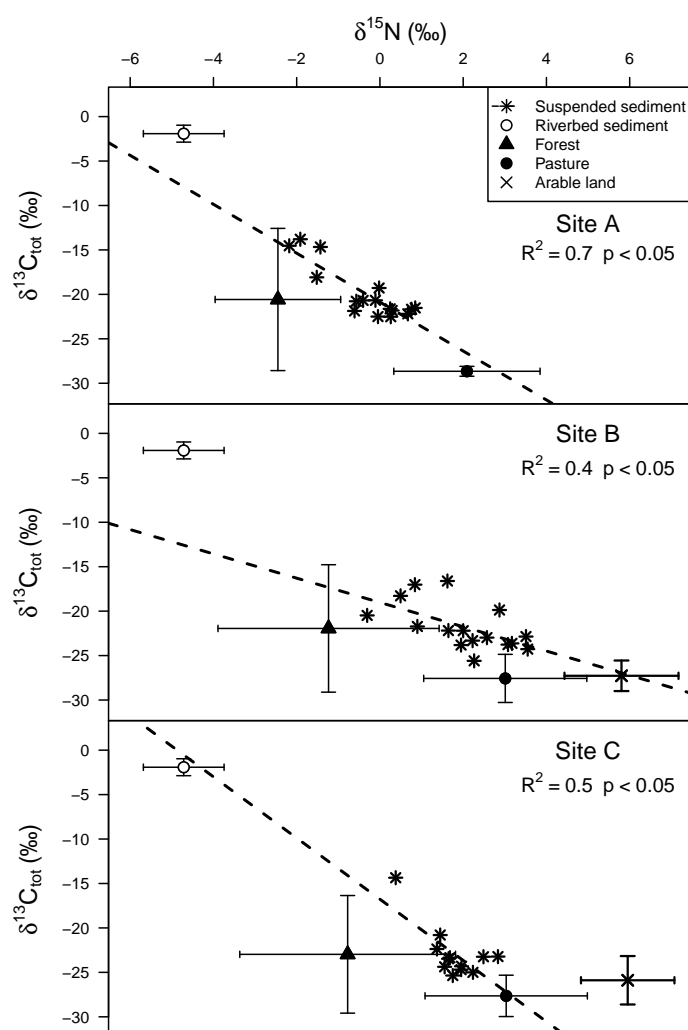


Figure 3.5: $\delta^{13}\text{C}_{\text{tot}}$ and $\delta^{15}\text{N}$ values of SS and soil samples collected above each sites (average \pm sd). Dashed line: SS regression line.

distinguishable (Fig. 3.5), resulting in well-defined *IsoSource* outcomes (Fig. 3.6). During base flow, the majority (up to $75 \pm 1\%$) of the SS originated from pasture soils. These percentages were relatively constant during the entire spawning season with an overall mean of 57%, even though the catchment was temporarily covered with snow (Fig. 3.6, Table 3.3). The percentage of SS deriving from the upper watershed riverbed sediment increased significantly with increasing maximal mean daily water level of a week (linear regression, $R^2 = 0.69$). The highest values with up to $52.8 \pm 0.8\%$ of the SS originating from the riverbed sediment in the upper watershed were measured during the high discharge events in December and January with high SS loads. In general, the smallest part of the SS at site A originated from forest soils with an overall mean of 16% (Table 3.3). The contribution of forest soils increased only after periods of higher temperature and thus snow melting periods (Fig. 3.5). Spearman rank correlation tests support this assumption with a significant correlation between SS deriving from forest and maximal mean daily temperature of a week ($\rho = 0.26$). These findings indicate the importance of

3.4. RESULTS AND DISCUSSION

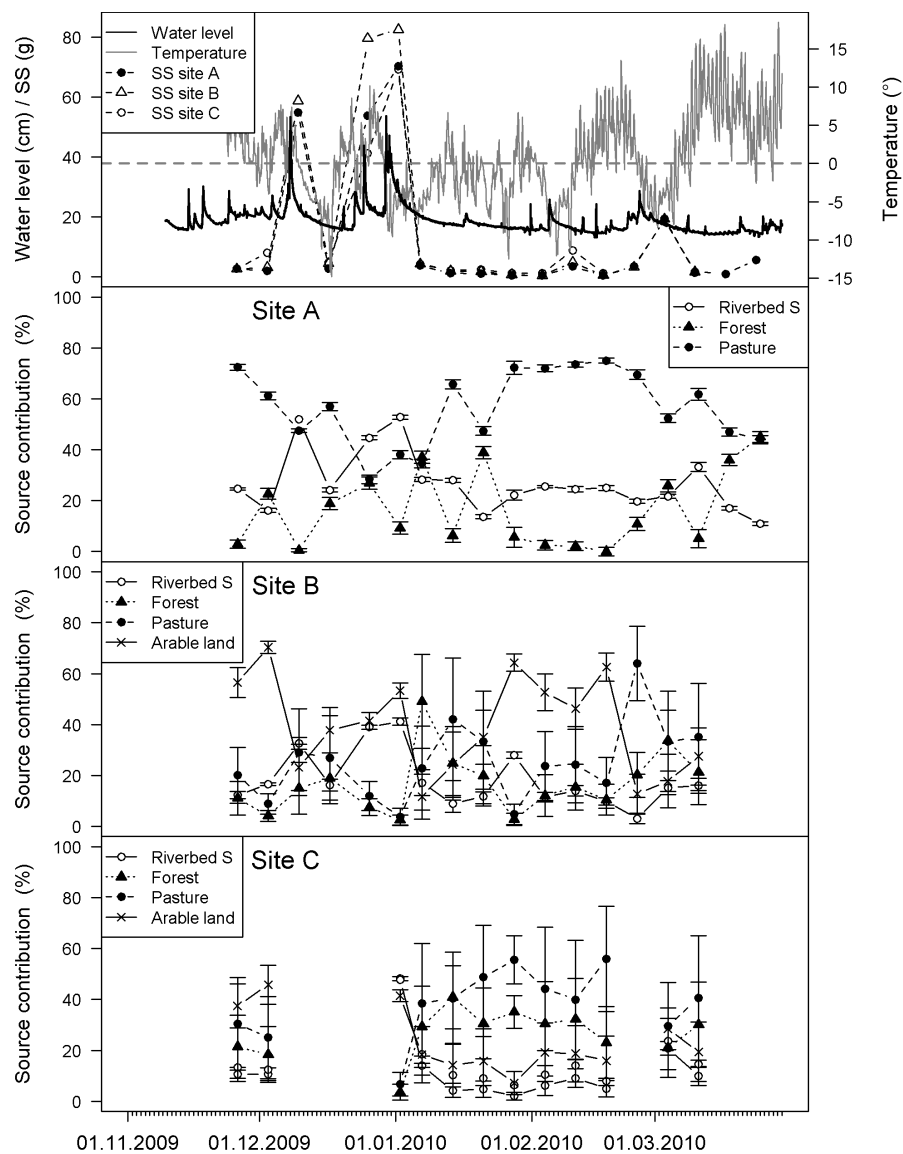


Figure 3.6: Total suspended sediment (SS) per week at the three sites and soil source contribution from the three/four possible sources to SS at the three sites, determined with the dual isotope mixing model *IsoSource*. Air temperature was measured close to site B in Hergiswil.

forest-covered land to reduce SS delivery to the river to prevent negative effects of SS on the aquatic ecosystem.

Arable land represents an additional possible source for SS at sites B and C. The modeling results of these sites have higher uncertainty as there are four ($n + 2$) possible sources for the downstream sites with two (n) isotope groups and thus, an under-determined equation system. In addition, the distinction of the isotopic compositions of the possible sources was not as clear as at site A (Fig. 3.5). Nevertheless, some general conclusions were possible.

During base flow conditions, SS at site B originated mainly from arable land followed by

Table 3.3: Mean (range and standard deviation) source contribution (%) to the suspended sediment at the three sites. Riverbed S = riverbed sediment.

Source	Site A	Site B	Site C
Riverbed S	27.0 (11.0 ± 0.7–52.8 ± 0.8)	18.3 (3.1 ± 2.0–41.2 ± 1.5)	12.1 (2.0 ± 1.5–48.2 ± 0.8)
Forest	16.0 (0 ± 1.7–45 ± 2.2)	16.8 (2.5 ± 1.9–49.1 ± 18.5)	26.4 (3.6 ± 3.1–40.9 ± 12.4)
Pasture	56.9 (28.4 ± 1.7–75 ± 1.0)	25.1 (3.8 ± 3.4–64.0 ± 14.6)	38.0 (6.7 ± 4.6–56.0 ± 20.7)
Arable land		39.9 (11.7 ± 5.1–70.4 ± 2.4)	23.5 (7.2 ± 4.5–45.8 ± 7.7)

pasture and forest soils (Fig. 3.6). On average, about 40 % of the SS originated from arable land (Table 3.3). The amount of SS originating from arable land increased significantly with increasing temperature ($\rho = 0.31$). The percentages were analyzed by multiple regression, using the highest mean daily temperature of a week (Temp), the maximal daily precipitation (Rain), and the quadratic terms of the two variables as regressors. The regression was a rather good fit ($R^2 = 0.56$) with an overall significant relationship and no interactions between the variables ($F_{4,91} = 20.1$, $p < 0.05$):

$$\text{SS from arable land} = 29.7 + 4.5 \text{ Temp} - 0.35 \text{ Temp}^2 - 0.5 \text{ Rain} + 0.002 \text{ Rain}^2 \quad (3.1)$$

These results indicate erosion processes on the fallow fields during rainy periods when the fields were neither snow-covered nor frozen. During high flow conditions, riverbed sediment of the upper watershed was the main source of SS, resulting in a significant positive correlation between SS with riverbed sediment origin and water level ($\rho = 0.56$). The feasible contributions of forest and pasture soils to SS often overlapped, making the distinction between their contributions impossible. Consequently, the mean contribution values in Table 3.3 have to be regarded with caution. For this reason, statistics were conducted with the sum of the SS fraction originating from forest and from pasture soils. Spearman correlations indicate a significant decrease of SS originating from forest and pasture soils with increasing temperature ($\rho = -0.31$) and precipitation ($\rho = -0.21$). This increase of forest and pasture soils sediment contributions during drier and colder periods might indicate a transportation of SS with percolating water during snow-covered periods. Forest and pasture areas upstream to site B are mainly located on the hillside on the right side of the river where the bedrock is relatively close to the surface (Fig. 3.7). This probably triggers a relatively fast subsurface flow. Moist soil in the warmer season and ice formation during the winter on the right side of the channeled riverbed support the assumption that subsurface water and groundwater is draining from the hillside to the river. Arable land is located on the flat planes on the left side of the river. Groundwater modeling as well as observations of riverine groundwater (head, temperature and electric conductivity) indicate infiltration processes on the left-sided river board dominating the local groundwater flow regime (Huber et al., 2013, Chapt. 5; Fig. 3.7). Thus, forest and pasture soils represent basically the main sediment sources at site B during undisturbed conditions. Sediments originating in arable land predominate, however, these natural processes due to erosion.

The majority of the SS during base flow conditions at site C came from pasture (29 ± 17 to 56 ± 20 %) and forest soils (21 ± 12 to 41 ± 12 %; Fig. 3.6). Both fractions increased significantly during colder and drier periods (Spearman rank correlations, pasture vs. precipitation $\rho = -0.39$, pasture vs. temperature $\rho = -0.37$, forest vs. precipitation $\rho = -0.41$ and forest vs. temperature $\rho = -0.61$.) Multiple regression models with maximal

3.5. CONCLUSIONS

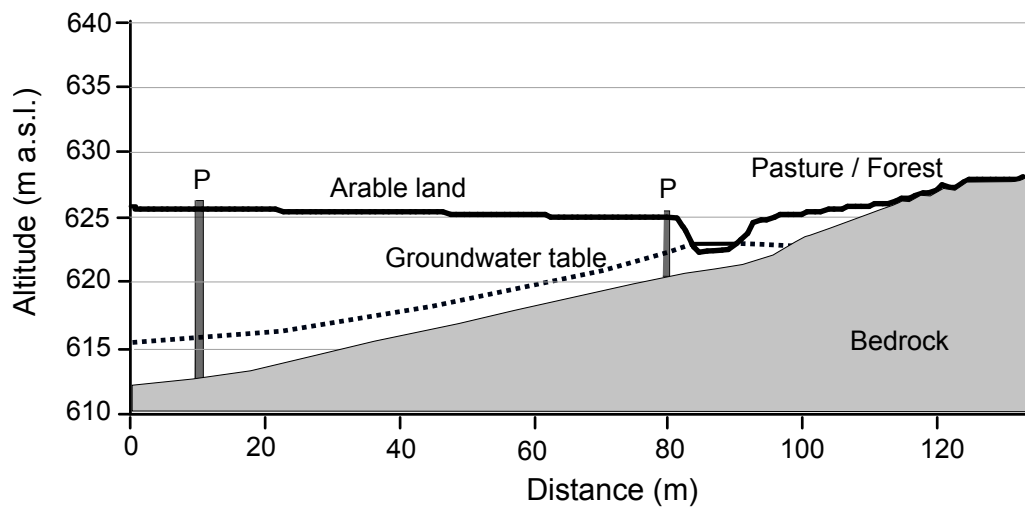


Figure 3.7: Schematic view of the groundwater table and bedrock at site B with the installed piezometers (P).

daily precipitation and mean daily temperature of a week could explain 58 % of the SS originating from pasture and 61 % of the SS originating from forest ($p < 0.05$). This indicates again a transportation of SS through percolating water from the hillside during snow-covered periods. The percentage of SS deriving from arable land was between 7.2 ± 4.5 and 45.8 ± 7.7 % with increasing values with higher temperature (linear regression, $R^2 = 0.49$, $p < 0.05$) and precipitation (linear regression, $R^2 = 0.36$, $p < 0.05$; Table 3.3). Maximum daily precipitation and maximum daily mean temperature of a week together explain 74 % of the amount of SS originated from arable land (multiple regression, $p < 0.05$). Unfortunately, only one sample from an extreme flow event was assessed due to the loss of SS samplers. Nevertheless, the mean percentage of SS deriving from the upper watershed riverbed sediment depended significantly on the maximal daily mean water level (linear regression, $R^2 = 0.95$). During low flow conditions, riverbed sediment accounted for only 2 ± 1.5 % of the SS, during high flow for 48.2 ± 0.8 % (Table 3.3).

These observations have important implications for arable land management strategies. Anticipated warmer winters with more frequent heavy rain events (IPPC, 2007) are likely to enhance the SS delivery from arable land at site B and C as well as DOC and nitrate input to the river. Besides the negative effects on the arable land (loss of soil and organic material to the river), brown trout eggs can be negatively impacted by the enhanced input of SS and organic material (Greig et al., 2005, 2007b). A possible adaption could be a wider protecting strip next to the river with natural vegetation or greening of the arable fields during the winter.

3.5 Conclusions

The concentration of C_{org} as well as TN in the IS and SS varied highly during the brown trout spawning season. The highest values were assessed during low flow periods with small sediment loads, the lowest values during high flow periods with high sediment loads. This is suggested to be related to the dilution with mineral matter deriving from

terrigenous soil erosion or the remobilizing of mineral matter of the riverbed. Organic matter concentrations of IS and SS are relatively low. Their impact on brown trout eggs is therefore expected to be low. The organic matter concentration of the sediment as well as nitrate in the river and interstitial water increased from the upstream site A to the two downstream sites B and C, which is attributable to leaching from pasture and arable land. C/Na and $\delta^{13}C_{org}$ values indicate an allochthonous source of the organic matter in the SS during the brown trout spawning season. C_{tot} and N isotopes were used to trace the source of SS in respect to time and space using the visual basic program *IsoSource*. The fraction of SS originating from the riverbed sediment of the upper watershed increased at all sites during high flow. At site A, these fractions were the highest with values between $11.0 \pm 0.7\%$ to $52.8 \pm 0.8\%$ (mean = 27.0%). Smallest contributions from the riverbed sediment were detected at site C. The SS source contributions varied between sites during base flow conditions: at site A SS mainly originated from pasture, at site B mainly from arable land and pasture, and at site C from pasture and forest. Increasing winter temperatures and precipitation led to a higher contribution of SS from arable land at both downstream sites, indicating soil erosion from the bare fields during snow-free and snow-melting periods. The increased DOC and nitrate concentration during high flow support these *IsoSource* calculations. These data indicate an increase of soil erosion processes on snow-free pasture and arable land during the anticipated warmer winter with more frequent torrential rain events (IPPC, 2007). An increase of SS and of organic matter concentration in the SS during the brown trout spawning season is a probable consequence. Both of these affect brown trout eggs negatively (Greig et al., 2005, 2007b)

Acknowledgments This study was funded by the Swiss national foundation (SNFK-32K1-32K1-120486/1). We would like to thank Torsten Vennemann and three anonymous reviewers for the constructive comments. They were a great help towards improving the manuscript. We thank Christian Michel, Sandra Rudolf and Bastian Brun for their help in the field, Mark Rollog, Marianne Caroni and Ruth Strunk for laboratory assistance and measurements and Claude Schneider for technical support. DOC and nitrate values were kindly provided by Bastian Brun from his bachelor thesis.

Chapter 4

Evaluation of a new method to measure riverbed colmation

4.1 Abstract

Fine sediment deposition can reduce pore space of the riverbed sediment and thus decrease the hydraulic conductivity and consequently triggering lower interstitial oxygen concentration. This increase of fine sediment in the top layer of the riverbed and subsequent clogging of the riverbed sediment is called "internal colmation". Up to now, no method exists to assess the degree of internal colmation in the entire riverbed in a high spatiotemporal scale, which does not harm the intra-gravel structure and is easy to handle. For this purpose, a hand penetrometer, used in soil science to assess soil compaction, was applied. Results suggest that penetration depths can predict to some extent the riverbed sediment composition. High penetration depths indicate river sediment that are not colmated. Small penetration depths were obtained at spots with high silt and clay fractions or with large gravel. Both are unfavorable for brown trout spawning. The former clogs the riverbed, the latter may be too large to be moved by the spawning fish. Consequently, penetration measurements can indicate favorable brown trout spawning habitats. This could also be seen in the mapped brown trout redds, which were all located at places with intermediate to deep penetration. The major drawback of the method was its bad reproducibility. Furthermore, comparability between two operators was low, which is probably due to large gravels, disturbing the penetration randomly and causing large scatter. This makes the method unfeasible to assess riverbeds with relatively small differences in internal colmation.

4.2 Introduction

The negative effects of excessive fine sediment (sediment < 2 mm) deposition on the aquatic ecosystem have been evaluated in several studies (for a review see Bilotta and Brazier, 2008). Pore spaces get reduced with the intrusion and deposition of fine sediment, resulting in smaller hydraulic conductivity (Schälchli, 1995). Thereby, interstitial oxygen concentrations decrease, lowering the survival success of gravel spawning fish embryos as e.g., brown trout *Salmo trutta* (e.g., Bilotta and Brazier, 2008; Greig et al., 2005). Clogging of the top layer of riverbed sediments is called colmation (e.g., Brunke and Gonser, 1997). Two main types of riverbed colmation, named internal and external colmation, have been identified in laboratory and field studies (Blaschke et al., 2003; Brunke, 1999; Schälchli, 1995). External colmation refers to fine sediment settling on the top of the riverbed in areas of low water velocity, building up an additional fine sediment layer on the riverbed. Internal colmation describes an increase of fine material in the existing top centimeters or decimeters of the riverbed. It depends on many factors as e.g., shear stress, hydraulic gradient, grain size distribution of the riverbed and suspended sediment concentrations (e.g., Brunke and Gonser, 1997). Internal colmation is often not visible on the riverbed surface and due to the complex process, no easy computational approaches exist (Schälchli et al., 2002).

Schälchli et al. (2002) developed a method to explicitly estimate the internal colmation of riverbed by visually classifying the percentage of fine sediment of the overall river sediment below rocks. A major drawback of the method is the limitation to dry gravel banks. To assess internal colmation in rivers, the boot-method can be applied (Schälchli et al., 2002). This method is based on an estimation of the force needed to "kick" in the riverbed and break up the sediment structure by feet. This method is connected with low effort for the operator, but the estimation of colmation is subjective (Schälchli et al., 2002). Furthermore, freeze core samples or bulk samples of the riverbed sediment can be taken to analyze the amount of fine sediment by sieving (e.g., Blaschke et al., 2003; Zimmermann et al., 2005). The effort to obtain and sieve sediment samples is, however, very high.

The term "embeddedness" describes a similar concept as the term colmation. Several definitions of embeddedness exist in the literature (e.g., Sennatt et al., 2006; Sylte and Fischenich, 2002). Some definitions only refer to the degree to which fine sediments surround coarse substrates on the surface of a streambed. Other authors also refer to the subsurface conditions and define embeddedness as "the amount of fine sediment that is deposited in the interstices between larger stream substrate particles" (e.g., Sennatt et al., 2006; Sylte and Fischenich, 2002). Sylte and Fischenich (2002) provide a comprehensive review of these different concepts and a comparison of the measurement techniques. Most of the techniques are visual, some others require samples to be taken, which destroy the substrate. Sylte and Fischenich (2002) concluded that very large differences in methodologies exist and that none of them can provide the appropriate details needed for field application. They suggest that a fundamental change in approach may be necessary. Similarly, Sennatt et al. (2006) compared different embeddedness methods to identify differences between a regulated and an unregulated stream. All methods showed a trend of increasing embeddedness downstream of a dam, but the quantitative values differed significantly and none of the methods stands out as the best and most useful technique (Potyondy and Sylte, 2008).

4.3. MATERIALS AND METHODS

The aim of this project was to find and evaluate a new technique to measure internal colmation. The method has to be applicable in the entire riverbed to identify feasible spawning habitats and to assess the spatial and temporal colmation dynamic during the spawning season and its potential harmful effects on the developing eggs. The method should not harm intra-gravel structures and should be easy to handle. Results have to be comparable between different rivers and operators. For this, the idea was to use hand penetrometers, which are common in soil science to measure soil compaction.

4.3 Materials and methods

The study was conducted during the spawning season 2008 / 2009 at three sites named A, B and C from up- to downstream at the river Enziwigger, Canton of Lucerne, Switzerland. River and site characteristics are described in details in Schindler Wildhaber et al. (2012b,a)(Chap. 2 and 3). The Enziwigger is heavily modified with lateral steps for stabilizations and terraces with a length of approximately 10 m created by these steps. Brown trout redds were mapped in November 2008. Penetration depth was investigated at three steps each site between January and April 2009.

A hand penetrometer from Eijkelkamp (Eijkelkamp Agrisearch Equipment, Giesbeek, Netherlands) was used to measure internal colmation. Hand penetrometer are used in soil science to assess soil compaction by measuring the force needed to press a metallic cone into the soil (for a review see Hemmat and Adamchuk, 2008). Penetration depth with a force of 400 N was measured every 50 cm in the cross section of the river in one meter sections along the river. At each measuring point, penetration depth was measured twice. Mean values were mapped with Esri ArcGis and values were interpolated for the entire terrace by kriging. Based on this map, two spots with deep penetration depths and two spots with small penetration depths were assessed. Freeze core samples with a length of roughly 350 mm were taken at these spots to determine the amount of fine sediment in different layers (0 - 10 cm, 10 - 20 cm, 20 - 30 cm, > 30 cm). The procedure of freeze core sampling and sediment analyses are described in details in Schindler Wildhaber et al. (2012b)(Chapt. 2).

4.4 Results and discussion

4.4.1 Comparing penetration depth with the sediment size of the riverbed

Penetration depth decreased significantly with higher clay fraction (sediment $< 2 \mu\text{m}$, Figure 4.1A) in the upper 10 cm of the riverbed as well as with higher silt and clay fraction (sediment $< 63 \mu\text{m}$, Figure 4.1B). The latter relationship was, however, not significant. With the increase of total fine sediment ($< 2 \text{mm}$) penetration depth significantly increased (Figure 4.1C). This indicates that penetration depth can predict to some extent silt and clay fraction. According to Schälchli (1995), internal colmation is mainly depending on fine particles (3 - 30 μm) that can fill up pores between coarser particles and very fine particles ($< 3 \mu\text{m}$), forming an almost impermeable skin at the interface between the

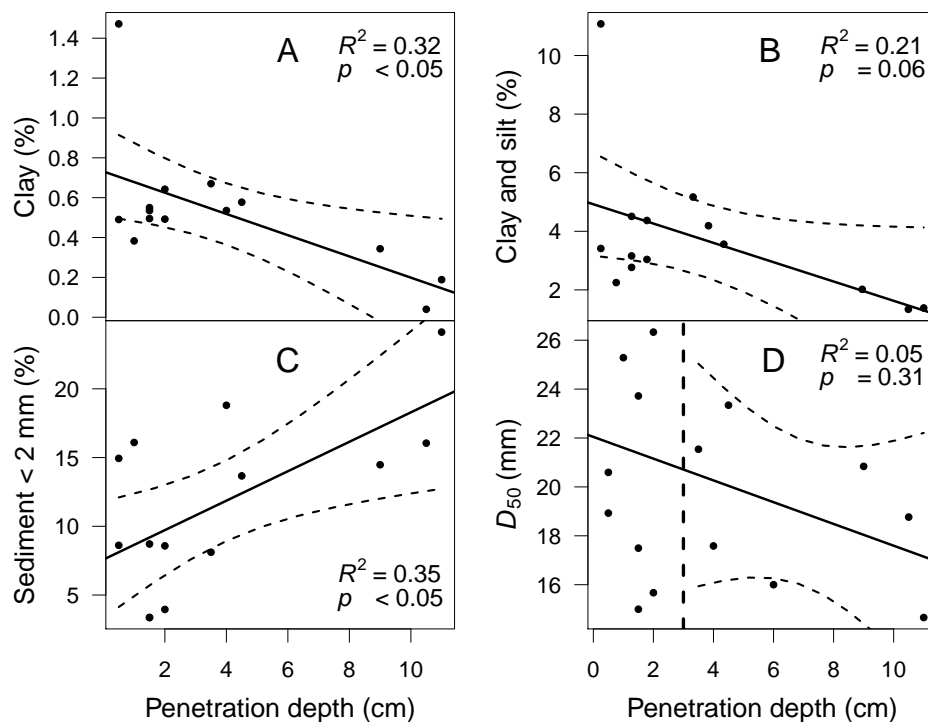


Figure 4.1: Correlation between penetration depth and (A) clay fraction of the upper 10 cm of the riverbed sediment (u10), (B) clay and silt fraction of u10, (C) sediment < 2 mm fraction of u10, and (D) D_{50} of the riverbed sediment. Linear regression line is only for data with penetration depth > 3 cm. Dashed lines are the 95 % confidence intervals.

surface and subsurface layers. Thus, penetrometer measurement might be able to predict internal colmation.

However, small penetration depths can also be caused by large gravel that can not be moved by the cone of the penetrometer. Figure 4.1D indicates a decrease in penetration depth with bigger D_{50} (50th percentile grain size diameter of the whole freeze core sample). These findings suggest that high penetration depths stand for a riverbed sediment which is not colmated. Low penetration depths, on the other hand, could either indicate colmated sediments with a high silt and clay fraction or riverbeds with large gravels.

4.4.2 Spatial distribution of penetration depths and redd locations

Penetration depth varied remarkably within a terrace (Figure 4.2). There was, however, no general relationship of the penetration depth and the location within a terrace. Mapped brown trout redds were all in locations with medium or high penetration depth (Figure 4.2). In total, five redds were mapped in locations with a penetration depth of 5-8 cm, five redds in locations with a penetration depth of 2-5 cm and no redd was found where penetration depth was below 2 cm. This finding can be interpreted in two ways: Penetration could be deeper at spots where redds have been cut due to the spawning activity, since the gravel gets loosen and the porosity increases during cutting (Crisp and Carling, 1989). Or, brown trout only spawn at locations where gravel is loose already. The latter is probably true, since redds were usually located within a bigger area of deep

4.4. RESULTS AND DISCUSSION

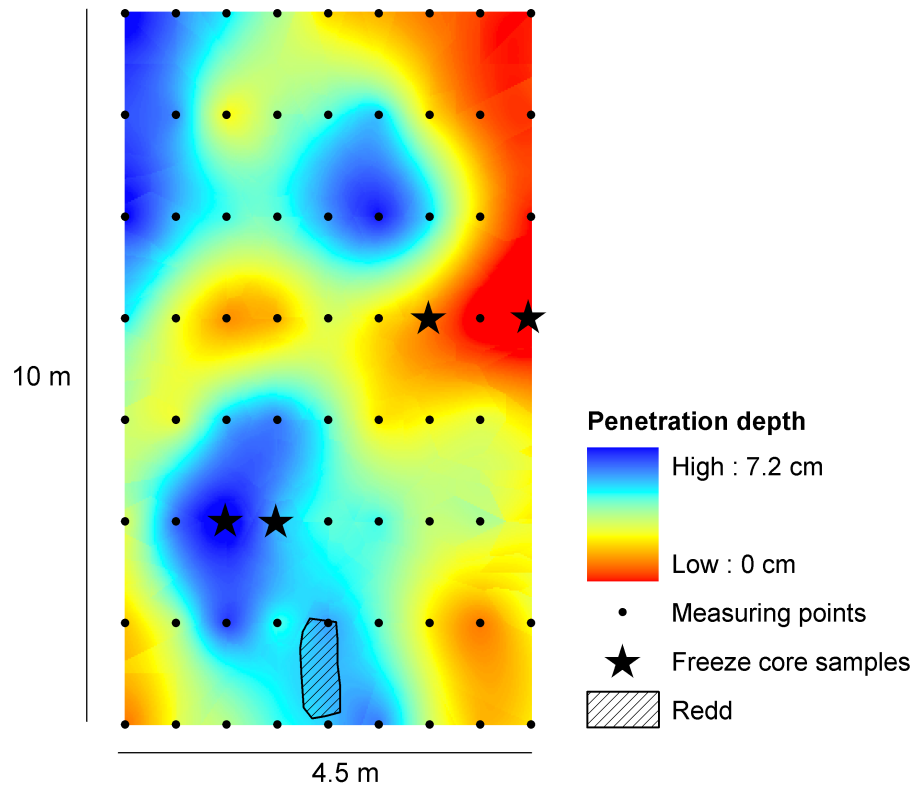


Figure 4.2: Mean penetration depth of two measurements per measuring point at the site B, terrace 4.

penetration (Figure 4.2). Additionally, the higher permeability of the redd substratum is expected to be obliterated within a few months by riverbed gravel displacements and fine sediment infiltration (Schindler Wildhaber et al., 2014, Chap. 6), thus, it would probably not have been measurable anymore in February. Low penetration depth could be due to big gravel in the riverbed or due to colmation. Both would hinder brown trouts to successfully cut a redd (Kondolf, 2000).

The mean penetration depth increased along the river with the significantly smallest mean penetration depth at site A and highest mean penetration depth at site C (Table 4.1). This is consistent with the highest fine sediment accumulation at site A assessed with sediment accumulation baskets (Table 4.1; Schindler Wildhaber et al., 2012b, Chap. 2). The silt and clay accumulation in the baskets differed, however, not significantly between the sites. Another, possibly more reliable reason for the increase in penetration depth along the river could be the decrease in D_{50} of the riverbed sediment (Table 4.1; Schindler Wildhaber et al., 2012b, Chap. 2). Larger riverbed gravel can hinder deep penetration, as they can block the cone of the penetrometer (Figure 4.1D).

4.4.3 Reproducibility and comparability of the method

The biggest drawback of the penetrometer method is its poor reproducibility and comparability. The two penetration measurement made at approximately the same spot (within

Table 4.1: Mean \pm standard deviation of the penetration depths and number of integrated values at the three sites A, B and C. Each value consists of two replicates. Data of fine sediment (< 2 mm) accumulation, fraction of sediment $< 63 \mu\text{m}$ of the fine sediment and D_{50} of the riverbed sediment (defined by freeze core samples and with line-number-analyses; Fehr, 1987) are taken from Schindler Wildhaber et al. (2012b)(Chap. 2).

	A	B	C
Penetration depth (cm)	$3.3 \pm 1.9^*$	4.3 ± 2.8	$5.2 \pm 5.7^*$
Number of values	194	285	202
Fine sediment (%)	$20.1 \pm 4.5^*$	18.7 ± 4.5	$13.9 \pm 2.8^*$
Clay and silt	5.1 ± 1.7	4.8 ± 1.1	5.0 ± 2.5
D_{50} (freeze core) (mm)	20 ± 4	19 ± 6	16 ± 1
D_{50} (line-nr-analysis) (mm)	25 ± 8	25 ± 4	$16 \pm 4^*$

* Differs significantly from the two other sites (ANOVA, $p < 0.05$).

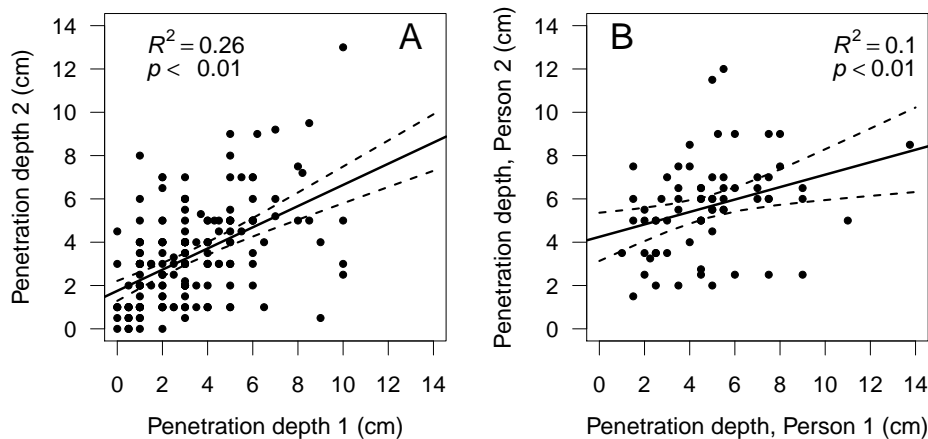


Figure 4.3: Relationship between penetration depths conducted twice at the same spot by (A) the same person and (B) two persons. Dashed lines are the 95% confidence intervals.

5 cm) correlated significantly, but they showed a very high scatter (Figure 4.3A). This emphasizes the importance of conducting at minimum two measurements at each spot to get a more reliable result. The comparison of penetration depths obtained by two persons at approximately the same spot showed only a weak correlation (Figure 4.3B). Consequently, the results of different operators are hardly comparable, which makes the method unfeasible. These bad correlations between replicates and between two operators are probably due to large riverbed gravel, disturbing the penetration of the cone as discussed above.

4.5 Conclusion and outlook

Penetration measurements can predict to some extent the riverbed sediment composition and the degree of colmation. High penetration depths were measured in riverbeds which were not colmated. Small penetration depths were obtained at spots with a high silt

4.5. CONCLUSION AND OUTLOOK

and clay fractions as well as at spots with large gravel. Both are unfavorable for brown trout spawning. The former clogs the riverbed, the latter may be too large to be moved during redd cutting (Crisp, 1996; Kondolf, 2000). Thus, penetration measurements can indicate favorable brown trout spawning habitats. All mapped brown trout redds were located at locations where intermediate to deep penetration was possible, supporting this hypothesis.

The repeatability and comparability of results obtained by different operators is, however, poor. The corresponding uncertainty is larger than the differences in the degree of clogging at the river Enziwigger, where none of the sites had strongly colmated river sediment. The method could possibly serve to indicate bigger colmation differences, for example between upstream and downstream of a dam, as assessed with different methods by Sennatt et al. (2006). A further study could be conducted to answer this hypothesis.

Big gravels below the armor layer are probably the biggest problem of the penetrometer-method, since they decrease penetration depth randomly, which causes large scatter. Another idea to characterize internal colmation without this disturbance would be a "spring balance-method". This method would base on the measurement of the force needed to tear a stone out of the riverbed. Thereby, the area, weight and water level above the stone have to be considered. This idea could also be tested in a further study.

CHAPTER 4. EVALUATION OF A NEW METHOD TO MEASURE RIVERBED COLMATION

Chapter 5

Multidimensionale Untersuchung der Fluss-Grundwasser-Interaktion

This chapter is published as:

Huber E, Huggenberger P, Epting J, Schindler Wildhaber Y. Zeitliche und räumliche Skalen der Fluss-Grundwasser Interaktion: Ein multidimensionaler hydrogeologischer Untersuchungsansatz. Grundwasser. 2013. DOI 10.1007/s00767-013-0220-x

Spatiotemporal scales of river-groundwater interaction: A multidimensional hydrogeological investigation approach

Abstract: River-groundwater interactions show strong scale-dependencies and are often strongly transient. In this regard, small-scale flow conditions in the hyporheic zone at the interface between surface- and groundwater can be important for process-understanding. This especially includes questions concerning flow conditions in salmonid redds of gravel-bed rivers. The Swiss subalpine river Enziwigger was chosen as an example for a small channelized river with artificial steps within the riverbed. Several methods were developed, tested and combined that capture the four dimensions (three spatial and one temporal) of the interactions between surface water, the hyporheic zone and groundwater, for individual river segments. The setup of a monitoring network as well as the realization of field-measurements provided data for groundwater flow models. Continuous time series of hydraulic data, temperature and electrical conductivity within the river and the riverbed, as well as within the riverine groundwater, allowed identifying zones with significant exchange of surface water and groundwater. Additionally, the data helped describe the transient character of groundwater flow-paths under various hydrological boundary conditions. Results of the field-measurements in combination with transient groundwater flow modeling and scenario analyses illustrate the relevance of dynamically changing infiltration and exfiltration patterns within the riverbed.

5.1 Zusammenfassung

Die Prozesse der Fluss-Grundwasser-Interaktionen sind stark skalenabhängig und im Allgemeinen stark instationär. Einen für das Prozessverständnis wichtigen Aspekt betreffen die kleinräumigen Strömungsverhältnisse an der Grenzschicht zwischen Oberflächengewässer und Grundwasser im hyporheischen Interstitial. Dies betrifft insbesondere auch Fragestellungen zu Strömungsverhältnissen in Forellenlaichgruben kiesführender Flüsse.

Exemplarisch für kleinere mit Sohlschwellen verbaute und kanalisierte Fließgewässer wurden am voralpinen Schweizer Fluss Enziwigger verschiedene Methoden entwickelt, getestet und kombiniert, die es erlauben die vier Dimensionen (drei räumliche und eine zeitliche) der Interaktion Oberflächengewässer-Interstitialraum-Grundwasser für einzelne Flussabschnitte zu erfassen.

Der Aufbau eines Messnetzes sowie die Durchführung von Feldmessungen lieferten Grundlagen für eine Grundwasserströmungsmodellierung. Kontinuierliche Zeitreihen der Hydraulik, Temperatur und elektrischen Leitfähigkeit im Fließgewässer, an der Gewässersohle sowie im flussnahen Grundwasser dienten zudem der Identifizierung von Zonen mit signifikantem Fluss-Grundwasser-Austausch und von zeitlich instationären bevorzugten Fließpfaden im Grundwasser bei unterschiedlichen hydrologischen Randbedingungen. Die Resultate der Feldmessungen in Kombination mit der instationären Modellierung und Szenarienentwicklung illustrieren die Bedeutung von sich dynamisch verändernden Infiltrations- und Exfiltrationsmustern im Flussbett.

5.2 Einleitung

Die Prozesse der Fluss-Grundwasser-Interaktion sind wesentlich durch die Abflussdynamik der Oberflächengewässer geprägt und entsprechend instationär. Die Durchlässigkeiten von Flussbett und Uferzone variieren in Abhängigkeit von Abfluss, Temperatur und Partikeldynamik an der Grenzschicht zwischen Oberflächengewässer und Grundwasser. Zudem machen Heterogenitäten in der Korngrößenzusammensetzung der Flusssohle ein „Upscaling“ der hydraulischen Parameter (Porosität und Permeabilität) über einen bestimmten Abschnitt des Flussbetts schwierig.

Trotz der Bedeutung für die Wasserressourcenbewirtschaftung, die Gewässerökologie und den Grundwasserschutz ist das Verständnis dieser Austauschprozesse ungenügend. Dies betrifft auch die lückenhaften Kenntnisse von Prozessabläufen im hyporheischen Interstitial. Eine besondere Herausforderung sind die verschiedenen Einflüsse auf das Grundwasserfließregime in den unterschiedlichen Maßstabebereichen, einschließlich der Dynamik der verschiedenen Randzuflüsse sowie der Morphologie und Zusammensetzung des Flussbettes.

Die meisten Feldexperimente bei hohen Abflüssen geben nur bedingt Aufschluss über die effektive Dynamik des Geschiebe- und Partikeltransportes (Ashmore, 1988). Experimente, welche die Prozesse untersuchen, die zur Verringerung der Durchlässigkeit der Deckschicht führen, wurden zudem im Labor- und nicht im Feldmasstab entwickelt (Schälchli, 1993, 1995). Dass im Feldmasstab räumlich komplexe Muster von

5.3. UNTERSUCHUNGSGBIET

Veränderungen in der Durchlässigkeit der Flusssohle im Verlauf einzelner Hochwasserereignisse regelmässig auftreten, zeigen zahlreiche Untersuchungen (z.B. Doppler et al., 2007; Hoehn and Cirpka, 2006; Naegeli et al., 1995).

Im Rahmen eines interdisziplinären Forschungsprojektes des Schweizer Nationalfonds K-32K1-120486 wurden Methoden entwickelt, um den Einfluss von Feinsedimenten in Flüssen auf die Entwicklung von Forellenlaichgruben in Kiesbänken zu quantifizieren. Primär stand die Frage im Vordergrund, wie die Entwicklung von Fischlaich in den Laichgruben der Kiesbänke jeweils in der Laichperiode von November bis Ende März des darauffolgenden Jahres von der Dynamik dieser Austauschprozesse beeinflusst wird. Von Bedeutung war insbesondere der Einfluss der Sedimentinfiltration in die Poren der Flussbettablagerungen sowie das Erfassen der Instationarität der hydraulischen Verhältnisse, einschliesslich der Veränderung von Up- und Downwelling Zonen (Schindler Wildhaber et al., 2014, Chap. 6). Für die Untersuchungen war es notwendig verschiedene Erkundungsmethoden miteinander zu kombinieren, welche es erlauben, Aussagen über die Austauschprozesse (direkte Infiltration) an der wassergesättigten Grenzschicht zwischen Oberflächengewässer und Grundwasser im Massstab der Laichgruben zu machen.

Mit diesem Beitrag sollen, am Beispiel des verbauten Schweizer Mittelgebirgsflusses Enziwigger und dem regionalen alluvialen Grundwassersystem, die Austauschprozesse Fliessgewässer-Interstitialraum-Grundwasser sowie das Grundwasserfliessregime in verschiedenen Massstabsbereichen mit dem Schwerpunkt auf die Dynamik der Strömungsverhältnisse in Forellenlaichgruben charakterisiert werden. Dabei werden verschiedene Betrachtungsmassstäbe unterschieden (Table 5.1): A) regional als Teil des Grundwasserkörpers im Tal (100er m bis km); B) Bereiche eines Flussabschnittes (10er bis 100 m); und C) lokal im Bereich der Schwellen, Kiesbänke und Forellenlaichgruben (1er bis 10er m).

Der Schwerpunkt der Untersuchungen lag auf der Erfassung der zeitlichen und räumlichen Skalen der Fluss-Grundwasser-Interaktion. Die Haupthypothese der vorliegenden Arbeit ist, dass sich im Bereich von Sohlenschwellen lokale Grundwasserfliessregime entwickeln, die zu einer Abfolge von Up- und Downwelling Zonen führen und damit die Strömungsverhältnisse in den Laichgruben beeinflussen. Oberhalb der Flussschwellen infiltriert Flusswasser aufgrund des erhöhten hydraulischen Gradienten. Das infiltrierte Wasser strömt um und unter der Schwelle und exfiltriert unterhalb der Schwelle wieder in das Fliessgewässer. Diese lokalen Prozesse werden überlagert von regionalen instationären Prozessen der In- und Exfiltration zwischen dem Fliessgewässer und dem regionalen Grundwasserfliessregime. Abschliessend werden qualitative Aspekte auf der lokalen Skala der untersuchten künstlich angelegten Fischlaichgruben im Zusammenhang mit dem instationären lokalen Grundwasserfliessregime diskutiert.

5.3 Untersuchungsgebiet

Die Untersuchungen wurden am kleinen voralpinen Fluss Enziwigger im Schweizer Kanton Luzern im Hügelland südlich von Willisau durchgeführt (Fig. 5.1). Die Enziwigger entspringt am Nordhang des Napfes auf 1300 m ü.M. und mündet nach 17 km in die Wigger. Das gesamte Einzugsgebiet der Enziwigger beträgt 38 km². Im Haupttal,

CHAPTER 5. MULTIDIMENSIONALE UNTERSUCHUNG DER
FLUSS-GRUNDWASSER-INTERAKTION

Tabelle 5.1: Fragen und Ziele für die verschiedenen Untersuchungsskalen sowie Untersuchungsmethoden und Ergebnisse.

Skala	Fragen/Ziel	Untersuchungsmethode	Ergebnisse
Einzugsgebiet* & regionale Grundwasserkörper (100er m bis km)	<ul style="list-style-type: none"> · Niederschlag u. Abfluss · Flächenhaft versickerndes Niederschlagswasser · Regionaler Grundwasserströmung und Hangzustrom 	<ul style="list-style-type: none"> · Auswertung meteorologischer Daten, Grundwasser- und Flusspegel · Regionales Grundwasserströmungsmodell 	<ul style="list-style-type: none"> · Das Einzugsgebiet hat kaum Speicherkapazität · Geringe Grundwasserneubildung aus flächenhaft versickerndem Niederschlagswasser · Hangzustrom: vernachlässigbar, hat jedoch lokalen Einfluss
Flussabschnitt, mehrere Schwellen (10er bis 100 m)	Zeitliche und räumliche Charakterisierung der Fluss-Grundwasser Interaktion	<ul style="list-style-type: none"> · Auswertung von Grundwasser- und Flussdaten (P^a, T^b, LF^c) · Regionales und lokales Grundwasserströmungsmodell 	<ul style="list-style-type: none"> · Regionalen Skale: Flussinfiltration in Grundwasser · Lokale Grundwasserflussregime sind komplexer
Schwelle, Kiesbänke, Laichgrube (1er bis 10er m)	<ul style="list-style-type: none"> · Einfluss der Morphologie (Eintiefung des Flusses, Schwellen, Kolke, Topographie Flusssohle) und der Durchlässigkeit der Flusssohle · Dynamik In-/Exfiltration · Erosion/Verringerung der Flussbettdurchlässigkeit · Definition von Schwellenwerten 	<ul style="list-style-type: none"> · Vermessung Flussbett · Auswertung von Grundwasser- und Flussdaten (P^a, T^b, LF^c) · Lokales Grundwasserströmungsmodell · Analyse Flussbetttemperatur 	<ul style="list-style-type: none"> · Schwelle-Kolk Reihenfolge prägt lokale Grundwasserflussregime stark · Starke Hochwasserereignisse mit deutlichen Änderungen der Austauschprozesse an der Flusssohle

* nur Betrachtung Abflussbildung, ^a Pegel, ^b Temperatur ^c elektrische Leitfähigkeit

5.3. UNTERSUCHUNGSGEBIET

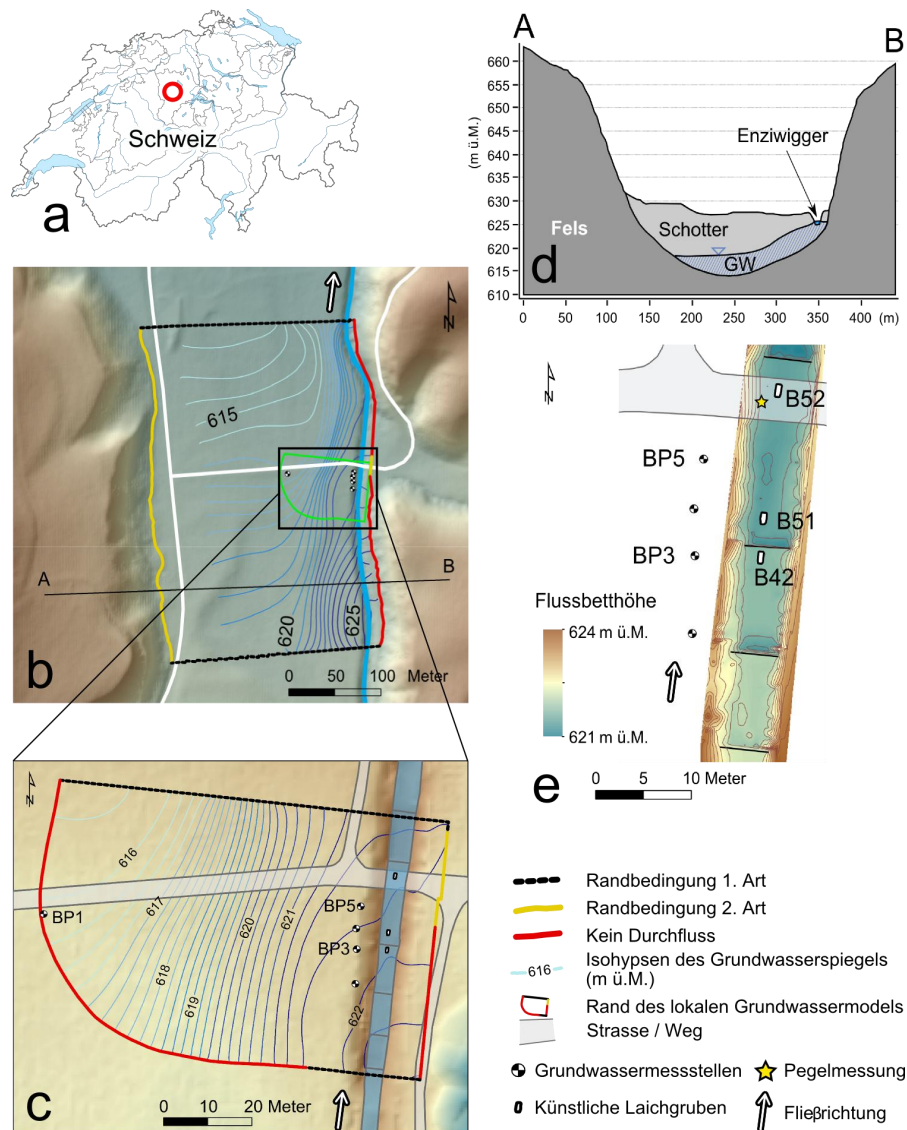


Abbildung 5.1: Untersuchungen auf verschiedenen Skalen. **a)** Lage des Untersuchungsgebiets in der Schweiz. **b)** Digitales Höhenmodell (5 m-Auflösung) des Untersuchungsgebiets und Modellperimeter für das regionale Grundwasserströmungsmodell. Dargestellt ist die Verteilung von berechneten Grundwassergleichen (1 m-Äquidistanz) während einer Mittelwassersituation (siehe Abb 5.2). **c)** Digitales Höhenmodell (5 m-Auflösung) und Modellperimeter des lokalen Grundwasserströmungsmodells. Dargestellt sind die Verteilung von berechneten Grundwassergleichen (0.2 m-Äquidistanz) während einer Mittelwassersituation (siehe Fig. 5.2) sowie die Lage der Grundwassermessstellen, Sohlschwellen und künstlich angelegten Forellenlaichgruben. **d)** 5-fach überhöhtes laterales Höhenprofil durch den Talgrundwasserleiter der Enziwigger, dargestellt mit einem, aus den Bohrtiefen abgeleiteten Schotter-Grundwasserkörper; die Enziwigger wurde über weite Bereiche an den östlichen Talrand verlegt. **e)** Darstellung des untersuchten Flussbettabschnittes und Ergebnisse der Flussbettvermessungen zusammen mit der Lage der ufernahen Grundwassermessstellen, Sohlschwellen und künstlich angelegten Forellenlaichgruben.

welches von Süden nach Norden verläuft, wurde die Enziwigger durch Begradigung und Kanalisierung im 20. Jahrhundert stark verkürzt und über weite Strecken auf die östliche Talseite verlegt. Heute sind ca. 60% der Enziwigger stark beeinträchtigt (Schager and Peter, 2001, 2002). Um die Tiefenerosion der Flusssohle zu verhindern oder wesentlich zu reduzieren wurde die Sohle mit Schwellen stabilisiert und die Böschungen mit Blocksteinen gesichert. Die Sohlschwellen mit einer Metallarmierung wurden alle 10 bis 15 m in die Flusssohle eingebracht. Dadurch ist das Fließregime hinsichtlich von Strömung und Wassertiefe vergleichsweise monoton. Unterhalb einiger dieser Schwellen haben sich Kolke gebildet, welche lokal die Flusstiefe stark erhöhen. Trotz dieser Flussverbauungen gilt die Enziwigger als gutes Forellenlaichgewässer (Schager and Peter, 2001, 2002). Die Gewässerbettstruktur der Enziwigger ist charakteristisch für viele voralpine Fließgewässer wie auch Mittelgebirgsflüsse und erlaubt es den Einfluss von wasserbaulichen Massnahmen, wie z.B. Sohlschwellen, auf die Austauschprozesse der Fluss-Grundwasser-Interaktion in den verschiedenen Massstabsbereichen zu evaluieren.

Das Untersuchungsgebiet selbst ist ca. 0.1 km² gross und liegt auf einer mittleren Höhe von ca. 624 m ü. M. (Fig. 5.1). Hier ist der Talgrundwasserleiter charakterisiert durch teilweise gering mächtige Quartärbedeckung (bis ca. 13 m in der Talmitte, Bohrtiefe BP1; Fig. 5.1d), bestehend aus Bachschuttkegeln, Gehängebildungen, fluvialen Sedimenten hochwürmeiszeitlicher Niederterassenschotter (Landeshydrologie und -geologie, 1994) und rezenten Alluvionen. Der Grundwasserstauer ist charakterisiert durch Konglomerate und Sandsteine der oberen Meeres- und oberen Süsswassermolasse.

Die durchschnittliche Jahressumme des Niederschlags im Zeitraum von 2000 bis 2009 beträgt 1055 mm (Messstelle LU 08 Willisau). Hydrologisch ist das Einzugsgebiet durch Schnee im Winter (Dezember bis April) und das Auftreten von starken konvektiven Niederschlägen im Sommer gekennzeichnet. Das Wasserrückhaltevermögen der Böden im Quellgebiet und somit die Speicherkapazität im Einzugsgebiet ist klein. Dadurch ist der Abfluss stark durch Starkniederschlagsereignissen beeinflusst. Der mittlere Abfluss der Enziwigger beträgt ca. 2 m³ s⁻¹, der minimale Abfluss lag bei ca. 1 m³ s⁻¹ und der maximale Abfluss lag bei ca. 10 m³ s⁻¹ (Messreihe von Mitte November 2007 bis Mitte November 2008, welche im Rahmen eines Bauprojektes in Willisau aufgezeichnet wurde).

5.4 Methoden und Datengrundlagen

Der multidimensionale Untersuchungsansatz umfasst unterschiedliche Methoden und Skalenbereiche: I) Erfassen der hydrologischen und Grundlagendaten im Einzugsgebiet der Enziwigger und Darstellung in einem Datenbank-GIS-System; II) Installation von Messsystemen zur Aufzeichnung hydraulischer und physikalischer Daten im Fließgewässer, in der Gewässersohle und im flussnahen Grundwasser; III) Aufnahme der Flussbetttopographie; sowie IV) Grundwasserströmungsmodellierung und Szenarienberechnungen.

5.4.1 Hydrologische Grundlagen

Die meteorologischen Grundlagendaten basieren auf Messungen der Station Willisau (MeteoSchweiz Stationsnummer 6130). Für die Abschätzung des Beitrags der Schnee-

5.4. METHODEN UND DATENGRUNDLAGEN

schmelze am Gesamtabfluss wurden Lufttemperaturmessungen aus Hergiswil südlich von Willisau (Messintervall 5 min; MeteoSchweiz, Stationsnummer 6133) sowie tägliche Schneetiefen aus dem 4 km entfernten Nebental Luthern (MeteoSchweiz Stationsnummer 6630) verwendet.

5.4.2 Messsysteme zur Aufzeichnung hydraulischer und physikalischer Parameter

Mit der Direct-Push Technik (Geoprobe Kansas / USA) wurden für Standort B insgesamt 5 Grundwassermessstellen im Talbereich und am Flussufer errichtet (Sondiergrösse von 2,152" für den Ausbau von 1" Messstellen Rammsondierung, Fig. 5.1). Die Sondierungen konnten bis zur Felsoberfläche (Annahme) in Tiefen von ca. 12.8 m im Talbereich und von ca. 4.4 m am Flussufer abgeteuft werden. Die Sondierung in der Talmitte (BP1) sowie zwei Sondierungen am Flussufer (BP3, BP5) sind als Grundwassermessstellen ausgebaut und mit Messsonden zur kontinuierlichen Aufzeichnung des Grundwasserpegels, der Grundwassertemperatur und der elektrischen Leitfähigkeit (nur BP3 und BP5) ausgestattet. Während mit den Messungen im Uferbereich die lokalen Austauschprozesse im Bereich der Flussabschnitte untersucht werden, diente die Messung in der Talmitte der Abschätzung des Einflusses des regionalen auf lokalen Grundwasserfließregimes. Die Analyse von Fluss- und Grundwasserpegeldaten im Uferbereich und in der Talmitte ermöglichten eine erste Abschätzung der In- und Exfiltrationsverhältnisse.

Für die Untersuchungen in der Gewässersohle wurde die Temperatur in zwei unterschiedlichen Tiefen (zwischen 10 und 38 cm) in drei künstlich angelegten Laichgruben kontinuierlich gemessen (Fig. 5.1). Die tägliche Temperaturamplitudendifferenz zwischen dem Oberflächen- und Interstitialwasser wurde verwendet um die spezifische Austauschrate q zu berechnen (Hatch et al., 2006; Keery et al., 2007). Eine hohe spezifische Austauschrate führte zu einer Annäherung der Temperaturverläufe in den zwei Tiefen an den Temperaturverlauf des Oberflächenwassers, eine niedrige Austauschrate zu einem abgeflachten Verlauf in der Tiefe. Exfiltrierendes Grundwasser konnte bei einer zusätzlich verstärkten Abflachung ermittelt werden. Diese Methode erlaubte es, zwei q -Werte pro Tag zu berechnen. Somit konnte lokal der zeitlichen Verlauf der Durchlässigkeiten nach dem Bau der Laichgruben im November bis zum Schlupf der Eier im März beschrieben werden (Schindler Wildhaber et al., 2014, Chap. 6). Die berechneten Durchlässigkeitswerte der Monate Februar und März wurden gemittelt, in der Annahme, dass sich bis dahin die anfänglich erhöhte Durchlässigkeit durch den Bau der Laichgrube auf einem natürlichen Level stabilisiert hat.

5.4.3 Flussbetttopographie

Da Änderungen der Struktur und Zusammensetzung der Flusssohle nach starken Hochwässern mehrmals festgestellt wurden, fanden insgesamt drei Neuvermessungen der Flussbetttopographie statt (Fig. 5.1e). Differenzkarten von aufeinanderfolgenden Messungen ermöglichten es, Bereiche in den untersuchten Flussabschnitten auszuweisen, in denen Akkumulations- oder Erosionsprozesse während der Hochwasserereignisse dominiert haben (Schindler Wildhaber et al., 2014, Chap. 6).

Tabelle 5.2: Definition Modellrandbedingungen (Fig. 5.1).

Randbedingung	Art	Beschreibung
Regionale Grundwasserflüsse ins Modellgebiet hinein (Süden) und hinaus (Norden)	1. Art (Festpotenzial, variabel über die Zeit)	Regionales Modell: Lineare Interpolation von Piezometerhöhen zwischen zwei im Haupttal liegenden Grundwasserpegeln
Seitenzuflüsse aus den Hangbereichen	2. Art (Randzufluss und -abfluss, variabel über die Zeit)	Zuflüsse entsprechen Grundwasserneubildung (meteo. Daten, siehe Sec. 5.4.2) integriert auf Hangeinzugsgebietflächen, die mittels hydrologischer Oberflächenmodellierung auf Basis des digitalen Höhenmodells evaluiert wurden
Enziwigger	3. Art (halbdurchlässiger Rand, variable Abflusstiefe über Zeit + Austauschrate)	Regionales Modell: Linie mit "RiverPackage Lokales Modell: flächig als "General Head Boundary"(GHB); Austauschrate (Conductance-Wert): kalibriert
Grundwasserneubildung durch flächig versickerndes Niederschlagswasser		Täglicher Niederschlag, mit Berücksichtigung Schneehöhen, Lufttemperatur und Jahreszeiten. Abschätzung der Schneeschmelze basiert auf Temperaturindex Modell: Summe der stündlich gemessen Lufttemperatur negativ: Niederschläge = Schnee. Wenn diese Summe positiv: Schneeschmelzvorrat wird proportional zur Temperatursumme und zu Schneeschmelzfaktor vom 0.01 (Tag x °C) ⁻¹ verringert (Debele et al., 2010). Wasservolumen von Niederschlag bei Temperaturen über 0°C trägt mit Faktor von 0.3 zur Grundwasserneubildung bei.

5.4.4 Grundwasserströmungsmodell und Szenarienberechnungen

Die Grundwasserströmungsberechnungen wurden in einem regionalen und lokalen Massstab durchgeführt und dienen der Abschätzung von räumlichen und zeitlichen Variationen des Grundwasserfließregimes (Grundwasserfließfeld, -fließgeschwindigkeiten und Wasserbilanzen). Mit den Modellen wurden verschiedene Prozesse detailliert untersucht, einschliesslich der Sensitivität von Randbedingungen sowie des zeitlich und räumlich instationären Charakters der Fluss-Grundwasser-Interaktion. Ein Schwerpunkt liegt auf der Beantwortung der Frage nach dem Zusammenhang zwischen Oberflächenmorphologie des Fließgewässers und der Wasserwegsamkeit im hyporheischen Interstitial. Eine Abschätzung der Einflüsse von verschiedenen Parametern und Randbedingungen (z.B. Flussbettmorphologie, Verteilung der Flussbettdurchlässigkeit), beruht auf Szenarienberechnungen mit dem kalibrierten Grundwassermodell.

Die Grundwasserströmungsberechnungen erfolgten mit GMS (Groundwater Modeling System 7.1; Environmental Modeling Systems, 2002) auf der Basis von MODFLOW (McDonald and Harbaugh, 1996). Die Randbedingungen des regionalen Modells (230 m x 340 m, Auflösung 2 m x 2 m) wurden auf die Randbedingungen des lokalen Modells (110 m x 60 m, Auflösung 0.5 m x 0.5 m) übertragen (Fig. 5.1). Für die Beschreibung des Verlaufs der Felsoberfläche wurden Angaben zu Eindringtiefen der Direct-Push Erkundung herangezogen. Für das regionale Modell wurde weiterhin angenommen, dass im Bereich der westlichen und östlichen Hangbereiche die Hangsteigung im Zusammen-

5.5. RESULTATE

hang mit dem Verlauf des Grundwasserstauers steht (Fig. 5.1b,d). Für das lokale Modell wurden zudem die hochaufgelösten Flussbettvermessungen berücksichtigt (Fig. 5.1e). Die Randbedingungen für die Grundwasserströmungsmodellierung werden in Table 5.2 zusammengefasst. Aufbauend auf flusssedimentologischen Überlegungen und dem Vorhandensein von Grundwassermessungen wurden die Durchlässigkeiten des Grundwasserleiters und an der Flusssohle instationär (220 Tage, Tagesauflösung) invers kalibriert (Pilot Point, PEST; Doherty, 1994) sowie eine Sensitivitätsanalyse der relevanten Parameter durchgeführt. Kalibrierte Durchlässigkeiten des Grundwasserleiters bewegen sich zwischen 10^{-2} und 10^{-4} m s^{-1} . Im Bereich des Hauptgrundwasserstroms und im unmittelbaren Bereich der Enziwigger sind die kalibrierten Durchlässigkeiten tendenziell höher. In Fig. 5.3 sind die kalibrierten Durchlässigkeiten (19 bis 62 d^{-1}) der Flusssohle für die verschiedenen Gewässerabschnitte dargestellt.

Mit dem kalibrierten lokalen Grundwasserströmungsmodell wurden anschliessend Szenarien definiert. Zusätzlich zum Ausgangsmodell (Szenario 1) wurde ein Modellszenario nur mit den Sohlschwellen und ohne differenzierte Flussbetttopographie (Szenario 2) sowie ein Modellszenario mit einem gleichmässigen Gefälle ohne Sohlschwellen und Flussbetttopographie (polynomial, 2. Grad interpoliert, Szenario 3) vorbereitet. Die Szenarienberechnungen erlauben es, die Austauschraten und Fliessgeschwindigkeiten zwischen dem Modell mit hochaufgelöster Flussbetttopographie mit den Modellszenarien mit monotonerer Flussbetttopographie zu vergleichen.

5.5 Resultate

5.5.1 Hydrologie

Fig. 5.2 zeigt die Zeitreihen der Tagessummen des Niederschlags, der Schneetiefe, der Lufttemperatur im Einzugsgebiet der Enziwigger und den Verlauf des Flusspegels für den Zeitraum von November 2010 bis Ende März 2011. Deutlich ist ein Zusammenhang von einzelnen Niederschlagsereignissen und dem Flusspegellauf in der Enziwigger und zwischen Schneetiefe und Temperaturverlauf zu beobachten. Temperaturanstiege bei einer vorhandenen Schneedecke führen zu Schmelzereignissen, welche durch die Erhöhung des Oberflächenabflusses zu einem Anstieg des Flusspegels führen. Sowohl bei Niederschlag- als auch auf Schneeschmelzereignissen steigt der Flusspegel rasch an. Dies ist ein Hinweis für eine kleine Speicherkapazität des Molasseuntergrundes im Einzugsgebiet ohne wesentliche Pufferwirkung des Grundwassers.

5.5.2 Hydraulische und physikalische Parameter

Table 5.3 fasst die wesentlichen Resultate der Messungen im Fluss, im Grundwasser und in den Laichgruben zusammen. Die Untersuchungen orientierten sich vor allem an den Laichperioden 2009/2010 und 2010/2011. Messungen des Flusspegels erstreckten sich für die erste Laichperiode über den Zeitraum von November 2009 bis August 2010 (teilweise blieben einzelne Messgeräte im Fluss länger installiert) und für die zweite Laichperiode über den Zeitraum von November 2010 bis Ende März 2011. Die Messungen in den Grundwasserpegeln lieferten kontinuierliche Zeitreihen über den gesamten Zeit-

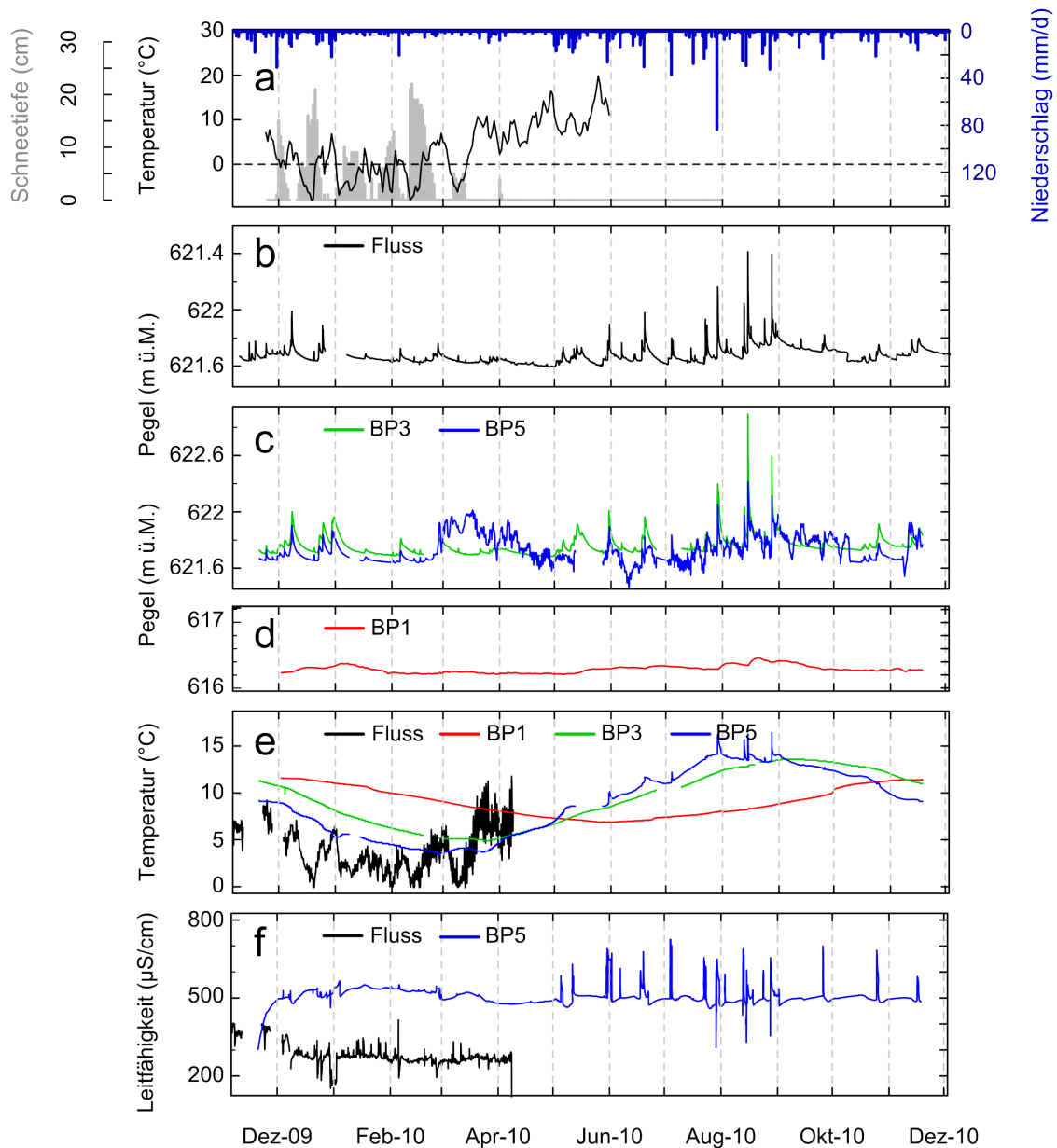


Abbildung 5.2: Zeitreihen von: **a)** meteorologischen Daten im Einzugsgebiet der Enziwigger; **b)** Pegeldaten im Fluss; **c)** Pegeldaten im ufernahen Grundwasser (BP3 und 5); **d)** Pegeldaten im Talgrundwasserleiter (BP1); **e)** Temperaturdaten im Fluss und im Grundwasser (BP1, 3 und 5); und **f)** Daten der elektrischen Leitfähigkeiten im Fluss und im Grundwasserpegel BP5 (BP5). Für die Lage der Grundwassermessstellen siehe Fig. 5.1.

raum vom November/Dezember 2009 bis Dezember 2010. Die im Rahmen dieser Arbeit diskutierten Austauschprozesse im Skalenbereich der Laichgruben konzentrieren sich auf die erste Laichperiode und den Zeitraum vom November bis Ende März 2010.

Der Grundwasserpegel in der Messstelle BP1 im Tal (Fig. 5.1) zeigt ein gedämpftes Signal des Pegelverlaufs. Ein Minimum des Grundwasserpegels kann zwischen Februar und März 2010 beobachtet werden, welches darauf zurückgeführt werden kann, dass

5.5. RESULTATE

Tabelle 5.3: Zusammenfassung der Resultate der Fluss- und Grundwassermessungen (BP1, 3 und 5, siehe Fig. 5.1 und 5.2), der Temperaturanalysen in den Forellenlaichgruben (B42, 51 und 52, siehe Fig. 5.1) und der Grundwasserströmungsmodellierung. Mittelwerte \pm Standardabweichung. T = Temperatur, P = Pegel, GW=Grundwasser

	Messzeitraum P (m ü. M.) (MM.YY)	P (m ü. M.)	T (°C)	Saisonal T- amplitude α (°C)	Saisonale Verzögerung im Ver- gleich zum Flussignal τ_T (d)	Berechnete spezifische Aus- tauschra- ten (md^{-1}) T-analyse	Berechnete spezifische Aus- tauschra- ten (md^{-1}) GW- modell
Fluss	11.09 - 08.10 11.10 - 03.11	621.66 ± 0.05	9.47	7.07			
BP1	12.09 - 04.11	616.28 ± 0.05	9.15	2.2	124.1		
BP3	11.09 - 04.11	621.75 ± 0.07	9.7	4.2	47.97		
BP5	11.09 - 03.11	621.72 ± 0.09	9.25	5.14	29.47		
B42	02.10 - 03.10		3.32 ± 2.16			0.13 ± 0.01	1.35 ± 0.02
B51	02.10 - 03.10		3.19 ± 2.11			0.11 ± 0.02	-0.24 ± 0.04
B52	02.10 - 03.10		3.39 ± 2.09			0.12 ± 0.01	0.59 ± 0.06

in diesem Zeitraum wenige Hochwasserereignisse stattfanden. Generell ist der Grundwasserpegel im Vergleich zum Flusspegel über 5 m niedriger. Auf der regionalen Skala dominiert somit der Gradient vom Fluss zum Grundwasser und der Prozess der Flusswasserinfiltration (Fig. 5.1, 5.2 und Table 5.1, 5.3). Auch die Temperaturdaten in der Grundwassermessstelle BP1 im Tal zeigen ein gedämpftes Signal im Jahresverlauf und eine saisonalen Verzögerung im Vergleich zum Verlauf der Lufttemperatur von ca. 124 Tagen. Diese Retardation resultiert in einem im Vergleich zum Verlauf der Lufttemperatur verzögerten Auftreten von Extremwerten. Temperaturmaxima werden im Dezember und Temperaturminima im Juni beobachtet.

Fig. 5.2 zeigt auch den Verlauf der Grundwassermessungen in den beiden Messstellen am Flussufer BP3 und BP5 im Vergleich zu den Messungen im Fluss und im Talgrundwasserleiter (Fig. 5.1 und Table 5.3). Lokal im Bereich von Messstelle BP3 oberhalb einer Sohlschwelle dominieren flusswasserinfiltrierende und im Bereich von Messstelle BP5 unterhalb einer Sohlschwelle exfiltrierende Verhältnisse. Die Grundwasserpegeldaten in den Grundwassermessstellen am Flussufer verlaufen ähnlich wie der Flusspegel. Im Frühling ist in Grundwassermessstelle BP5, welche ansonsten einen gleichen Pegelverlauf wie BP3 zeigt, ein abweichender Pegelverlauf erkennbar. Diese Abweichung wird auf den Einfluss des Hangzustroms nach Schneeschmelzereignissen zurückgeführt (Fig. 5.2). Saisonale Verzögerungen der Grundwassertemperaturen im Vergleich zum Verlauf der Lufttemperatur liegen bei 29 bis 50 Tagen. Generell haben die Grundwassertemperaturen eine kleinere Temperaturamplitude als der Fluss und das Signal ist verzögert (Fig. 5.2). Tägliche Temperaturschwankungen im Fluss können im flussnahen Grundwasser nicht mehr beobachtet werden. Temperaturmessungen in Grundwassermessstelle BP5 unterhalb einer Sohlschwelle zeigen eine stärkere Reaktion auf Temperaturschwankungen des Flusswassers als jene in BP3 oberhalb der Schwelle in der eine grössere Dämpfung und Verzögerung von Temperatursignalen aus dem Fluss beobachtet werden kann (eine Interpretation für diese Beobachtung wäre, dass nur bei vergleichsweise grossen Hochwasserereignissen eine direkte Infiltration von Flusswasser stattfindet).

Die elektrischen Leitfähigkeiten wurden nur im Fluss und in der Grundwassermessstelle BP5 gemessen. Die mittlere elektrische Leitfähigkeit im Fluss liegt bei $276 \mu\text{S cm}^{-1}$ und bei Grundwassermessstelle BP5 bei $504 \mu\text{S cm}^{-1}$. Wohingegen bei kleineren und mittleren Hochwasserereignissen ein Ansteigen der elektrischen Leitfähigkeit beobachtet werden kann, kann bei grossen Hochwasserereignissen ein Abfallen der elektrischen Leitfähigkeit beobachtet werden (Eine Interpretation für diese Beobachtung wäre, dass während kleinerer und mittlerer Hochwasserereignissen Niederschlagswasser lokal über die ungesättigte Zone und bevorzugte Fliesspfade (Makroporen) versickert. Da das Gebiet landwirtschaftlich genutzt wird führt der Transport von nitrathaltigem Wasser über die ungesättigte Zone zu den Anstiegen der elektrischen Leitfähigkeit. Bei grossen Hochwasserereignissen hingegen führt die Infiltration von Flusswasser mit niedrigen elektrischen Leitfähigkeiten zu einem Abfallen der elektrischen Leitfähigkeit im ufernahen Grundwasser).

Die Resultate der Temperaturmessungen in den künstlichen Forellenlaichgruben (Fig. 5.1) werden in Schindler Wildhaber et al. (2014) in Detail beschrieben (Chap. 6). In Table 5.3 werden die für die vorliegende Arbeit relevanten wesentlichen Resultate zusammengefasst. Mittlere Temperaturen im Flussbett für Messstandort B42 liegen bei 3.32°C , für Messstandort B51 bei 3.19°C und für Messstandort B52 bei 3.39°C . Berechnete Austauschraten durch das Flussbett liegen für Messstandort B42 bei 0.13 m d^{-1} , für Messstandort B51 bei 0.11 m d^{-1} und für Messstandort B52 bei 0.12 m d^{-1} .

5.5.3 Lokales und regionales Grundwasserströmungsmodell

Die Quantifizierung des zeitlichen Verlaufs der Fluss-Grundwasser-Interaktion erfolgt mit Hilfe regionaler und lokaler hochauflösender kalibrierter Grundwasserströmungsmodelle. Fig. 5.1 zeigt das berechnete Grundwasserfliessregime für das regionale und lokale Grundwasserströmungsmodell für eine Mittelwassersituation am 20. April 2010 (Fig. 5.2). Das berechnete Grundwasserfliessregime für den regionalen Massstabsbereich bildet vor allem die regionale Grundwasserströmung im Talgrundwasserleiter von Süden nach Norden sowie den Einfluss der Flusswasserinfiltration im ufernahen Bereich nach. Deutlich ist der hydraulische Gradient vom Fliessgewässer zum Talgrundwasserleiter zu erkennen. Das berechnete Grundwasserfliessregime für den lokalen Massstabsbereich bildet vor allem den Einfluss der Flusswasserinfiltration im ufernahen Bereich und den Übergang zur regionalen Grundwasserströmung nach.

Die berechneten Wasserbilanzen für das regionale und lokale Grundwasserströmungsmodell lassen sich wie folgt zusammenfassen. Im regionalen Maßstabsbereich können 70% der Gesamtwasserbilanz der Flusswasserinfiltration und 30 % dem Talgrundwasserzustrom aus dem Süden (inflow) sowie 12 % der Gesamtwasserbilanz der Grundwasserexfiltration und 88 % dem Talgrundwasserabstrom gegen Norden (outflow) zugeschrieben werden. Im lokalen Maßstabsbereich können 86 % der Gesamtwasserbilanz der Flusswasserinfiltration, 12 % dem Talgrundwasserzustrom aus dem Süden und 2 % dem Hangwasserzustrom (inflow) sowie 30 % der Gesamtwasserbilanz der Grundwasserexfiltration und 70 % dem Talgrundwasserabstrom gegen Norden (outflow) zugeschrieben werden. Die Zahlen verdeutlichen die Abhängigkeit der Gesamtwasserbilanzen vom betrachteten Maßstab. Im regionalen Maßstab machen In- und

5.5. RESULTATE

Tabelle 5.4: Berechnete Aufenthaltszeiten (t) und Fliesspfade (d) zu den Grundwassermessstellen (BP1, 3 und 5, siehe Fig. 5.1) für die regionale und lokale Grundwasserströmungsmodellierung und die verschiedenen Szenarienberechnungen.

		Regionales Model	Lokales Model		
			scn1	scn2	scn3
BP1	t (d)	12.3 ± 0.4	14.2 ± 0.5	14.1 ± 0.5	14.1 ± 0.5
BP1	d (m)	92.6 ± 1.7	90.4 ± 0.7	89.4 ± 0.8	89.6 ± 0.9
BP3	t (d)	0.5 ± 0.2	4.3 ± 1.2	4.5 ± 1.4	3.2 ± 0.5
BP3	d (m)	9.5 ± 2.8	21.3 ± 3.8	20.2 ± 3.3	21.9 ± 1.8
BP5	t (d)	0.8 ± 0.2	4.2 ± 3.2	4.3 ± 3.2	3.3 ± 1.7
BP5	d (m)	11.6 ± 2.0	13.3 ± 0.5	13.3 ± 0.5	23.6 ± 4.8

Exfiltration von Fluss- und Grundwasser 70 % und 12 % im lokalen Maßstab hingegen 86 % und 30 % der Gesamtwasserbilanz aus.

Table 5.4 fasst die berechneten Aufenthaltszeiten sowie die Länge der Fliesspfade von Flussinfiltrat zwischen der Enziwigger und den verschiedenen Grundwassermessstellen zusammen. Infiltriertes Flusswasser benötigt demnach für einen Fliesspfad von ca. 93 m ca. 12 Tage um Grundwassermessstelle BP1 im Tal zu erreichen. Hingegen erreicht infiltriertes Flusswasser die ufernahen Grundwassermessstellen auf Fliesspfaden von ca. 10 und 12 m schon nach ca. 0.5 und 0.8 Tagen.

Fig. 5.3 zeigt die räumliche Verteilung der berechneten Flussinfiltration und Grundwasserexfiltration im Flussbett des untersuchten Gewässerabschnittes für verschiedene Wasserstände (Fig. 5.2). Deutlich ist, unabhängig vom Wasserstand, die Dominanz der Infiltration oberhalb und der Exfiltration unterhalb der Sohlschwellen. Vor den Schwellen erreicht die Infiltration von Flusswasser in das Grundwasser Werte zwischen 2 und 3.5 m d⁻¹, die Exfiltration von Grundwasser in den Fluss unterhalb erreicht Werte zwischen 2 und 3.5 m d⁻¹. Im Bereich zwischen den Schwellen dominiert die Infiltration von Flusswasser in das Grundwasser, was auch durch das regionale Grundwasserfließregime und dem hohen Gradienten vom Fluss zum Talgrundwasserleiter bedingt ist (vgl. Fig. 5.1). Der Einfluss des regionalen Grundwasserfließregimes manifestiert sich durch einen Anstieg der Austauschraten zwischen den Schwellen zum linken Ufer hin. Der Einfluss von Hochwasserereignissen lässt sich hingegen eher am zeitlichen Verlauf der In- und Exfiltration beschreiben.

Fig. 5.4 zeigt den zeitlichen Verlauf von In- und Exfiltrationsraten welche für die drei künstlich angelegten Forellenlaichgruben berechnet wurden (Fig. 5.1). Die grössten Austauschraten wurden für Forellenlaichgrube B42 berechnet gefolgt von Forellenlaichgrube B52. Beide Forellenlaichgruben befinden sich in Bereichen vor einer Sohlschwelle und somit in Zonen des Flussbettes in denen die Infiltration von Flusswasser in das Grundwasser dominiert. Negative Austauschraten wurden für B51 berechnet. Diese Forellenlaichgrube befindet sich in Bereichen hinter einer Sohlschwelle und somit in Zonen des Flussbettes in denen die Exfiltration von Grundwasser in das Flusswasser dominiert. Mit dem Grundwassermodell berechnete Austauschraten durch das Flussbett im Bereich der Forellenlaichgruben liegen für Messstandort B42 bei 1.35m d⁻¹ mit einer Standardabweichung von 0.02 m d⁻¹, für Messstandort B51 bei -0.24 m d⁻¹ mit einer Standardabweichung von 0.04 m/s und für Messstandort B52 bei 0.59 m d⁻¹ mit einer Standardabweichung von 0.06 m d⁻¹ (Table 5.3). Wohingegen die Grundwassermodellierung es

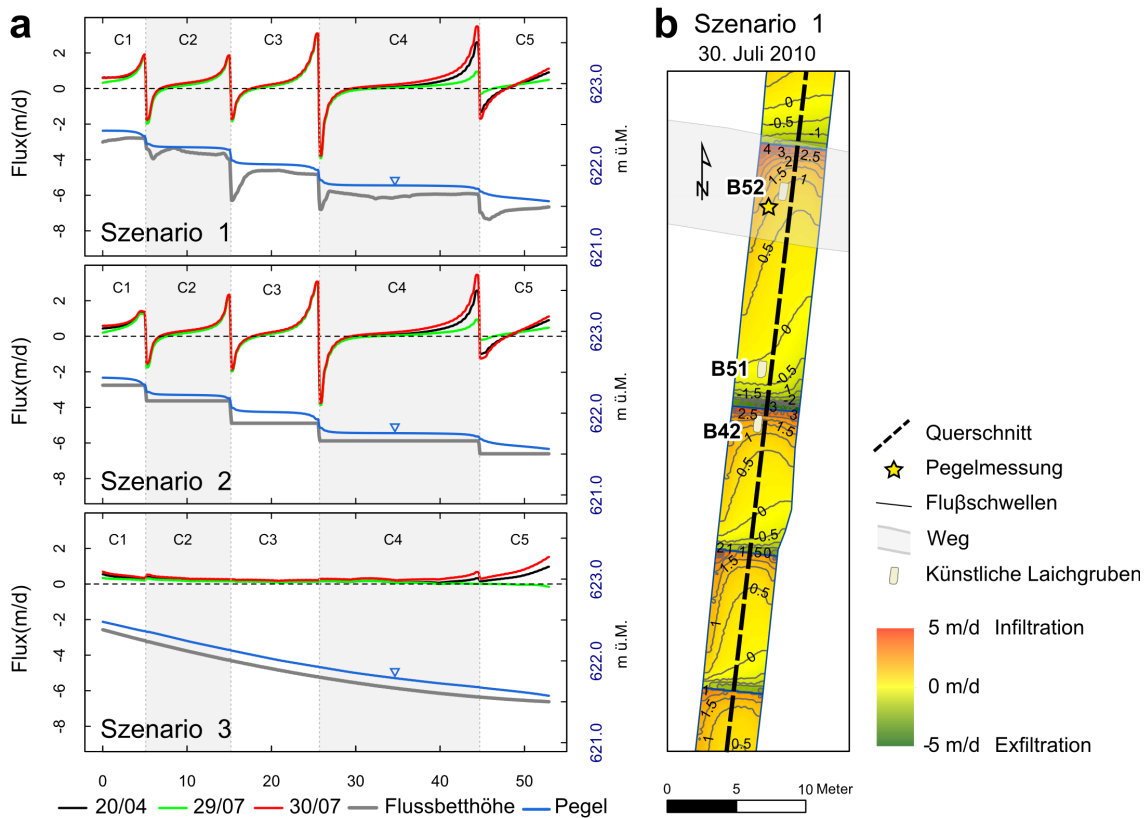


Abbildung 5.3: a) Berechnete Austauschraten für drei Szenarien während Mittel- und Hochwasser (Fig. 5.2). Auch dargestellt sind der Flusspegel und der Verlauf des Flussbettes in der Mitte der Enziwigger. Der 20. April 2010 sowie der 29. Juli 2010 entsprechen einem niedrigen Wasserstand, während der 30. Juli 2010 fand ein Hochwasserereignis statt (Fig. 5.2). Positive Werte entsprechen einer Infiltration vom Flusswasser in das hyporheische Interstitial; negative Werte entsprechen einer Exfiltration vom Grundwasser in den Fluss. b) Räumliche Verteilung der Austauschraten im Flussbett des untersuchten Gewässerabschnitts der Enziwigger für das lokale Grundwasserströmungsmodell (Szenario 1).

erlaubt Austauschraten über das gesamte Flussbett zu berechnen sind die spezifischen Austauschraten welche aus der Temperaturmethode abgeleitet wurden nur für die lokale Skala der Forellenlaichgrube charakteristisch (dm-Bereich).

5.5.4 Szenarienberechnungen mit dem lokalen Grundwasserströmungsmodell

Zusätzlich zum Ausgangsmodell (Szenario 1) wurden mit dem kalibrierten lokalen Grundwasserströmungsmodell Modellszenarien definiert. Ein Szenario (Szenario 2) berücksichtigt nur die Sohlschwellen nicht aber die differenzierte Flussbetttopographie (Fig. 5.3b, 5.5). Ein weiteres Szenario (Szenario 3) berücksichtigt lediglich ein gleichmässiges Gefälle ohne Sohlschwellen und Flussbetttopographie (polynomial, 2. Grad) interpoliert, Fig. 5.3).

Fig. 5.3a zeigt den Verlauf des Flussbettes in der Mitte der Enziwigger für die drei Szena-

5.5. RESULTATE

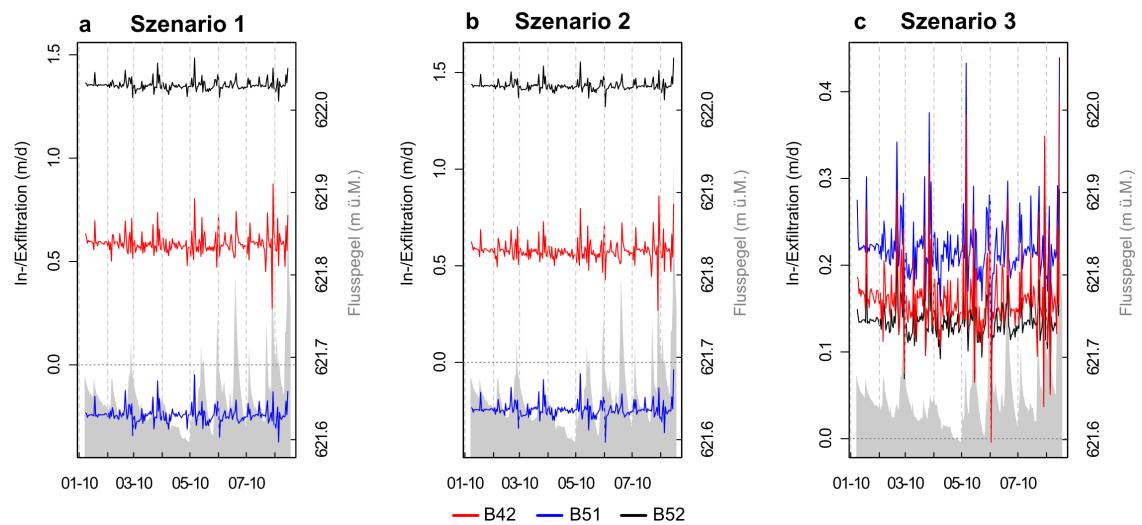


Abbildung 5.4: Flusspegel in der Enziwigger und zeitliche Verläufe der berechneten Austauschraten durch die künstlich angelegten Forellenlaichgruben (B42, 51 und 52, siehe Fig. 5.1) für den gesamten instationär modellierten Zeitraum. Positive Werte entsprechen einer Infiltration vom Flusswasser in das hyporheische Interstitial; negative Werte entsprechen einer Exfiltration vom Grundwasser in den Fluss. Die Unterschiedliche Skalierung bei Szenario 3 ist zu beachten.

rien sowie berechnete Austauschraten für den gesamten simulierten Gewässerabschnitt. In Szenarien 1 und 2 ist zu erkennen, dass vor den Sohlschwellen die Infiltration von Flusswasser in das hyporheische Interstitial und hinter der Sohlschwelle die Exfiltration von Grundwasser in das Flusswasser dominiert. Bezüglich der Verteilung von In- und Exfiltrationsraten ist der Unterschied zwischen den Szenarien 1 und 2 gering. Die Exfiltration von Grundwasser in den Fluss unterhalb der Sohlschwellen nimmt wegen der fehlenden Kolke für Szenario 2 leicht ab. Die Berechnungen für Szenario 3 zeigen einen sehr ausgeglichenen Verlauf mit ausschliesslich Infiltration von Flusswasser in das hyporheische Interstitial. Infiltrationsmengen liegen unter $0.5 \text{ m}^2 \text{ d}^{-1}$. Austauschprozesse werden vom regionalen Grundwasserfließregime und bevorzugter Infiltration von Flusswasser in das hyporheische Interstitial dominiert. Ein Ansteigen der Austauschraten am unteren Ende des untersuchten Flussabschnittes ist modelltechnisch begründet.

Fig. 5.4 zeigt die zeitliche und räumliche Verteilung von In- und Exfiltration in den künstlich angelegten Forellenlaichgruben und entlang des untersuchten Flussabschnittes für die drei berechneten Szenarien. Auch hier bestehen für die Szenarien 1 und 2 kaum Unterschiede. Berechnete Austauschraten durch die Forellenlaichgruben sind für Szenario 3 stark reduziert. Für die Szenarien 1 und 2 dominiert vor der Sohlschwelle die Infiltration von Flusswasser in das hyporheische Interstitial. Hinter der Sohlschwelle hingegen dominiert die Exfiltration von Grundwasser in das Flusswasser. Dazwischen existieren Zonen, in denen, in Abhängigkeit der Lage des Flusspegels, In- und Exfiltration abwechseln können. Die Berechnungen für Szenario 3 hingegen zeigen, dass vor allem zum linken Ufer hin, die Infiltration von Flusswasser in den Grundwasserleiter zunimmt. Zum rechten Ufer können In- und Exfiltration abwechseln. Ausschliesslich Exfiltration, wie in den Szenarien 1 und 2, kann nicht mehr beobachtet werden. Alle drei Szenarien

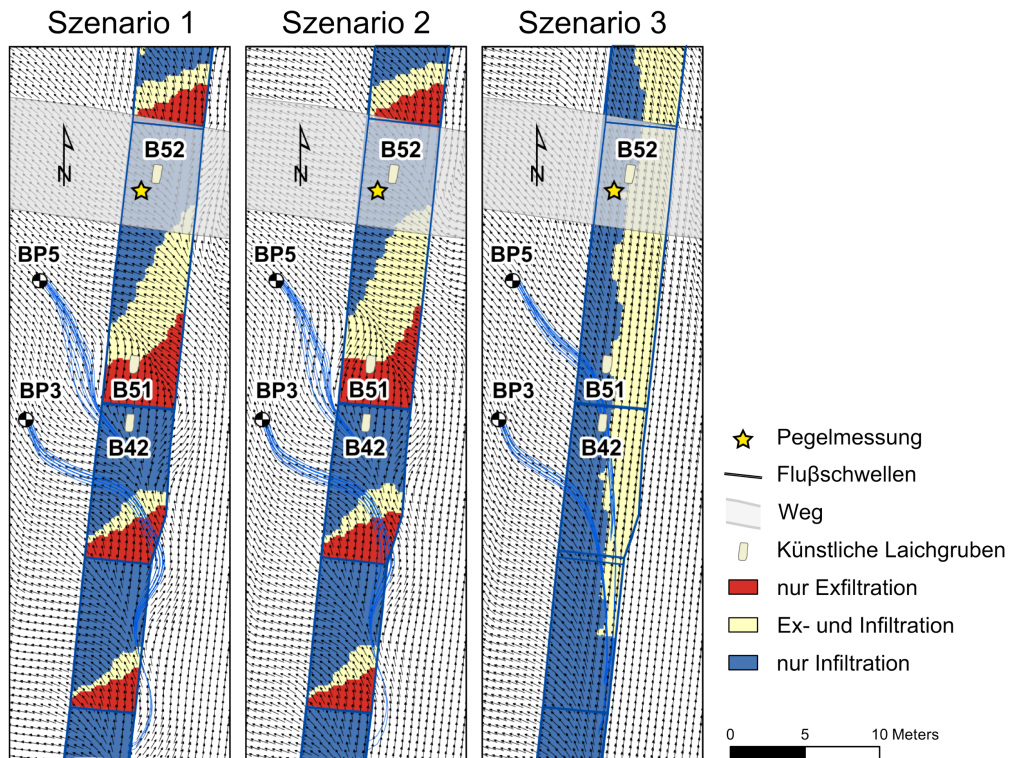


Abbildung 5.5: a) Strömungsvektoren und Zuströmbereiche zu den Grundwassermessstellen dargestellt für die drei Szenarien. b) Räumliche Verteilung der Austauschprozesse für die drei berechneten Szenarien über die gesamte Simulationszeit. Kalibrierte Durchlässigkeit der Flusssohle: $C1 = 19 \text{ (m}^2 \text{ d}^{-1}) \text{ m}^{-2}$, $C2 = 50 \text{ (m}^2 \text{ d}^{-1}) \text{ m}^{-2}$, $C3 = 42 \text{ (m}^2 \text{ d}^{-1}) \text{ m}^{-2}$, $C4 = 62 \text{ (m}^2 \text{ d}^{-1}) \text{ m}^{-2}$, $C5 = 19 \text{ (m}^2 \text{ d}^{-1}) \text{ m}^{-2}$.

zeigen, dass der Einfluss des regionalen Grundwasserfließregimes und Infiltrationsprozesse zum linken Ufer hin ansteigen.

Fig. 5.5 veranschaulicht auch das Grundwasserfließregime für die verschiedenen Szenarien anhand von Fließvektoren und Zuströmbereichen zu den verschiedenen Grundwassermessstellen. Der Einfluss der Sohlschwelle ist für die Szenarien 1 und 2 deutlich zu erkennen. Interessant ist der Zuströmbereich zu Grundwassermessstelle BP3; Flusswasser infiltriert oberhalb einer Sohlschwelle in das hyporheische Interstitial und fließt unterhalb des Flussbettes der Grundwassermessstelle BP3 zu. Das Grundwasserfließfeld für Szenario 3 ist hingegen, wie zu erwarten, sehr viel gleichmäßiger.

Table 5.4 fasst die berechneten Aufenthaltszeiten sowie die Länge der Fließpfade von Flussinfiltrat zwischen der Enziwigger und den verschiedenen Grundwassermessstellen zusammen. Für das lokale Modell und alle drei Szenarien benötigt infiltriertes Flusswasser für einen Fließpfad von ca. 90 m ca. 14 Tage um Grundwassermessstelle BP1 im Tal zu erreichen. Im ufernahen Bereich unterscheiden sich Länge der Fließpfade und Fließzeiten hingegen für die ersten beiden und das letzte Szenario. Für die beiden ersten Szenarien benötigt infiltriertes Flusswasser für Fließpfade von ca. 13 und 21 m Fließzeiten von ca. 4.2 und 4.3 Tage um die ufernahen Grundwassermessstellen zu erreichen. Für

5.6. DISKUSSION

das letzte Szenario hingegen erreicht infiltriertes Flusswasser die ufernahe Grundwassermessstelle schon nach ca. 3.2 und 3.3 Tagen und Fliesspfaden von ca. 22 und 24 m.

5.6 Diskussion

Die Ergebnisse der Datenanalysen und der Grundwassermodellierung zeigen die grosse zeitliche und räumliche Variabilität der Austauschraten zwischen Oberflächengewässern und dem Grundwasser in Abhängigkeit der lokalen und regionalen Grundwasserfliessregime. Diese Prozesse wiederum verändern die Strömungsdynamik, die Anteile an Wasserkomponenten unterschiedlicher Herkunft sowie die Wassertemperatur im hyporheischen Interstitial und im Bereich der Laichgruben. Die verschiedenen Faktoren, welche einen unterschiedlich starken Einfluss auf die Prozesse der Fluss-Grundwasser-Interaktion haben, werden nachfolgend anhand der Untersuchungsergebnisse diskutiert.

Niederschlags- und Schneeschmelzereignisse im Zusammenhang mit dem Verlauf der Lufttemperatur können indirekt über die Abflussbildung im Fliessgewässer und lokal über oberflächige und unterirdische Hangzuflüsse einen starken Einfluss darstellen. Dies wird durch Zeitreihenanalysen der meteorologischen Daten betätigt, welche zeigen, dass Hochwasser mit Niederschlags- oder Schneeschmelzereignissen korrelieren. Die Grundwasserneubildung durch flächig versickerndes Niederschlagswasser und der direkte Einfluss auf das regionale Grundwasserfliessregime sind gering (<1% der Gesamtwasserbilanz). Ober- und unterirdische Hangzuflüsse haben einen mittleren Einfluss auf die Flussdynamik und lokale Fliessregime in der hyporheischen Zone. Berechnete In- und Exfiltrationsraten zeigen, dass Variationen der In- und Exfiltration vor allem auf den Verlauf des Flusspegels zurückzuführen sind (Fig. 5.3). Die Exfiltration von Grundwasser in das Fliessgewässer ist mengenmässig im Vergleich zum Abflussvolumen klein.

Im Untersuchungsgebiet der Enziwigger führt die Geometrie des Grundwasserleiters sowie der starke Gradient vom Fluss zum Niveau des regionalen Grundwasserstroms dazu, dass auf der regionalen Skala der Prozess der Flusswasserinfiltration dominiert (Fig. 5.1, 2 und Table 5.1, 5.3). Auf der lokalen Skala im ufernahen Bereich und im Bereich der Sohlschwellen hingegen wechseln in- und exfiltrierende Verhältnisse in rascher Abfolge. Wichtigste Parameter für den Wechsel von In- und Exfiltration sind das Verhältnis von Fluss- zum ufernahen Grundwasserpegel, die Durchlässigkeit der Flusssohle sowie die Flussbettmorphologie (Fig. 5.3, 5.5). Die Datenanalysen von Grundwasserpegel und -temperaturen zeigen, dass das regionale Grundwasserregime zeitverzögert das Signal aus Hochwasserereignissen widerspiegelt (Fig. 5.2 und Table 5.3). Das Signal aus Hochwasserereignissen wird in der hyporheischen Zone gedämpft. Dabei dominieren lokal in Bereichen oberhalb von Sohlschwellen infiltrierende und in Bereichen unterhalb von Sohlschwellen exfiltrierende Verhältnisse. Weiterhin kann eine thermische Retardation zwischen dem Verlauf der Luft- und den Grundwassertemperaturen beobachtet werden.

Vergleicht man die Resultate der verschiedenen hydraulischen und physikalischen Parameter, so lassen sich folgende Aussagen ableiten: I) Eine Auswertung der Fluss- und Grundwasserpegeldaten zeigt wie während Hochwasserereignissen die Druckfortpflanzung stattfindet; dabei muss kein eigentlicher Massentransport von Flusswasser in den Grundwasserleiter stattfinden; II) Die Analyse der Fortpflanzung von Temperaturverläufen vom Oberflächengewässer in den Grundwasserleiter kann durch kon-

duktiven Wärmetransport dominiert werden, wobei auch kein eigentlicher mit der Infiltrationsströmung verbundener advektiver Massentransport stattfinden muss; und III) Änderungen der elektrischen Leitfähigkeiten im Grundwasser deuten auf echten Massentransport im hyporheischen Interstitial sowie Grundwasserleiter hin.

Mit den hochaufgelösten Grundwasserströmungsmodellen konnte das lokale und regionale Grundwasserfließregime beschrieben und Wasserbilanzen für die verschiedenen Untersuchungsskalen abgeleitet werden. In Abhängigkeit der betrachteten Skala machen die Prozesse der In- und Exfiltration im lokalen Massstab insgesamt 58% und im regionalen Massstab 41% der Gesamtwasserbilanz aus. Der fehlende Anteil an der Gesamtwasserbilanz kann vor allem der Hauptgrundwasserstrom im Tal zugewiesen werden. Der Einfluss, welcher die Instationarität des Grundwasserfließregimes ausmacht, kann auf die zeitliche und räumliche Verteilung der In- und Exfiltrationsprozesse zurückgeführt werden. Gleichzeitig konnte mit dem lokalen Modell die räumliche und zeitliche Instationarität von Austauschraten untersucht werden. Die mit den Modellen berechneten Fließgeschwindigkeiten liegen im ufernahen Bereich bei ca. 3 bis 5 m d^{-1} und vom Fluss zum Talgrundwasserleiter bei ca. 6 bis 7 m d^{-1} . Die grösseren Fließgeschwindigkeiten im Bereich des Talgrundwasserleiters sind auf den starken hydraulischen Gradienten vom Fluss zur Talmitte zurückzuführen. Die berechneten Fließgeschwindigkeiten sind in der gleichen Grössenordnung wie Untersuchungsergebnisse aus vergleichbaren Grundwasserleitern (Hoehn and Von Gunten, 1989).

Vor den Sohlschwellen nimmt die Infiltration von Flusswasser in das hyporheische Interstitial stark zu. Unterhalb der Schwellen findet eine Exfiltration von Grundwasser in den Fluss statt. Mit dem Grundwassermodell berechnete Austauschraten durch das Flussbett liegen im Bereich von -0.24 bis 1.35 m d^{-1} . Die aus den Temperaturanalysen in den künstlichen Forellenlaichgruben abgeleiteten Austauschraten liegen im Bereich von 0.11 bis 0.13 m d^{-1} . Sowohl die mit dem Modell als auch mit der Temperaturanalyse berechneten Austauschraten sind mit erhobenen Werten in anderen Schweizer Fließgewässern vergleichbar (Hoehn, 2002; Huggenberger et al., 2006).

Die Szenarienberechnungen erlaubten es, die Austauschraten und Fließgeschwindigkeiten des Modells mit hochaufgelöster vermessener Flussbetttopographie mit den Modellszenarien mit monotonerer Flussbetttopographie zu vergleichen. Alle drei Szenarien zeigen den Einfluss des regionalen Grundwasserfließregimes und die Zunahme der Infiltrationsprozesse zum linken Ufer hin. Für die ersten beiden Szenarien ist der Unterschied der räumlichen und zeitlichen Verteilung von Austauschraten vernachlässigbar. Die Ergebnisse lassen sich wie folgt interpretieren: Szenario 1 beschreibt die aktuelle Situation mit heterogenen Flussbettstrukturen, einschliesslich gebildeten Kiesbänken und Kolkerscheinungen unterhalb der Sohlschwellen. Szenario 2 hingegen beschreibt die Situation eines stark verbauten Flusses kurz nach der Fertigstellung von flussbaulichen Massnahmen. Die Modellresultate deuten also darauf hin, dass vor allem die "harten Verbauungen" (Sohlschwellen) im Flussbett die Austauschraten Massgeblich beeinflussen. Kleinskaligere Heterogenitäten spielen hingegen eher für die Wasserzirkulation im hyporheischen Interstitial der Kiesbänke eine Rolle. Szenario 3 beschreibt die Situation eines monotonen Flussbettverlaufs.

Die Ergebnisse der Detailuntersuchungen in den künstlich angelegten Forellenlaichgruben werden in Schindler Wildhaber et al. (2014) und Michel et al. (acc) behandelt (Chap. 6 und 7). Zusammenfassend können die folgenden Aussagen gemacht werden: I) Die

5.7. SCHLUSSFOLGERUNGEN

Sauerstoffmessungen in den künstlich angelegten Forellenlaichgruben B51 (Laichperiode 2009/2010 und 2010/2011) und B52 (Laichperiode 2010/2011) zeigen, dass während einem Grossteil der Untersuchungsperioden für die Eientwicklung ausreichend Sauerstoff ($>7\text{mg l}^{-1}$; Crisp, 2000) vorhanden war. Erst während dem letzten Drittel vor Schlupf sanken die Werte zeitweise unter 7mg l^{-1} ; II) der Anteil von überlebenden Fischeiern liegt bei B52 bei 17% und bei B42 bei 27%. Die Laichgrube B51 wurde in der Laichperiode 2009/2010 während eines Hochwasserereignisses im Dezember komplett weggeschwemmt. Während beider untersuchten Laichperioden wurden keine kritischen Temperaturen erreicht, welche die Fischeierentwicklung negativ beeinflusst hätten. Auch die modellierte hohe Variabilität der lokalen Grundwasserfließregime im hyporheischen Interstitial sowie die im Feld beobachtete eher geringe Beeinflussung der Flussbettdurchlässigkeit deuten auf einen positiven Einfluss bei der Eientwicklung hin. Trotzdem war das Überleben der Eier in der Enziwigger eher mässig bis gering.

5.7 Schlussfolgerungen

Die Resultate der Untersuchungen zeigten, dass Grundwasserfließregime in einzelnen Flussabschnitten und im Bereich von einzelnen Laichgruben nicht isoliert von übergeordneten hydrologischen Randbedingungen betrachtet werden können. Der zeitlich und räumlich stark instationäre Charakter der Fluss-Grundwasser-Interaktion in den verschiedenen Skalen (regionales Grundwasserfließregime, Einfluss Sohlschwellen, Forellenlaichgruben) kann nur erfasst werden indem man die regionalen und lokalen hydrologischen Randbedingungen mit Grundwasserströmungsmodellen simuliert.

Das regionale Grundwasserfließregime hat einen starken Einfluss auf die räumliche Verteilung der Austauschraten an der Gewässersohle der Enziwigger. Vor allem bedingt durch die Sohlschwellen im Fluss entwickeln sich lokale Grundwasserfließregime im hyporheischen Interstitial, welche in einer kleinräumigen Verteilung von Up- und Downwelling Zonen resultieren. Oberhalb der Flussschwellen infiltriert Flusswasser aufgrund des erhöhten hydraulischen Gradienten. Das infiltrierte Wasser strömt um und unter der Schwelle und exfiltriert unterhalb der Schwelle wieder in das Fließgewässer. Diese lokalen Prozesse werden überlagert die instationären Prozesse der In- und Exfiltration zwischen dem Fließgewässer und dem regionalen Grundwasserfließregime.

Die Abflussdynamik hat in verbauten Fließgewässern wie der Enziwigger einen vergleichbar geringen Einfluss auf die Flussmorphologie und Flussbettdurchlässigkeit, umgekehrt ist der Einfluss der Flussmorphologie und Flussbettdurchlässigkeit auf die Strömungsdynamik vergleichsweise gross. Die Abflussdynamik hat einen starken Einfluss auf das lokale Fließregime in der hyporheischen Zone. Die Grundwasserzirkulation im hyporheischen Interstitial hängt u.a. von der Geometrie des Grundwasserleiters, dem Oberflächenabfluss, bzw. der Abflusstiefe, der Durchlässigkeit der Flusssohle und der Flussbettmorphologie ab. Eine Evaluation von Szenarien erlaubte eine Beurteilung inwiefern zusätzliche Information des Flussbettes Modellresultate beeinflussen und welche Auflösung des Flussbettes für das Prozessstudium der Fluss-Grundwasser-Interaktion notwendig und relevant ist.

CHAPTER 5. MULTIDIMENSIONALE UNTERSUCHUNG DER FLUSS-GRUNDWASSER-INTERAKTION

Verdankung Die Untersuchungen fanden in Rahmen des Schweizer Nationalfondsprojekts (K-32K1-120486) statt. Die Autoren wollen sich bei Daniel Altdorff und seinen Kollegen vom UFZ und Christian Michel für die gemeinsam durchgeführte Feldarbeit bedanken.

Chapter 6

Effects of river morphology, hydraulic gradients, and sediment deposition on water exchange and oxygen dynamics in salmonid redds

This chapter is published as:

Schindler Wildhaber Y*, Michel C*, Epting J, Wildhaber RA, Huber E, Huggenberger P, Burkhardt-Holm P, Alewell C. *Effects of river morphology, hydraulic gradients, and sediment deposition on water exchange and oxygen dynamics in salmonid redds. Science of the total Environment* 470-471, 2013. *SHARED FIRST AUTHORSHIP

6.1 Abstract

Fine sediment decreasing gravel permeability and oxygen supply to incubating salmonid embryos, is often considered the main contributing factor for the observed decline of salmonid populations. However, oxygen supply to salmonid embryos also depends on hydraulic conditions driving water flow through the redd. A more generalized perspective is needed to better understand the constraints on successful salmonid incubation in the many heavily modified fluvial ecosystems of the Northern Hemisphere. The effects of hydraulic gradients, riverbed and redd morphology as well as fine sediment deposition on dissolved oxygen (DO) and water exchange were studied in 18 artificial redds at three sites along a modified river. Fifty percent of the redds in the two downstream sites were lost during high flow events, while redd loss at the upstream site was substantially lower (8%). This pattern was likely related to increasing flood heights from up- to downstream. Specific water infiltration rates (q) and DO were highly dynamic and driven on multiple temporal and spatial scales. Temporally, the high permeability of the redd gravel and the typical pit-tail structure of the new built redds, leading to high DO, disappeared within a month, when fine sediment had infiltrated and the redd structure was leveled. On the scale of hours to days, DO concentrations and q increased during high flows, but decreased during the falling limb of the water level, most likely related to

exfiltration of oxygen depleted groundwater or hyporheic water. DO concentrations also decreased under prolonged base flow conditions, when increased infiltration of silt and clay particles clogged the riverbed and reduced q . Spatially, artificial log steps affected fine sediment infiltration, q and interstitial DO in the redds. The results demonstrate that multiple factors have to be considered for successful river management in salmonid streams, including riverbed structure and local and regional hydrogeological conditions.

6.2 Introduction

Native salmonid populations are declining in numerous countries around the world, including populations of brown trout *Salmo trutta* in Switzerland (Burkhardt-Holm and Scheurer, 2007), Atlantic salmon *Salmo salar* in the United Kingdom (Youngson et al., 2002) and coho Salmon *Oncorhynchus kisutch* in North America (Brown et al., 1994). Habitat degradation is considered a major threat for native salmonids (e.g., Brown et al., 1994; Burkhardt-Holm and Scheurer, 2007; Hicks et al., 1991). In this regard, fine sediment (< 2 mm) deposition has been argued as the single contributing factor (e.g., Jensen et al., 2009, and studies cited therein). Deposited fine sediment can decrease redd gravel permeability and interstitial flow (e.g., Brunke, 1999; Schälchli, 1995), which, in turn, hinders oxygen supply to incubating salmonid embryos, thereby affecting their survival (Greig et al., 2005, 2007a; Heywood and Walling, 2007). However, the oxygen supply to incubating salmonids embryos depends on several further factors such as the relative contribution of oxygenated river water infiltration and exfiltration of oxygen depleted groundwater or interstitial water in the redd (Malcolm et al., 2006, 2009) or the oxygen demand of organic material (Greig et al., 2007b). Although these factors vary extensively both temporally and spatially (Brunke and Gonsler, 1997; Greig et al., 2007b; Malcolm et al., 2006), only a few studies have resolved these processes on appropriate temporal and spatial scales.

Modeling approaches on the redd scale indicate that hyporheic velocities and dissolved oxygen (DO) concentrations within the egg pocket are enhanced due to the spawning activity, leading to reduced fine sediment and thus higher hydraulic conductivity (Tonina and Buffington, 2009; Zimmermann and Lapointe, 2005a). Redd scale hyporheic exchange, measured on a centimeter to meter scale, can also be induced by the pit-tail structure of salmonid redds (Fig. 6.1A, ToninaBuffington2009). This initial structure cannot, however, be expected to remain intact during high flow events (Ottaway et al., 1981). Hence hydraulic conditions on the redd scale likely change during the incubation season. Moreover, recent research clearly indicates the need for a multi-scale approach when investigating the dynamics of abiotic conditions in salmonid redds (Baxter and Hauer, 2000; Zimmermann and Lapointe, 2005a): The local scale covers a single redd with an applied data grid resolution down to single centimeters (Fig. 6.1A). The intermediate scale covers the wider redd surrounding area of the riverbed including the relevant neighboring riverbed steps (Fig. 6.1B). The chosen data grid for this intermediate scale is in the range of meters. The regional scale considers a larger section of the river with a length and width of tenths of meters up to several kilometers (Fig. 6.1C). Hydraulic processes driven at all these scales can be expected to affect water exchange in a particular redd, and hence oxygen supply to the incubating embryos (Baxter and Hauer, 2000; Malcolm et al., 2008).

6.2. INTRODUCTION

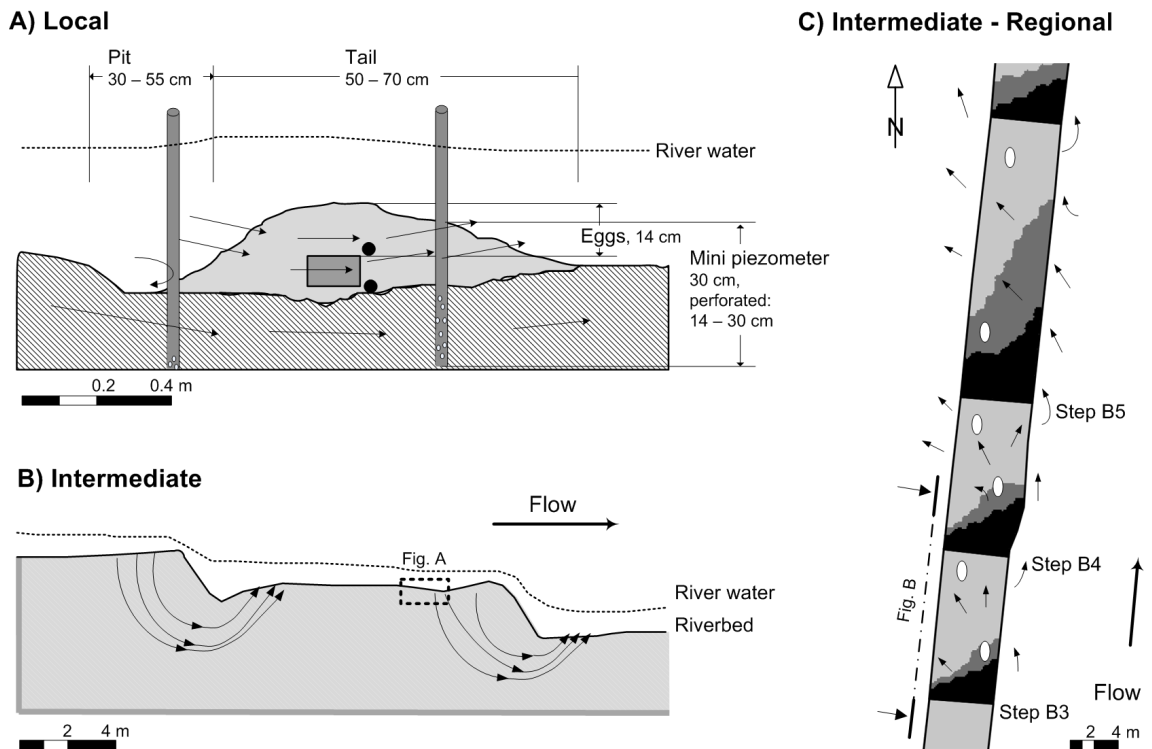


Figure 6.1: Schematic view of (A) longitudinal section of an artificial redd (modified after Greig et al., 2007b) including the location of the mini piezometers, the egg pockets (square) and temperature probes (bullet points) with the local scale flow pattern, (B) the hyporheic flow on an intermediate scale induced by riverbed steps according to the model calculations of Huber et al. (2013) (Chap. 5), and (C) the intermediate and regional scale water exchange processes (top view). Modeled data from Huber et al. (2013) (Chap. 5). Black: only exfiltration, gray: ex- and infiltration, light gray: only infiltration. Arrows indicate the main direction of the interstitial- / groundwater flow, ovals represent the position of the redds (for naming see Fig. 6.2).

In Western Europe and North America many rivers with viable salmonid populations are heavily modified, i.e., channelized and with lateral stabilizations and artificial steps introduced for slope reduction (Brookes, 1988; Wohl, 2006). In channelized rivers, the lack of geomorphic features can substantially reduce hyporheic exchange (Malcolm et al., 2010), whereas hydraulic gradients related to artificial steps can markedly increase hyporheic exchange (Endreny et al., 2011). Artificial steps generate predictable flow-paths, with increased river water downwelling above steps and upwelling of hyporheic water below steps (Fig. 6.1B, e.g., Huber et al., 2013; Kasahara and Hill, 2006). Accordingly, artificial steps can increase hyporheic exchange in modified rivers (Kasahara and Hill, 2006; Sawyer et al., 2011) and could thereby also affect water exchange and oxygen supply in salmonid redds. Despite this, the effects of artificial steps on abiotic conditions in salmonid redds have, to our knowledge, not been investigated. This knowledge would provide important input for process-based river management in the many heavily modified salmonid streams of the Northern Hemisphere.

To this end, the current study evaluates the relative contribution of fine sediment, hydraulic gradients, river morphology, and regional geomorphology to specific water infiltration and oxygen dynamics in artificial brown trout redds in the Enziwigger, a heavily

modified headwater river of the Swiss Plateau in the Canton of Lucerne. The Enziwigger also maintains a viable brown trout population (Schager et al., 2007).

The objective of this study was to provide a detailed investigation of the factors affecting the abiotic redd environment in a heavily modified river including I) an investigation of fine sediment deposition, hydraulic conditions (i.e. specific infiltration q , vertical and horizontal hydraulic gradients, and water level) and their effects on oxygen dynamics in the redds, II) an assessment of the morphological change of the riverbed and of the characteristic pit and tail structure of the redds and III) a comparison of the measured data with the results of a groundwater flow model, which was set up for one of the three experimental sites (cf. Huber et al., 2013) (Chap. 5). This model predicts zones of increased downwelling river water above steps, of hyporheic water upwelling below steps and zones with altering upwelling, downwelling and horizontal advection zones between the two steps.

In contrast to most previously published studies, data were collected with high spatial and temporal resolution (i.e. weekly or continuously) to explicitly characterize the temporal and spatial dynamics of the measured parameters. Measured parameters affect brown trout embryo survival in the redds and our results can thus be integrated with studies monitoring survival success of salmonid embryos (Michel et al., acc) (Chap. 7), providing a more complete perspective on the factors affecting salmonid incubation success in comparable anthropogenically modified river environments.

6.3 Materials and methods

6.3.1 Study site and general setup

The river Enziwigger is a small channelized river located near Willisau, Canton of Lucerne, Switzerland with a total watershed area of about 31 km² (Fig. 6.2). Mean discharge, measured in Willisau (Fig. 6.2) by the Cantonal authorities (Nov. 2007 - Nov. 2008) was 2.1 m³ s⁻¹, minimum and maximum discharge were 1.1 m³ s⁻¹ and 10.1 m³ s⁻¹, respectively. During the 20th century the Enziwigger was straightened and channelized, and cross-channel log steps were installed as slope breakers to prevent deep channel erosion and bed-scouring during flood events (Fig. 6.2). Thus, like for most rivers in the Swiss Plateau, its morphology is strongly modified: only 5% is close to natural or natural, 21% is slightly affected and 74% is strongly affected or even artificial (classified with the Swiss modular stepwise procedure for ecomorphology after Huetten and Niederhauser, 1998; EBP-WSB-Agrofutura, 2005). Despite these extensive modifications, its biological condition, classified with the macrozoobenthos module of the Swiss modular stepwise procedure (Stucki, 2010), is considered good (EBP-WSB-Agrofutura, 2005). The only fish species in the Enziwigger is the brown trout *S. trutta*, which maintains a viable population (EBP-WSB-Agrofutura, 2005; Schager et al., 2007). The flow regime of the Enziwigger is affected neither by hydro-power facilities nor by effluents from waste water treatment plants.

Measurements were conducted at three experimental sites along the river named A, B and C (from upstream to downstream; Fig. 6.2) at altitudes from 757 to 583 m a.s.l.. The groundwater flow model was set up for site B (Huber et al., 2013) (Chap. 5). The

6.3. MATERIALS AND METHODS

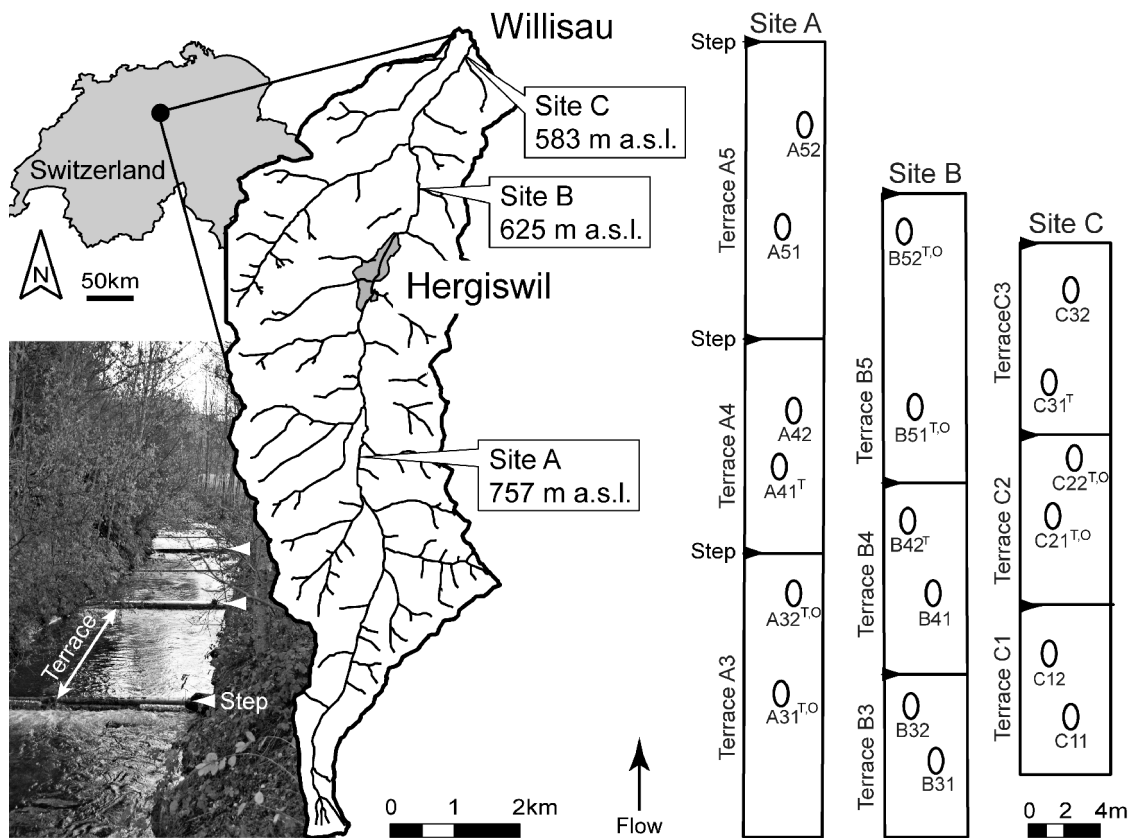


Figure 6.2: Location of the Enziwigger watershed in Switzerland. The photograph shows the step and terrace structure at study site B. The watershedmap of the river Enziwigger and the towns Willisau and Hergiswil (Canton of Lucerne, Switzerland) shows the locations of the three field sites A, B and C, while the schematic on the right illustrates the location of the redds within each field site. Here, superscripts indicate redds with continuous temperature (T) and oxygen (O) measurements.

riverbed at all sites is stabilized with artificial log steps, which strongly affect hyporheic exchange on an intermediate scale with river water infiltration upstream of the steps and exfiltration of hyporheic water downstream of the steps (Fig. 6.1B). At site A, the bedrock beneath the riverbed lies at a depth of a few decimeters and the hydrogeologic settings are assumed to be dominated by lateral inflow or the exfiltration of groundwater and/or hyporheic water. Piezometer measurements at sites B and C and the groundwater flow modeling at site B indicate on a regional scale a hydraulic gradient from the river to the main valley aquifer on the left side of the river and consequently a domination of river water infiltration (Fig. 6.1C, Huber et al., 2013) (Chap. 5). The influence of river flow stage and transient hillside groundwater flow has a minor impact on these intermediate and regional flow patterns (Huber et al., 2013) (Chap. 5).

Each site was equipped with six artificial salmonid redds in places wherein natural brown trout redds had been mapped in November 2008. The artificial redds were built to create a structure that resembles the structure of natural brown trout redds (Crisp and Carling, 1989). A detailed description of the redd structure and how it was built is given in Michel et al. (accepted). In the Enziwigger, these locations are mostly consistent from year to

year (P. Amrein, Fish and Wildlife Service, Canton of Lucerne, pers. comm.). Data were collected during two spawning seasons (season 1 (S1): November 2009 to end of March 2010; season 2 (S2): November 2010 to end of March 2011) in 18 artificial redds per year ($n = 36$ redds in total). Redds were built in the same location each season (Fig. 6.2) with the exception of redds A31 and A32, which were covered in ice in January and February, making sampling impossible. Redds are labeled after the site (A, B, C), the terraces between two steps (1-5), the redd location within a terrace (1 and 2) and the season (S1 and S2). For example, redd A41.S1 identifies the first redd in the fourth investigated terrace at site A during the first season (Fig. 6.2). A detailed description of the river characteristics and field locations is given in Schindler Wildhaber et al. (2012b)(Chap. 2).

6.3.2 Sediment collections and analyses

Each redd was equipped with two sediment baskets to assess weekly fine sediment infiltration and net fine sediment accumulation during the entire field season (cf. Acornley and Sear, 1999; Greig et al., 2005; Heywood and Walling, 2007). One of them was emptied at weekly intervals to measure the weekly infiltration rates (= infiltration basket). The second set of sediment baskets was emptied at the end of the incubation season to measure net accumulation of fine sediment during the incubation period (= accumulation basket, Sear et al., 2008). At each site, the sediment basket data were complemented with four to seven freeze core samples to characterize the sediment stratification of the undisturbed river gravel. For a detailed description of the used baskets, the freeze core technique and their handling see Schindler Wildhaber et al. (2012b) (Chap. 2).

Grain size distribution was measured in a subsample of the fine sediment fraction of the freeze cores' layers 0-10 cm, 10-20 cm and 20-30 cm and in two subsamples of the fine sediment collected in accumulation baskets. Representative subsamples were obtained by a sample divider (Retsch, Haan, Germany). Additionally, grain size distributions of weekly infiltrated fine sediment samples ($n = 80$) were determined. The rest of the infiltrated fine sediment was pooled for each redd and a subsample was analyzed to obtain a mean grain size distribution of the infiltrated fine sediment. Grain size fractions were named according to the German soil taxonomy standard (DIN EN ISO 14688-1): Sand: $63 \mu\text{m} - 2\text{mm}$, silt: $2 \mu\text{m} - 63 \mu\text{m}$ and clay: $< 63 \mu\text{m}$ (Sponagel et al., 2005).

Porosity (n) was calculated for each site on the basis of sediment grain size distributions of the freeze core samples by the formula

$$n = 48.6 \cdot C_u^{-0.2} \quad (6.1)$$

Where $C_u = d_{60} / d_{10}$ (diameter of grain size at the 60th and 10th percentile of the cumulative sample mass) (Schälchli, 1995). The *fredle index* of the accumulation baskets and of the freeze core samples was calculated by the formula

$$fredle\ index = \frac{d_g}{S_o} \quad (6.2)$$

Where d_g is the geometric mean grain size and S_o is the sorting coefficient derived by taking the square root of the quotient of the grain size at the 75th percentile divided by that at the 25th percentile (Lotspeich and Everest, 1981). The *fredle index* is a central tendency quality index of the redd gravel composition, which gets smaller with smaller permeability of the sediment.

6.3. MATERIALS AND METHODS

6.3.3 Oxygen

Continuous oxygen measurements were conducted with Aanderaa oxygen optodes 3835 (Aanderaa data instruments, Bergen, Norway) buried at the same depth as the incubating brown trout embryos (approx. 14 cm, cf. Michel et al., acc). Oxygen contents in mg l^{-1} as well as saturation (%) were measured every ten seconds and mean values were logged in ten minute intervals. One optode per site was installed during season 1 (redds A32, B51 and C21) and two during season 2 (Fig. 6.2). Moreover, oxygen concentrations in each redd were measured manually every second week in mini piezometers located in the pit and tail of each redd (Fig. 6.1A) with PreSens oxygen dipping probe mini-sensor (PreSens Precision Sensing GmbH, Regensburg, Germany). Each manual oxygen measurement was conducted twice: once in the "old" interstitial water and once in the reflux "new" water approximately 30 minutes after the "old water" had been extracted.

6.3.4 Riverbed and redd morphology

Riverbed morphology was mapped in a 0.5 m horizontal resolution in season 2009/2010 shortly after redd constructions (October 26th 2009) and on December 27th after high flow events to assess morphological alterations in a river segment scale due to high flows. Additionally, the morphology of each redd was assessed weekly by measuring the water level above the pit and tail to quantify the temporal change of the typical redd structure.

6.3.5 Hydraulic investigations

Flow-stage at each site was measured every 15 seconds with pressure transmitter probes (STS, Sensor Technik Sirnach, Switzerland) and average values were logged at 10 minutes intervals during both field seasons.

Water levels above pit and tail of each redd were recorded weekly to assess its heterogeneity within sites. Vertical hydraulic gradients (VHG) in redds were measured weekly in mini piezometers after Baxter et al. (2003) installed in the pit and tail of each redd. Mini piezometers are described in detail in Schindler Wildhaber et al. (2012b)(Chap. 2). VHG is a dimensionless parameter calculated by the formula

$$\text{VHG} = \frac{\Delta h}{\Delta l} \quad (6.3)$$

where Δh is the difference in head between the water level in the piezometer and the level of the stream surface and Δl is the depth from the streambed surface to the first holes in the piezometer (Baxter et al., 2003). Positive values indicate an energy gradient potentially sufficient to produce upwelling and negative values indicate an energy gradient potentially sufficient to produce downwelling. In the following, the VHG values are reported as upwelling or downwelling processes, although they are actually only a measure of upwelling and downwelling potential (Baxter and Hauer, 2000). The differences in VHGs between the pit and the tail piezometer of each redd were defined as the horizontal hydraulic gradients (HHG), which is an indicator for hydraulic gradients driving water flow through the redd.

To obtain the temporal and spatial change of specific infiltration rate (q) in the interstitial, the one-dimensional heat pulse method was used (e.g., Hatch et al., 2006). For this, stream water temperature and temperatures at two different depths just above and below the incubating brown trout embryos (approx. 12 and 20 cm, respectively) were recorded every minute using thermocouple temperature probes (Campbell Scientific 105 E). Three redds per site were equipped with one or two temperature probes (Fig. 6.2). In redds equipped with two temperature probes, q could be calculated for the upper part (q_u , 0 to about 12 cm), the bottom part (q_b , about 12 cm to about 20 cm) and the total part (q_t , 0 to about 20 cm). In redds with one temperature probe, q could only be assessed in the upper part. The diurnal amplitude variations in temperature in the different depths and the diurnal phase variations were used to calculate q , but only the results of the former method were incorporated into further interpretations because of their higher stability. The method used allowed the calculation of two specific infiltration rate values per day.

The diurnal sinusoidal alternation was filtered from the temperature data by a discrete bandpass filter (FIR-filter with Hamming-window, 5001 filter coefficients, cut-off frequency $0.8 \cdot f_{Day} / 1.5 \cdot f_{Day}$). All field temperature data were sampled with a frequency of one measurement per minute. When field sample periods exceeded one minute, e.g., due to technical problems, linear interpolation was used to fill gaps of up to 10 minutes. Data gaps exceeding 10 minutes were marked as missing and not further evaluated. Data-points with time offset between the daily minima or maxima peaks of the corresponding sinusoidal temperature curves at the different depths exceeding 20% of a day period (i.e. 288 minutes) were also removed from further processing. The resulting temperature amplitude ratio (A_r) was used to estimate q .

The specific infiltration rate q and the vertical flow velocity (v_f) are extracted according to equation 6.4 (Ingebritsen et al., 2006) and equation 6.5 (slightly transposed after Hatch et al., 2006).

$$q = v_f \cdot n \quad (6.4)$$

$$v_f = \left(\frac{\rho \cdot c}{\rho_f \cdot c_f} \right) \cdot v \quad (6.5)$$

For parameter definition and values see Table 6.1. The vertical fluid velocity (v) can be determined by the amplitude ratio (A_r), identified as v_{Ar} . We gained the values by a numerical solver from the equations 6.6 and 6.7 (Hatch et al., 2006)

$$\frac{2\kappa_e}{\Delta z} \ln \left(A_r + \sqrt{\frac{\alpha(v_{Ar}) + v_{Ar}^2}{2}} - v_{Ar} \right) = 0 \quad (6.6)$$

where

$$\alpha(v) = \sqrt{v^4 + (8\pi \cdot f_{Day} \cdot \kappa_e)^2} \quad (6.7)$$

The effective thermal diffusivity (κ_e) is estimated according to Hatch et al. (2006) by the equation

$$\kappa_e = \frac{\sigma}{\rho \cdot c} + \beta \cdot |v_f| \quad (6.8)$$

where the components of the first term are gained from:

$$\sigma = n \cdot \sigma_f + (1 - n) \cdot \sigma_s \quad (6.9)$$

$$\rho = n \cdot \rho_f + (1 - n) \cdot \rho_s \quad (6.10)$$

6.4. RESULTS AND DISCUSSION

$$c = \frac{n\rho_f c_f + (1-n)\rho_s c_s}{n\rho_f + (1-n)\rho_s} \quad (6.11)$$

The second term of the equation 6.8 was excluded from the calculations as its contribution to the value of κ_e is negligible with the thermal dispersivity (β) = $1 \cdot 10^{-3}$ as proposed by Hatch et al. (2006) and Keery et al. (2007) but it would strongly increases the complexity of the analysis (Keery et al., 2007).

Heat is mainly transferred through riverbed sediments by advection and conduction. Heat advection describes the heat transfer occurring while water flows through the sediment, heat conduction the molecular transport of thermal energy (e.g., Constantz, 2008). The relative contribution of advection and conduction on the heat transfer can be calculated by determining the dimensionless Peclet number (Pe ; Silliman et al., 1995).

$$Pe = \frac{v_f \cdot n \cdot l}{D} \quad (6.12)$$

where l is the characteristic length and set as 0.01 m due to the range of the setup. The thermal diffusivity D is given by:

$$D = \frac{K_e}{c_s \cdot \rho_s} \quad (6.13)$$

where K_e is the thermal conductivity of the saturated sediment (Table 6.1). If Pe is smaller than approximately $2 \cdot 10^{-4}$, advection component of the solution has little impact for fluxes and conductive heat transport dominates (Silliman et al., 1995).

Median Peclet numbers were between approximately 0.01 and 0.1, indicating that heat is transported not only by molecular transport of thermal energy (conduction) but also by water flow (advection) (Silliman et al., 1995).

6.3.6 Groundwater flow modeling

Groundwater flow models for site B were setup in GMS (Groundwater Modeling System 7.1, Environmental Modeling Systems, 2002) on the basis of MODFLOW (McDonald and Harbaugh, 1996). Details can be found in Huber et al. (2013) (Chap. 5). Boundary conditions of a regional scale groundwater model (extension 230 m \times 340 m, resolution 2 m \times 2 m) were transferred to an intermediate scale groundwater model (extension 110 m \times 60 m, resolution 0.5 m \times 0.5 m). For the description of the bedrock surface penetration depth of Direct-Push boreholes were used. For the intermediate scale model the high-resolution measurements of riverbed morphology were considered. Based on continuously measured groundwater heads, the distribution and magnitude of hydraulic conductivities as well as the riverbed conductance were inversely calibrated for a transient data set (220 days, resolution 1d, PEST, Doherty, 1994).

6.4 Results and discussion

6.4.1 Spatiotemporal changes in riverbed and redd morphology

The riverbed morphology of the Enziwigger changed substantially during high flow events, despite the steps to prevent deep scouring. This was especially true for the two

Table 6.1: Physical parameters used for calculating specific infiltration rates q in alphabetic order (1. Roman letters, 2. Greek letters).

Symbol	Values	Unit	Parameter
A		$^{\circ}\text{C}$	Amplitude of thermal oscillation
A_r		-	Temperature (T) amplitude ratio (upper / lower T amplitude)
c		$\text{J kg}^{-1} \text{ } ^{\circ}\text{C}^{-1}$	Specific heat of sediment-fluid system
c_f	4208	$\text{J kg}^{-1} \text{ } ^{\circ}\text{C}^{-1}$	Specific heat of fluid (water at 4°C ; Lemmon et al., 2012)
c_s	775	$\text{J kg}^{-1} \text{ } ^{\circ}\text{C}^{-1}$	Specific heat of sediments, average between values of Schön (1996) (cited by Rau et al., 2010) and Revil (2000) (cited by Keery et al., 2007)
f_{Day}	$11.5 \cdot 10^{-6}$	s^{-1}	Frequency of a day period (24h)
K_e	1	$\text{J m}^{-1}\text{s}^{-1}\text{K}^{-1}$	Thermal conductivity of the saturated sediment (after Carslaw and Jaeger, 1959; Silliman et al., 1995)
n	0.23	-	Porosity, assessed from freeze core samples
q		m s^{-1}	Specific infiltration rate
v		m s^{-1}	Velocity of thermal front
v_{Ar}		m s^{-1}	Velocity of thermal front derived from the amplitude ratio A_r
v_f		m s^{-1}	Vertical fluid velocity, positive number = down welling (Goto et al., 2005)
β	$1 \cdot 10^{-3}$	m	Thermal dispersivity (cited by Hatch et al., 2006)
κ_e		$\text{m}^2 \text{ s}^{-1}$	Effective thermal diffusivity
ρ		kg m^{-3}	Density of saturated sediment
ρ_f	1000	kg m^{-3}	Density of fluid (water at 4°C ; Kuchling, 1976)
ρ_s	2650	kg m^{-3}	Density of sediment (e.g., Kuntze et al., 1994)
σ	1.50	$\text{W m}^{-1} \text{ K}^{-1}$	Thermal conductivity of saturated sediment (Constantz, 2008)
σ_f	0.60	$\text{W m}^{-1} \text{ K}^{-1}$	Thermal conductivity of fluid (water; Ingebritsen et al., 2006)

6.4. RESULTS AND DISCUSSION

downstream sites B and C (Fig. 6.2), where flood events in December 2009 triggered river gravel accumulation or scouring up to 0.9 m (Fig. 6.3). All redds at site B were strongly affected by scouring, while at site C the gravel bed scoured predominately in the pools below steps and accumulated towards the right bank of the river. Sediment displacements varied from terrace to terrace within a site. For example, changes of the riverbed morphology below step 3 at site C were much smaller than at the other two examined steps (Fig. 6.3, right). This was probably due to the slightly wider riverbed (5.0-5.5 m at step C3, 4.5-5 m at step C2 and 4.5 m at step C1) causing lower water levels and hence less shear stress. These data also agree with the suggestion that sediment transport in rivers is a discontinuous process and sediment often moves in pulses (Klingemann and Emmett, 1982) affected by bed-form and associated sediment sorting (Cudden and Hoey, 2003) or by debris flows (Hoffman and Gabet, 2007). Hence, bed scouring and gravel deposition is not easy predicted, at least on an intermediate scale within individual river sections. Along the entire river (i.e. regional scale) increased gravel displacement was evident at sites B and C as compared to site A (visual interpretation). In total, half of the redds in sites B and C were lost (Fig. 6.3), while only 8% of the redds were lost at the most upstream site A. This pattern is most likely related to increased bed shear stress in sites B and C caused by higher water levels and only marginally smaller slopes (Schindler Wildhaber et al., 2012b) (Chap. 2), as also indicated by increasing bedloads and suspended sediment loads from upstream to downstream (Schindler Wildhaber et al., 2012b) (Chap. 2). In support of this notion the probability of redd excavation increased with the water level above the redd (glm, $p < 0.05$).

Winter flood events in some Swiss rivers and also in rivers worldwide have increased over the last decade (Birsan et al., 2005; Scheurer et al., 2009) and are expected to further increase, both, in respect to intensity and frequency, due to climate change (IPPC, 2007; Middelkoop et al., 2001; Thodsen, 2007). In the Enziwigger, high-flow events in early winter are unusual, but it has been suggested that they have increased in recent decades (P. Amrein, Fish and Wildlife Service, Canton of Lucerne, Switzerland, pers. comm.). Accordingly, the high redd loss reported here raises concerns about how the observed and predicted increases of winter floods affect salmonid recruitment in confined rivers like the Enziwigger with small egg-burial depths (0-9 cm Riedl and Peter, 2013) making salmonid embryos more susceptible to scouring.

High-flow events also strongly affected the morphology of the remaining redds. Initially, the mean difference between the depth of the tail and pit of newly built redds was 9.4 ± 2.8 cm (Fig. 6.4A). After one month and some high flow events, most redds were basically leveled (Fig. 6.4A) and a high amount of fine sediment had infiltrated (Schindler Wildhaber et al., 2012b) (Chap. 2). These observations agree with Ottaway et al. (1981) who documented a flattening of brown trout redds after only the first high water event subsequent to spawning. Both, flattening of the redd and fine sediment content are known to affect the water exchange in redds, either by reducing horizontal pumping flow or by decreasing redd gravel permeability (e.g., Greig et al., 2005; Schälchli, 1995). The concept of enhanced downwelling of oxygenated water due to the redd morphology is still widely discussed (e.g., Greig et al., 2007b; Tonina and Buffington, 2009; Zimmermann and Lapointe, 2005a). Our results clearly indicate that redd morphology contributes to local redd scale exchange processes only during the first few weeks after redd building (see below). Once the pit-tail structure has been leveled, exchange processes on intermediate

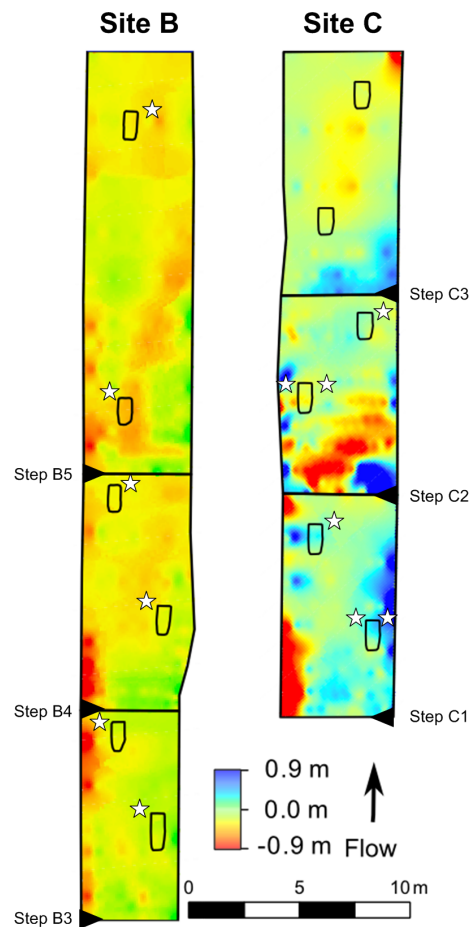


Figure 6.3: Differences between the riverbed topography measured in October and December 2009 at the two downstream sites B and C. Negative values indicate gravel bed erosion, and positive values indicate sediment deposition. Black ovals are the positions of the artificial redds. Redds lost during season 1 are marked by a star on the left side, while redds lost during season 2 are marked by a star on the right side.

or regional scales gain importance for water-exchange and oxygen supply to developing embryos. In many modified rivers, such processes driven on these scales have to be clearly incorporated into management plans to ensure sufficient salmonid incubation success.

6.4.2 Hydraulic dynamics in redds

Spatial patterns of the hydraulic dynamics

Vertical hydraulic gradients (VHG) measured in mini piezometers did not parallel the expected intermediate scale downwelling and upwelling patterns induced by steps (Fig. 6.1B, e.g., Huber et al., 2013; Kasahara and Hill, 2006). Most redds were located more than one meter before or after a step. Accordingly, they were not located in the main upwelling and downwelling zones predicted by the model, but in areas where down-

6.4. RESULTS AND DISCUSSION

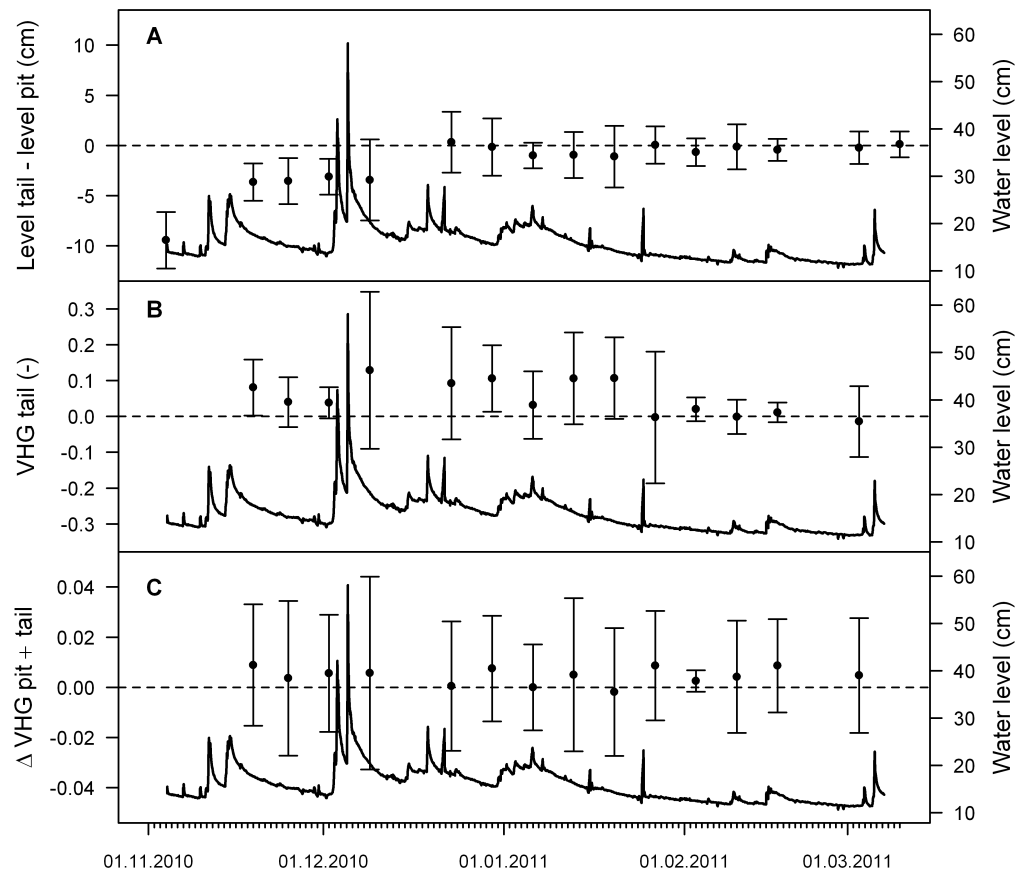


Figure 6.4: In each panel, the black graph represents the flowstage at site B. Symbols within panels denote (A) the mean \pm standard deviation (SD) of the riverbed level differences between tail and pit (B) mean \pm SD of the vertical hydraulic gradients (VHGs) in the tail of the redds, and (C) mean \pm SD of the horizontal hydraulic gradients (HHGs) between pit and tail of the redds. Values were calculated from all 18 redds during season 2. A positive hydraulic gradient indicates upwelling, and a negative gradient indicates downwelling.

welling, upwelling and horizontal advection alternate (Fig. 6.1C). Hence, the applied mini piezometer approach was most likely not able to integrate the hydraulic gradients that jointly drove water exchange in redds, i.e. both vertical and horizontal. In redd A32.S1, which provides an exception being located only 0.65 m above a step, considerable downwelling potential was measured (-0.07 ± 0.06). When this redd was located 1.65 m upstream of the step in season 2 (redd A32.S2; Fig. 6.2), VHGs changed between upwelling and downwelling conditions with a mean close to zero (0.03 ± 0.08). This confirms the model predictions. In general, vertical hydraulic gradients on the redd scale can be expected to show substantial temporal variation related to water level fluctuations and also changes in riverbed morphology (cf. beginning of section 6.4.2).

Specific infiltration rates q , calculated from continuous data, confirmed the predictions from the groundwater flow modeling. Mean q_t increased with smaller distance to the next downstream step and hence confirmed the increased downwelling above steps (Table 6.2). Similarly, in redds located further upstream smaller and also negative q_t values were found, which again agrees with model predictions (Fig. 6.1C). Also, weekly fine

sediment infiltration increased with shorter distance to the downstream step (Spearman rank correlation, fine sediment: $\rho = -0.45$, $p < 0.05$, silt: $\rho = -0.52$, $p < 0.05$, clay: $\rho = -0.57$, $p < 0.01$), likely related to increased river water infiltration above steps. Increased weekly fine sediment infiltration had no negative effect on specific water infiltration in redds (Table 6.2). However, the net fine sediment accumulation did not increase with shorter distance to the step (all $p > 0.12$). Fine sediment accumulation depends not only on fine sediment infiltration, but also on the water level, since higher water levels lead to resuspension of fine sediment (see also Schindler Wildhaber et al., 2012b). The specific infiltration rate q decreased significantly in redds with higher fine sediment accumulation and increased with a higher maximal water level above the redd (Table 6.2).

Hydraulic exchange processes can vary remarkably within a single redd. In most redds q was lower in 12-20 cm depth as compared to the upper 12 cm of redd gravel (t-test, $p < 0.01$; Fig. 6.5). Freeze core samples of undisturbed gravel in the study area confirmed a significantly lower silt and clay level in the upper part (0-10 cm) compared to the deeper part (i.e., 10 - 20 cm and 20 - 30 cm, Schindler Wildhaber et al., 2012b, Chap. 2). A comparable increase in fine sediment content paralleled by a decreased hydraulic conductivity was also found in the studies of Brunke (1999) and Sear (1993). Accordingly, the decrease of q with depth reported here suggests higher fine sediment content around our brown trout eggs (i.e. at 12-20 cm depth) compared with the entire redd gravel. A similar distinction between the upper and lower part of the redd gravel was made by Meyer (2003). Our study further documents that this increased fine sediment accumulation around the eggs can decrease water exchange around the eggs, which could hinder oxygen supply to the embryos (see section 6.4.3) and hence salmonid embryo survival.

At redd A32.S1, the specific infiltration q was higher in the bottom part than the upper part of the redd (Fig. 6.5, see Fig. 6.2 for location of the redd), which was probably related to the lower mean water level above this redd (9.8 ± 2.0 cm), triggering high fine sediment deposition and only limited scouring (Schindler Wildhaber et al., 2012b) (Chap. 2). Redd A32.S1 was also the only redd equipped with temperature probes that was temporally covered with ice, which could have caused decreased water flow over the redd. In addition, VHG measurements indicated substantial downwelling potential in this redd (VHG = -0.07 ± 0.06 , see above). Both factors possibly increased the fine sediment input

Table 6.2: Spearman rank correlation coefficients between median specific infiltration rate q in the upper part (ca. 0 - 12 cm; q_u) and the total part (ca. 0 - 20 cm, q_t) with total accumulated fine sediment (< 2 mm), accumulated silt and clay fraction, sum of the weekly infiltrated fine sediment, *fredle index* of the accumulation baskets, maximal water level above the redd and distance of the redd to the upstream and downstream step. The sample size (n) is given in parentheses.

	q_u (m s^{-1})	q_t (m s^{-1})
Fine sediment accu. (%)	-0.79, $p = 0.03$ (8)	-0.89, $p = 0.03$ (6)
Silt and clay accu. (%)	-0.52, $p = 0.20$ (8)	-0.49, $p = 0.36$ (6)
Fine sediment infiltration (g)	-1.9, $p = 0.58$ (8)	-0.18, $p = 0.57$ (6)
Fredle index (-)	0.71, $p = 0.06$ (8)	0.77, $p = 0.09$ (6)
Water max. (cm)	0.60, $p = 0.03$ (13)	0.66, $p = 0.03$ (10)
Distance upstream step (cm)	0.15, $p = 0.62^a$ (13)	0.61, $p = 0.06^a$ (10)
Distance downstream step (cm)	-0.17, $p = 0.58^a$ (13)	-0.68, $p = 0.03^a$ (10)

^a Mean q of February and March to get a mean q value of the undisturbed river gravel.

6.4. RESULTS AND DISCUSSION

in the entire gravel column of this redd (Brunke, 1999; Schindler Wildhaber et al., 2012b; Seydell et al., 2009) and hence decreased specific water infiltration q also in the upper part. A low q was also found in the upper part of redd A31_S1 (Fig. 6.5), which also had a very low mean water level (2.5 ± 1.7 cm). During the second field season, the locations of two redds were changed to locations with deeper mean water levels (A31_S2: 15.1 ± 3.5 cm, A32_S2: 12.4 ± 3.5 cm). This resulted in less fine sediment accumulation (Schindler Wildhaber et al., 2012b) (Chap. 2) and higher specific infiltration rates q were found (Fig. 6.5). Further, these patterns of q were closely paralleled by the oxygen dynamics in these redds (see section 6.4.3).

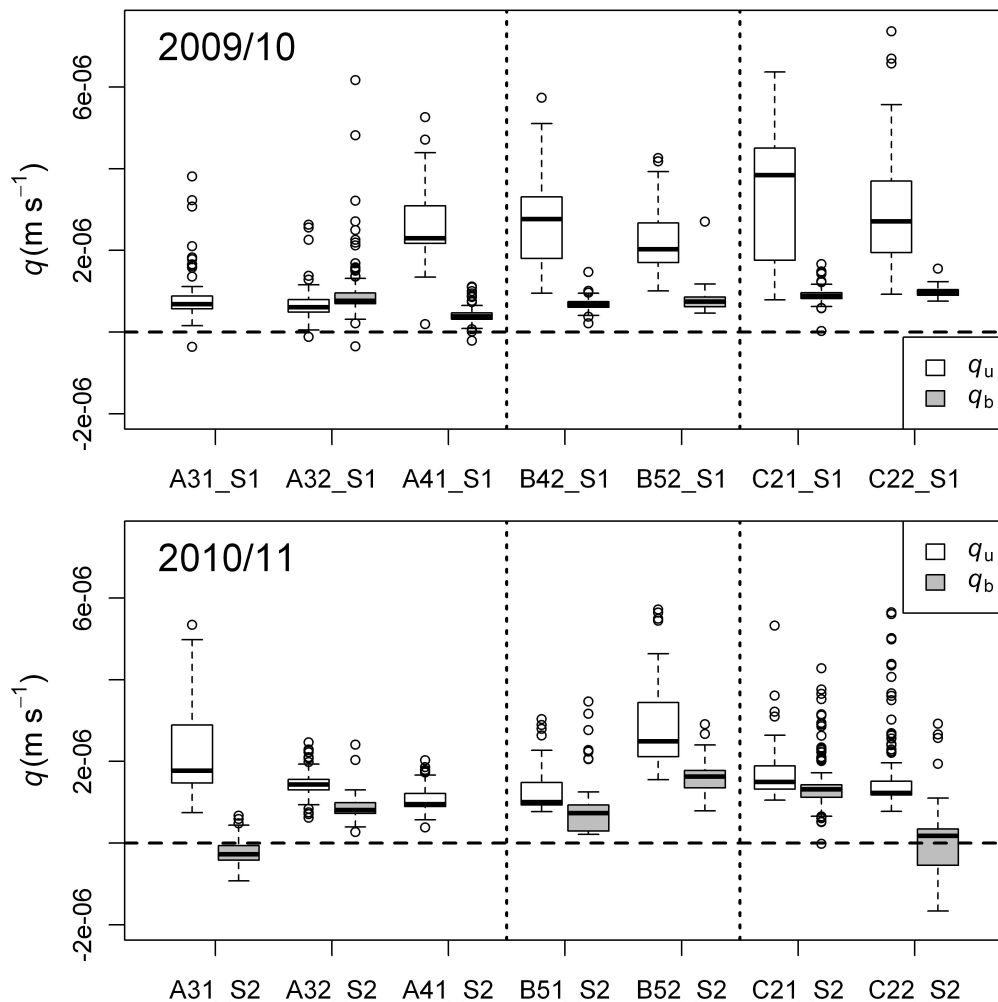


Figure 6.5: Specific infiltration rate in the upper (q_u) and the bottom part (q_b) of the redds during the two seasons. Negative values indicate upwelling, positive values indicate downwelling. For each redd the horizontal line indicates the median, the box interquartile range (i.e., center 50% of the data), whiskers mark maximum and minimum values, and points denote values exceeding 1.5 times the interquartile range. Among seasons, redds were built in the same location (Fig. 6.2) with the exception of redds A31 and A32 (see beginning of Section 6.4.2).

Temporal pattern of the hydraulic dynamics

Slightly positive VHGs, indicating upwelling processes, were measured in the tail of most redds at the beginning of the incubation period (Fig. 6.4B). In contrast, horizontal hydraulic gradients (HHG) between pit and tail did not indicate increased horizontal pumping flows between pit and tail (Fig. 6.4C). The often suggested redd scale flow pattern, with downwelling in the pit and upwelling in the tail (Tonina and Buffington, 2009), was therefore not confirmed by the HHG measurements. One reason for this might be the influence of the riverbed morphology or the water levels on the vertical and horizontal hydraulic gradients, as indicated by significant correlations between VHGs and the water level ($\rho = 0.4 - 0.6$, $p < 0.05$ in 8 of the 18 redds, Fig. 6.6).

During base flow, VHGs were mostly negative or around zero, indicating downwelling or horizontal advection flow, which agrees with model predictions (Huber et al., 2013) (Chap. 5). Upwelling or lateral flow dominated for VHG values measured at higher water levels (Fig. 6.6). On an intermediate scale, upwelling increases below steps (Huber et al., 2013; Kasahara and Hill, 2006). On a regional scale, upwelling can occur when increasing riparian groundwater levels are paralleled by decreasing stream water levels, e.g., during the recession limb of flood events (Geist et al., 2008; Malcolm et al., 2006, 2003b; Soulsby et al., 2009). In the Enziwigger, VHG measurements during the rising limb or flood events were not possible because of dangerous physical conditions. Most of the higher water levels in Fig. 6.6 therefore represent data points measured during the recession limb of flood events. Therefore, the positive hydraulic gradients (Fig. 6.6)

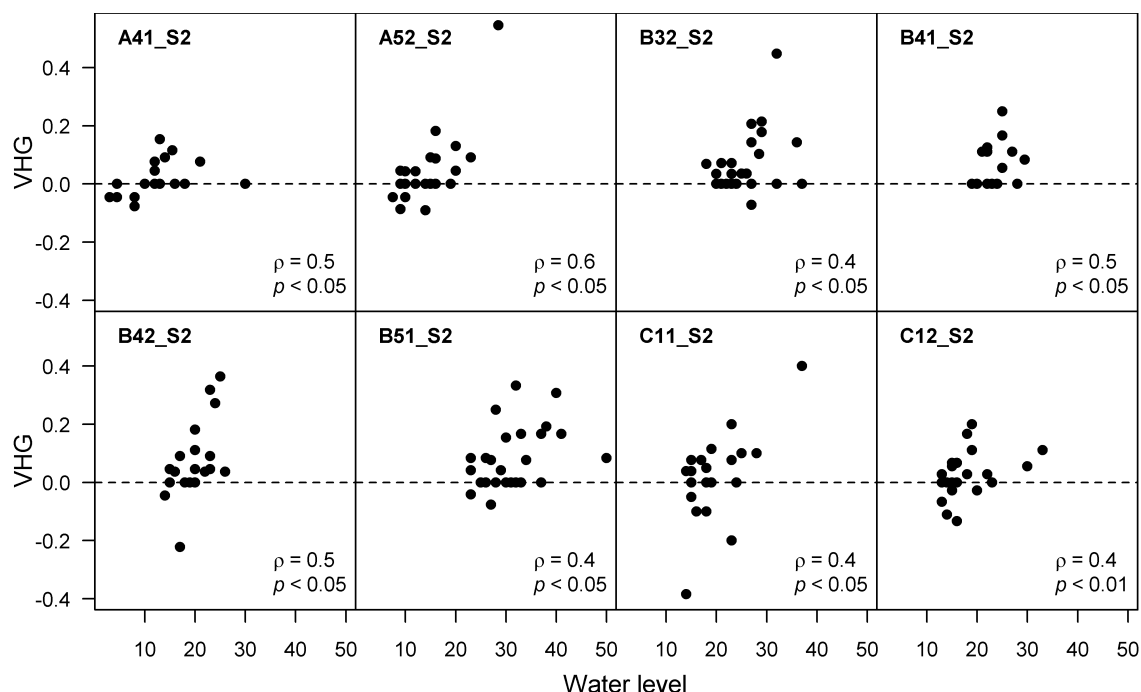


Figure 6.6: Relationship between water level and vertical hydraulic gradient (VHG) for individual redds from season 2. Within each panel Spearman correlation coefficient ρ and the p -value are given. Positive VHG indicates upwelling, and negative VHG indicates downwelling. The location of each redd is given in Fig. 6.2.

6.4. RESULTS AND DISCUSSION

indicate most likely recharge of groundwater on a regional scale and related upwelling in the redds.

Hyporheic flow paths in rivers can be very complex and also change with discharge and morphology (Tonina and Buffington, 2007). In our study, these complex temporal dynamics can best be seen in the specific water infiltration rates. Initially, q values in most redds were consistently high ($6 - 7 \cdot 10^{-6} \text{ m}^2 \text{ s}^{-1}$), decreased markedly within a month - likely related to fine sediment accumulation and changes in redd morphology - to finally stabilize around $1 - 2 \cdot 10^{-6} \text{ m}^2 \text{ s}^{-1}$ for the rest of the incubation season (Fig. 6.7, Fig. 6.5). Nonetheless, on the scale of hours and days, q remained responsive to water-level fluctuations, when it increased during high-flow events and returned to baseline levels afterwards (Fig. 6.7). The most likely explanation for this are local changes in groundwater heads in combination with increased gravel permeability related to remobilization of fine sediment (e.g., Brunke, 1999; Keery et al., 2007; Schälchli, 1995).

Temporally negative q values, and hence upwelling were found in the bottom part (approx. 12-20 cm) of two redds (A31_S2 and C22_S2) where consistent downwelling occurred in the upper part (Fig. 6.5). Redd C22 (Fig. 6.8) was located just above a step, where downwelling predominates (Huber et al., 2013) (Chap. 5). Further, it was located on the right side of the Enziwigger, close to a small tributary river driving exfiltration of groundwater (Fig. 6.2). Given this specific location, we suspect that river water infiltrated in the upper part of this redd (positive q), while groundwater exfiltrated into the lower part (negative q). As discussed above, this groundwater exfiltration increased during the recession limb of high flow events (Fig. 6.8). Altogether, these data clearly indicate that exchange processes in salmonid redds are driven on different scales, and that these processes altogether determine water-exchange patterns in the egg pocket, which will then have an influence on the likelihood of embryo survival (Michel et al., acc) (Chap. 7).

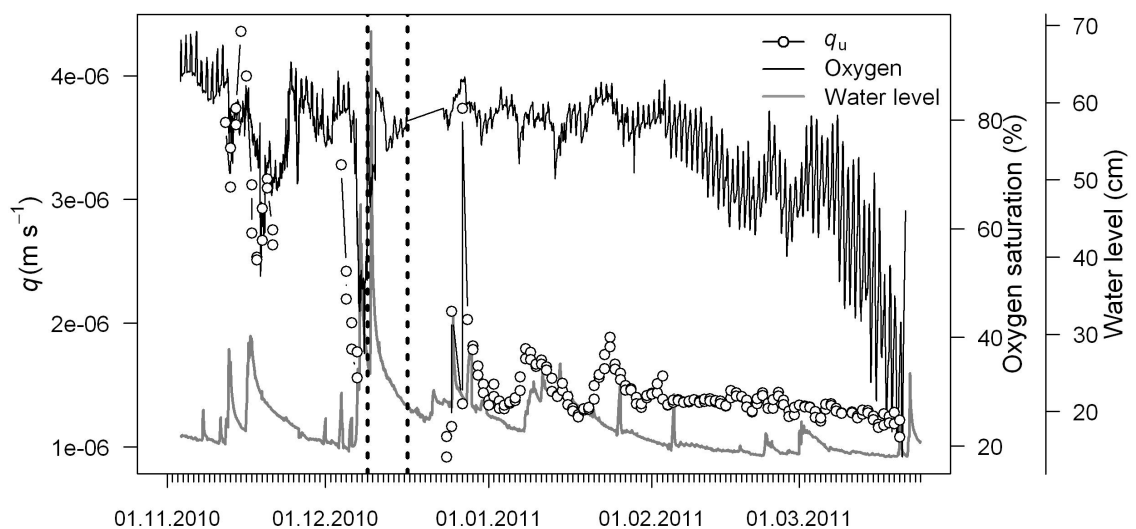


Figure 6.7: Example of the temporal dynamics of the specific infiltration q in the upper part of the redd gravel (q_u), the oxygen concentration and the water level. Shown are data from redd C21_S2 (cf. Fig. 6.2). A period when oxygen and temperature probes were dug out is marked with vertical dashed lines.

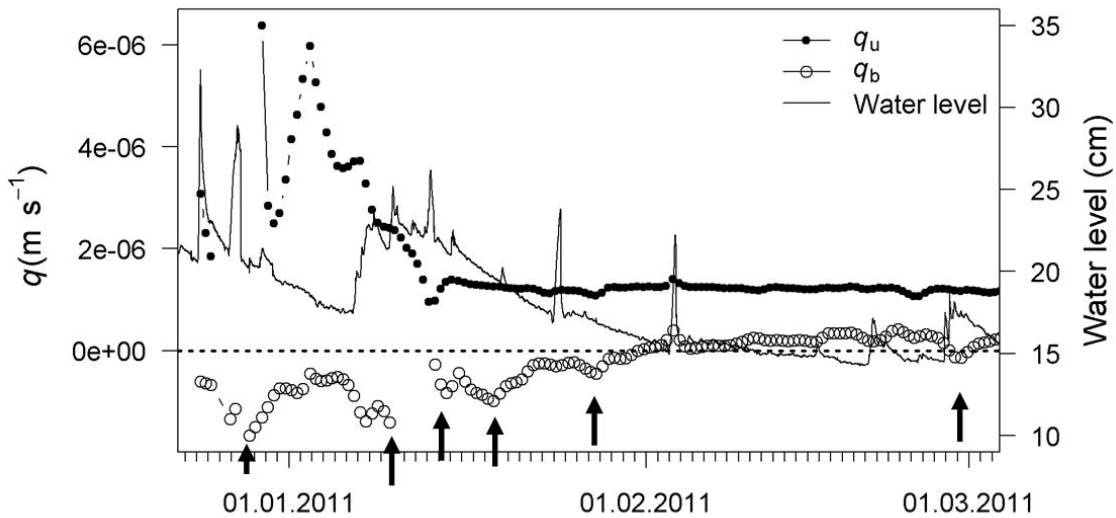


Figure 6.8: Temporal changes of the specific infiltration rate q in the upper and the bottom part of the redd C22_S2 (cf. Fig. 6.2 for location of the redd). Negative values indicate upwelling, positive values indicate downwelling. The arrows point to periods with increased upwelling during the falling limb of high flow events.

Specific water infiltration rates q calculated with the intermediate groundwater flow model for specific redd locations in downwelling zones ranged between $8.5 \cdot 10^{-7} \text{ m s}^{-1}$ and $1.5 \cdot 10^{-5} \text{ m s}^{-1}$ (for season 1, Huber et al., 2013) (Chap. 5). Measured daily q_t values at redd B42_S1 correlated with the modeled values (Pearson correlation: 0.3, $p < 0.05$). At redd B52_S1, no significant correlation was found. The groundwater flow model was set up using hydraulic heads of the river and groundwater as well as the local and regional topography. In contrast, the actual q in the redds further depends on the hydraulic conductivity, affected by fine sediment deposition and hydraulic gradients on the redd scale. These differences could have contributed to the lack of correlation in the latter redd, since water exchange rates on the redd scale can vary strongly, either depending on reach scale bedform character and barriers (Baxter and Hauer, 2000) or differences in hydraulic conductivities (Brunke and Gonser, 1997). These results indicate that groundwater flow modeling as applied in Huber et al. (2013) (Chap. 5) can predict exchange processes on the regional and intermediate scales, but is limited in predicting exchange processes on the redd scale.

Altogether, these findings illustrate that water exchange processes in salmonid redds are complex and driven on multiple scales. Consequently, fine sediment effects on salmonid embryo survival can be expected to differ depending on the redd location relative to river morphology and structure and also on regional aspects, such as river interactions with the valley aquifer.

6.4. RESULTS AND DISCUSSION

6.4.3 Oxygen

Manual vs. continuous oxygen measurements

Manual oxygen measurements, conducted on bi-weekly intervals during season 2 in mini-piezometers, indicated a high interstitial dissolved oxygen (DO) concentration in the redds ($10.1 \pm 2.2 \text{ mg l}^{-1}$ / $75.7 \pm 15.7\%$). However, DO concentrations measured manually did not correlate with DO concentrations from permanent oxygen measurements. Oxygen concentrations in salmonid redds can vary substantially with time (Heywood and Walling, 2007, this study), and hence even weekly or bi-weekly measuring intervals have a high risk of underestimating extreme values (Malcolm et al., 2006). Manual measurements in piezometers could therefore over- or underestimate the amount of oxygen present in salmonid redds, being a poor descriptor for oxygen dynamics during the incubation season. Given these limitations and the methodological bias of the manual DO data, further interpretations are based only on the continuous DO measurements.

Spatial oxygen dynamics

Dissolved oxygen concentrations from continuous measurements in redds documented a high variability on small spatial scales (i.e. between redds), and also a general increase from upstream to downstream (Table 6.3). Interstitial oxygen concentrations at site A (redd A32_S1) were especially low during season 1 with DO concentrations below 3 mg l^{-1} during 44 of total 135 days of egg incubation time. DO concentrations of 3 mg l^{-1} are considered as a critical threshold for salmonid embryo survival (Michel et al., acc) (Chap. 7). The low DO concentrations in this redd could be related to low specific water infiltration q (see beginning of section 6.4.2). This is supported by the observation that, when this redd was moved to a location with a higher water level during season 2, not a single day below 3 mg l^{-1} occurred (redd A32_S2; Table 6.3). In contrast, redd A31_S2, built about six meters upstream of A32_S2, had 14 days with DO concentrations below 3 mg l^{-1} , likely related to upwelling of DO depleted hyporheic water, as discussed in beginning of section 6.4.2 (Fig. 6.5). Days below 3 mg l^{-1} were far less frequent at sites B and C (Table 6.3). These observed low oxygen concentrations at site A could be related to the artificial log steps, breaking down the river slope, inhibiting natural river gravel movements and thus triggering high fine sediment accumulation at sites with low water levels. At the downstream sites, water levels and shear stress were generally higher, leading to a flushing of infiltrated fine sediment, and less accumulation (Schindler Wildhaber et al., 2012b) (Chap. 2).

Only a small number of accumulation baskets in redds with permanent oxygen measurements survived floods, resulting in a very small data set ($n = 4$) across the two field seasons (Schindler Wildhaber et al., 2012b) (Chap. 2). However, these four data points were surprisingly evenly spread and showed a perfect linear decrease of the mean DO concentration with increasing fine sediment accumulation (Supplementary information, Fig.6.11). This has been repeatedly demonstrated before (e.g. Heywood and Walling, 2007), and indicates that also in our study river increased fine sediment accumulation could negatively affect embryo survival by decreasing oxygen supply.

Temporal oxygen dynamics

On the scale of hours and days, DO concentrations decreased during the falling limb of high flow events. This pattern was most pronounced when temporal water exfiltration was measured, e.g., redd A31.S2 (Fig. 6.9, see also section 6.4.2), and thus most likely related to intermittent exfiltration of depleted groundwater or hyporheic water through the redd (sections 6.4.2). The same has been reported in other studies (Malcolm et al., 2010, 2006; Soulsby et al., 2009). Nonetheless, decreasing DO concentrations during the falling limb of high flow events were also found in locations where no exfiltration was measured (e.g., redd C21.S2, Fig. 6.7). Here interstitial DO quickly returned to normal levels after the rising limb of high flow events, also suggesting that this pattern is related to groundwater exfiltration rather than increased fine sediment deposition, which would have likely caused more prolonged effects (Fig. 6.7).

In addition to these changes in interstitial DO on the scale of hours and days, two general trends over the entire incubation period were evident. The first trend could be observed

Table 6.3: Mean oxygen concentrations calculated from continuous measurement with permanent oxygen probes in one redd per site during season 1 (S1) and two redds per site during season 2 (S2). Given are mean \pm standard deviations, minimum (Min) and number of days wherein oxygen concentration was below 7 mg l^{-1} .

Site	Mean \pm sd O_2 (mg l^{-1})			Min O_2		Days $\text{O}_2 < 7 \text{ mg l}^{-1}$		
	S1	S2	Mean S1 & S2	S1	S2	S1	S2	Mean S1 & S2
A	4.7 ± 3.3	8.4 ± 3.4	6.6 ± 3.8	0.0	0.1	94	38 & 2	45 ± 47
B	9.6 ± 2.1	10.0 ± 2.3	9.8 ± 2.2	3.2	0.0	22	25 & 10	19 ± 8
C	9.6 ± 1.8	10.3 ± 1.3	10.0 ± 1.6	0.6	3.8	10	10 & 3	8 ± 4

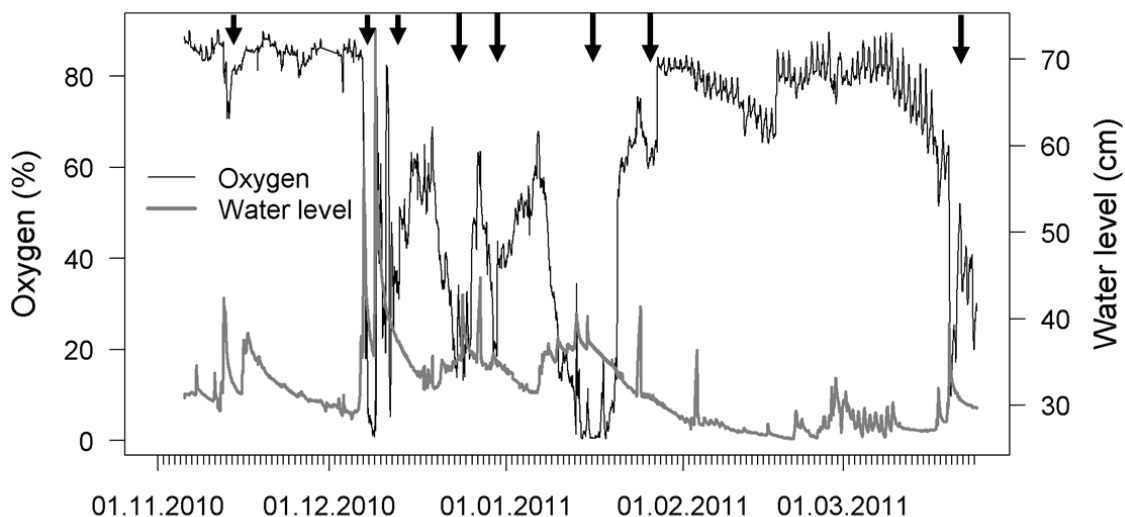


Figure 6.9: Example for temporal oxygen concentration and water level dynamics (redd A31.S2, see Fig. 6.2 for location of the redd). Arrows mark the decrease of oxygen concentrations during the falling limb of high flow events.

6.4. RESULTS AND DISCUSSION

at the beginning of the incubation season: shortly after redd construction, DO was generally high and paralleled by high specific water infiltration rates q (10-12 mg l⁻¹, or 80-90% oxygen saturation; for an example see Fig. 6.7). Within a few weeks, interstitial DO decreased in parallel with q , as also reflected in significant correlations between these two parameters (Fig. 6.10). The different form of this relationship among redds (Fig. 6.10) could be related to local conditions at the redd location that also affect interstitial DO (e.g., organic content, groundwater influence). The second trend could be observed at the end of the incubation season, when several redds showed a distinct decrease in interstitial oxygen during spring, i.e. just before hatching (Fig. 6.7, Fig. 6.9). This decrease was usually preceded by prolonged periods of base flow, when smaller sediment particles infiltrated in the redds (Schindler Wildhaber et al., 2012b) (Chap. 2). These silt and clay sized particles can effectively induce siltation of the riverbed, thereby decreasing hydraulic conductivity (Schälchli, 1995). Moreover, the organic matter concentration of the infiltrated fine sediment increased during base flow conditions (Schindler Wildhaber et al., 2012a) (Chap. 3). Together with rising water temperatures during spring, the latter likely further decreased the oxygen concentration in the redds (Greig et al., 2007b). This decrease towards the time of hatching, when oxygen demand of the salmonid embryos

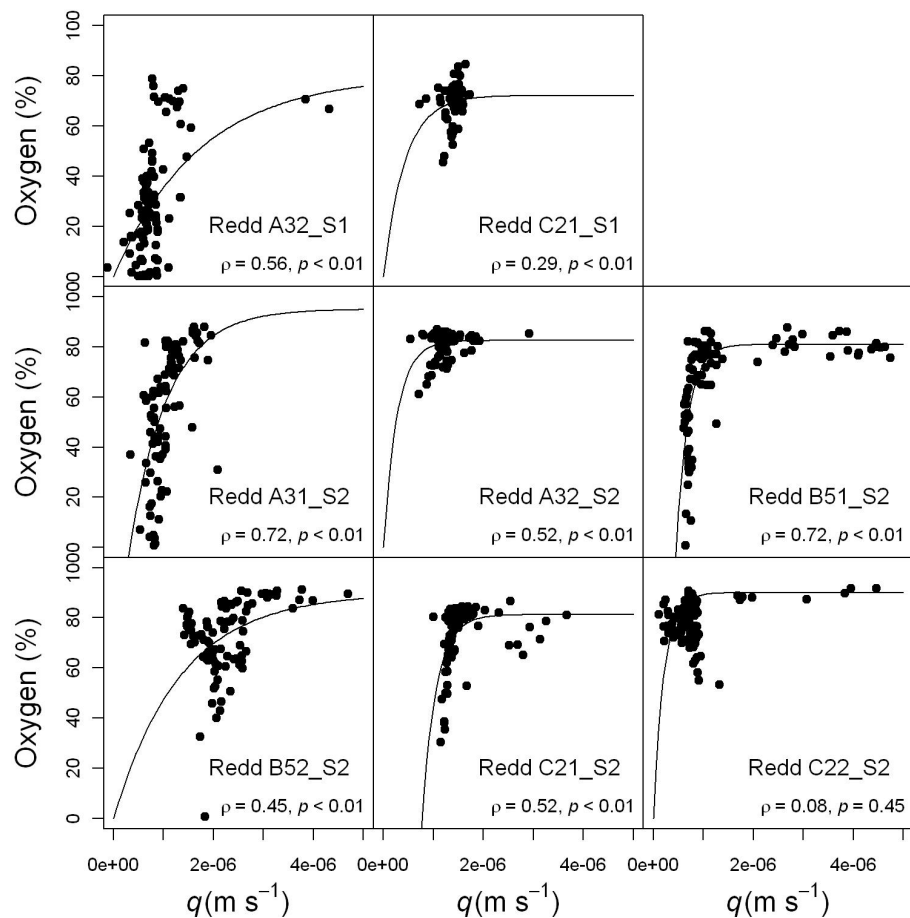


Figure 6.10: Relationships between the mean daily oxygen concentrations in redds and the specific infiltration rates q_t with non-linear regression lines. Within each panel Spearman correlation coefficient ρ and the p -value are given. See Fig. 6.2 for location of the redds.

is at maximum (Greig et al., 2007b), might have also affected embryo survival in some redds (Michel et al., acc) (Chap. 7).

6.5 Conclusion

Artificial steps in channelized rivers can have positive or negative effects on incubating salmonid embryos. In downstream sections, where canalization of the riverbed cause higher water level and an increased slope, resulting in a higher sediment transport capacity, artificial steps decrease river gravel movements and thus scouring of the riverbed. Additionally, artificial steps increase hyporheic exchange processes. Further upstream, in low flow sections, where slopes would naturally be higher, artificial steps inhibit natural river gravel movements due to the decreased riverbed slope. This triggers higher fine sediment infiltration and accumulations, resulting in lower specific water infiltration rates (q) and hyporheic oxygen.

Our data further more demonstrate that q and dissolved oxygen (DO) concentrations in salmonid redds are highly dynamic and driven on multiple scales. Clearly, q and interstitial DO in salmonid redds are affected by conditions at the redd location, such as the amount of accumulated fine sediment, organic content and redd morphology. However, local factors of the magnitude of centimeters to meters are regularly superimposed by processes driven on the intermediate scale (in the range of meters) and regional scale (in the range of tenths of meters to kilometers). On an intermediate scale artificial steps can affect patterns of fine sediment accumulation, water exchange in salmonid redds and hence interstitial DO.

Our results document for the first time an effect of artificial steps on water exchange and oxygen concentrations in salmonid redds. Given the complex interaction of all the processes studied here, multiple factors have to be considered to predict salmonid embryo survival, which is highly time and work intensive. Multiple predictors should include oxygen and fine sediment measurements, riverbed structure such as artificial steps or the channelized riverbed and the hydrological setting of the river in the valley aquifer.

Acknowledgments This study was funded by the Swiss National Science Foundation (SNSF projects K-32K1-120486 and CR23I2_138025). We thank Sandra Rudolf, Bastian Brun and Annina Gysel for their help in the field, Marianne Caroni and Ruth Strunk for their laboratory assistance and measurements, Johannes Fritsche for his help with R analyses and Claude Schneider and Lukas Zimmermann for their technical support. The corrections of Andrew Clarke improved language and grammar of the manuscript, thank you. Finally, we greatly acknowledge the extensive support of Phillip Amrein (Fish and Wildlife Service, Canton of Lucerne, Sursee, Switzerland).

6.6 Supplementary information

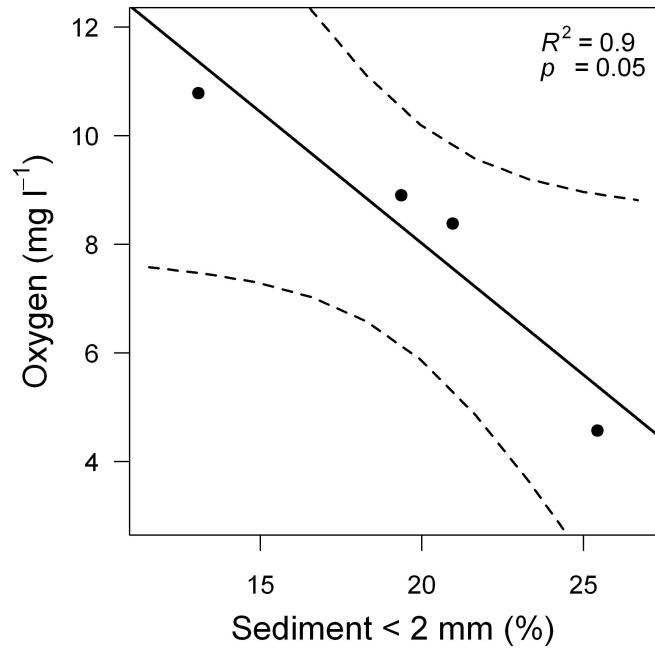


Figure 6.11: Correlation between dissolved oxygen and accumulated fine sediment in the redds. Dashed lines are the 95% confidence intervals.

CHAPTER 6. EFFECTS OF RIVER MORPHOLOGY, HYDRAULIC GRADIENTS, AND
SEDIMENT DEPOSITION ON WATER EXCHANGE AND OXYGEN DYNAMICS IN SALMONID
REDDS

Chapter 7

Artificial steps mitigate fine sediment effects on brown trout embryo survival in a heavily modified river

This chapter is accepted for publication:

Michel C, Schindler Wildhaber Y*, Epting J, Thorpe, KL, Huggenberger P, Alewell C, Burkhardt-Holm P. Artificial steps mitigate fine sediment effects on brown trout embryo survival in a heavily modified river. Journal of Freshwater Biology. *SHARED FIRST AUTHORSHIP*

7.1 Summary

1. Understanding the factors that determine successful salmonid embryo incubation in the many structurally modified river systems of the Northern hemisphere is crucial for maintaining healthy salmonid populations. In this context, the joint impact of fine sediment accumulation together with anthropogenic river modifications on salmonid embryo survival has been rarely investigated.
2. We investigated brown trout embryo survival to hatch (STH) together with ten physicochemical, hydraulic and morphological parameters in artificial brown trout redds in a heavily modified stream (i.e. channelized, artificial log steps) in central Switzerland. We were interested to understand 1) if STH is more sensitive to the timing and duration of low oxygen rather than a mean oxygen concentration, 2) if STH was negatively affected by increased fine sediment deposition decreasing redd gravel permeability, 3) if higher water levels, causing fine sediment re-suspension, benefit STH, 4) if STH was negatively affected by organic content in the redds, and especially 5) if hydraulic gradients related to redd scale bed-form and/or the artificial step structure benefit embryo STH, and hence could mitigate the negative impact of fine sediment and/or organic content.
3. Up to 50% brown trout embryos survived with interstitial oxygen exceeding 3 mg l^{-1} . Embryos endured up to six days $\leq 1 \text{ mg l}^{-1}$ but were more sensitive to oxygen depletion close to hatch. Therefore, timing and duration of low oxygen

were important for embryo STH, and hence oxygen dynamics need to be considered when assessing in redd conditions for salmonid STH.

4. Partial least squares regression identified the horizontal hydraulic gradient, fredle index, distance to artificial log steps upstream, and amount of accumulated fine sediment as influential predictors for embryo STH. The water level above the redd and total organic carbon content in the redd were not influential. Among the identified influential predictors, 70.9% of the variation in STH could be explained by a logistic regression model containing redd distance to the next upstream step (26.4%, $p = 0.004$), fredle index (27.2%, $p = 0.003$), and horizontal hydraulic gradient (10.1%, $p = 0.04$). In the logistic regression, the amount of accumulated fine sediment ($p = 0.75$), field seasons ($p = 0.93$) and field sites ($p = 0.66$) were non-significant.
5. In summary, brown trout STH was sensitive to redd gravel permeability, which was measured as fredle index and affected by fine sediment deposition. At the same time, hydraulic gradients related to artificial log steps, which enhanced hyporheic exchange, benefited embryo STH, and hence mitigated fine sediment impact. This result can be likely transferred to other surface-water dominated river systems with good hyporheic water quality. To what extent it can be transferred to river systems with other hydraulic boundary conditions, remains to be evaluated. Altogether, our results clearly indicate that the impact of fine sediment on salmonid incubation success needs to be understood in the hydrological and morphological context of the particular river system.

7.2 Introduction

Native salmonid populations are reported to be in decline in Switzerland (Burkhardt-Holm et al., 2005), the United Kingdom (Youngson et al., 2002), and North-America (Brown et al., 1994; Huntington et al., 1996). Among others, habitat degradation is considered a major contributing factor (e.g., Brown et al., 1994; Burkhardt-Holm and Scheurer, 2007; Hicks et al., 1991) with numerous studies focusing on fine sediment as a single factor for decreased salmonid embryo survival (e.g., Jensen et al., 2009, and studies cited therein). However, recent research substantiates that a more generalized perspective is necessary to understand the constraints for salmonid incubation success in degraded and modified river environments (Malcolm et al., 2010).

During spawning, salmonid fish deposit their eggs in distinct gravel structures, called redds, where the embryos incubate for several months (Crisp, 2000). Embryo survival during this intra-gravel stage depends strongly on oxygen supply to the developing embryos, which itself depends on the water-flow through the egg pocket and the interstitial oxygen concentration (Malcolm et al., 2008). Deposited fine sediment can decrease redd gravel permeability and hence hinder oxygen supply (Greig et al., 2007a; Heywood and Walling, 2007). However, water exchange in salmonid redds also depends on river morphology and hydraulic gradients driving interstitial flow (Malcolm et al., 2010, 2006; Soulsby et al., 2001a). Laboratory studies indicate that hydraulic gradients can to some degree counterbalance the negative effect of fine sediment on interstitial flow and salmonid incubation success (Lapointe et al., 2003). In rivers hyporheic exchange is

7.2. INTRODUCTION

strongly influenced by gravel permeability and hydraulic boundary conditions, which also depend on local geomorphic features (Baxter and Hauer, 2000; Brunke and Gonser, 1997; Kasahara and Wondzell, 2003). Altogether, it can be expected that several parameters in combination affect water-flow and quality in salmonid redds, and hence embryo survival (Greig et al., 2007b).

In channelized rivers the lack of morphological diversity can substantially decrease hyporheic water exchange (Boulton, 2007), whereas hydraulic gradients related to artificial in-stream structures (e.g., steps, gabions, weirs) can increase hyporheic exchange (Boulton, 2007; Hester and Doyle, 2008). These river modifications, present in many structurally modified fluvial ecosystems (Brookes, 1988; Wohl, 2006), could therefore also affect salmonid incubation success. Despite this, no field study has, to our knowledge, simultaneously investigated the relative importance of fine sediment, hydraulic gradients and structural modifications for salmonid embryo survival. Such a study could help to better understand the factors contributing to successful embryo incubation in heavily modified rivers, thereby providing new perspectives for management decisions to maintain viable salmonid populations.

The current study disseminates the relative importance of ten factors that could affect brown trout *Salmo trutta* embryo survival to hatch (STH) in a small and heavily modified headwater stream of the Swiss Plateau (Enziwigger, Canton of Lucerne, Switzerland; Fig. 7.1a). River modifications in the Enziwigger, introduced during land reclamation in the 20th century, include a straightened and laterally stabilized river channel and cross-channel log steps to prevent bed scouring during flood events. As in many other rivers, these modifications had a profound effect on the hydro-morphological functioning of the river (Schindler Wildhaber et al., 2012b) (Chap. 2). Despite this, the Enziwigger maintains a viable brown trout *Salmo trutta* population (Schager et al., 2007), making it a suitable river to assess the relative importance of fine sediment, hydraulic gradients and river structure for salmonid embryo survival in a heavily modified river environment.

The hypotheses tested in the current study are based on our knowledge obtained during a four year interdisciplinary project. Integrating over the whole project, a process-based conceptual summary (Fig. 7.1) of the interaction of the investigated parameters (Table 7.1) and how they could affect brown trout embryo survival (Table 7.1) was developed: In the Enziwigger, fine sediment deposition decreases gravel permeability and water exchange in the redds, while higher water levels decrease fine sediment accumulation by increasing fine sediment re-suspension (Schindler Wildhaber et al., 2012b) (Chap. 2). Hydraulic gradients, either related to localized (redd scale) bed-morphology and/or the artificial step structure, together with gravel permeability then jointly drive hyporheic water exchange in the redds. Oxygen concentrations in the redds increase with hyporheic water exchange and decrease with accumulated fine sediment. Therefore, we hypothesized that (hypothesis A) the hydraulic gradients mentioned above could partly mitigate the negative impact of increased fine sediment. This was suggested before by laboratory studies (Lapointe et al., 2003) but not yet tested in a field setting. Moreover, oxygen concentrations in redds decreased in spring which was most likely related to prolonged periods of base flow, causing infiltration of smaller sediment particles with higher organic matter content. Together with rising water temperature, this increased organic oxygen demand, which could negatively affect embryo STH (Schindler Wildhaber et al., 2014, hypothesis B) (Chap. 7). Finally, the oxygen concentrations in the redds are highly variable, leading

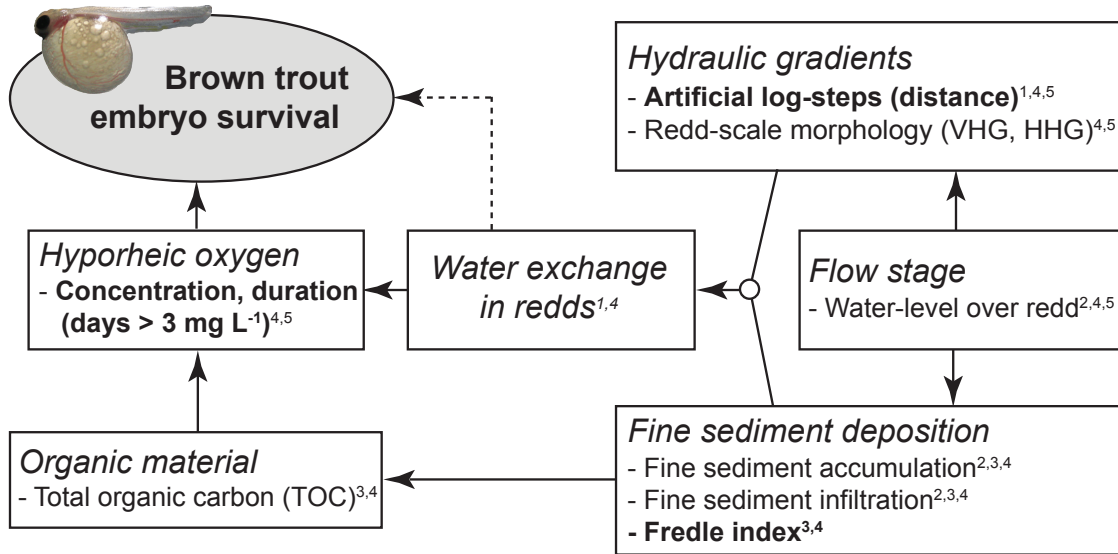


Figure 7.1: Conceptual process-based summary of the interaction of investigated parameters and how they relate to brown trout embryo survival in our heavily modified study river. In each box a general descriptive term (in italics) is given on top, with parameters investigated in our project listed below. Superscripts indicate References: 1- Huber et al. (2013) (Chap. 5), 2 - Schindler Wildhaber et al. (2012b) (Chap. 2), 3 - Schindler Wildhaber et al. (2012a) (Chap. 3), 4 - Schindler Wildhaber et al. (2014) (Chap. 7), and 5 - this study (bold parameters are identified most important variables). Arrows indicate that parameter affects the response parameter directly, and the open circle indicates that parameters jointly affect the response parameter. Dashed arrow indicates that water exchange might also affect embryo STH directly, e.g., by removing metabolic waste, but this was not tested in the current study.

us to hypothesize (C) that the frequency and duration of periods of low oxygen, rather than just a mean oxygen concentration, determines effects salmonid embryo survival.

To approach these hypothesis we investigated in the current manuscript 1) if brown trout STH is sensitive to the timing and duration of low oxygen rather than a mean oxygen concentration; 2) if brown trout embryo STH decreases with increasing fine sediment deposition and hence decreasing redd gravel permeability, 3) if higher water levels, causing fine sediment re-suspension, benefit brown trout embryo STH, 4) if brown trout embryo STH in the Enziwigger is negatively affected by organic content in the redds, and most important 5) if hydraulic gradients, either related to local (redd scale) bed-form or the artificial step structure of the river, benefit embryo STH, and hence mitigate the negative impact of either fine sediment or organic content. Altogether, the current study provides a novel perspective on salmonid embryo survival in heavily modified rivers by identifying the most important factors affecting brown trout embryo survival.

7.2. INTRODUCTION

Table 7.1: Explanatory variables included in multivariate analyses. For each variable a short description and references (Ref.) describing the methodology how the parameter was measured are given. The hypothesized effect on embryo STH (\uparrow = increase; \downarrow = decrease) based on the process understanding developed in our project (Fig. 7.1) are also given. Finally, the variable influence on prediction score (VIP) inferred in the partial least squares regression analysis is given. The most important predictor variables identified in the multivariate logistic regression analysis are marked in bold.

Variable	Description	Ref.	Effect	VIP
Infiltrated fine sediment	Mean amount of weekly deposited fine sediment in the redd	1,2	\downarrow	0.88
Accumulated fine sediment	Net amount of fine sediment deposited over the entire incubation season	1,2	\downarrow	1.18
Fredle index	Gravel quality index that correlates positively with gravel permeability	2,3	\uparrow	1.41
Water level	Mean water level over the redd calculated from measured water levels above each redd and continuous flow stage measurements at each field site	2	\uparrow	0.03
Vertical hydraulic gradient	The vertical hydraulic gradient driving up- and downwelling through redd	2,4	\uparrow	0.40
Horizontal hydraulic gradient	Pit-tail hydraulic gradient driving horizontal pumping flow through redd	2	\uparrow	1.61
Interstitial oxygen	Mean oxygen concentration calculated from bi-weekly manual measurements in mini-piezometers	2	\uparrow	0.62
Total organic carbon	Net amount of organic carbon deposited in the redd during the incubation season	5	\downarrow	0.56
Distance to upstream step	Distance of the redd to the next step located upstream in the terrace	2,6	\downarrow	1.29
Distance to downstream step	Distance of the redd to the next step located downstream in the terrace	2,6	\downarrow	0.85

References: 1 - Schindler Wildhaber et al. (2012b) (Chap. 2), 2 - Schindler Wildhaber et al. (2014) (Chap. 7), 3 - Lotspeich and Everest (1981), 4 - Baxter et al. (2003), 5 - Schindler Wildhaber et al. (2012a) (Chap. 3), 6 - Huber et al. (2013) (Chap. 5).

7.3 Methods

7.3.1 Study River and experimental setup

The Enziwigger is a straightened and channelized stream located in Central Switzerland (Canton of Lucerne). It has a total watershed area of about 31 km² (Fig. 7.2a). Mean discharge, measured in Willisau by the cantonal authorities (Nov. 2007 - Nov. 2008) was 2.1 m³ s⁻¹, minimum and maximum discharge were 1.1 m³ s⁻¹ and 10.1 m³ s⁻¹, respectively. Like most rivers in the Swiss Plateau, the morphology of the Enziwigger is strongly modified: 5% is natural or close to natural, 21% is little affected and 74% is strongly affected or artificial (EBP-WSB-Agrofutura, 2005). Artificial in-stream structures include lateral stabilizations and steps to prevent deep channel erosion and bed-scouring during flood events (Fig. 7.2a). Despite the strong morphological modifications, the biological condition is considered good (EBP-WSB-Agrofutura, 2005). The only fish species in the Enziwigger is the brown trout, which maintains a viable population (Schager et al., 2007). No stocking is carried out and the river is neither affected by hydropower nor by effluents of wastewater treatment plants.

In winter 2009/10 (season 1) and winter 2010/11 (season 2) artificial brown trout redds (Fig. 7.1b) were set up at three sites along the river (Fig. 7.2a). The most upstream site A is

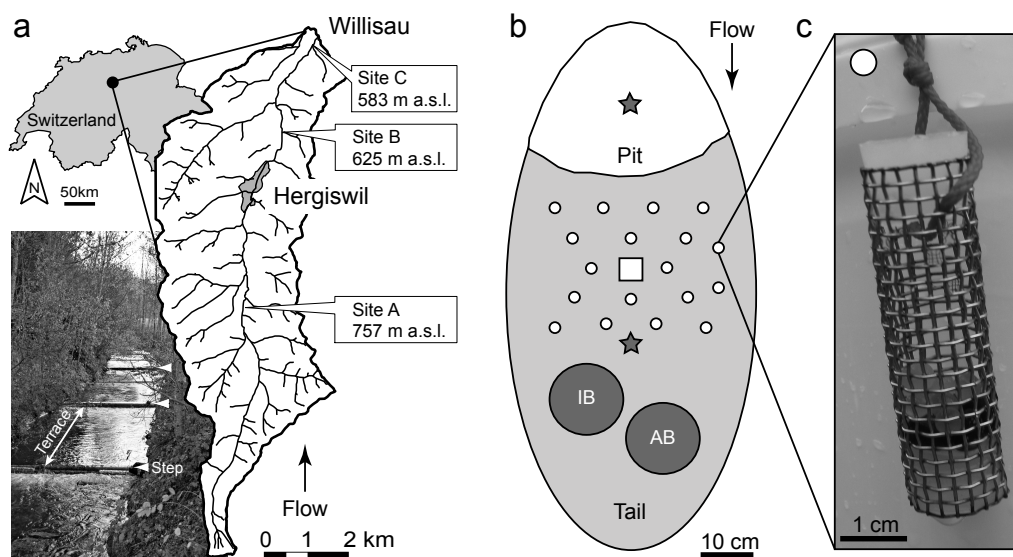


Figure 7.2: Study river and experimental setup. (a) Location of the Enziwigger watershed in Switzerland. The photograph shows the step and terrace structure at study site B. The watershed map of the river Enziwigger shows the towns Willisau and Hergiswil (Canton of Lucerne, Switzerland) and the location of the three field sites, (b) Schematic of the experimental setup, showing a top view on one of the artificial redds with the pit (white) and tail (light grey) areas. Symbols mark the position of the piezometer pipes (grey stars), egg capsules (white circles), and the Aandera oxygen probe (white rectangle) introduced in some redds for continuous oxygen monitoring. The fine sediment infiltration (IB) and accumulation (AB) baskets were located just behind the egg-capsules. For a schematic lateral view on one of the artificial redds see Fig. 6.1 in Schindler Wildhaber et al. (2014) (Chap. 7) and (c) egg-capsule used to incubate brown trout embryos.

7.3. METHODS

located in an area surrounded by forest and pasture. Sites B and C are in areas dominated by pasture and arable land. All sites contain artificial steps and terraces, which create a repetitive step-pool-glide morphology (Fig. 7.2a).

In each season six artificial redds were built per site, resulting in a total of 36 investigated redds. A subset of these redds ($n = 9$) was also equipped with continuous oxygen measurement probes (Fig. 7.2b; cf. Schindler Wildhaber et al., 2014) (Chap. 7). Redds were located in areas where natural brown trout redds are regularly observed (pers. obs.; P. Amrein, Fish and Wildlife Service, Canton of Lucerne). All redds were built with natural gravel obtained at the redd location to resemble natural brown trout redds in structure and dimension (Crisp and Carling, 1989). Within terraces artificial redds were built in glide sections, always one towards the downstream step and one more towards the upstream step. See Fig. 7.2 in Schindler Wildhaber et al. (2014) (Chap. 7) for the exact location of the redds in the terraces. In each redd a number of sampling devices was installed (Fig 2b) to quantify seven physicochemical and hydraulic parameters that could potentially affect brown trout embryo STH (Table 7.1). The water-level above each redd was inferred from weekly manual measurements above every redd and continuous flow-stage measurements at each site (Table 7.1 Schindler Wildhaber et al., 2014) (Chap. 7). Finally, for each redd the distance to the next step located downstream and upstream in the terrace was measured manually (Table 7.1). In the following, when referring to a particular redd and season, the redd name (e.g., C31) is extended by *_S1* (for season 1) or *_S2* (for season 2), respectively.

7.3.2 Quantification of embryo survival

Brown trout embryo survival to hatch (STH) was assessed with egg-capsules (e.g., Dumas and Marty, 2006; Scrivener, 1988) inserted in the redd gravel. The egg capsules (Fig. 7.2c) used in our study were made of individually manufactured stainless steel mesh-cylinders (DIN 1.4401 AISI316 material, length = 60 mm, diameter = 16 mm, mesh-size = 2 mm, G. Bopp & Co. AG, Zürich, Switzerland) and closed on both ends with biologically inert silicone stoppers (Carl Roth. AG, Arlesheim, Switzerland). Each capsule had a red line attached on its top to locate and remove the capsule during sampling (Fig. 7.2c). Eggs in the capsules were located at a depth of 12-14 cm, which is the range of egg-burial depths observed for similar sized riverine brown trout (Crisp and Carling, 1989; DeVries, 1997). Twenty capsules per redd were planted, each with ten fertilized brown trout eggs ($n = 200$ eggs per redd). Fertilized eggs were obtained during routine collection of spawners by the cantonal authorities in early November, and fertilization was conducted at the fish holding facility of the cantonal fish warden in Willisau (P. Amrein, Fish and Wildlife Service, Canton of Lucerne). For the experiment, eggs stripped from ripe females (season 1: $n = 16$, length = 25.1 ± 1.8 cm and season 2: $n = 10$, length = 27.9 ± 2.6 cm; mean \pm sd) were pooled and artificially inseminated with pooled milt (season 1: $n = 8$ males, length = 29.5 ± 1.8 cm and season 2: $n = 7$, length = 26.1 ± 1.3 cm; mean \pm sd). Fish of this size represent first time spawners in the Enziwigger (Schager et al., 2007). After water hardening, eggs were transferred into capsules and transported to field sites in buckets filled with spring water originating from the Enziwigger watershed. The water temperature was slowly adjusted to that of the river, and capsules were planted in redds within less than six hours post fertilization. As control, fertilized eggs ($n = 300$) were placed directly

after water hardening in an egg incubator at the holding facility. To control for the effect of transportation, a further 300 eggs were transported to the field locations, returned to the holding facility, and placed in the egg incubator. The egg incubator was supplied with spring water originating from the Enziwigger watershed. The STH in the incubator was used to determine the natural mortality of the egg batches within each season. Prior to data analyses, survival data within each season was normalized to the respective transportation control, which is a common method to account for differences in egg quality between years (cf. Rubin and Glimsäter, 1996).

7.3.3 Statistical analysis

All data were analyzed with the software R v2.12.0 using multivariate methods. In total, ten parameters were included as explanatory variables (Table 7.1). To identify the most important predictors for brown trout STH among these ten explanatory variables we first used partial least squares regression to screen for the influential variables (PLS regression; Eriksson et al., 2006). PLS regression was used first because it provides a robust approach to evaluate the relative influence of multiple predictor variables on a response variable in co-linear and small-sized data-sets (Wold et al., 2001). Its good performance has been also demonstrated for comparable ecological data-sets (Carrascal et al., 2009). PLS regression was conducted with the function `pls` (`pls` package; Mevik and Wehrens, 2007). The response variable (proportion survival to hatch; STH) was arcsine transformed prior to the analysis (Quinn and Keough, 2002). Once the model was fit, the variable influence on projection score (VIP; calculated in reference to Chong and Jun, 2005) was used to evaluate the influence of each predictor variable on embryo STH. Variables with a $VIP > 1$ were considered influential (cf. Eriksson et al., 2006).

Following this screening, the individual relationship between the identified influential predictor variables ($VIP > 1$) and embryo STH was quantified by multivariate logistic regression (quasi-binomial error structure, logit link function; Faraday, 2006). Prior to this analysis, the Pearson product-moment correlation coefficient was used to quantify the amount of co-variation among influential variables. Variance inflation factors (VIF; function `corvif`, `AED` package) were applied to test if the amount of co-variation among influential explanatory variables prohibits using them in a single multivariate regression model. To account for effects of our sampling design, field seasons and field sites, as well as their interaction, were included as categorical explanatory variables in the initial full model. Significant predictor variables were then identified via step-wise model simplification using pair-wise model comparisons. As recommended for logistic regression models with a quasi-binomial error structure F-tests were applied in pair-wise comparisons (function: `drop1`; Faraday, 2006). Significance was accepted at $p \leq 0.05$.

7.4 Results

7.4.1 Redd loss during bed scouring

Overall, 12 of the 36 initially installed redds (33%) were lost during bed scouring events, leaving a final data-set of 24 redds for the multivariate analysis. Five of the 9 redds with

7.4. RESULTS

continuous oxygen monitoring were also lost; as a consequence the continuous oxygen data could not be included in the multivariate analysis, but is discussed qualitatively (see below). Further egg capsules were also lost from the surviving redds, during bed-scouring events, therefore, embryo STH in redds was determined from different numbers of capsules per redd: The mean number of capsules sampled per redd was 13 (min = 10, max = 14) in season 1 and 17 (min = 9, max = 20) in season 2. Altogether, STH was determined from a mean of 138 (min = 90, max = 200) fertilized brown trout eggs per redd.

7.4.2 Embryo survival among years and sites

Mean brown trout survival to hatch (STH) in the control/transportation control was 73% / 76% and 72% / 60% in seasons 1 and 2, respectively. The corrected mean \pm SEM brown trout STH in the Enziwigger was $34 \pm 4\%$, and ranged from a minimum of zero survival in a redd at site A (redd A31_S1) to a maximum of 74% at the downstream site C (redd C31_S2). The mean STH within seasons showed fluctuations between years (Fig. 7.3a) and field sites (Fig. 7.3b). Compared to the other explanatory variables these differences were non-significant in the multivariate logistic regression analysis (see below).

7.4.3 Oxygen dynamics and embryo survival

Oxygen concentrations during the incubation season are compared to a reference value of 3 mg l^{-1} , because brown trout embryos have been documented to survive well with this oxygen level.

In redd A32_S1 interstitial oxygen was initially high, but dropped sharply in early December occasionally reaching complete depletion (Fig. 7.4a). Altogether, interstitial oxy-

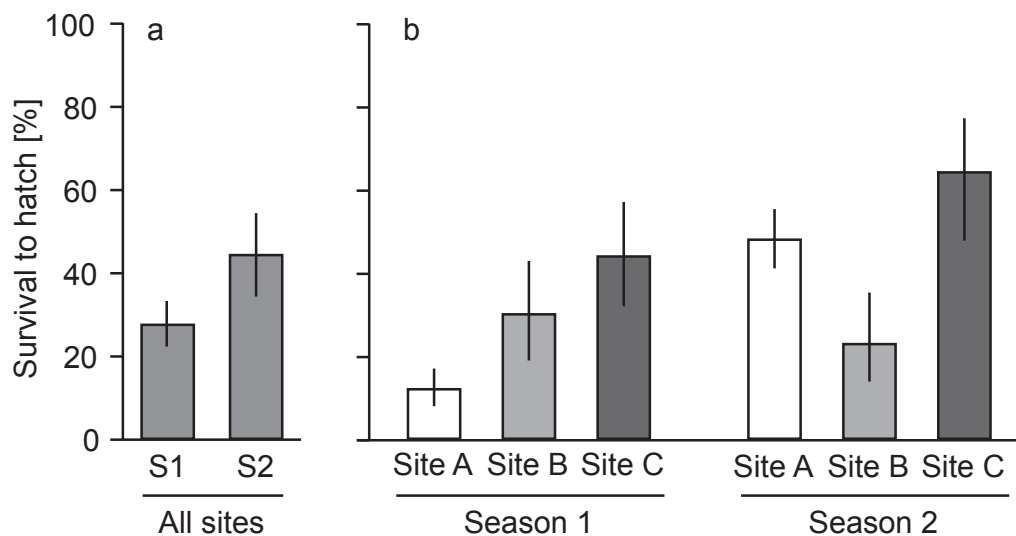


Figure 7.3: (a) mean embryo survival to hatch for all study sites during seasons 1 (S1) and 2 (S2) and (b) Mean embryo survival to hatch in the individual field sites (A, B and C) for seasons 1 and 2. Bars represent mean \pm SEM.

gen was below 3 mg l^{-1} on 44 days in this redd, and below 1 mg l^{-1} for 22 of these days. The mean \pm sd oxygen concentration was $4.6 \pm 3.3 \text{ mg l}^{-1}$, and embryo STH was 10%. In redd A32_S2 oxygen concentrations were mostly above 8 mg l^{-1} , and no day below 3 mg l^{-1} occurred (Fig. 7.4b). The mean \pm sd oxygen concentration was $10.8 \pm 1.8 \text{ mg l}^{-1}$ and embryo STH was 49%. In redd A31_S2, which was built about six meters upstream of A32_S2, interstitial oxygen was more variable throughout the incubation season and altogether 14 days with less than 3 mg l^{-1} occurred (Fig. 7.4c). Moreover, embryos in this redd experienced six days with less than 1 mg l^{-1} oxygen in mid-January. The mean \pm sd oxygen concentration was $8.4 \pm 3.4 \text{ mg l}^{-1}$, and embryo STH was 47%. In redd B51_S2 oxygen concentrations were mostly above 5 mg l^{-1} until early March, but then oxygen levels dropped below 3 mg l^{-1} until hatch, in this period also four days with less than 1 mg l^{-1} occurred (Fig. 7.4d). The mean \pm sd oxygen concentration was $8.9 \pm 2.5 \text{ mg l}^{-1}$, and embryo STH was 35%. For a discussion of the continuous oxygen data from all investigated redds see Schindler Wildhaber et al. (2014) (Chap. 7).

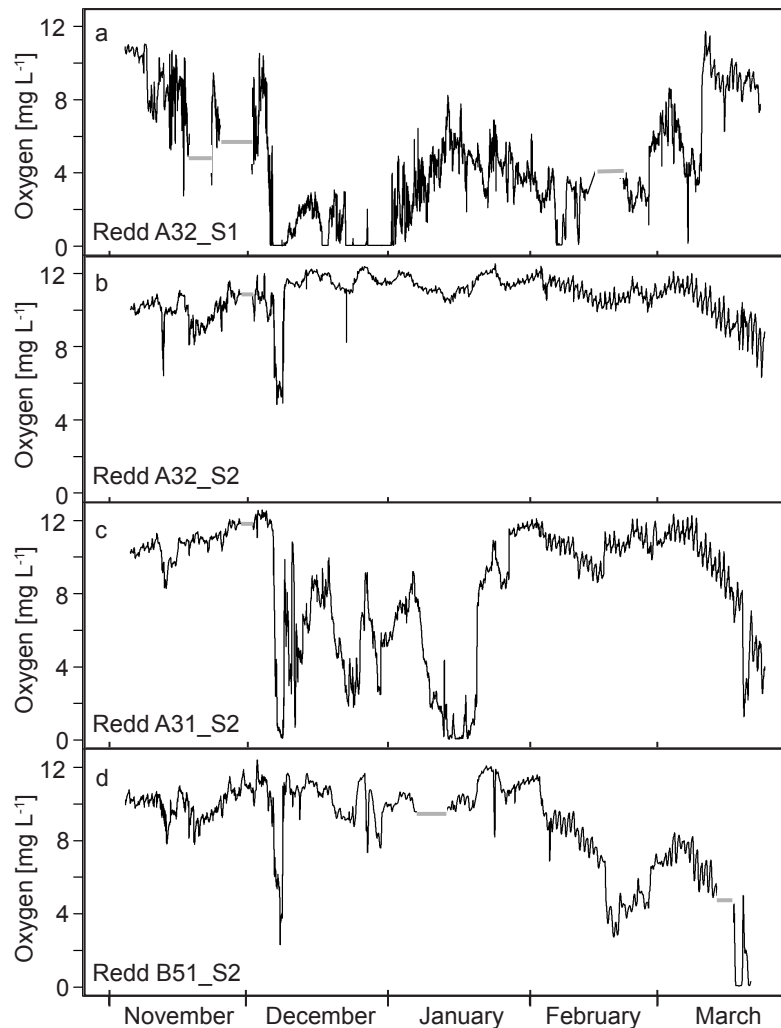


Figure 7.4: Interstitial oxygen concentration in the four redds where continuous measurements and embryo survival to hatch data were available. Horizontal gray bars mark periods of missing data.

7.5. DISCUSSION

Table 7.2: Results of the multivariate logistic regression analyses. Given are the explained deviance (D_{exp}), parameter estimates (Estimate) and their standard error (SE), as well as their significance levels (p) from the optimal logistic regression model. Dist. step up = distance to upstream step, HHG = Horizontal hydraulic gradient, see also Table 7.1.

Variable	D_{exp}	Estimate	SE	p
Intercept		-1.09	0.42	0.021
Fredle index	27.2%	0.15	0.04	0.003
Dist. step up	26.4%	-0.15	0.04	0.004
HHG	10.1%	10.19	4.57	0.045
Total	70.9%			

7.4.4 Fine sediment, river structure and embryo survival

The PLS regression identified the horizontal hydraulic gradient, the fredle index, the distance to the upstream step, and the amount accumulated fine sediment as influential predictors for embryo STH in the Enziwigger ($VIP > 1$; Table 7.1). The PLS regression model containing these four influential parameters explained 71.4% of the variance in embryo STH. The only significant correlation among influential predictor variables could be observed between the fredle index and the amount of accumulated fine sediment (Fig 7.6). Variance inflation factors permitted using all influential variables in a single multivariate regression model (all VIFs ≤ 2.57 ; Zuur et al., 2010). Among influential predictor variables step-wise logistic regression analysis identified the fredle index, the distance to the upstream step, and the horizontal hydraulic gradient as significant explanatory variables (Table 7.2). The logistic regression model containing these three explanatory variables explained 70.9% of the total deviance in embryo STH (Table 7.2). The fredle index and the distance to the next upstream step explained equal proportions of 27.2% and 26.4%, respectively. The horizontal hydraulic gradient was just significant explaining 10.1% (Table 7.2), but this result was mostly related to two influential data-points (Fig. 7.5c) from a single redd consistently located below a step in site C. Altogether, embryo STH decreased with distance to the next upstream step (Fig. 7.5a) and increased with the fredle index (Fig. 7.5b), and the horizontal hydraulic gradient (Fig. 7.5c). The amount of accumulated fine sediment ($p = 0.75$), field seasons ($p = 0.93$) and field sites ($p = 0.66$) did not contribute significantly.

7.5 Discussion

Many salmonid streams of the northern hemisphere are structurally modified (Brookes, 1988; Wohl, 2006), but little is known about if and how these modifications, together with fine sediments, may influence salmonid embryo survival (but see Malcolm et al., 2010). This knowledge could contribute valuable information for restoring native salmonid populations. To this end, we applied a generalized approach, integrating the sciences of geomorphology, hydrology and freshwater ecology, to better understand the factors affecting brown trout incubation success in a degraded and modified river environment.

CHAPTER 7. ARTIFICIAL STEPS MITIGATE FINE SEDIMENT EFFECTS ON BROWN TROUT EMBRYO SURVIVAL IN A HEAVILY MODIFIED RIVER

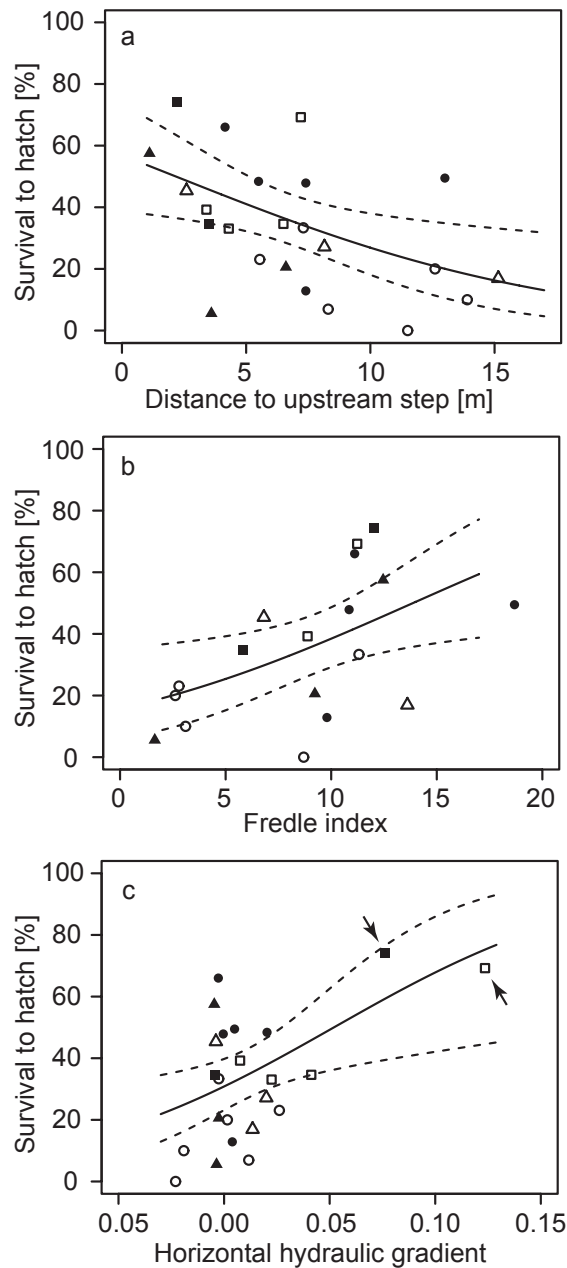


Figure 7.5: Relationship between brown trout survival to hatch and significant predictor variables identified in the multivariate logistic regression (Table 7.2). Lines are mean regression line \pm 95% point-wise confidence intervals as predicted from the fitted generalized linear model. Symbol filling denotes seasons (2009/10 = open, 2010/11 = filled) and shape denotes field sites (\circ = Site A, \triangle = Site B, and \square = Site C). Arrows in graph c mark influential data-points mentioned in the results section.

7.5.1 Embryo survival among years and sites

The corrected brown trout embryo survival to hatch (STH) in the Enziwigger (mean = 34%, min = 0%, max = 74%) was comparable to similar field studies in other Western

7.5. DISCUSSION

European streams (Dumas et al., 2007; Rubin and Glimsäter, 1996). Control STH in our study was in the range of similar sized spawners, but lower than for larger brown trout (Dumas et al., 2007; Rubin, 1995; Rubin and Glimsäter, 1996). Brown trout available for our experiment were most likely first time spawners, which can have a lower embryo survival (Brooks et al., 1997). Also differences in genetic composition of the spawners may have contributed (Brooks et al., 1997). Altogether, control embryo survival in our experiment was consistent among both field seasons, and hence conclusions about the factors affecting embryo STH in our study river remain valid.

Differences in embryo survival between years and sites similar to the ones observed here are common in natural river systems: In French streams brown trout embryo survival fluctuated up to five-fold among sampling sites and years (Bagliniere et al., 2005; Dumas et al., 2007). Atlantic salmon *Salmo salar* embryo STH differed up to seven-fold among sampling sites in the Sainte-Marguerite River system, Canada (Julien and Bergeron, 2006). Coho salmon *Oncorhynchus kisutch* embryo STH in a small coastal stream of north-western California varied four-fold between study years (Meyer, 2003). All these studies attributed the differences in embryo STH to differences in redd gravel quality (e.g., organic content, gravel permeability, or fine sediment). In support of this notion, we found that redd gravel permeability and accumulated fine sediment also affected brown trout STH in our heavily modified study river. In contrast, we did not find any indication that organic material, measured as total organic carbon, had a marked influence (hypothesis B), most likely because values in our redds were far below other river systems.

7.5.2 Oxygen dynamics in redds and embryo survival

Sufficient interstitial oxygen is crucial for the survival of salmonid embryos during their intra-gravel incubation (Greig et al., 2007b; Malcolm et al., 2008). This can be seen in redd A32_S1, where oxygen concentrations were below 3 mg l^{-1} on 44 days and of these below 1 mg l^{-1} on 22 days. These periods of severe oxygen depletion likely caused the low embryo survival of 10% in season 1 - especially since embryo STH was markedly increased at this redd location in season 2 (redd A32_S2), when no day with less than 3 mg l^{-1} occurred. Embryo STH in redd A31_S2 (47%), where oxygen was $< 3 \text{ mg l}^{-1}$ for 14 days and $< 1 \text{ mg l}^{-1}$ for six days in mid-January, was similar to redd A32_S2 (49%). Finally, in redd B51_S2, where the oxygen level dropped below 3 mg l^{-1} and reached almost complete depletion just before hatch, embryo STH was lower (39%). This might have contributed to the lower survival observed in this redd, since salmonid embryos are most sensitive to oxygen depletion close to hatch (Greig et al., 2007b). Altogether, these data indicate that up to 50% brown trout STH can occur in redds when oxygen concentrations exceed 3 mg l^{-1} during most of the incubation season. This agrees with laboratory studies demonstrating an average brown trout embryo STH of 74% and 54% with oxygen concentrations of 3.0 and 2.3 mg l^{-1} , respectively. Moreover, a threshold of 3 mg l^{-1} is in the range of the lower critical oxygen concentration of 4.06 mg l^{-1} suggested for Atlantic salmon close to hatch (Crisp, 2000). In support of hypothesis C, brown trout embryos in our study were even able to endure up to a week with less than 3 mg l^{-1} interstitial oxygen. This threshold value would most likely be higher with increasing water temperature, since the oxygen demand of salmonid embryos increases with temperature (Crisp,

2000). In any case, we suspect that brown trout embryos in our experiment probably adjusted their developmental and metabolic rates to cope with these phases of low oxygen (Geist et al., 2006; Miller et al., 2008). This could have affected growth and muscle development as well as fitness and survival post-emergence. In our opinion, such carry-over effects in later fry stages necessitate further research, since survival post-emergence can have a profound effect on recruitment in salmonid populations.

As demonstrated here and elsewhere oxygen concentrations in salmonid redds are highly variable, both spatially and temporarily (Malcolm et al., 2006). In this regard, it has been also recognized that manual oxygen measurement might not accurately reflect the oxygen concentration affecting salmonid embryo survival (Malcolm et al., 2010, 2006). In our study, mean oxygen concentrations calculated from bi-weekly manual point-wise measurements, which were most likely biased (cf. Schindler Wildhaber et al., 2014) (Chap. 7), had no explanatory power in our multivariate analyses. Moreover, our continuous oxygen data discussed in the previous paragraph suggests that embryo mortality could be related to short phases of severe oxygen depletion, e.g., close to hatch, which point measurements could easily miss. Timing and duration of such phases is closely linked to the hydro-morphological setting of the particular river system, and hence can be highly variable. These data clearly indicate that not only the oxygen concentration, but also the river system, water temperature and related processes affecting vertical hyporheic exchange and oxygen dynamics in salmonid redds have to be considered (hypothesis C).

7.5.3 Factors affecting brown trout embryo survival

Most interesting, our results provide first empirical evidence that in some heavily modified river systems artificial in-stream structures could mitigate the negative effect of fine sediment on salmonid embryo survival, supporting hypothesis A. Like in other river systems (Kasahara and Hill, 2006) the steps markedly affected hyporheic water exchange within terraces. This was also reflected in specific water infiltration rates in our redds. Without the steps hyporheic exchange in the Enziwigger would be markedly reduced (Fig. 7.3 in Schindler Wildhaber et al., 2014) (Chap. 7), which is a common phenomenon in channelized rivers with limited morphological diversity (Malcolm et al., 2010). Altogether, these data clearly highlight the importance of the artificial step structure for hyporheic exchange in the Enziwigger, and, as we could demonstrate, also for brown trout embryo survival.

Comparable studies that specifically investigated the effect of artificial in-stream structures on salmonid embryo survival are sparse. Klassen and Northcote (1988) investigating the effect of gravel filled cross-channel wire cages (i.e. weir gabions) on pink salmon *Oncorhynchus gorbuscha* embryo survival, did not report any effect. Yet, the authors compared the mean embryo survival between gabion sites and reference locations, without considering the redd position relative to the structures. This might explain why they did not find any effect, because the positive effect of artificial in-stream structures on hyporheic exchange strongly depends on the distance to the structure (Endreny et al., 2011).

Steps in general, either natural or artificial, have a marked influence on hyporheic water exchange in streams (Kasahara and Wondzell, 2003; Tonina and Buffington, 2007). Usually down-welling occurs just above the step, whereas upwelling of hyporheic water

7.5. DISCUSSION

dominates downstream of the step (Endreny et al., 2011; Kasahara and Hill, 2006). This exchange pattern also occurs in the Enziwigger. Thus, our results indicate that brown trout embryo STH increased in or close to the upwelling zone below steps. Positive effects of upwelling water for brown trout embryo survival was observed for sockeye salmon *Oncorhynchus nerka* (Garrett et al., 1998) as well as for brook trout *Salvelinus fontinalis* and brown trout in the Midwest and eastern regions of the USA. One necessity for this is a good hyporheic water quality. This is the case in the Enziwigger, where most hyporheic water originates from well oxygenated surface water and not from ground water.

Our results further corroborate the well-established fact that increased fine sediment can decrease salmonid embryo survival by decreasing redd gravel permeability, interstitial water exchange and hence oxygen supply (Greig et al., 2007b; Jensen et al., 2009). In support of this notion we demonstrated that increased fine sediment decreased water exchange and oxygen concentrations in our redds, and that this also affected brown trout embryo survival (this study). Although the amount of accumulated fine sediment was an influential predictor in the PLS regression this parameter did not reveal significance in the multivariate logistic regression, which recommends to use PLS as initial screening tool. The fredle index was a slightly better predictor for brown trout embryo STH than the amount of accumulated fine sediment. This has been reported before, especially in redds with good hyporheic water quality (Malcolm et al., 2008; Sowden and Power, 1985), such as in our study river (see above). Our results altogether corroborate that increased fine sediment can decrease salmonid embryo survival by decreasing redd gravel permeability, and hence water exchange and oxygen supply to the embryos.

We cannot pin-point the exact mechanism by which the hyporheic exchange pattern introduced by the steps benefited the embryos, but we see two main possibilities: Firstly, upwelling water below the steps could have decreased fine sediment accumulation and/or packing of the redd sediment (e.g., Seydell et al., 2009), which could have benefited water exchange. Secondly, the upwelling generated by the steps could have generated a more stable incubation environment. In our study the fredle index and the amount of accumulated fine sediment did not correlate with the distance to the steps (this study; Schindler Wildhaber et al., 2012b) (Chap. 2). Thus the upwelling water possibly provided a more stable incubation environment, such as for example a more stable thermal regime (Bjorn and Reiser, 1991; Hansen, 1975).

Acknowledgments The study was funded by the Swiss National Science Foundation (SNSF projects: K-32K1-120486 and CR2312.138025). We thank Sandra Rudolf, Bastian Brun, Annina Gysel, Patrick Schwartz, Maria a Marca, Heidi Schiffer, Venla Kontiokari, Nadja Haefeli and Sepp Lustenberger for their help in the field. Further we thank Claude Schneider and Lukas Zimmermann for technical support, and Phillip Hirsch for help during the PLS regression analysis. We greatly acknowledge the extensive support of Phillip Amrein (Fish and Wildlife Service, Sursee, Canton of Lucerne) during the experiment. Finally, we appreciate and acknowledge the very constructive and supportive comments of our editor and two anonymous reviewers. All authors declare no conflict of interests.

7.6 Supplementary information

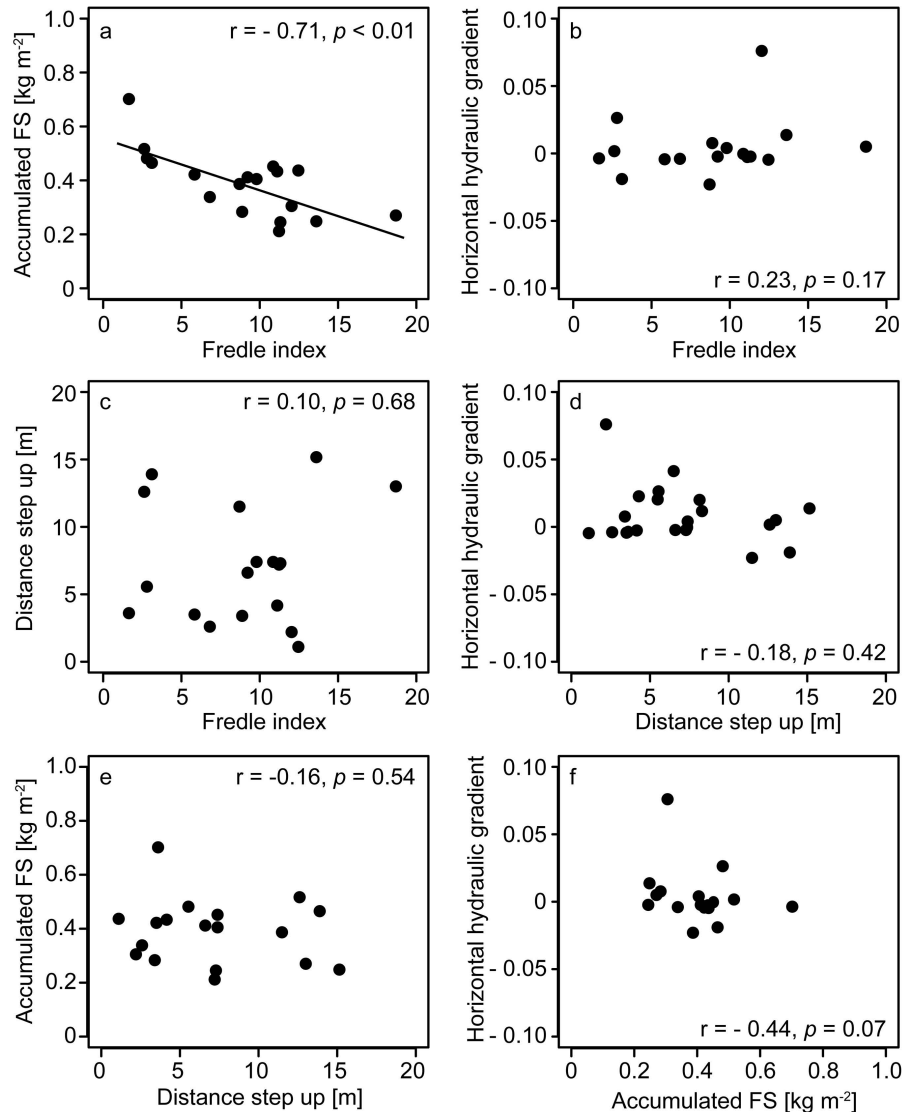


Figure 7.6: Relationship between influential predictor variables identified in partial least squares regression ($\text{VIP} > 1, 7.4$). Pearson product-moment correlation coefficients (r) and the p-values (p) are given. The black line is the best fit line. Abbreviations: FS = fine sediment, Distance step up = Distance to next upstream step.

Chapter 8

Final remarks and outlook

The attempt to measure internal colmation with a hand penetrometer was not successful. The corresponding uncertainty was larger than the differences in the degree of clogging in the river Enziwigger, where none of the three study sites had strongly colmated riverbed sediments. Bigger differences in colmation could possibly be indicated by the method, but further studies would be necessary to test this hypothesis.

A comparison of the different methods to measure fine sediment loads to other studies as well as a cross-comparison between methods indicated a general agreement between the methods. Fine sediment loads and their C_{org} and TN concentrations showed strong spatiotemporal dynamics. Consequently, a dense measuring network is necessary to capture this variability. Furthermore, all methods were connected with some instrumental and sampling errors, which cannot always be distinguished from spatial heterogeneity in the river. This calls for laboratory tests to assess the instrumental biases under controlled hydraulic and sedimentological conditions. The flushing of measuring devices during high flows remains a difficult to resolve problem. This is especially problematic with devices which can not be renewed as e.g., the accumulation baskets that were used to obtain the total sediment accumulation over the entire egg incubation season or the egg capsules.

Despite these methodical challenges, the effects of anthropogenic river modifications on water exchange processes and sediment composition in salmonid redds could be shown for the first time. Embryo survival increased at all investigated sites with shorter distance to the upstream step. This is probably related to upwelling interstitial water, triggering a more stable incubation environment. At site A, the most upstream site, the introduced steps are likely to drive higher fine sediment accumulation since they reduce the riverbed slope and thus flow velocity remarkably. Additionally, increased water infiltration above steps caused higher fine sediment infiltration and accumulation in the associated downwelling zones upstream of a step, triggering low specific infiltration rates q and thus low dissolved oxygen (DO) concentrations in redds. This resulted in a low embryo survival rate of less than 10% in the redd located directly above a step. At the downstream sites B and C, sediment accumulation was smaller than at the upstream site A even though suspended sediment (SS) loads and concentrations were higher. This was likely due to flushing of fine sediments due to higher water levels downstream. Here, the inserted steps tend to favor the embryo survival, since they increase the groundwater/interstitial water - surface water exchange. The increased fine sediment infiltration above steps which paralleled the increased downwelling of river water did not affect the net fine

sediment accumulation. Again, this was attributable to regularly flushing of fine sediments. Furthermore, the relocation of the river to the right valley side at site B and C caused hydraulic conditions that favor river water infiltration in redds, mostly towards the left bank of the river. Only during the falling limb of the river water, oxygen depleted groundwater locally exfiltrated, causing a decline in DO concentrations in redds.

Anthropogenic canalized river highly increase downstream water levels and flow velocity. Consequently, high flow events became a high risk for redd scouring. As a consequence, 50% of all redds at the two downstream sites B and C were lost. Redd loss at the upstream site was with 8% substantially lower. In a canalized river like the Enziwigger, where steps were inserted to break down the slope, this increased scouring from up- to downstream was probably related to increasing water levels, and hence bed shear stress. This high scouring could be of concern since the predicted and observed increases in winter precipitation (IPPC, 2007) can be expected to trigger similar events of even higher frequency in the future. This could potentially lead to a decline in brown trout population at the downstream sites. At the upstream site A, trout population was not affected by high scouring, however, as discussed above, fine sediment accumulation was significantly higher and DO concentration significantly lower at the upstream site, making the redd environment less favorable for the egg survival.

The source of SS at the three sites changed during the egg incubation season. The fraction of SS originating from the riverbed sediment of the upper watershed increased at all sites during high flow. Smallest contributions from the riverbed sediment were detected at site C. During baseflow, SS mainly originated from pasture and arable land. Increasing winter temperatures and precipitation led to a higher contribution of SS from arable land at both downstream sites, indicating soil erosion from the bare fields during snow-free and snow-melting periods. These data indicate an increase of soil erosion processes on snow-free pasture and arable land during the anticipated warmer winter with more frequent torrential rain events (IPPC, 2007). An increase of SS and of organic matter concentration in the SS during the brown trout spawning season is a probable consequence. Both could affect brown trout eggs negatively.

During this PhD project, an insight into the complex behavior of fine sediments in the river system Enziwigger was gained and numerous methods were developed and evaluated. It could be shown that salmonid embryo survival depends on many factors as amount of fine sediments, hydraulic exchange processes or scouring of the riverbed. These factors all change on a small temporal and spatial scale and many are interrelated, making their assessment difficult. Overall, brown trout survival in the river Enziwigger is at present not alarming, given that their population is stable since 1996 without any artificial stocking (Schager and Peter, 2002). The expected climate change, however, raises concerns about the future of brown trout as well as of other gravel riverbed species as e.g., macrozoobenthos, which are less mobile and thus possibly even more affected by sediment deposition.

Acknowledgements

I was only able to succeed successfully with this dissertation thanks to numerous people. I would like to express my gratitude to all of them.

- I especially want to thank Prof. Dr. Chrisine Alewell for the competent scientific lead in this project. She always took the time to discuss questions, came up with many ideas, helped in the field and generally provided a friendly work environment.
- I greatly enjoyed the collaboration with Christian Michel during the last four years. The many discussions in our numerous "business lunches", not only about scientific topics, were very inspiring. Furthermore, he made the sometimes hard and challenging field work enjoyable and fun.
- Further I want to thank all the other scientists involved in the project: Prof. Dr. Peter Huggenberger, Dr. Jannis Epting and Emanuel Huber from the *Applied and Environmental Geology*, Prof. Dr. Patricia Burkhardt-Holm from *Man-Society-Environment* and Dr. Dominik Bänninger. It was always good and interesting to get inputs from another angle of view.
- I also appreciated the technical support of Claude Schneider, the laboratory assistance of Marianne Caroni and Ruth Strunk and the help in the field of Annina Gysel, Sandra Rudolf, Bastian Brun and many other master students.
- The field work would not have been possible without the help from local people. Namely I want to thank Philipp Amrein and Sepp Lustenberger.
- The whole UGW-team for the many shared coffee breaks, lunches, swims in the Rhine, laughs and frustrations.
- Last but not least I want to thank Reto Wildhaber. He went with me through many ups and downs, brought up lots of new ideas, saved my nerves several times with computer related problems, always cheered me up and was my second technical supporter.

Bibliography

- Acornley, R. M. and Sear, D. A. (1999). Sediment transport and siltation of brown trout (*Salmo trutta* L.) spawning gravels in chalk streams. *Hydrol. Process.*, 13(3):447–458.
- Alewell, C., Meusburger, K., Brodbeck, M., and Bänninger, D. (2008). Methods to describe and predict soil erosion in mountain regions. *Landsc. Urban Plan.*, 88(2-4):46–53.
- Amundson, R., Austin, A. T., Schuur, E. A. G., Yoo, K., Matzek, V., Kendall, C., Uebersax, A., Brenner, D., and Baisden, W. T. (2003). Global patterns of the isotopic composition of soil and plant nitrogen. *Glob. Biogeochem. Cycle*, 17(1):11.
- Ashmore, P. E. (1988). Bed-load transport in braided gravel-bed stream models. *Earth Surf. Process. Landf.*, 13(8):677–695.
- Asselman, N. E. M., Middelkoop, H., and van Dijk, P. M. (2003). The impact of changes in climate and land use on soil erosion, transport and deposition of suspended sediment in the River Rhine. *Hydrol. Process.*, 17(16):3225–3244.
- Bagliniere, J. L., Marchand, F., and Vauclin, V. (2005). Interannual changes in recruitment of the Atlantic salmon (*Salmo salar*) population in the river Oir (Lower Normandy, France): relationships with spawners and in-stream habitat. *Ices Journal of Marine Science*, 62(4):695–707.
- Baumann, P., Kirchhofer, A., and Schälchli, U. (2012). *Sanierung Schwall/Sunk - Strategische Planung: Ein Modul der Vollzugshilfe Renaturierung der Gewässer*. Umwelt-Vollzug Nr. 1203, 126 S., Bundesamt für Umwelt, Bern.
- Baxter, C. V. and Hauer, F. R. (2000). Geomorphology, hyporheic exchange, and selection of spawning habitat by bull trout (*Salvelinus confluentus*). *Can. J. Fish. Aquat. Sci.*, 57(7):1470–1481.
- Baxter, C. W., Hauer, F. R., and Woessner, W. W. (2003). Measuring groundwater-stream water exchange: New techniques for installing minipiezometers and estimating hydraulic conductivity. *T. Am. Fish. Soc.*, 132(3):493–502.
- Bilotta, G. S. and Brazier, R. E. (2008). Understanding the influence of suspended solids on water quality and aquatic biota. *Water Res.*, 42(12):2849–2861.
- Birsan, M. V., Molnar, P., Burlando, P., and Pfaundler, M. (2005). Streamflow trends in Switzerland. *Journal of Hydrology*, 314(1-4):312–329.

- Bjorn, T. and Reiser, D. (1991). *Habitat requirements of salmonids in streams*. In: Influences of forest and rangeland management on salmonid fishes and their habitats, Special Publication, vol. 19. Ed.: Meehan, WR; American Fisheries Society, Bethesda.
- Blaschke, A. P., Steiner, K. H., Schmalfuss, R., Gutknecht, D., and Sengschmitt, D. (2003). Clogging processes in hyporheic interstices of an impounded river, the Danube at Vienna, Austria. *International Review of Hydrobiology*, 88(3-4):397–413.
- Bond, N. R. (2002). A simple device for estimating rates of fine sediment transport along the bed of shallow streams. *Hydrobiologia*, 468(1-3):155–161.
- Boulton, A. J. (2007). Hyporheic rehabilitation in rivers: Restoring vertical connectivity. *Freshwater Biology*, 52(4):632–650.
- Bowman, G. T. and Delfino, J. J. (1980). Sediment oxygen-demand techniques - A review and comparison of laboratory and insitu systems. *Water Research*, 14(5):491–499.
- Brookes, A. (1988). *Channelized Rivers: Perspectives for Environmental Management*. Wiley, Chichester.
- Brooks, S., Tyler, C. R., and Sumpter, J. P. (1997). Egg quality in fish: what makes a good egg? *Reviews in Fish Biology and Fisheries*, 7(4):387–416.
- Brown, L. R., Moyle, P. B., and Yoshiyama, R. M. (1994). Historical decline and current status of coho salmon in California. *North American Journal of fisheries management*, 14(2):237–261.
- Brun, B. (2011). Zeitliche und räumliche Dynamik der Geochemie in der Enziwigger (Kanton Luzern, Schweiz). *Bachelor thesis, Bachelor of Science in geosciences*, pages 1–36.
- Brunke, M. (1999). Colmation and depth filtration within streambeds: Retention of particles in hyporheic interstices. *Int. Rev. Hydrobiol.*, 84(2):99–117.
- Brunke, M. and Gonser, T. (1997). The ecological significance of exchange processes between rivers and groundwater. *Freshw. Biol.*, 37(1):1–33.
- BSF (2012). *Statistisches Lexikon der Schweiz: Landwirtschaftliche Nutzfläche*. Url: <http://www.bfs.admin.ch/bfs/portal/de/index/themen/07/03/blank/data/01/02.html>, Bundestamt für Statistik, Neuenburg.
- Bucher, R. (2002). *Feinsedimente in schweizerischen Fliessgewässern, Fischnetz-Publikation*. Projekt "Netzwerk Fischrückgang Schweiz". Teilprojekt 01/07, EAWAG, Dübendorf.
- Burkhardt-Holm, P. (2007). Project Fischnetz: Decline of fish catch in Switzerland. *Aquatic Sciences*, 69(1):1–2.
- Burkhardt-Holm, P., Alewell, C., and Bänninger, D. (2008). Methodologies to measure and characterize fine sediment input to rivers and their effect on health and reproduction of gravel spawning brown trout. *Proposal for the Swiss National Science Foundation*, K-32K1-120486.
- Burkhardt-Holm, P., Giger, W., Guttinger, H., Ochsenbein, U., Peter, A., Scheurer, K., Segner, H., Staub, E., and Suter, M. J. F. (2005). Where have all the fish gone? *Environmental Science and Technology*, 39(21):441a–447a.

BIBLIOGRAPHY

- Burkhardt-Holm, P. and Scheurer, K. (2007). Application of the weight-of-evidence approach to assess the decline of brown trout (*Salmo trutta*) in Swiss rivers. *Aquatic Sciences*, 69(1):51–70.
- Carrascal, L. M., Galvan, I., and Gordo, O. (2009). Partial least squares regression as an alternative to current regression methods used in ecology. *Oikos*, 118(5):681–690.
- Carslaw, H. and Jaeger, J. (1959). *Conduction of Heat in Solids*. Oxford University, New York, 2nd edition.
- Chong, I. G. and Jun, C. H. (2005). Performance of some variable selection methods when multicollinearity is present. *Chemometrics and Intelligent Laboratory Systems*, 78(1-2):103–112.
- Conen, F., Zimmermann, M., Leifeld, J., Seth, B., and Alewell, C. (2008). Relative stability of soil carbon revealed by shifts in delta N-15 and C : N ratio. *Biogeosciences*, 5(1):123–128.
- Constantz, J. (2008). Heat as a tracer to determine streambed water exchanges. *Water Resources Research*, 44.
- Craft, J. A., Stanford, J. A., and Pusch, M. (2002). Microbial respiration within a floodplain aquifer of a large gravel-bed river. *Freshwater Biology*, 47(2):251–261.
- Crisp, D. T. (1996). Environmental requirements of common riverine european salmonid fish species in fresh water with particular reference to physical and chemical aspects. *Hydrobiologia*, 323(3):201–221.
- Crisp, D. T. (2000). *Trout and Salmon: Ecology, conservation and rehabilitation*. Fishing News Books, Blackwell Sciece.
- Crisp, D. T. and Carling, P. A. (1989). Observations on siting, dimensions and structure of salmonid redds. *Journal of Fish Biology*, 34(1):119–134.
- Cudden, J. R. and Hoey, T. B. (2003). The causes of bedload pulses in a gravel channel: The implications of bedload grain-size distributions. *Earth Surf. Process. Landf.*, 28(13):1411–1428.
- Dawson, J. J. C., Soulsby, C., Tetzlaff, D., Hrachowitz, M., Dunn, S. M., and Malcolm, I. A. (2008). Influence of hydrology and seasonality on DOC exports from three contrasting upland catchments. *Biogeochemistry*, 90(1):93–113.
- Dawson, J. J. C., Tetzlaff, D., Speed, M., Hrachowitz, M., and Soulsby, C. (2010). Seasonal controls on DOC dynamics in nested upland catchments in NE Scotland. *Hydrol. Process.*, 25(10):1647–1658.
- Debele, B., Srinivasan, R., and Gosain, A. K. (2010). Comparison of process-based and temperature-index snowmelt modeling in SWAT. *Water Resources Management*, 24(6):1065–1088.
- DeVries, P. (1997). Riverine salmonid egg burial depths: Review of published data and implications for scour studies. *Can. J. Fish. Aquat. Sci.*, 54(8):1685–1698.

- Doherty, J. (1994). *PEST Model-Independent Parameter Estimation*. Watermark Computing, Corinda, Australia.
- Doppler, T., Franssen, H. J. H., Kaiser, H. P., Kuhlman, U., and Stauffer, F. (2007). Field evidence of a dynamic leakage coefficient for modelling river-aquifer interactions. *Journal of Hydrology*, 347(1-2):177–187.
- Downing, J. (2006). Twenty-five years with OBS sensors: The good, the bad, and the ugly. *Cont. Shelf Res.*, 26(17-18):2299–2318.
- Dumas, J., Bassenave, J. G., Jarry, M., Barriere, L., and Glise, S. (2007). Effects of fish farm effluents on egg-to-fry development and survival of brown trout in artificial redds. *Journal of Fish Biology*, 70(6):1734–1758.
- Dumas, J. and Marty, S. (2006). A new method to evaluate egg-to-fry survival in salmonids, trials with atlantic salmon. *Journal of Fish Biology*, 68(1):284–304.
- Duvert, C., Gratiot, N., Evrard, O., Navratil, O., Nemery, J., Prat, C., and Esteves, M. (2010). Drivers of erosion and suspended sediment transport in three headwater catchments of the Mexican Central Highlands. *Geomorphology*, 123(3-4):243–256.
- EBP-WSB-Agrofutura (2005). *Ganzheitliche Gewässerplanung im Einzugsgebiet Wiggertal*. Bau- und Umwelt und Wirtschaftsdepartement des Kantons Luzern und Baudepartement des Kantons Aargau, Luzern und Aarau.
- Endreny, T., Lautz, L., and Siegel, D. I. (2011). Hyporheic flow path response to hydraulic jumps at river steps: Flume and hydrodynamic models. *Water resources research*, 47.
- Environmental Modeling Systems, I. (2002). *GMS: Groundwater Modeling System*. South Jordan, Utah.
- EPA (2007). *Wadeable Stream Assessment, a collaborative survey of the Nations's streams*. United States Environmental Protection Agency, Washington, DC.
- EPA (2009). *National Water Quality Inventory: Report to Congress*. United States Environmental Protection Agency, Washington, DC.
- Eriksson, L., E., J., J., K.-W., Trygg, C., C., W., and Wold, S. (2006). *Multi- and Megavariate data analysis - principles and applications*. Umetrics AB.
- Faraday, J. (2006). *Extending the linear model with R*. Chapman and Hall.
- Fehr, R. (1987). Einfache Bestimmung der Korngrößenverteilung von Geschiebematerial mit Hilfe der Linienzahlanalyse. *Schweizer Ingenieur und Architekt*, 38:1104–1109.
- Fischnetz (2004). *Dem Fischrückgang auf der Spur. Schlussbericht des Projektes Netzwerk Fischrückgang Schweiz "Fischnetz"*. Eawag, BUWAL, Dübendorf, Bern.
- Fox, J. F., Davis, C. M., and Martin, D. K. (2010). Sediment source assessment in a lowland watershed using nitrogen stable isotopes. *J. Am. Water Resour. Assoc.*, 46(6):1192–1204.
- Fox, J. F. and Papanicolaou, A. N. (2007). The use of carbon and nitrogen isotopes to study watershed erosion processes. *J. Am. Water Resour. Assoc.*, 43(4):1047–1064.

BIBLIOGRAPHY

- Gail, M., Krickeberg, K., Samet, J., Tsiatis, A., and Wong, W. (2009). *Mixed effects models and extensions in ecology with R*. Springer Science + Business Media, New York.
- Gao, Q. Z., Tao, Z., Yao, G. R., Ding, J., Liu, Z. F., and Liu, K. X. (2007). Elemental and isotopic signatures of particulate organic carbon in the Zengjiang River, southern China. *Hydrol. Process.*, 21(10):1318–1327.
- Garrett, J. W., Bennett, D. H., Frost, F. O., and Thurow, R. F. (1998). Enhanced incubation success for kokanee spawning in groundwater upwelling sites in a small Idaho stream. *North American Journal of fisheries management*, 18(4):925–930.
- Geist, D. R., Abernethy, C. S., Hand, K. D., Cullinan, V. I., Chandler, J. A., and Groves, P. A. (2006). Survival, development, and growth of fall chinook salmon embryos, alevins, and fry exposed to variable thermal and dissolved oxygen regimes. *Transactions of the American Fisheries Society*, 135(6):1462–1477.
- Geist, D. R., Arntzen, E. V., Murray, C. J., McGrath, K. E., Bott, Y. J., and Hanrahan, T. P. (2008). Influence of river level on temperature and hydraulic gradients in chum and fall Chinook salmon spawning areas downstream of Bonneville Dam, Columbia river. *North American Journal of Fisheries Management*, 28(1):30–41.
- Gibbs, M. M. (2008). Identifying source soils in contemporary estuarine sediments: A new compound-specific isotope method. *Estuaries Coasts*, 31(2):344–359.
- Goto, M., Matsukara, N., and Hagiwara, Y. (2005). Heat transfer characteristics of warm water flow with cool immiscible droplets in a vertical pipe. *Exp. Therm. Fluid Sci.*, 29(3):371–381.
- Greig, S., Sear, D., and Carling, P. (2007a). A field-based assessment of oxygen supply to incubating Atlantic salmon (*Salmo salar*) embryos. *Hydrol. Process.*, 21(22):3087–3100.
- Greig, S. M., Sear, D. A., and Carling, P. A. (2005). The impact of fine sediment accumulation on the survival of incubating salmon progeny: Implications for sediment management. *Sci. Total Environ.*, 344(1-3):241–258.
- Greig, S. M., Sear, D. A., and Carling, P. A. (2007b). A review of factors influencing the availability of dissolved oxygen to incubating salmonid embryos. *Hydrol. Process.*, 21(3):323–334.
- Hansen, E. A. (1975). Some effects of groundwater on brown trout redds. *Transactions of the American Fisheries Society*, 104(1):100–110.
- Hatch, C. E., Fisher, A. T., Revenaugh, J. S., Constantz, J., and Ruehl, C. (2006). Quantifying surface water-groundwater interactions using time series analysis of streambed thermal records: Method development. *Water Resources Research*, 42(10):1–14.
- Hemmat, A. and Adamchuk, V. I. (2008). Sensor systems for measuring soil compaction: Review and analysis. *Comput. Electron. Agric.*, 63(2):89–103.
- Hester, E. T. and Doyle, M. W. (2008). In-stream geomorphic structures as drivers of hyporheic exchange. *Water resources research*, 44(3).

- Heywood, M. J. T. and Walling, D. E. (2007). The sedimentation of salmonid spawning gravels in the Hampshire Avon catchment, UK: implications for the dissolved oxygen content of intragravel water and embryo survival. *Hydrol. Process.*, 21(6):770–788.
- Hicks, B. J., Beschta, R. L., and Harr, R. D. (1991). Long-term changes in streamflow following logging in Western Oregon and associated fisheries implications. *Water Resources Bulletin*, 27(2):217–226.
- Hoehn, E. (2002). Hydrogeological issues of riverbank filtration - a review. In Ray C. (ed) *Riverbank Filtration: Understanding Contaminant Biogeochemistry and Pathogen Removal*:17-41. Kluwer Academic Publisher, Dordrecht, The Netherlands.
- Hoehn, E. and Cirpka, O. A. (2006). Assessing residence times of hyporheic ground water in two alluvial flood plains of the southern alps using water temperature and tracers. *Hydrology and Earth System Sciences*, 10(4):553–563.
- Hoehn, E. and Von Gunten, H. R. (1989). Radon in groundwater - a tool to assess infiltration from surface waters to aquifers. *Water Resources Research*, 25(8):1795–1803.
- Hoffman, D. E. and Gabet, E. J. (2007). Effects of sediment pulses on channel morphology in a gravel-bed river. *Geological Society of America Bulletin*, 119(1-2):116–125.
- Hornberger, G. M., Bencala, K. E., and McKnight, D. M. (1994). Hydrological controls on dissolved organic carbon during snowmelt in the Snake River near Montezuma, Colorado. *Biogeochemistry*, 25(3):147–165.
- Horowitz, A. J., Rinella, F. A., Lamothe, P., Miller, T. L., Edwards, T. K., Roche, R. L., and Rickert, D. A. (1990). Variations in suspended sediment and associated trace-element concentrations in selected riverine cross-sections. *Environ. Sci. Technol.*, 24(9):1313–1320.
- Huber, E., Huggenberger, P., Epting, J., and Schindler Wildhaber, Y. (2013). Zeitliche und räumliche Skalen der Fluss-Grundwasser Interaktion: Ein multidimensionaler Untersuchungsansatz - Spatiotemporal scales of river-groundwater interaction: A multidimensional investigation approach. *Grundwasser*, 18(3):159–172.
- Huette, M. and Niederhauser, P. (1998). *Ökomorphologie Stufe F. Methoden zur Untersuchung und Beurteilung der Fliessgwaesser in der Schweiz*. Bundesamt für Umwelt, Wald und Landschaft, Mitteilungen zum Gewässerschutz, Bern.
- Huggenberger, P., Epting, J., Spottke, I., Regli, C., and Zechner, E. (2006). *INTERREG III A-Projekt MoNit "Modellierung der Grundwasserbelastung durch Nitrat im Oberrheingraben"*. Teilprojekte Nitratherkunft (Nitrat-Transportmodellierung) und Fluss-Grundwasser-Interaktion (regionale hydrologische Grundlagendaten). Landesanstalt für Umwelt, Messungen und Naturschutz Baden-Württemberg, Karlsruhe.
- Huntington, C., Nehlsen, W., and Bowers, J. (1996). A survey of healthy native stocks of anadromous salmonids in the Pacific Northwest and California. *Fisheries*, 21(3):6–14.
- Inamdar, S. P., Christopher, S. F., and Mitchell, M. J. (2004). Export mechanisms for dissolved organic carbon and nitrate during summer storm events in a glaciated forested catchment in New York, USA. *Hydrol. Process.*, 18(14):2651–2661.

BIBLIOGRAPHY

- Ingebritsen, S., Sanford, W., and Neuzil, C. (2006). *Groundwater in Geologic Processes*. Cambridge University Press, New York, second edition.
- Ingendahl, D. (1999). *Der Reproduktionserfolg von Meerforelle und Lachs in Korrelation zu den Milieubedingungen des hyporheischen Interstitials*. Inaugural-Dissertation, Universität Köln.
- IPPC (2007). *Climate Change 2007: The Physical Science Basis, Summary for Policymakers*. Intergovernmental panel on climate change, Cambridge University Press, Cambridge, United Kingdom and New York, NY, USA.
- IUSS (2006). *World reference base for soil resources*. FAO, Rome.
- Jensen, D. W., Steel, E. A., Fullerton, A. H., and Pess, G. R. (2009). Impact of fine sediment on egg-to-fry survival of pacific salmon: A meta-analysis of published studies. *Rev. Fish. Sci.*, 17(3):348–359.
- Julien, H. and Bergeron, N. (2006). Effect of fine sediment infiltration during the incubation period on Atlantic salmon (*Salmo salar*) embryo survival. *Hydrobiologia*, 563:61–71.
- Kasahara, T. and Hill, A. R. (2006). Hyporheic exchange flows induced by constructed riffles and steps in lowland streams in southern Ontario, Canada. *Hydrol. Process.*, 20(20):4287–4305.
- Kasahara, T. and Wondzell, S. M. (2003). Geomorphic controls on hyporheic exchange flow in mountain streams. *Water resources research*, 39(1).
- Keery, J., Binley, A., Crook, N., and Smith, J. W. N. (2007). Temporal and spatial variability of groundwater-surface water fluxes: Development and application of an analytical method using temperature time series. *Journal of Hydrology*, 336(1-2):1–16.
- Kendall, C., editor (1998). *Isotope tracer in catchment hydrology*. Elsevier, Amsterdam.
- Klassen, H. D. and Northcote, T. G. (1988). Use of gabion weirs to improve spawning habitat for pink salmon in a small logged watershed. *North American Journal of fisheries management*, 8(1):36–44.
- Klingemann, P. and Emmett, W. (1982). Gravel bedload transport processes. In Hey, R., Bathurst, J., and Thorne, C., editors, *Gravel-bed Rivers*, pages 145–169. Wiley, Chichester.
- Kondolf, G. M. (2000). Assessing salmonid spawning gravel quality. *Transactions of the American Fisheries Society*, 129(1):262–281.
- Kuchling, H. (1976). *Taschenbuch der Physik*. Verlag Harri Deutsch, Thun.
- Kuntze, H., Roeschmann, G., and Schwerdtfeger, G. (1994). *Bodenkunde*. Ulmer UTB für Wissenschaft, Stuttgart.
- Lapointe, M., Bergeron, N., Berube, F., Pouliot, M., and Johnston, P. (2003). Interactive effects of substrate sand and silt contents, redd-scale hydraulic gradients, and interstitial velocities on egg-to-emergence survival of atlantic salmon (*salmo salar*). In *Symposium on Status of Atlantic Salmon*, pages 2271–2277, Quebec, CANADA.

- Lemmon, E., McLinden, M., and Friend, D. (2012). "Thermophysical Properties of Fluid Systems". NIST Chemistry WebBook, NIST Standard Reference Database Number 69, Eds. P.J. Linstrom and W.G. Mallard, National Institute of Standards and Technology, Gaithersburg MD, <http://webbook.nist.gov>, retrieved February 1.
- Leser, H., Haas, H.-D., Meier, S., Mosimann, T., and Paesler, R. (2005). *DIERCKE Wörterbuch Allgemeine Geographie*. Deutscher Taschenbuchverlag, München.
- Levasseur, M., Bergeron, N., Lapointe, M., and Berube, F. (2006). Effects of silt and very fine sand dynamics in Atlantic salmon (*Salmo salar*) redds on embryo hatching success. *Can. J. Fish. Aquat. Sci.*, 63:1450–1459.
- Liechti, P. (2010). *Methoden zur Untersuchung und Beurteilung der Fließgewässer. Chemisch-physikalische Erhebungen, Nährstoffe*. Umwelt-Vollzug Nr. 1005, Bundesamt für Umwelt, Bern.
- Liechti, R. (2011). Bestimmung der sedimentherkunft in der enziwigger anhand von Kohlenstoff- und Stickstoff-Isotopen. *Bachelor thesis, Bachelor of Science in geosciences*, pages 1–38.
- Lisle, T. E. (1989). Sediment transport and resulting deposition in spawning gravels, North Coastal California. *Water Resour. Res.*, 25(6):1303–1319.
- Lisle, T. E. and Lewis, J. (1992). Effects of sediment transport on survival of salmonid embryos in a natural stream - a simulation approach. *Can. J. Fish. Aquat. Sci.*, 49(11):2337–2344.
- Liu, W. C., Chen, W. B., and Kimura, N. (2009). Measurement of sediment oxygen demand to simulate dissolved oxygen distribution: Case study in the main Danshuei river estuary. *Environmental Engineering Science*, 26(12):1701–1711.
- Lotspeich, F. and Everest, F. (1981). *A new method for reporting and interpreting textural composition of spawning gravel*. United States Department of Agriculture, Forest service, Pacific Northwest Forest and Range Experiment Station.
- Malcolm, I. A., Greig, S. M., Youngson, A. F., and Soulsby, C. (2008). Hyporheic influences on salmon embryo survival and performance. In *Salmonid Spawning Habitat in Rivers: Physical Controls, Biological Responses, and Approaches to Remediation*, volume 65 of *American Fisheries Society Symposium*, pages 225–248. American Fisheries Society.
- Malcolm, I. A., Middlemas, C. A., Soulsby, C., Middlemas, S. J., and Youngson, A. F. (2010). Hyporheic zone processes in a canalised agricultural stream: implications for salmonid embryo survival. *Fundam. Appl. Limnol.*, 176(4):319–336.
- Malcolm, I. A., Soulsby, C., Youngson, A., and Tetzlaff, D. (2009). Fine scale variability of hyporheic hydrochemistry in salmon spawning gravels with contrasting groundwater-surface water interactions. *Hydrogeology Journal*, 17:161–174.
- Malcolm, I. A., Soulsby, C., and Youngson, A. F. (2006). High-frequency logging technologies reveal state-dependent hyporheic process dynamics: implications for hydroecological studies. *Hydrol. Process.*, 20(3):615–622.

BIBLIOGRAPHY

- Malcolm, I. A., Soulsby, C., Youngson, A. F., and Petry, J. (2003a). Heterogeneity in ground water-surface water interactions in the hyporheic zone of a salmonid spawning stream. *Hydrol. Process.*, 17(3):601–617.
- Malcolm, I. A., Youngson, A. F., and Soulsby, C. (2003b). Survival of salmonid eggs in a degraded gravel-bed stream: Effects of groundwater-surfacewater interactions. *River Research and Applications*, 19(4):303–316.
- McConnachie, J. L. and Petticrew, E. L. (2006). Tracing organic matter sources in riverine suspended sediment: Implications for fine sediment transfers. *Geomorphology*, 79(1-2):13–26.
- McDonald, M. and Harbaugh, A. (1996). Programmer's documentation for MODFLOW-96, an update to the U.S. Geological Survey modular finite-difference ground-water flow model. In *U.S. Geological Survey open-file report*, pages 96–486.
- Meusburger, K. and Alewell, C. (2008). Impacts of anthropogenic and environmental factors on the occurrence of shallow landslides in an alpine catchment (Urseren Valley, Switzerland). *Nat. Hazards Earth Syst. Sci.*, 8(3):509–520.
- Mevik, B. H. and Wehrens, R. (2007). The pls package: Principal component and partial least squares regression in r. *J. Stat. Softw.*, 18(2):23.
- Meybeck, M. (1982). Carbon, nitrogen, and phosphorus transport by world rivers. *Am. J. Sci.*, 282(4):401–450.
- Meyer, C. (2003). Importance of measuring biotic and abiotic factors in the lower egg pocket to predict salmon egg survival. *Journal of Fish Biology*, 62:534–548.
- Michel, C., Schindler Wildhaber, Y., Epting, J., Thorpe, K., Huggenberger, P., P., B.-H., and C., A. (acc.). Artificial steps mitigate fine sediment effects on brown trout embryo survival in a heavily modified river. *Journal of Freshwater Biology*.
- Middelkoop, H., Daamen, K., Gellens, D., Grabs, W., Kwadijk, J. C. J., Lang, H., Parmet, B., Schadler, B., Schulla, J., and Wilke, K. (2001). Impact of climate change on hydrological regimes and water resources management in the Rhine basin. *Climatic Change*, 49(1-2):105–128.
- Miller, S. C., Reeb, S. E., Wright, P. A., and Gillis, T. E. (2008). Oxygen concentration in the water boundary layer next to rainbow trout (*oncorhynchus mykiss*) embryos is influenced by hypoxia exposure time, metabolic rate, and water flow. *Canadian Journal of Fisheries and Aquatic Sciences*, 65(10):2170–2177.
- Minella, J. P. G., Merten, G. H., Reichert, J. M., and Clarke, R. T. (2008). Estimating suspended sediment concentrations from turbidity measurements and the calibration problem. *Hydrol. Process.*, 22(12):1819–1830.
- Mosimann, T. (2003). *Erosionsgefährdung und Schutz der Böden durch die Bewirtschaftung - Monitoring 1982 - 2002*. Amt für Umweltschutz und Energie, Kanton Basel-Land, Liestal.

- Naegeli, M. W., Hartmann, U., Meyer, E. I., and Uehlinger, U. (1995). POM-dynamics and community respiration in the sediments of a floodprone prealpine river (Necker, Switzerland). *Archiv für Hydrobiologie*, 133:339–347.
- Navratil, O., Esteves, M., Legout, C., Gratiot, N., Nemery, J., Willmore, S., and Grangeon, T. (2011). Global uncertainty analysis of suspended sediment monitoring using turbidimeter in a small mountainous river catchment. *J. Hydrol.*, 398(3-4):246–259.
- Newcombe, C. and Jensen, J. (1996). Channel suspended sediment and fisheries: A synthesis for quantitative assessment of risk and impact. *N. Am. J. Fish. Manage.*, 16:693–727.
- Newcombe, C. P. and MacDonald, D. (1991). Effects of suspended sediments on aquatic ecosystems. *North American Journal of fisheries management*, 11:72–82.
- Onstad, G. D., Canfield, D. E., Quay, P. D., and Hedges, J. I. (2000). Sources of particulate organic matter in rivers from the continental USA: Lignin phenol and stable carbon isotope compositions. *Geochimica Et Cosmochimica Acta*, 64(20):3539–3546.
- Ottaway, E. M., Carling, P. A., Clarke, A., and Reader, N. A. (1981). Observations on the structure of brown trout, *Salmo trutta* Linnaeus, redd. *Journal of Fish Biology*, 19(5):593–607.
- Owens, P., Batalla, R., Collins, A., Gomez, B., Hicks, D., Horowitz, A., Kondolf, G., Marden, M., Page, M., Peacock, D., Peticrew, E., Salomons, W., and Trustrum, N. (2005). Fine-grained sediment in river systems: Environmental significance and management issues. *River Res. Appl.*, 21:693–717.
- Packman, J., Comings, K., and Booth, D. (1999). Using turbidity to determine total suspended solids in urbanizing streams in the Puget Lowlands. In *Managing change in water resources and the environment*, Can. Wat. resour. association annual meeting, pages 158–165, Vancouver.
- Phillips, D. L. and Gregg, J. W. (2001). Uncertainty in source partitioning using stable isotopes. *Oecologia*, 127(2):171–179.
- Phillips, D. L. and Gregg, J. W. (2003). Source partitioning using stable isotopes: coping with too many sources. *Oecologia*, 136(2):261–269.
- Phillips, D. L., Newsome, S. D., and Gregg, J. W. (2005). Combining sources in stable isotope mixing models: alternative methods. *Oecologia*, 144(4):520–527.
- Phillips, J. M., Russell, M. A., and Walling, D. E. (2000). Time-integrated sampling of fluvial suspended sediment: a simple methodology for small catchments. *Hydrol. Process.*, 14(14):2589–2602.
- Pimentel, D. and Kounang, N. (1998). Ecology of soil erosion in ecosystems. *Ecosystems*, 1(5):416–426.
- Potyondy, J. P. and Sylte, T. L. (2008). Discussion - "Assessment of methods for measuring embeddedness: Application to sedimentation in flow regulated streams". *J. Am. Water Resour. Assoc.*, 44(1):259–261.

BIBLIOGRAPHY

- Prasuhn, V. (2011). Soil erosion in the Swiss midlands: Results of a 10-year field survey. *Geomorphology*, 126(1-2):32–41.
- Prasuhn, V. (2012). On-farm effects of tillage and crops on soil erosion measured over 10 years in Switzerland. *Soil Tillage Res.*, 120:137–146.
- Pusch, M. and Schwoerbel, J. (1994). Community respiration in hyporheic sediments of a mountain stream (Steina, Black-Forest). *Archiv Für Hydrobiologie*, 130(1):35–52.
- Quinn, G. and Keough, M. (2002). *Experimental Design and Data Analysis for Biologists*. Cambridge University Press.
- Rau, G. C., Andersen, M. S., McCallum, A. M., and Acworth, R. I. (2010). Analytical methods that use natural heat as a tracer to quantify surface water-groundwater exchange, evaluated using field temperature records. *Hydrogeology Journal*, 18(5):1093–1110.
- Revil, A. (2000). Thermal conductivity of unconsolidated sediments with geophysical applications. *Journal of Geophysical Research-Solid Earth*, 105(B7):16749–16768.
- Riedl, C. and Peter, A. (2013). Timing of brown trout spawning in alpine rivers with special consideration of egg burial depth. *Ecology of Freshwater Fish*, pages 1–14.
- Rubin, J. F. (1995). Estimating the success of natural spawning of salmonids in streams. *Journal of Fish Biology*, 46(4):603–622.
- Rubin, J. F. and Glimsäter, C. (1996). Egg-to-fry survival of the sea trout in some streams of gotland. *Journal of Fish Biology*, 48(4):585–606.
- Rudolf, S. (2010). Die Rolle des Niederschlages auf die Sedimentdynamik in der Enziwigger (Kanton Luzern, Schweiz). *Bachelor thesis, Bachelor of Science in geosciences*, pages 1–28.
- Ryan, P. A. (1991). Environmental-effects of sediment on New Zealand streams - a review. *N. Z. J. Mar. Freshw. Res.*, 25(2):207–221.
- Sawyer, A. H., Cardenas, M. B., and Buttles, J. (2011). Hyporheic exchange due to channel-spanning logs. *Water Resources Research*, 47.
- Schager, E. and Peter, A. (2001). *Bachforellensömmerlinge Phase 1*. Fischnetz-Publikation. Projekt "Netzwerk Fischrückgang Schweiz", EAWAG, Dübendorf.
- Schager, E. and Peter, A. (2002). *Bachforellensömmerlinge Phase 2*. Fischnetz-Publikation. Projekt "Netzwerk Fischrückgang Schweiz", EAWAG, Dübendorf.
- Schager, E., Peter, A., and Burkhardt-Holm, P. (2007). Status of young-of-the-year brown trout (*Salmo trutta fario*) in Swiss streams: factors influencing YOY trout recruitment. *Aquatic Sciences*, 69(1):41–50.
- Scheurer, K., Alewell, C., Bänninger, D., and Burkhardt-Holm, P. (2009). Climate and land-use changes affecting river sediment and brown trout in alpine countries - a review. *Environ. Sci. Pollut. Res.*, 16(2):232–242.

- Schindler Wildhaber, Y., Liechti, R., and Alewell, C. (2012a). Organic matter dynamics and stable isotope signature as tracers of the sources of suspended sediment. *Biogeosciences*, 9:1985–1996.
- Schindler Wildhaber, Y., Michel, C., Burkhardt-Holm, P., Bänninger, D., and Alewell, C. (2012b). Measurement of spatial and temporal fine sediment dynamics in a small river. *Hydrol. Earth Syst. Sci.*, 16:1501–1515.
- Schindler Wildhaber, Y., Michel, C., Epting, J., Wildhaber, R., Huber, E., Huggenberger, P., Burkhardt-Holm, P., and Alewell, C. (2014). Effects of redd morphology, hyporheic flow and sediment deposition on oxygen dynamics. *Science of the total Environment*, 470-471:488–500.
- Schälchli, Abegg, and Hunzinger (2002). *Kolmation - Methoden zur Erkennung und Bewertung*. EAWAG, Dübendorf.
- Schälchli, U. (1993). Die Kolmation von Fliessgewässersohlen: Prozesse und Berechnungsgrundlagen. *Versuchsanstalt für Wasserbau, Hydrologie und Glaziologie*, 142.
- Schälchli, U. (1995). Basic equations for siltation of riverbeds. *J. Hydraul. Eng.-Asce*, 121(3):274–287.
- Schälchli, U., Abegg, J., and Hunzinger, L. (2005). *Geschiebe- und Schwebstoffproblematik in Schweizer Fliessgewässern*. Schälchli, Abegg + Hunzinger, Zürich.
- Schön, J. (1996). *Physical properties of rocks: fundamentals and principles of petrophysics - handbook of geophysical exploration*. Pergamon, New York.
- Scrivener, J. C. (1988). Two devices to assess incubation survival and emergence of salmonid fry in an estuary streambed. *North American Journal of fisheries management*, 8(2):248–258.
- Sear, D. A. (1993). Fine sediment infiltration into gravel spawning beds within a regulated river experiencing floods - ecological implications for salmonids. *Regul. Rivers-Res. Manage.*, 8(4):373–390.
- Sear, D. A., Frostick, L., Rollinson, G., and Lisle, T. (2008). The significance and mechanics of fine-sediment infiltration and accumulation in gravel spawning beds. *Am. Fish. Soc. Symposium*, 65:149–173.
- Sennatt, K., Salant, N., Renshaw, C., and Magilligan, F. (2006). Assessment of methods for measuring embeddedness: Application to sedimentation in flow regulated streams. *Journal of American water resources association*, December:1671–1682.
- Seydell, I., Ibisch, R., and Zanke, U. (2009). Intrusion of suspended sediments into gravel riverbeds: influence of bed topography studied by means of field and laboratory experiments. *Advanc.Limnol.*, 61:67–85.
- Silliman, S. E., Ramirez, J., and McCabe, R. L. (1995). Quantifying downflow through creek sediments using temperature time-series - One-dimensional solution incorporating measured surface-temperature. *Journal of Hydrology*, 167(1-4):99–119.

BIBLIOGRAPHY

- Soulsby, C., Malcolm, I. A., Tetzlaff, D., and Youngson, A. F. (2009). Seasonal and inter-annual variability in hyporheic water quality revealed by continuous monitoring in a salmon spawning stream. *River research and applications*, DOI: 10.1002/rra.1241.
- Soulsby, C., Malcolm, I. A., and Youngson, A. F. (2001a). Hydrochemistry of the hyporheic zone in salmon spawning gravels: A preliminary assessment in a degraded agricultural stream. *Regul. Rivers-Res. Manage.*, 17(6):651–665.
- Soulsby, C., Youngson, A., Moir, H., and Malcolm, I. (2001b). Fine sediment influence on salmonid spawning habitat in a lowland agricultural stream: a preliminary assessment. *Sci. Total Environ.*, 265:295–307.
- Sowden, T. K. and Power, G. (1985). Prediction of rainbow trout embryo survival in relation to groundwater seepage and particle size of spawning substrates. *Transactions of the American Fisheries Society*, 114(6):804–812.
- Sponagel, H., Grottenthaler, W., Hartmann, K.-J., Hartwich, R., Janetzko, P., Joisten, H., Kuhn, D., Sabel, K.-J., and Traidl, R. (2005). *Bodenkundliche Kartieranleitung*. Bundesanstalt für Geowissenschaften und Rohstoffe, Hannover.
- Spreafico, M., Lehmann, C., Jakob, A., and Grasso, A. (2005). *Feststoffbeobachtung in der Schweiz*. Bundesamt für Wasser und Geologie / Swiss Federal Office for Water and Geology, Bern.
- Stucki, P. (2010). *Methoden zur Untersuchung und Beurteilung der Fliessgewässer. Makrozoobenthos Stufe F*. Bundesamt für Umwelt, Bern. Umwelt-Vollzug 1027, Bern.
- Sylte, T. and Fischenich, C. (2002). *Techniques for Measuring Substrate Embeddedness*. U.S. Army Engineer Research and Development Center, Missoula MT.
- Thodsen, H. (2007). The influence of climate change on stream flow in Danish rivers. *Journal of Hydrology*, 333(2-4):226–238.
- Todorova, Y., Belev, R., Topalova, Y., and Ribarova, I. (2009). Analogous simulation of nutrient transformation processes in stream sediments. *Water Sa*, 35(5):561–565.
- Tonina, D. and Buffington, J. M. (2007). Hyporheic exchange in gravel bed rivers with pool-riffle morphology: Laboratory experiments and three-dimensional modeling. *Water Resources Research*, 43(1):16.
- Tonina, D. and Buffington, J. M. (2009). A three-dimensional model for analyzing the effects of salmon redds on hyporheic exchange and egg pocket habitat. *Can. J. Fish. Aquat. Sci.*, 66(12):2157–2173.
- Wagner, L. E., Vidon, P., Tedesco, L. P., and Gray, M. (2008). Stream nitrate and DOC dynamics during three spring storms across land uses in glaciated landscapes of the Midwest. *Journal of Hydrology*, 362(3-4):177–190.
- Wohl, E. (2006). Human impacts to mountain streams. *Geomorphology*, 79(3-4):217–248.
- Wold, S., Sjostrom, M., and Eriksson, L. (2001). PLS-regression: a basic tool of chemometrics. *Chemometrics and Intelligent Laboratory Systems*, 58(2):109–130.

BIBLIOGRAPHY

- Young, M., Hubert, W., and Wesche, T. (1991). Biases associated with four stream substrate samplers. *Can. J. Fish. Aquat. Sci.*, 48(10):1882–1886.
- Youngson, A. F., MacLean, J. C., and Fryer, R. J. (2002). Rod catch trends for early-running MSW salmon in Scottish rivers (1952-1997): divergence among stock components. *Ices Journal of Marine Science*, 59(4):836–849.
- Zhang, S., Lu, X. X., Sun, H. Q., Han, J. T., and Higgitt, D. L. (2009). Geochemical characteristics and fluxes of organic carbon in a human-disturbed mountainous river (the Luodingjiang River) of the Zhujiang (Pearl River), China. *Sci. Total Environ.*, 407(2):815–825.
- Zimmermann, A., Coulombe-Pontbriand, M., and Lapointe, M. (2005). Biases of submerged bulk and freeze-core samples. *Earth Surf. Process. Landf.*, 30(11):1405–1417.
- Zimmermann, A. and Lapointe, M. (2005a). Integranular flow velocity through salmonid redds: sensitivity to fines infiltration from low intensity sediment transport events. *River research and applications*, 21:865–881.
- Zimmermann, A. E. and Lapointe, M. (2005b). Sediments infiltration traps: their use to monitor salmonid spawning habitat in headwater tributaries of the Cascadepedia River, Quebec. *Hydrol. Process.*, 19(20):4161–4177.
- Zuur, A., Ieno, E., and Elphick, C. (2010). A protocol for data exploration to avoid common statistical problems. *Methods in Ecology and Evolution*, 1(1):3–14.

Appendix A

Sediment oxygen demand

A.1 Objective

A detailed investigation of the effects of hydrological and hydrogeological conditions, riverbed structure, redd morphology and fine sediment deposition on oxygen concentrations in artificial brown trout redds has been conducted at the river Enziwigger, Lucerne, Switzerland during two spawning seasons (Schindler Wildhaber et al., 2014, Chap. 6). It was noted that during spring toward the end of the incubation season, oxygen generally decreased. This was linked to an increased infiltration of silt and clay sized particles, deposited during base flow periods and decreasing gravel permeability. Additionally, organic content in the deposited fine sediments was enhanced during base flow. Together with increasing river temperatures in spring this is likely to contribute to higher oxygen demands (Schindler Wildhaber et al., 2014, Chap. 6). The aim of this laboratory study was to assess the sediment oxygen demand (SOD) at the end of the incubation period, when oxygen demand of the developing embryos is at maximum (Greig et al., 2007b).

The term sediment oxygen demand (SOD) includes oxygen demand from two separate processes: I) Biological respiration of all living organisms in the sediment and II) Chemical oxidation of reduced substances in the sediment such as divalent iron and manganese, and sulfide (Bowman and Delfino, 1980). SOD can be measured in situ or in the laboratory, but it has been shown that laboratory techniques meet the criteria of consistency, reproducibility and efficiency better than in situ techniques (Bowman and Delfino, 1980). Today, laboratory studies to assess SOD for several research questions are conducted (e.g., Liu et al., 2009; Todorova et al., 2009).

A.2 Materials and methods

The study was conducted with sediments of the river Enziwigger, Lucerne, Switzerland. At this river, the sediment dynamics and the effects of sediments on brown trout eggs were investigated at three sites named A, B and C. Six artificial redds were built at each site and equipped with, among others, two accumulation baskets with a diameter of 125 mm and a depth of 160 mm. These baskets were buried in the riverbed sediment during the entire field season to measure the net fine sediment accumulation during the

brown trout egg incubation season. At the end of the field season 2010/2011 sediment accumulation baskets were taken to the laboratory to assess the SOD of the redds. Further information about the characteristics of the river, the three sites and the field methods can be found in Schindler Wildhaber et al. (2012a,b, 2014); Michel et al. (acc); Huber et al. (2013)(Chap. 2,3,5,6,7).

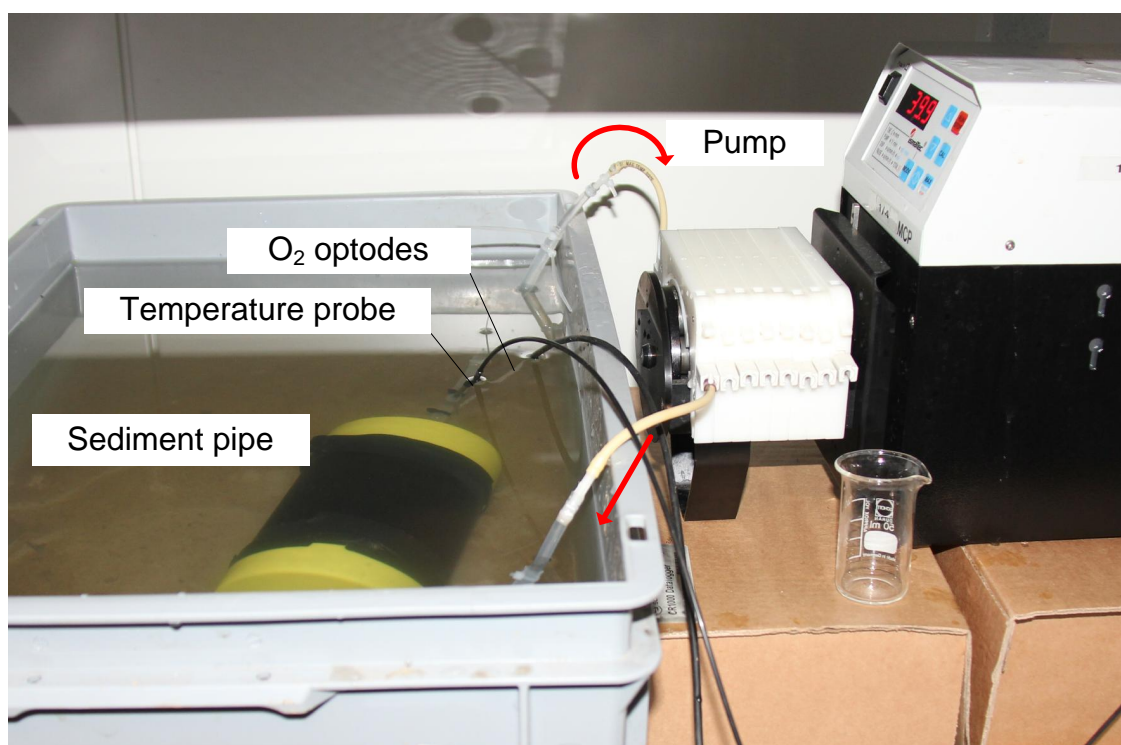


Figure A.1: Recirculation system used for measuring sediment oxygen demand (SOD). The red arrows indicate the flow direction.

The recirculating system to measure SOD consisted of a 170 mm long, commercially available PE pipes with an outer diameter of 110 mm and a wall thickness of 4.2 mm (Fig. A.1). The pipe was plugged with caps that had a central opening for a PharMed PBT tube with an inner diameter of 6 mm as inlet and outlet, which were covered with a nylon mesh. The tubes formed a recirculation system. The system was run with a peristaltic pump to maintain an internal circulation rate of approximately 40 ml min^{-1} , which is the same rate as used by Ingendahl (1999) and Craft et al. (2002). Dissolved oxygen (DO) and temperature were measured and logged every minute at the outlet of the sediment tube with a PreSens oxygen dipping probe mini-sensor (PreSens Precision Sensing GmbH, Regensburg, Germany). Temperature was kept constant at 4°C . The sediment tube was located in a box filled with water to minimize oxygen diffusion (Fig. A.1).

The accumulation baskets were transferred to the laboratory in stream water filled buckets and stored at 4°C . According to Pusch and Schwoerbel (1994), sediment samples can be stored up to 5 days without detectable effect on SOD. The sediments of one basket was filled in the sediment pipe. Afterward, the air was flushed from the system while filling in stream water that was taken in a separately container to the laboratory. The system

A.3. RESULTS, DISCUSSION AND OUTLOOK

was run until the negative slope of the DO curve was strongly reduced. One accumulation basket (basket A41) was run twice in order to assess differences in SOD which are due to a four day storage.

A.3 Results, discussion and outlook

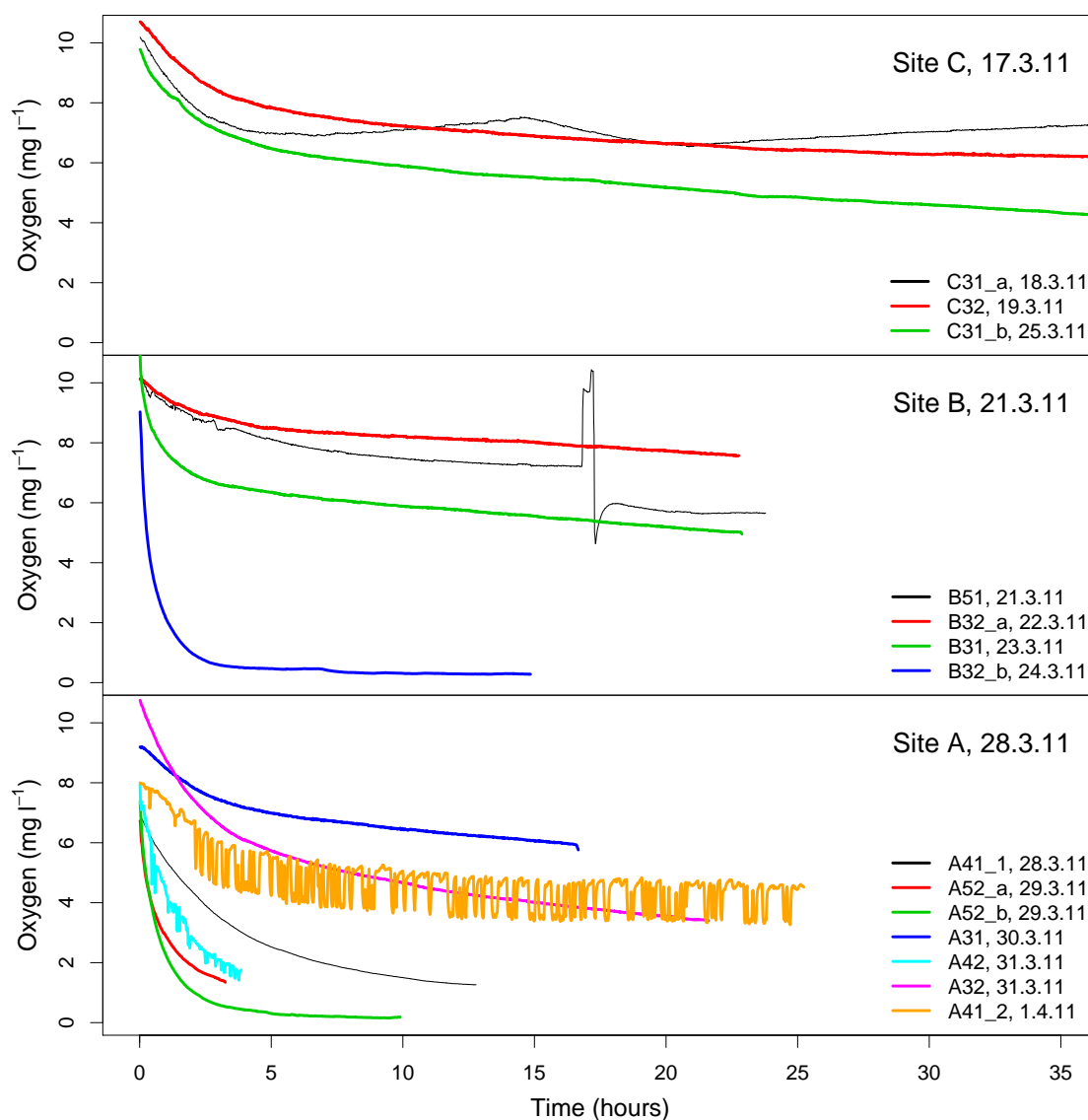


Figure A.2: Decline of oxygen concentration within the circulation system with sediment samples from the three sites A,B and C. Accumulation baskets from the same redd are indicated with _a and _b. ₁ and ₂ refers to the accumulation basket which was run twice. The samples are sorted after the date of procedure. The date behind the site label stands for the day when samples have been collected in the field.

DO concentration in the sediment tube was around 10 mg l⁻¹ at the start of the incubation experiment. This corresponds to an oxygen saturation of approximately 75% at 4°C. The

APPENDIX A. SEDIMENT OXYGEN DEMAND

concentration decreased remarkably within the first two hours (Fig. A.2). This decrease stopped, however, at around $6 - 8 \text{ mg l}^{-1}$ during the first six incubation runs. This may indicate that the system was not completely impermeable to oxygen. Some of the following experiments decreased until almost 0 mg l^{-1} , which is most probably associated with an improved handling and not with a higher SOD of the samples. Furthermore, it could be observed that the DO concentration increased immediately after a stop of the pump (run B51, Fig. A.2). After the restart of the pump, DO concentration decreased quickly to a lower level than it would have been expected by the curve. The reason for this behavior remained unknown. Finally, the two SOD-runs of the accumulation basket A41 triggered two quite different curves. Because of these uncertainties, the results of the SOD incubations were not further evaluated.

We are still confident that SOD would be of valuable interest in concern of the redd environment. But the laboratory experiments would have to be planned thoroughly and pretests must be conducted. These were not done because of a lack of time. Moreover, it would be recommendable to have more than one sediment tube to conduct several incubation runs in parallel.

Curriculum Vitae

Yael Schindler Wildhaber

born on 22nd March 1982 in Affoltern a.A., Switzerland

Education

- 09.2008 - 10.2012 **PhD** at Institute of Environmental Geosciences, University of Basel
Doctoral Thesis: *The impact of fine sediments in small rivers: Method development and effects on brown trout redds*
- 09.2012 - 04.2013 **Didactic certificate** in Environmental teaching, ETH Zürich
- 09.2006 - 08.2008 **Master of Science** in Environmental Geoscience, University of Basel
Master Thesis: *Wassererosion in Abhängigkeit der Oberflächenbeschaffenheit auf subalpinen Flächen, Quantifizierung mittels Regensimulatoren im Labor und Freiland*
- 10.2003 - 09.2006 **Bachelor of Science** in Geosciences, University of Basel, Switzerland
- 03.2006 - 07.2006 **Exchange Semester**, Université de Neuchâtel
- 08.1995 - 08.2002 **Matura**, Kantonsschule Glarus
- 08.1999 - 06.2000 **Exchange year**, Elkton High school, OR, USA

Professional Experience

- Since 11.2012 Postdoc at the department for Water Resources and Drinking Water, EAWAG, Dübendorf
- Since 08.2012 Education of environmental camp leaders, WWF Switzerland
- 11.2006 - 12.2007 Student assistance at the Institute of Environmental Geosciences, Basel
- 11.2006 - 02.2007 Internship in the ecology office Life Science AG, Basel
- 08.2008 - 10.2006 Internship at the Swedish University of Agricultural Science, Institute of Environmental Assessment, Uppsala.